7-2005

Long Term Monitoring of a Steel Bridge Constructed Using Phase Constructoin

Aaron Jon Yakel
University of Nebraska - Lincoln

Paulo Marchon

Atorod Azizinamini
University of Nebraska - Lincoln, aazizinamini1@unl.edu

NDOR Research Project Number SPR-PL-1 (038) P530

Long Term Monitoring of a Steel Bridge Constructed Using Phase Construction

Aaron J. Yakel
Paulo Marchon
Atorod Azizinamini

National Bridge Research Organization (NaBRO)
(http://www.NaBRO.unl.edu)
Department of Civil Engineering
College of Engineering and Technology

W150 Nebraska Hall
Lincoln, Nebraska 68588-0531
Telephone (402) 472-5106
FAX (402) 472-6658

Sponsored By

Nebraska Department of Roads

July, 2005

Table of Contents

List of Figures

List of Tables

Acknowledgement

Funding for this investigation was provided by the Nebraska Department of Roads. The authors would like to express their appreciation for this support. The authors would also like to express their thanks to Mr. Lyman Freemon, Gale Barnhill, and Sam Fallaha of the Bridge Division at the Nebraska Department of Roads (NDOR). The work being reported on has been carried out by various individuals, including: John Swendroski, Mark Otte, Reza Farimani, Dr. Kazem Moslem, Jeff Boettcher, Kazanori Minotani, Brian Hash, Nick Lampe, Patrick Mans, and Robb Pearce.

The opinions expressed in this report are those of the authors and do not necessarily represent the opinions of the sponsors.

Abstract

Phased construction allows for the replacement of a bridge while maintaining traffic flow during the construction. However, problems such as differential elevation of the phases and premature deterioration of the closure region joining the phases have been observed. Replacement of the Dodge Street Bridge over I-480 in Omaha, Nebraska, provided the opportunity to observe and closely monitor a phased constructed system.

The bridge was instrumented and then monitored during construction and for an additional 5 years of in-service use. Additionally, live load testing was performed on each of the phases. Selected data and results obtained from this extensive monitoring are presented in this paper. Deformations due to temperature changes along these years were thoroughly measured and a detailed analysis of deflections was made.

Executive Summary

Phased construction allows for the replacement of a bridge while maintaining traffic flow during the construction. The main objective of this project was to observe the behavior of a bridge using phased construction for a long period of time, when the short term deformations have already taken place and the main factors affecting the bridge are traffic, time, and environment.

Chapter

1 Introduction

Project Objective and Contents

This report is the second concerned with the replacement of the Dodge Street Bridge over I-480 in Omaha, Nebraska. The completed structure is shown in Figure 1-1. The replacement of this bridge provided an opportunity to monitor a project built utilizing phased construction. Phased construction, also known as staged construction, allows the replacement of a bridge while maintaining traffic flow. Dodge Street (US Highway 6) is a major arterial and complete closure to traffic during construction was to be avoided. Construction of the bridge occurred in two sequential phases with each phase roughly corresponding to half of the bridge. While one of the halves is being replaced, traffic is permitted to flow in the other one. Later, the two separate phases are joined together by means of a closure pour in order to make the deck of the new bridge transversely continuous. At first, these phases act independently and deflect differently, due to time dependent effects. Instrumentation was installed on the structure prior to

construction that allowed for monitoring the behavior both during construction and under regular in-service live loads.

Figure 1-1: Completed structure

1.1 OBJECTIVE

The main objective of this report is to investigate the strains, deflections, and expansion and contraction of the bridge under changes in temperature, both daily and seasonally. Currently, very conservative methods are used to address these movements. This can result in oversized, expensive bearing pads along with excessively wide expansion joints.

To allow measurement of the deflections and strains, the project continued with a monitoring system already installed on Dodge Street Bridge, for previous research.

1.2 Content of Report

The previously published report, *Development of a Design Guideline for Phase Construction of Steel Girder Bridges*, details the observations and monitoring results obtained during construction and for a period of time after completion of the structure. At the end of this period of time the monitoring equipment was still functional. It was therefore decided to continue the monitoring effort. This report presents the results obtained from that continued monitoring in addition to the previously reported data. The focus on the long term performance of the structure after construction was completed and the full bridge was opened to traffic.

A detailed description of the bridge and monitoring program can be found in Chapter 2. The theory and the data processing of temperature effects are presented in Chapter 4.

This report focuses on the strucure's responses occuring after the completion of the bridge. The longitudinal and vertical deformations are addressed separately, in chapters 5 and 6, respectively.

Contained in the Appendices is the complete data obtained from the monitoring of the Dodge Street Bridge over I-480.

Chapter

2 Monitoring Program Overview

Instrumentation of the Dodge Street Bridge Over I-480

This chapter has been taken directly from the previous report, *Development of a Design Guideline for Phase Construction of Steel Girder Bridges*. This provides the structural details and construction sequence of the bridge which serves as background for the data and discussions contained in the report. This section also provides an overview of the monitoring system that was used to collect the data. Additional details of the monitoring is provided in Appendix B. The previous report and the thesis by John Swendorski, *Field Monitoring of a Staged Construction Project*, contains extensive information as well.

2.1 Experimental Program Overview

Replacement of Dodge Street over I-480 in Omaha, Nebraska provided an opportunity to monitor a phase construction project. Each construction phase was monitored to gain behavioral insights. Gages were used to monitor steel strains, concrete strains, and deflections. Both short-term data, during construction events, and long term-data were investigated.

This report concerns the construction, gaging, and analysis of data collected from October 20, 1999 through May 23, 2005. Data has been analyzed to investigate long-term data trends concerning mainly temperature effects.

2.1.1 Challenges Faced in Field Monitoring

Several challenges were encountered in field monitoring. Gages were either placed in the field or at Lincoln Steel, where the girders were fabricated. Although proper procedures were followed to ensure gages were applied properly this makes the task cumbersome. Once gages are placed, wires from the gage to the data acquisition unit must be placed in the field. After installation on the bridge, girders are over 20 feet off the ground which made this process difficult and dangerous. Instrumentation locations are somewhat limited as frames to monitor deflection had to be placed so they would not interfere with construction equipment or I-480 traffic that runs under the bridge. Several large television transmission towers are also present near the bridge. Radio waves can interfere with the transmission of electrical signals through gage wires. Shielded wires were used to eliminate the problem.

Many construction events affect the loading on bridge girders, such as placement of heavy temporary barriers and removal of formwork. In order to understand the strain data collected from each girder, it is desirable to know exactly when these events occur. Unfortunately there is significant uncertainty regarding construction timing. As the bridge is 60 miles away

it is not possible to be there continuously observing construction. Furthermore, construction occurs at a rapid pace and not even the contractor knows in advance when certain events will occur so the drive to be there could be made. Communication with the construction manager enables dates of events to be obtained, however beginning and end times are not recorded. For instance, barriers may have been placed on June 4, 2001 but the start and ending times must be determined from analyzing data. As formwork removal takes a very long time, up to two months, it is impossible to determine the efffect that removing this load has.

The fact that monitoring occurs in an uncontrollable environment, versus a laboratory for example, also adds challenges. A laboratory environment stays relatively stable allowing the direct observation of long-term concrete effects. In the field, temperature and weather change. Not only does temperature increase or decrease seasonally but the temperature profile across the girder also changes daily as the sun warms the deck faster than the steel. These temperature changes affect bridge behavior. Environmental effects must be removed to directly observe how various construction events and long-term concrete behavior influence strains and deflections. These environmental effects have been studied and presented. Attempts have been made to remove these effects to more directly observe time dependent concrete effects but more work should be done to better understand this behavior. Finally, live load is present during monitoring as the phases carry traffic. This will cause some variation in readings and make it more difficult to directly observe long-term concrete behavior. Ideally this would not be present but there is no way to uncouple the live load effects.

2.2 Bridge Description

Replacement of Dodge Street Bridge over I-480 in Omaha, Nebraska provided an opportunity to monitor a project built utilizing staged construction. Dodge Street (US Highway 6) is a major arterial and complete closure

to traffic during construction was not feasible. The new bridge, which is a two span continuous steel plate girder bridge, replaces a 1963 eight span cast-in-place reinforced concrete box girder bridge. The new bridge will carry the same four traffic lanes and two pedestrian sidewalks as the old bridge. The completed new bridge consists of eight continuous steel plate girders spaced 9 ft., 5 in. apart spanning two equal 236.5 ft. spans. Each construction phase consisted of four girders topped by a 7.0 in. deep by 34ft. 10in. wide deck built compositely with the girders. The width of the closure pour joining the two phases is 40 in. After the closure pour, an overlay brought the final deck thickness to 8.5 in. and permanent railings were slip-formed. All plate girders were hybrid. Over the pier, girders utilize HPS-70W steel (High Performance Weathering Steel with 70 ksi yield strength) for both flanges. In the positive moment section, only the tension flanges use HPS-70W steel while the compression flanges use A709-50W steel. A709-50W steel was selected for web materials.

2.2.1 GIRDERS

The eight girders for the completed bridge are identical. Each girder changes section properties at five locations as shown in Figure 2-1. The girders are longitudinally symmetric about the pier. There are 4 field splices, two on each side of the pier, so each girder was manufactured in five sections. Girder spacing is 9 ft. 5 in. on center. Girders are named according to letter designation. Girders E, G, H and J are contained in Phase

I while A, B, C, and D are in Phase II. The five field sections are designated by girder letter and section number, such as A3.

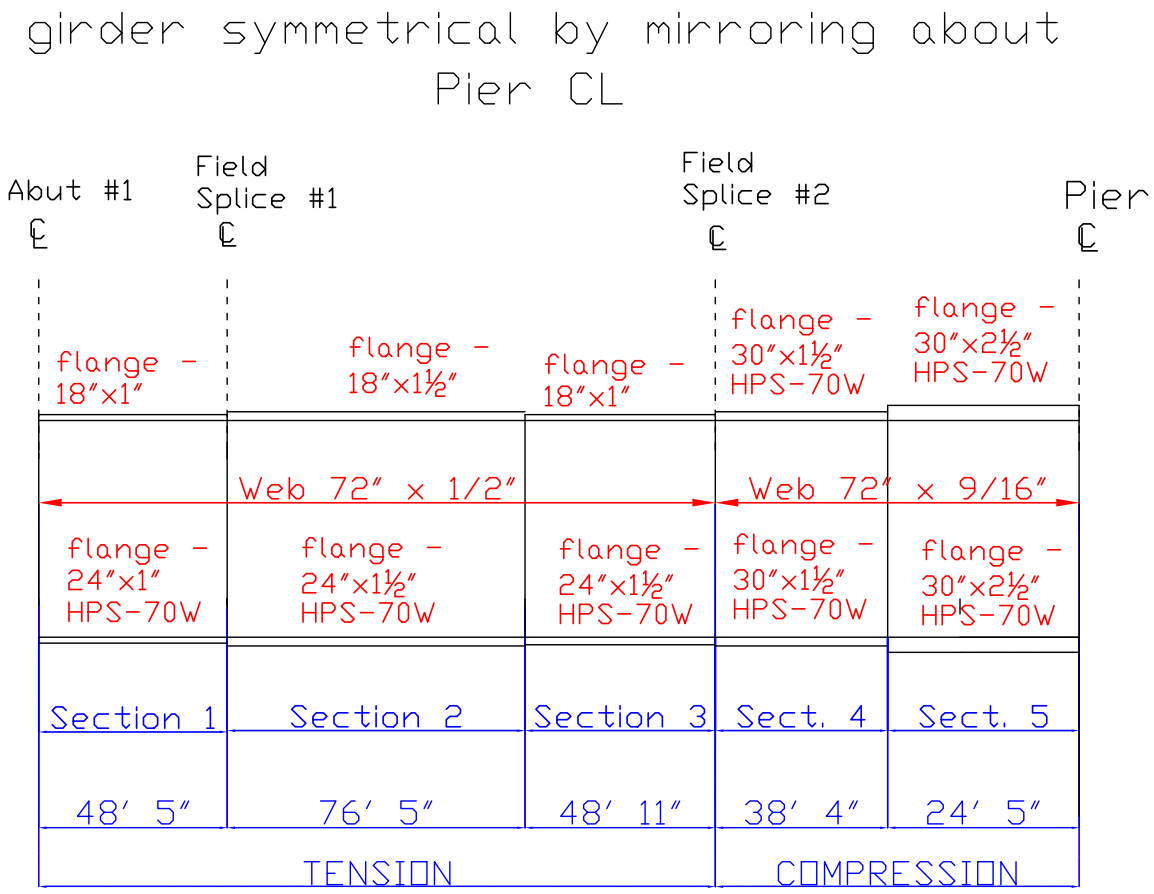

Figure 2-1: Girder plate dimensions. Note symmetry about the Pier CL. All steel is A709-50W unless noted otherwise.

Girder camber accounts for dead load deflections and the substantial vertical roadway curvature, accommodating nearly 7 ft of elevation difference between east and west abutments. The west abutment is higher than the

east. Figure 2-2 contains the blocking diagram from the bridge design and Figure 2-3 contains the blocking ordinates.

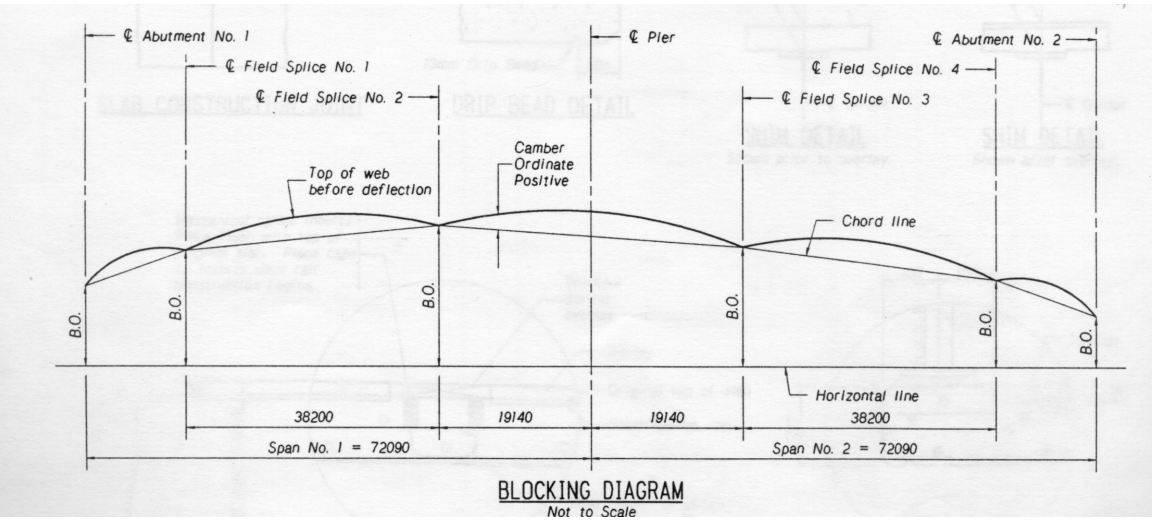

Figure 2-2: Blocking diagram for girders. Units are in mm.

DEFLECTION, CAMBER, AND BLOCKING ORDINATES FOR GIRDERS

Tenth Point	Deflection Ordinate (mm)	Camber Ordinate (mm)	Blocking Ordinate (mm)
1.0	0	0	2117
1.1	121	15	
1.2	217	2	
FS 1	220	0	2762
1.3	274	150	
1.4	293	234	
1.5	273	240	
1.6	221	176	
1.7	147	53	
FS 2	120	0	3165
1.8	73	11	
1.9	20	14	
2.0	0	13	2897
2.1	20	14	
2.2	73	11	
FS 3	120	0	2603
2.3	147	53	
2.4	221	176	
2.5	273	240	
2.6	293	234	
2.7	274	150	
FS 4	220	0	1078
2.8	217	2	
2.9	121	15	
3.0	0	0	0

Figure 2-3: Blocking ordinates for girders. Units are in mm.

Figure 2-4: Shear Studs on the top flange. Picture is taken looking West. From right to left are Girders E, G, H, and J during erection for Phase I.

Shear studs welded to the top flange will provide composite action with the deck. The shear studs are M7/8 x 5" with three per row spaced 24" between rows. An example of the shear stud placement can be seen in Figure 2-4.

2.2.2 Cross Frames

Figures 2-5 and 2-6 show cross frame locations and orientations. Cross frames were placed to provide compression flange bracing during con-

struction and transverse continuity. Cross frame locations are symmetric about the pier.

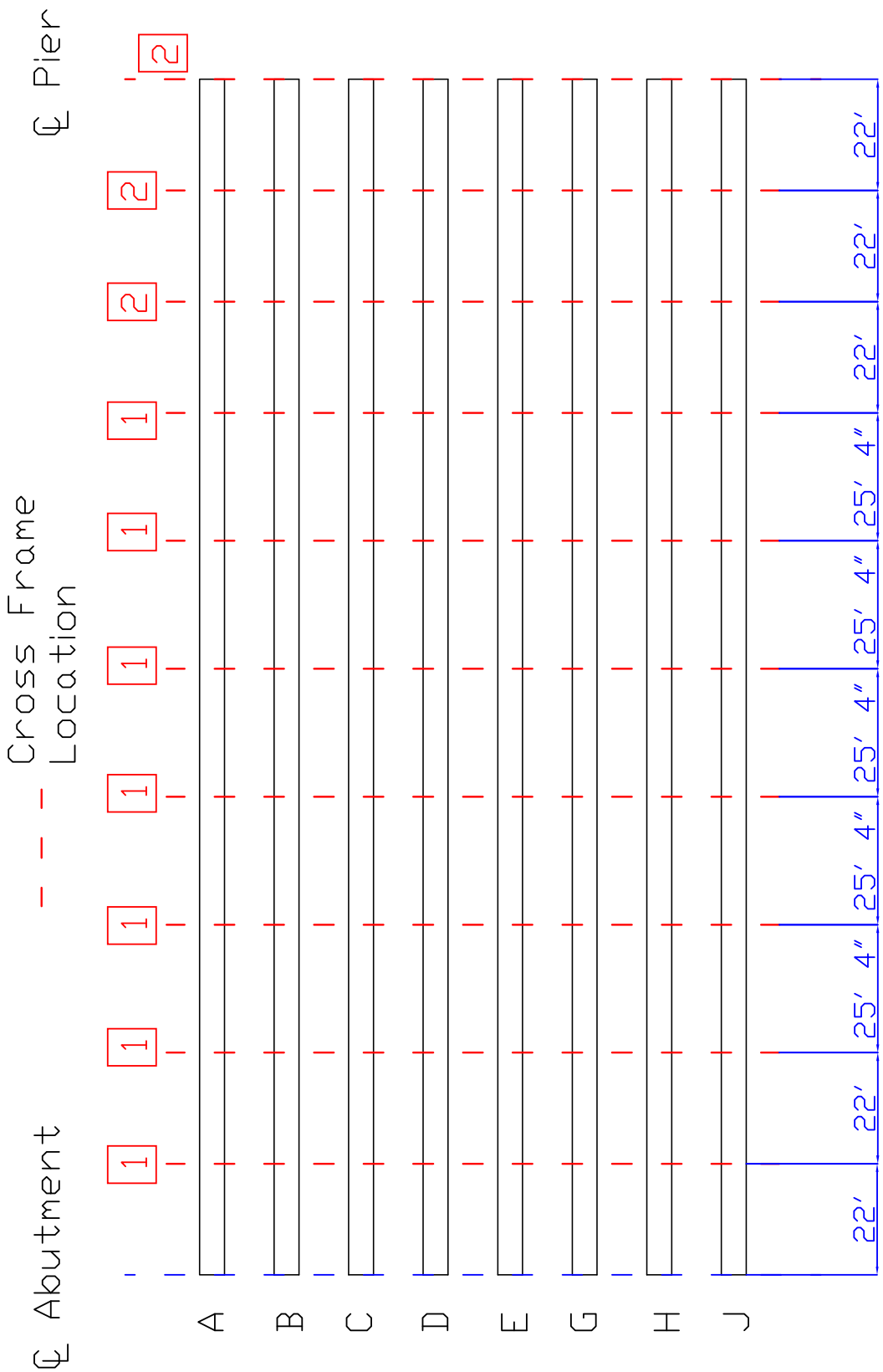

Figure 2-5: Location of Cross Frames. Refer to Figure 2.6 for orientation.

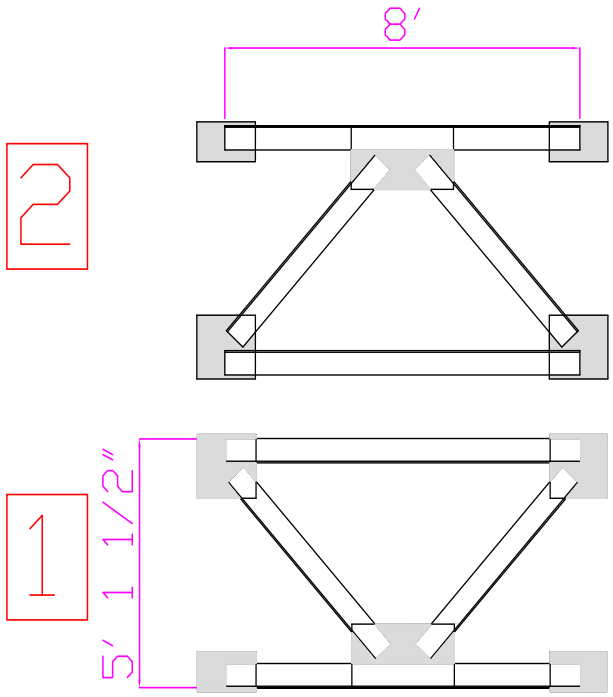

Figure 2-6: Orientation of Cross Frames. All members are L6x6x3/8

2.2.3 DECK

The slab for the completed bridge consists of three parts. The first two parts are the slabs cast in Phases I and II. These slabs are 7.0 in. thick by 34ft. 10in. wide built compositely with the girders. The third completed

deck section is the closure region which is 7 in. thick by 40 in. wide and connects the two phases as shown in Figure 2-7.

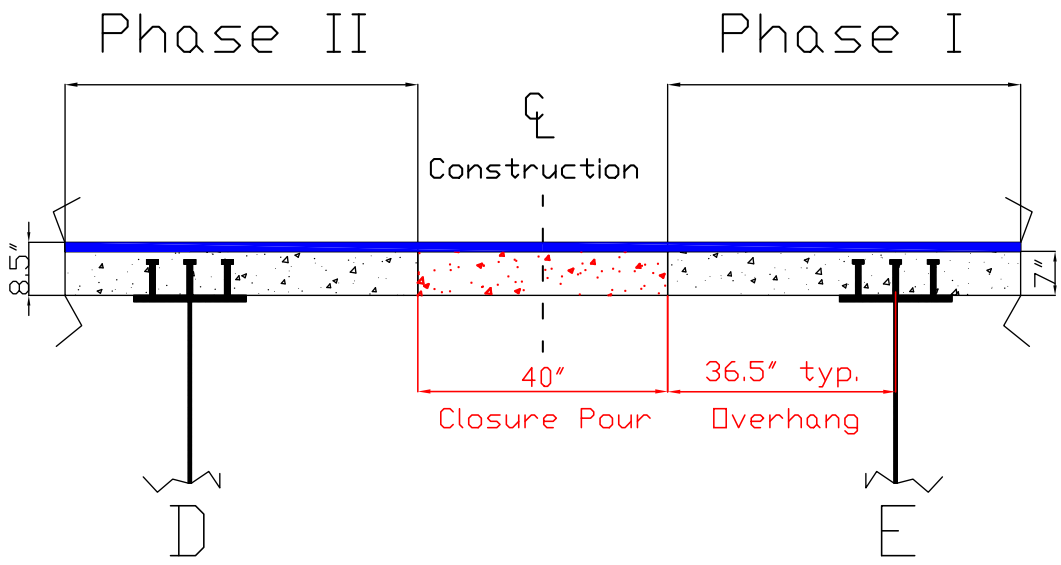

Figure 2-7: Deck thickness

Once the three sections of the deck are completed an overlay seals the joints and brings the total deck thickness to 8.5 in. as shown in Figure 2-7.

2.2.4 Permanent Railings

Once the overlay is complete, NDOR standard closed concrete rails are slip-formed on each side separating two 9 ft. sidewalks from 54 ft. of clear roadway. Figure 2-8 is a cross section of the completed bridge.

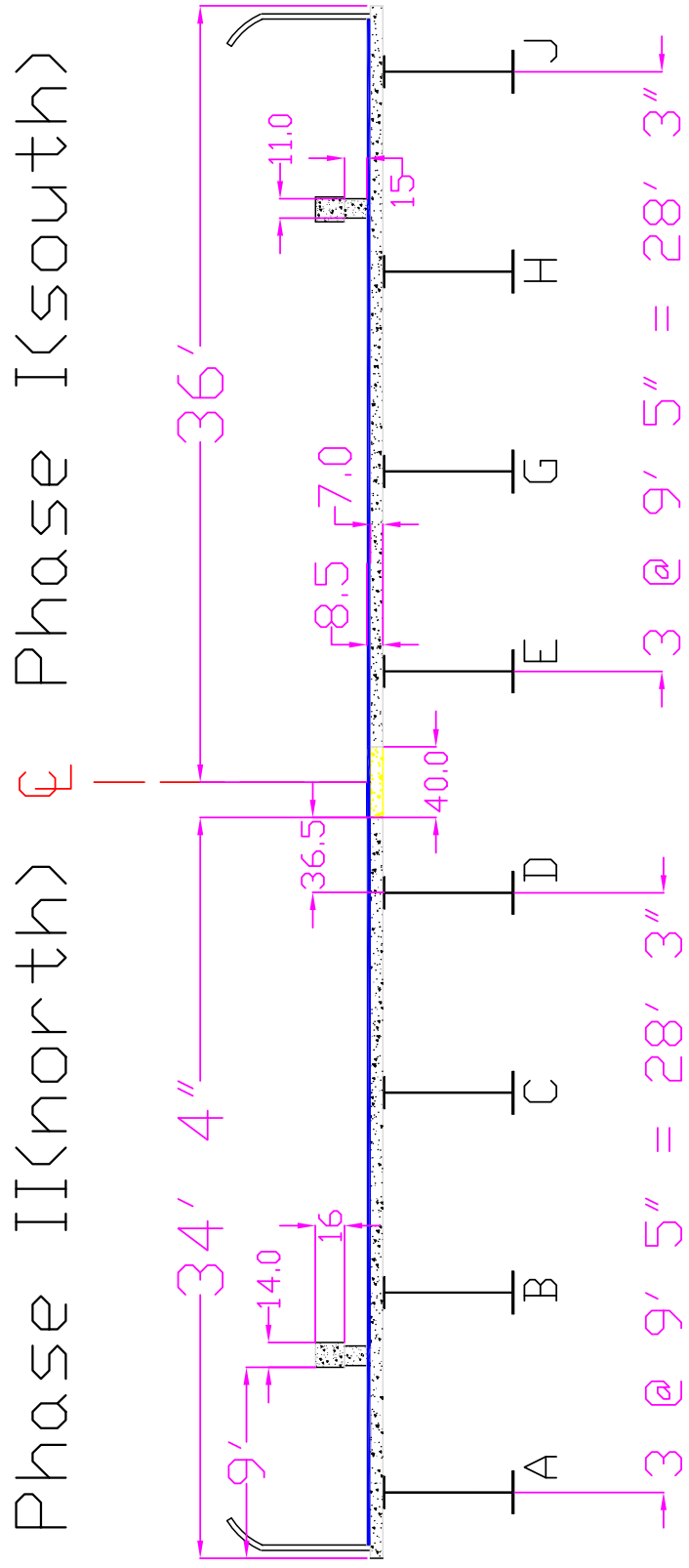

Figure 2-8: Completed bridge cross section. Note the phases are symmetric about the centerline. All dimensions are inches unless noted otherwise.

2.3 CONSTRUCTION SEQUENCE

The purpose of Staged Construction is to maintain traffic flow while an existing bridge is being replaced. To perform this task on Dodge Street over I-480, several steps were taken. First, the southern half of the existing bridge was removed allowing the construction of Phase I. During this time, temporary barriers were placed on the remaining half of the existing bridge allowing for two lanes of traffic and a pedestrian sidewalk.

Once Phase I was completed, temporary barriers were placed and traffic was switched onto the completed phase. The remaining half of the old bridge was then demolished. Phase II was constructed while Phase I carried traffic.

Once Phase II's deck was complete, the entire bridge was closed for 2 days while the closure pour operation joined the phases. Temporary barriers were used to maintain traffic flow while the overlay was placed first on the North side then on the South side. Next, permanent barriers were slip-formed utilizing temporary barriers to maintain traffic flow. Finally, all four traffic lanes and both pedestrian sidewalks were opened.

2.3.1 CONSTRUCTION OF PHASE I

After the southern half of the existing bridge had been removed and traffic was being carried on the existing bridge's remaining half, Phase I construction started. The first operations were those concerning the substructure: pile driving, constructing the concrete pier, and pile cap pouring. Once these operations were complete superstructure work could begin.

GIRDER ERECTION

Figure 2-9 is a graphical representation of the erection sequence. The like shaded girder sections were erected simultaneously and in the order indi-

cated below the figure. Table 2-1 includes the dates girder sections were erected.

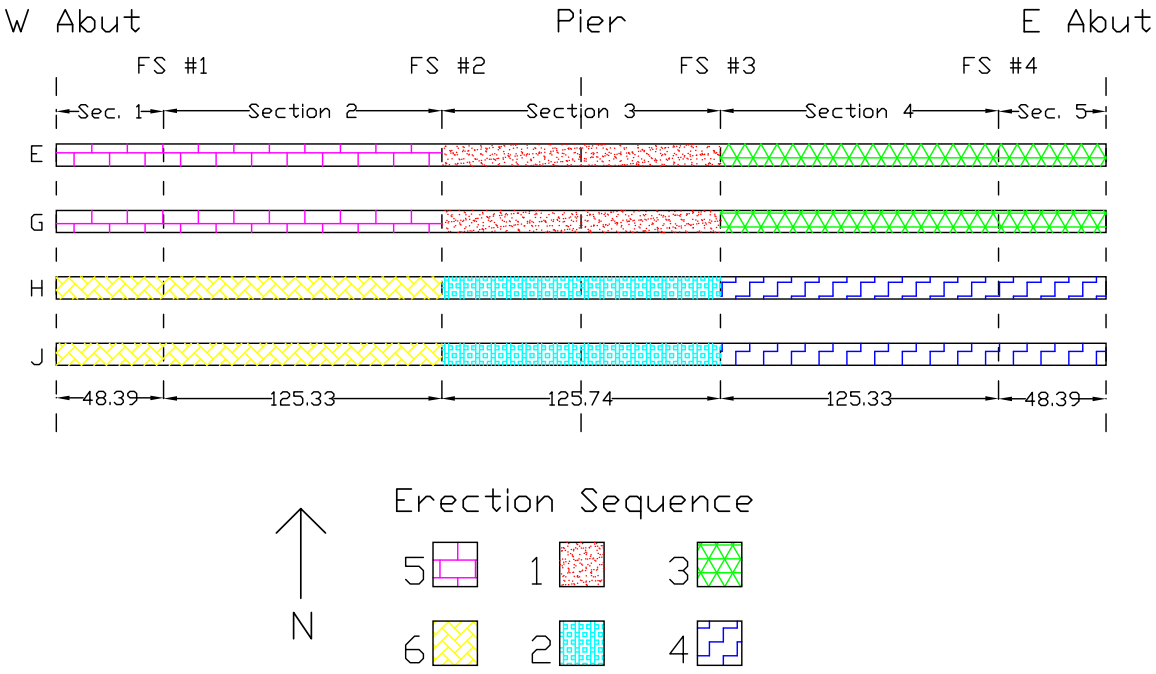

Figure 2-9: Girder erection sequence for Phase I

Event	Date Started	Date Completed
Pour of Pier		6/21/99
East Abutment Poured		7/15/99
West Abutment Poured		7/28/99
Girder Placement	8/31/99	9/14/99
Girders E3 and G3		8/31/99
Girders H3 and J3		9/1/99
Girders E4-E5 and G4-G5		9/3/99
Girders H4-H5 and J4-J5		9/8/99
Girders E1-E2 and G1-G2		9/10/99
Girders H1-H2 and J1-J2		9/14/99
Deck Formwork Placed	9/18/99	10/7/99
Rebar Placed for deck	10/4/99	10/13/99
Positive Region Pour		10/20/99
Negative Region Pour		10/28/99
Pedestrian Fencing Installed	11/5/99	11/9/99
Placement of Traffic Barriers on Ph. I	11/5/99	11/12/99
South Side Temporary		11/5/99
North Side Temporary		11/12/99
Phase I Opened to Traffic		11/15/99

Table 2-1: Construction Time Table for Phase I

Phase I girders were erected as follows. Sections E3 and G3 were connected by their cross frames while on the ground and placed on the pier. Temporary shoring supported the girders so wind would not blow them off. Next, Sections H3 and J3 were connected on the ground and placed on the pier. While in the air, cross frames between Girders G and H were placed. Now all girder sections over the pier were in place as seen in Figure 2-10. In the

figure Girder J is in forefront. Note the temporary shoring that is supporting the West (left) side.

Figure 2-10: Girder sections E3, G3, H3, and J3 placed over the pier

East span girder sections were erected after the pier sections were in place. While on the ground, sections 4 and 5 were spliced together for Girders E and G. The cross frames connecting Girder E to G and the cross frames that connect Girder G to H were placed before lifting. This unit was then spliced with girder section 3 while in the air and placed on the East abutment girder seats. Sections 4 and 5 of Girders H and J were placed in the same way. Figures 2-11 and 2-12 show these sections in place. Note in Figure 2-11 that Girder E is on the left and girder G is to the right. Also note the gird-

ers supported by the East abutment and cross frames ready to accept Girder H. Splice to section 3 is not visible.

Figure 2-11: Girder sections 4 and 5 of the East span

Figure 2-12: All four girders for East span in place.

The final girder sections erected for Phase I were those for the West Span. Sections 1 and 2 of Girders E and G were spliced together. The cross frames connecting them were placed along with the cross frames to accept Girder H. This unit was then spliced with girder section 3 in the air and placed on the west abutment girder seats. Girder sections 1 and 2 of Girders H and J were placed in the same way. Figure 2-13 shows the west span girders in place. Note in the figure that the west abutment and the temporary shoring to support section 3 has been removed as it is no longer needed. Girder J

is in forefront. Posts on top of the girders are for the safety of construction workers.

Figure 2-13: West span girders in place

Girder sections were spliced in the field using 22.2mm ASTM A325M bolts. Each side of the splice contained 2 lines of 5 bolts in top flange splices, 2 lines of 23 bolts in web splices, and 2 lines of 10 bolts in bottom flange splices. Splice plates utilized A709-50W steel. Top flange splice plates were 0.625" thick, web splice plates were 0.5" thick, and bottom flange splice

plates were 1.0" thick. Filler plates were of appropriate size. A typical splice is shown in Figure 2-14.

Figure 2-14: Girder splice

DECK POURING SEQUENCE

Once girder erection is complete the deck formwork and rebar can be placed. Forming the deck with plywood and metal hangers was carried out between 9/18/1999 to 10/7/1999. Placement of rebar took place between 10/4/1999 and 10/13/1999.

The concrete deck for Phases I and II was cast in the following sequence. Starting at a distance of 167' 4" from each abutment, concrete was poured simultaneously using two crews working towards each abutment as seen in Figure 2-15. The pour was 7" thick and 34' 4" wide. This pour is referred to as the positive region pour. The pour was performed 10/20/99 for Phase I.

The remaining portion of the deck was cast after the positive region concrete reached its 28 day design strength. This pour had a 138' 4" length. The pour started on the East span and ended on the West span. This “negative region pour” can be seen in Figure 2-16. This portion of the deck was poured 10/28/99 for Phase I.

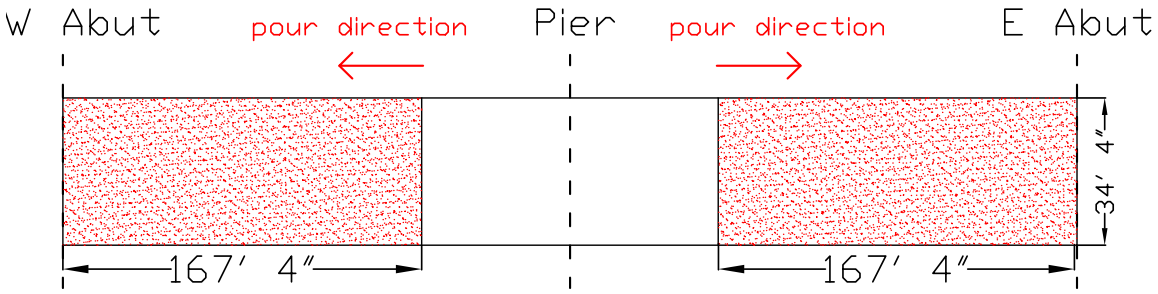

Figure 2-15: Positive region pour.

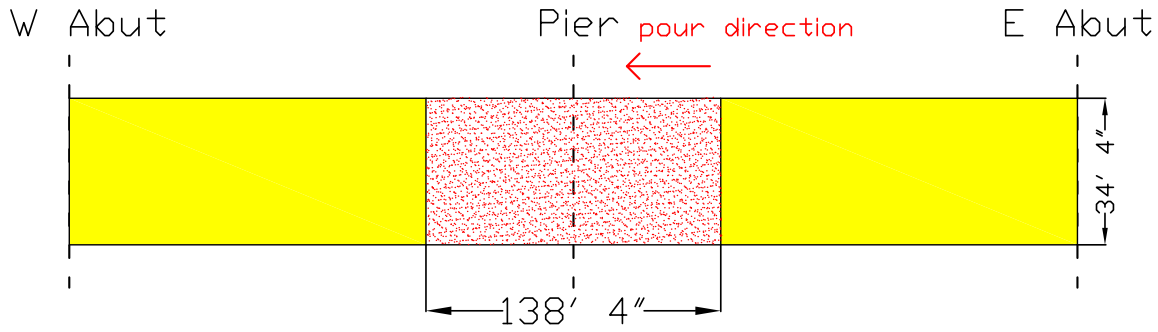

Figure 2-16: Negative region pour

Temporary Guardrail and Fencing

With the deck of Phase I complete it is nearly ready to carry traffic. Before that is possible pedestrian fencing must be placed and temporary barriers located to separate traffic lanes from the sidewalk. The fencing was placed on the south side of Phase I from 11/5/99 to 11/9/99. Temporary barriers were placed on the southern side of Phase I on 11/5/99. On 11/12/99 temporary barriers were placed on the North side, near the closure pour location. Barrier locations are shown in Figure 2-17. In the figure Girder E is on the North side and is closest to the closure region. The remaining half of the existing bridge would be North (right) of Girder E.

Phase I opens to Traffic

On 11/15/99 traffic was switched from the Northern half of the existing bridge to Phase I. Once Phase I was opened to traffic the formwork was removed from all regions except the closure region. After Phase I was carrying the traffic, the remaining half of the existing bridge was demolished as seen in Figure 2-18.

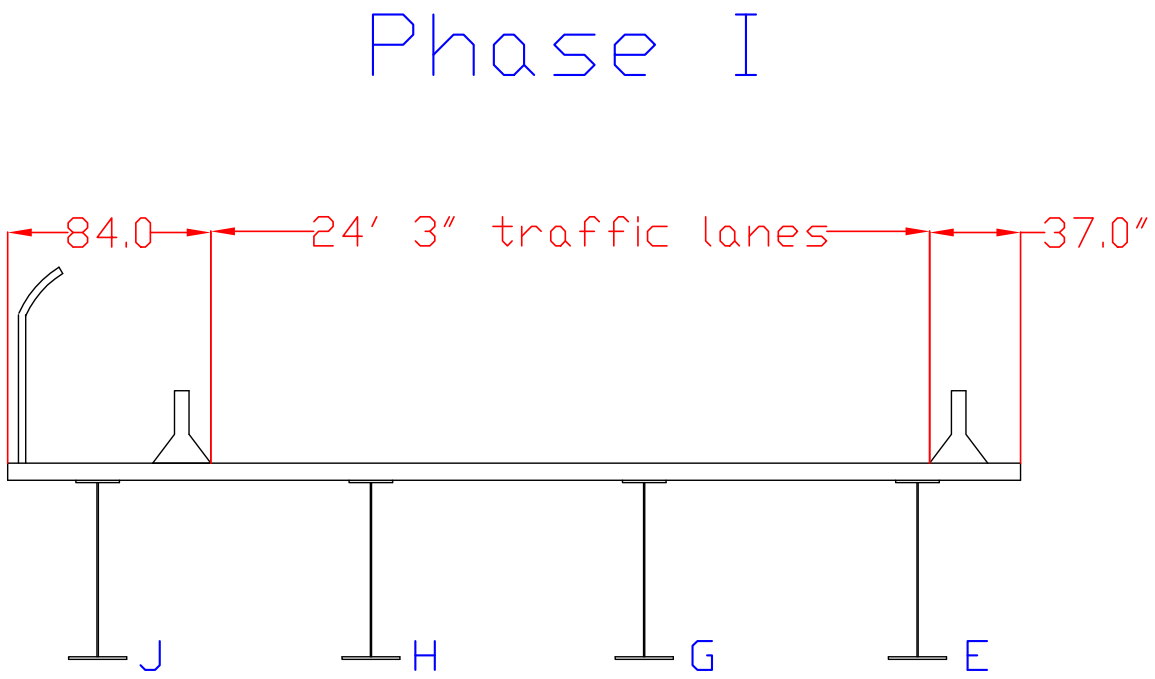

Figure 2-17: Location of Temporary barriers.

Figure 2-18: Demolition of the Northern half of the existing bridge

2.3.2 PHASE II CONSTRUCTION

After demolition of the existing bridge's northern half was completed, Phase II construction commenced. Again, the first operations were those concerning the substructure: pile driving, constructing the concrete pier, and pile cap pouring. Once these operations were complete superstructure work could begin. As the two phases are mirror images about the project centerline, construction steps were very similar. Therefore, an in-depth summary of Phase II's construction up to closure is unwarranted.

GIRDER ERECTION

Girders for Phase II were placed in a similar manner to those of Phase I with two joined by cross frames were set at once. The only difference was that the West span girders were placed before the East span girders. The order

of placement can be seen in Figure 2-19 and Table 2-2 shows the dates of erection.

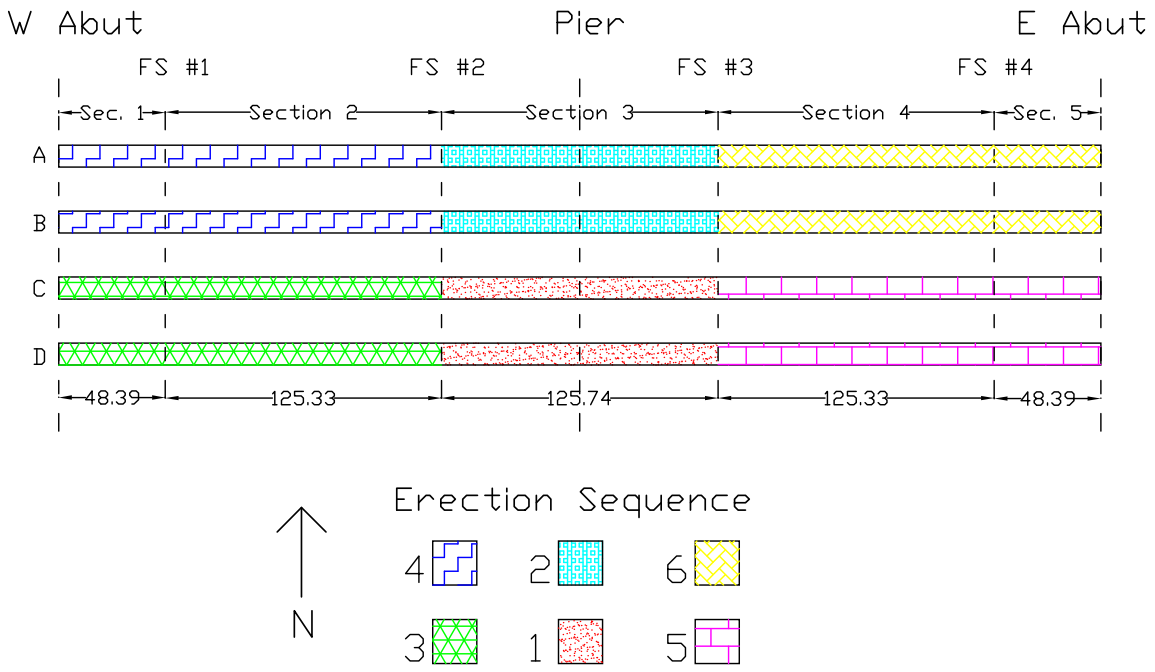

Figure 2-19: Girder erection sequence for Phase II.

Event	Started	Completed
Pour of Pier		12/28/1999
East Abutment Poured	1/19/00	1/21/00
West Abutment Poured	1/27/00	1/28/00
Girder Placement	2/1/00	2/21/00
Girders C3, D3, A3, and B3	2/1/00	2/5/00
Girders C1-C2 and D1-D2		2/8/00
Girders A1-A2 and B1-B2		2/13/00
Girders C4-C5 and D4-D5		2/20/00
Girders A4-A5 and B4-B5		2/21/00
Deck Formwork Placed	3/1/00	3/14/00
Positive Region Pour	4/18/00 8am	4/18/00 11am
Negative Region Pour	4/26/00 7am	4/26/00 9am
Live Load Tests	5/3/00	5/4/00
Bridge Closed to all Traffic		5/5/00 at 11pm
Closure Pour	5/6/00 5:15am	5/6/00 7:05am
Phase I Re-opened to Traffic		5/7/00 at 3pm
Overlay on Phase 2	5/22/00 2:25am	5/22/00 8:15am
Placement of Permanent N Side Barrier	6-2-00 2pm	6-2-00 4:30pm
Placement of Fence and Handrail on Phase II	6-5-00	6-8-00
Handrail Attached on Phase 2 Permanent Rail	6-12-00 6:30am	6-12-00 3pm
N Side Overhang Slab Formwork Removed	6-8-00 7pm	6-9-00 2am
Temporary Barriers Placed on S Side Phase 2	6-13-00 6am	6-13-00 9:30am
Phase 2 Opened to Traffic	6-13-00 10:30am	
Temporary Barriers Removed from Phase 1	6-13-00 10:30am	6-13-00 4pm
Formwork Removal from Phase II	6-18-00 11pm	6-19-00 3:30am
Final Cross Frames Placed between Phases	6-19-00 3:30am	6-19-00 5am
Formwork Removal from Phase 2 completed	6-19-00 11pm	6-20-00 6am
South Bridge Overlay	6-30-00 5am	6-30-00 10:30
South Bridge Sidewalk Overlay	7-8-00 7am	7-8-00 10am
Prep of Phase I bridge for concrete railing	7-10-00	7-13-00
Placement of Phase I permanent Barrier	7-14-00 8am	7-14-00 10 am
Bridge Completely opened to Traffic		8-10-00 3:30pm

Table 2-2: Construction Time Table for Phase II

DECK POURING SEQUENCE

Once girder erection was complete, the deck formwork and rebar was placed. Deck forming was carried out between 3/1/2000 to 3/14/2000. Placement of rebar took place between 4/2/2000 and 4/9/2000.

The concrete deck for Phase II was cast in the same sequence as Phase I. The positive region pour was performed 4/18/2000 and is shown in

Figure 2-20. The negative region pour was performed on 4/26/2000 and can be seen in Figure 2-21.

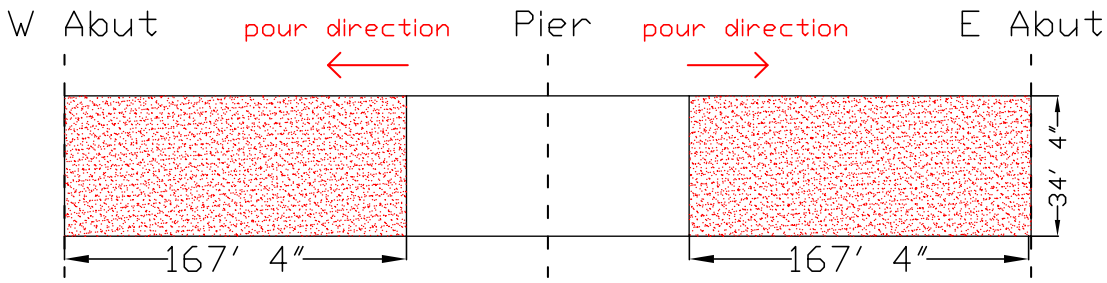

Figure 2-20: Positive region pour.

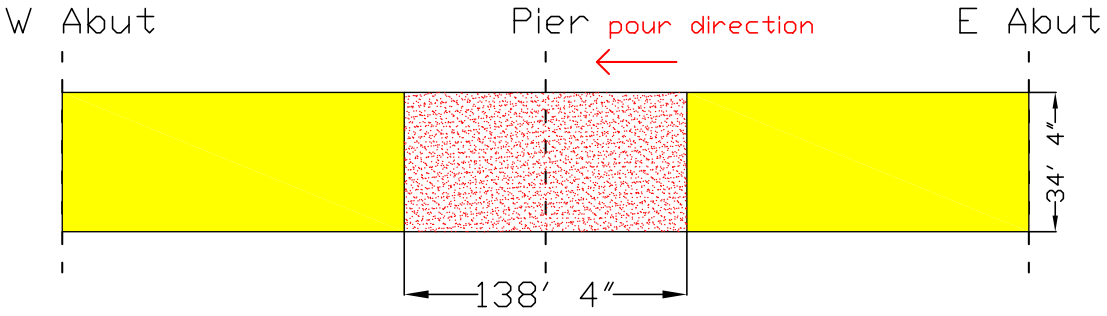

Figure 2-21: Negative region pour

2.3.3 Closure Pour

Before connecting the two phases with the closure pour, several things were done. First the construction crew removed some of the formwork from Phase II but left the overhangs needed for the closure concrete. Then some of the cross frames between Girders D and E were placed. All of the cross frames between these girders could not be placed because a differential elevation existed and cross frame bolt holes did not line up with those on the girders. The cross frames that were installed prior to the closure pour are shown in Figure 2-22. The other cross frames were placed after the closure operation. Longitudinal rebar was also placed in the closure region to provide strength. Transverse rebar consisted of extensions from the Phase I and II slabs. No additional rebar was placed in the transverse

direction, rather, the bars extending from the Phase I and II slabs were lapped and tied together.

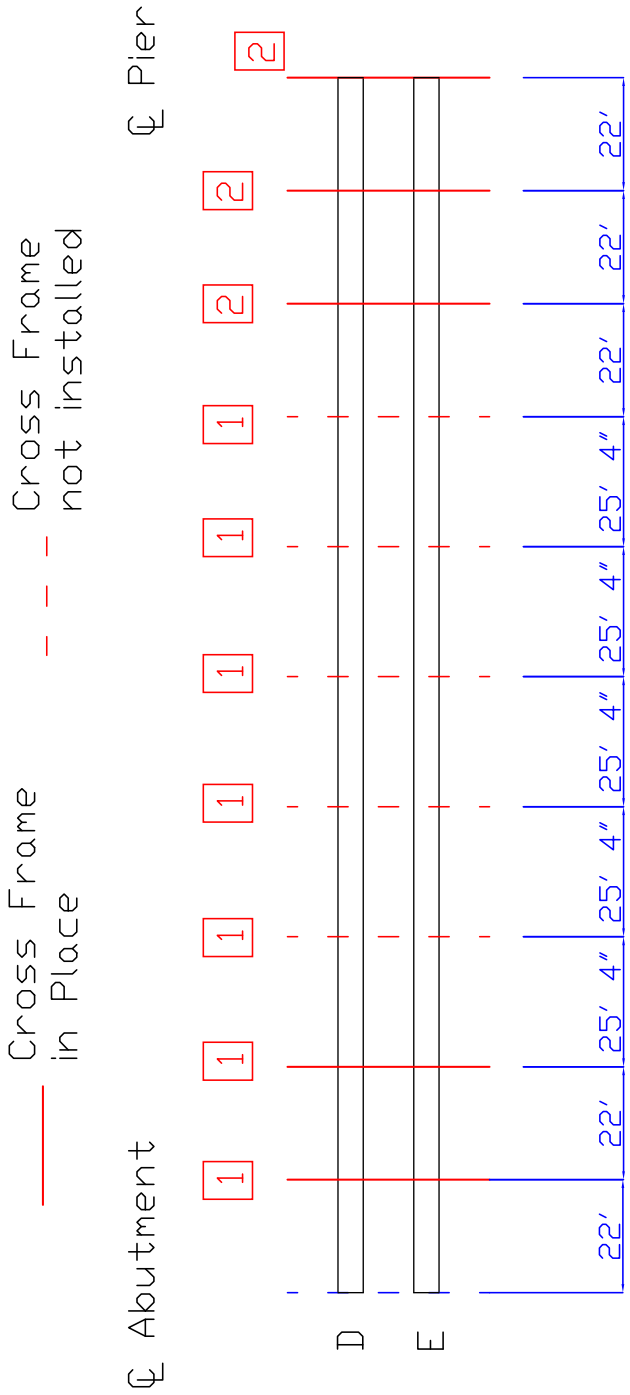

Figure 2-22: Cross frames that were installed at time of closure pour.

To perform the closure pour both phases were closed to traffic from 11pm May 5, 2000 to 3pm May 7, 2000. This was the only time during construction that traffic was entirely closed down. After the bridge was closed, all temporary barriers were removed from Phase I. The elevation of each phase was then obtained to determine the differential between the phases. Because Phase II was significantly higher than Phase I on the East span, barriers were placed on Phase II's East span as shown in Figure 2-23. These barriers reduced the differential elevation to 0.75" on the East Span. Barriers were placed from East abutment to pier. This reduced the differential elevation and was deemed an acceptable solution by Nebraska Department of Roads bridge engineers. The closure region formwork was then adjusted

by turning the leveling screw in the overhang brackets and plywood was screwed together to remove any gap in the forms.

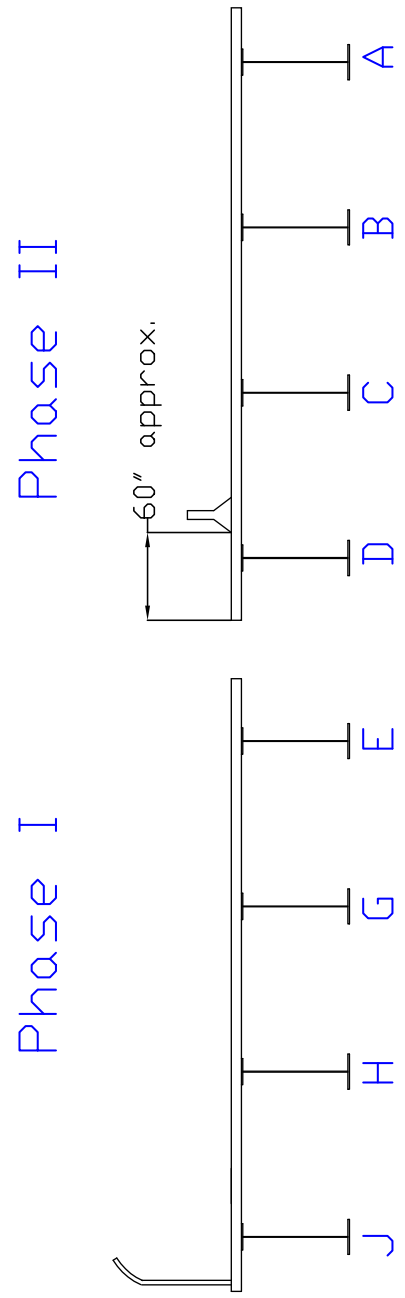

Figure 2-23: Location of barriers on Phase II

Concrete placement began 5:15am on May 6, 2000. Concrete trucks were not allowed on the bridge so concrete was either pumped or carted where it was needed with wheelbarrows. The closure pour was 40" wide and ran the entire bridge length. Pouring started at the East abutment and ended at the West abutment. The depth depended on the amount of differential elevation and was approximately the same as the Phase I and II decks, 7". Figure 2-24 shows the pour as it was being performed. The two decks from Phase I and II are clearly seen in the figure. Note transverse rebar tied together. This rebar consists of extensions of the rebar from the Phase I and II slabs to provide continuity. Longitudinal rebar was placed before the pour commenced. Figure 2-25 indicates the pouring direction.

Figure 2-24: Closure pour

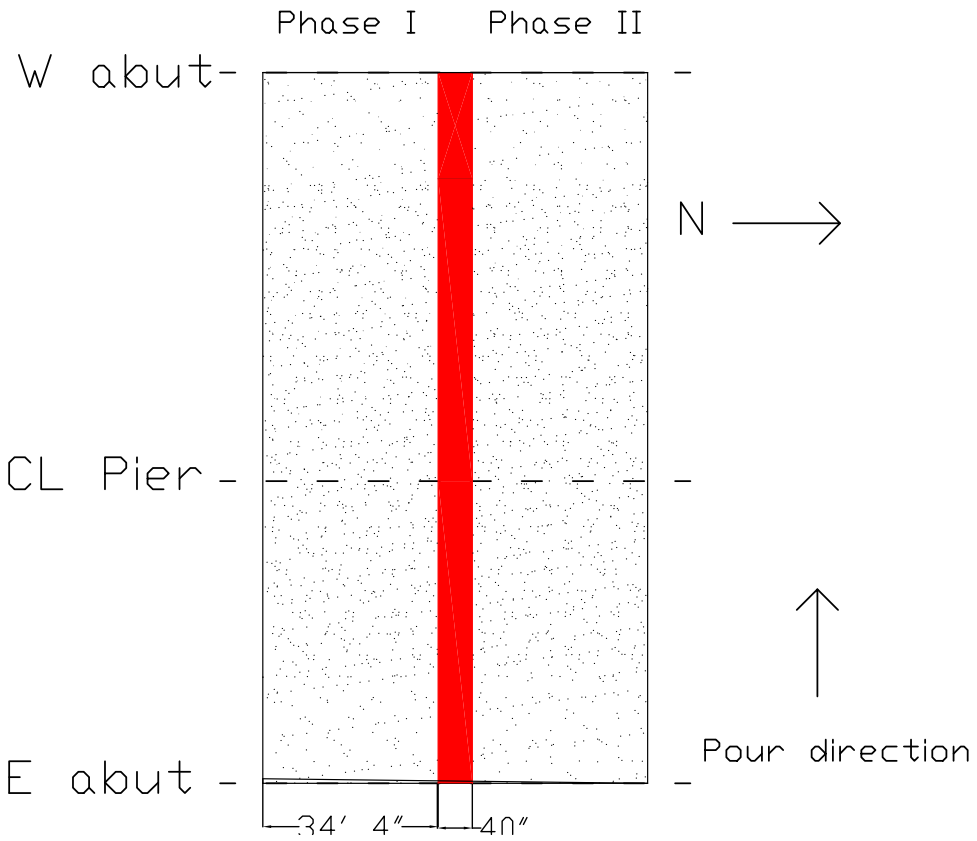

Figure 2-25: Direction of closure pour

After the concrete surface was finished it was covered with a curing agent and covered with wet burlap for 48 hours. The pour ended at 7:05am May 6, 2000.

Phase I was re-opened to traffic on May 7, 2000 at 3pm. Barriers were removed from Phase II and placed on Phase I as shown in Figure 2-26. This allowed only 32 hours for closure concrete to cure before barriers on the

East span of Phase II were removed. Data recorded during the closure operation will be presented later.

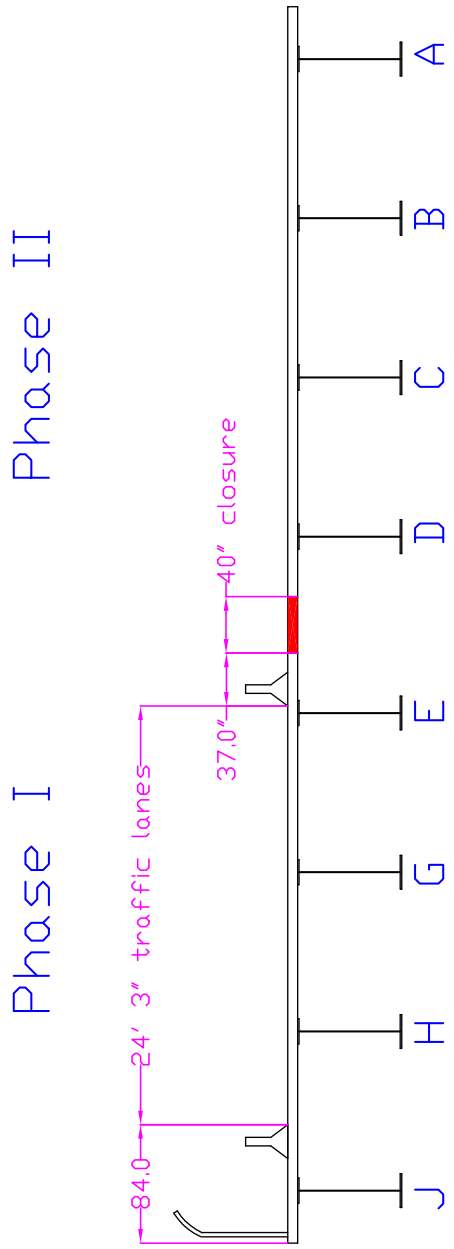

Figure 2-26: Phase I and II after closure pour

2.3.4 Overlay and Barriers

Once the primary structure had been completed, a few tasked remained including overlay of both phases and installation of the permanent barriers.

PHASE II OVERLAY

As traffic was once again on Phase I, the Phase II overlay was placed. Before this could be done, the deck of Phase II was prepared. This consisted of sandblasting 1/8" from the deck, blowing away dust using compressed air, and washing the surface with water. Wet burlap was then carefully placed from the West abutment to the East abutment. This was done in such a way that workers and trucks never stepped on the prepared surface. Instead they walked on wet burlap until the pour began.

Two concrete trucks were always on the bridge during the pour. They both backed down the bridge from the West abutment. One concrete truck contained a grout that was brushed onto the deck to help the overlay adhere to the original surface. The other concrete truck contained the overlay concrete. These trucks unloaded directly onto the bridge. The pour started at the East abutment and ended at the West. Burlap was pulled up as trucks drove forward to expose the prepared surface. A finishing machine and several workers did the finishing work. After work on a region was complete, it was recovered with burlap and sprinklers placed. The overlay was kept moist for 7 days to reduce shrinkage cracks and insure the best possible bond between the original deck and overlay.

The overlay of Phase II started at 2:25am May 22, 2000 and ended at 8:15am the same day. The final deck thickness was 8.5 in. yielding an approximate overlay thickness of 1.75 in. The area overlaid was one half

the deck width, from Phase II's edge to the closure region's center, as seen in Figure 2-27.

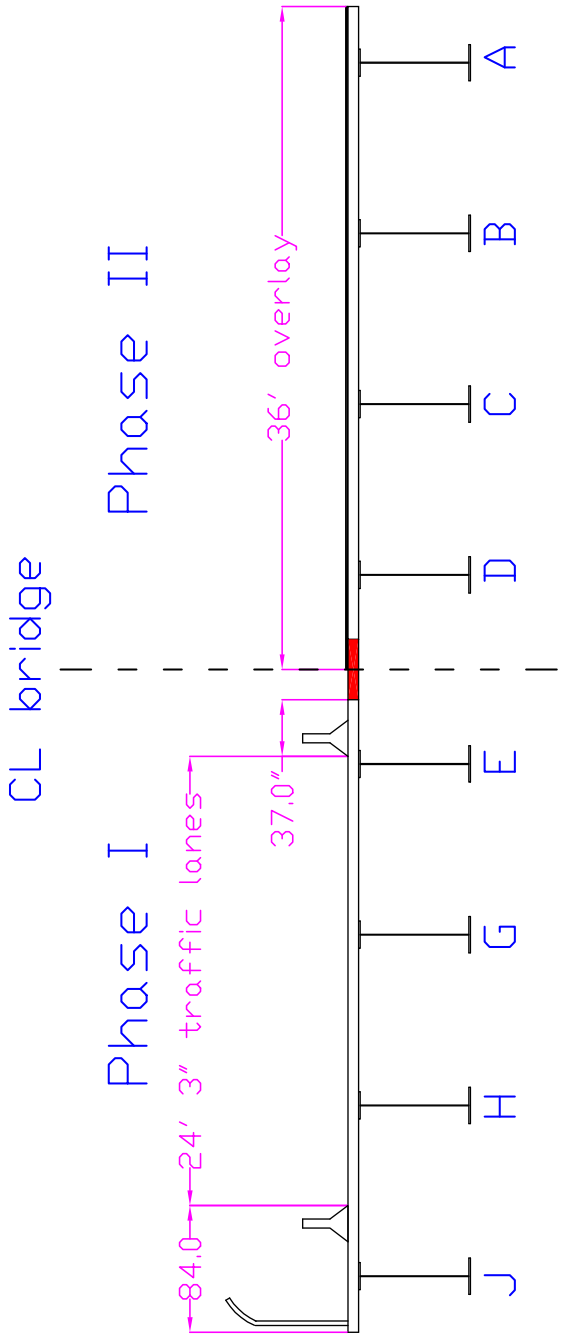

Figure 2-27: Configuration of bridge after Phase II overlay. Note bridges are joined by closure pour which has already occurred.

Phase II Permanent Railing

With the overlay on Phase II completed and traffic still being carried on Phase I, the permanent barrier on Phase II was placed. After the reinforcing steel was in place, the rail was slip-formed from the West to the East abutment from 2:00pm to 4:30pm on June 2, 2000. The rail was coated with a curing agent and left uncovered. Figure 2-28 shows the machine to slip form the rail and the reinforcing steel in place.

Figure 2-28: Phase II permanent barrier before casting. Note dowels epoxied into deck

After the railing cured pedestrian fencing was placed on Phase II and temporary barriers placed so traffic could be switched over and Phase I com-

pleted. A cross section of the bridge before the Phase I overlay is seen in Figure 2-29.

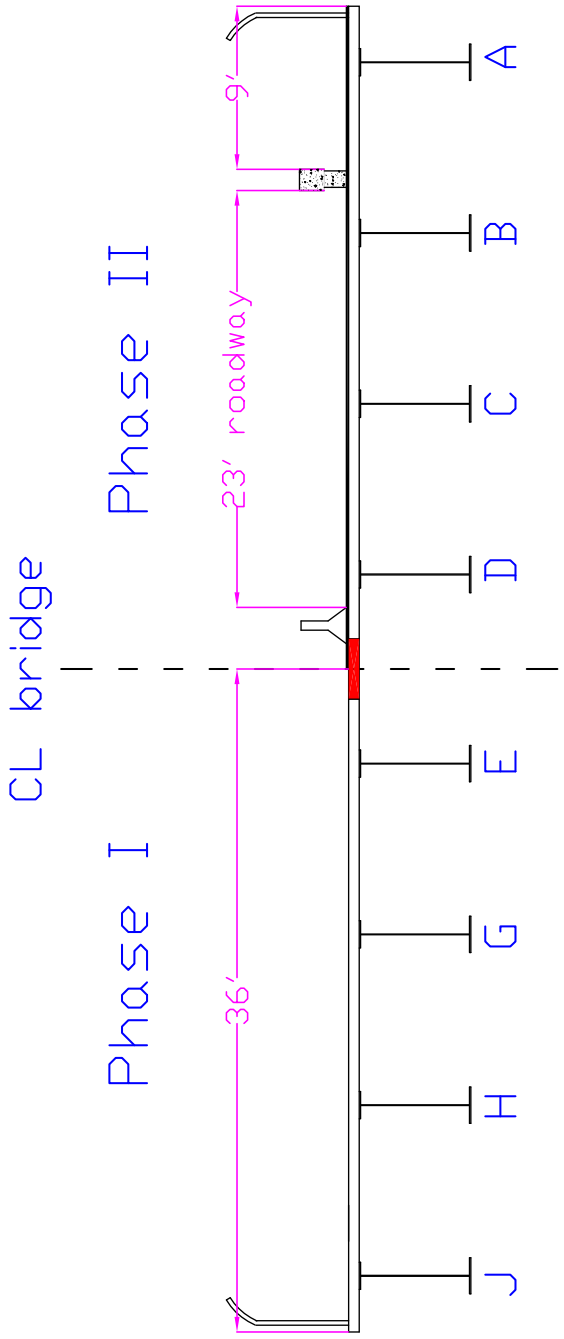

Figure 2-29: Configuration of bridge before Phase I overlay. Note traffic is being carried on Phase II as it is complete.

PHASE I OVERLAY

The Phase I overlay was very similar to that of Phase II. The deck preparations were performed in the same fashion and the concrete was placed the same way from East to West. The only difference is that Phase I had the pedestrian fencing in place at the time of the pour. Therefore the finishing machine rail had to be placed on the deck and the whole width could not be overlain at once. The majority of the overlay was placed from 5:00am to 10:30am on June 30, 2000. The remaining sidewalk overlay portion was completed on July 8, 2000 from 7:00am to 10:00am. As the sidewalk overlay was a small region all finishing work was done by hand. Both the main deck and sidewalk overlays were kept moist for one week to ensure a good

bond with the original deck and to reduce shrinkage cracking. Figure 2-30 shows the bridge cross section after the Phase I overlay was complete.

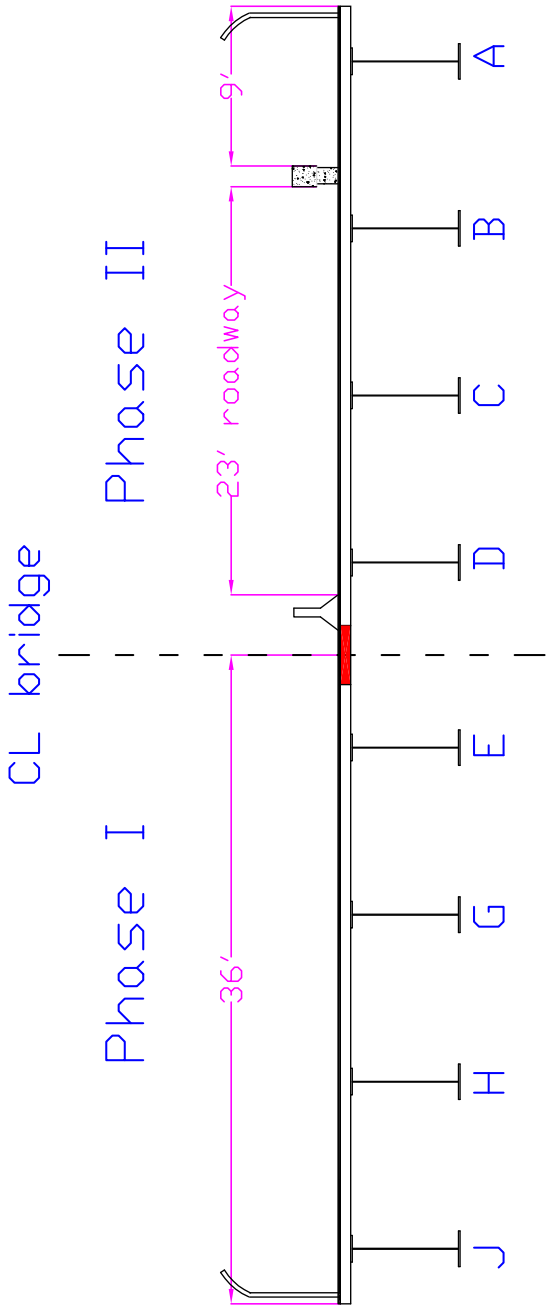

Figure 2-30: Configuration of Bridge after Phase I overlay.

PHASE I PERMANENT RAILING

Permanent rail for Phase I was cast on July 14, 2000 from 8:00am to 10:00am. This railing was also slip-formed from the West Abutment to the

East abutment as was Phase I. A photo of the finished rail is seen in Figure 2-31.

Figure 2-31: Finished permanent barrier. Note truck on bridge is grinding surface.

COMPLETION OF PROJECT

Before the bridge could be opened to traffic some of the deck had to be ground to bring the surface profile to the design 2% cross slope. During this operation the temporary barriers were removed from the bridge and traffic was limited to one phase or the other by barrels as seen on the left side of Figure 2-31.

Both phases of the bridge were officially opened to traffic on August 10, 2000 at 3:30pm. Construction lasted 14 months from the time the Phase I

pier was poured. A completed cross section of the bridge is shown in Figure 2-32.

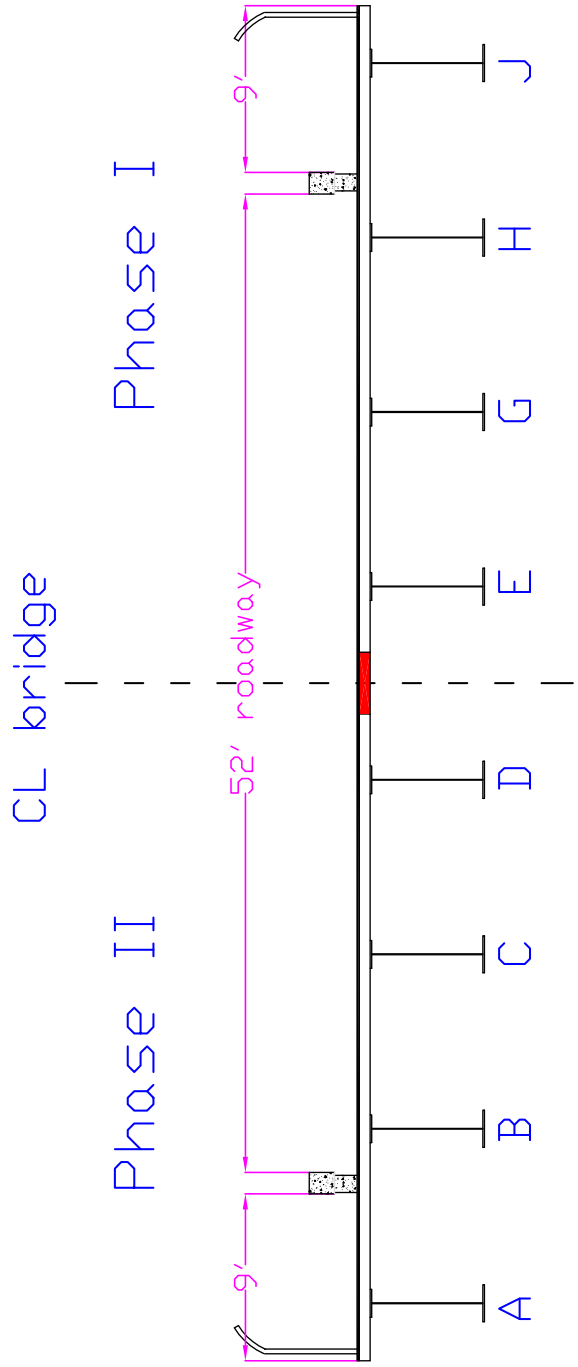

Figure 2-32: Completed bridge. Four traffic lanes and two sidewalks are clearly seen. Overall width of construction is 72'.

2.4 INSTRUMENTATION

The necessary data to obtain an understanding of the bridge behavior can be divided into two categories: strain and deflection. This data will provide information necessary to understand system behavior during short-term construction events such as deck casting, concrete barrier placement, closure pour, and live load tests. The data will also provide information necessary to understand long term bridge behavior such as creep, shrinkage, weather, and thermal effects.

2.4.1 DEVICES AND SENSORS USED IN MONITORING

Proper choice of instruments is essential for obtaining the required data. The strain data can be sub-divided into two categories: steel strain and concrete strain. The desired deflection data can also be divided into two categories: vertical girder deflection and longitudinal girder movement. A description of each instrument chosen to obtain the desired data follows.

Redundant instrumentation to obtain the desired data adds to the project cost and produces massive data files. Therefore, a cost effective instrumentation strategy was devised by judiciously selecting the location of gages.

Using the 1997 AASHTO LRFD Bridge Design Manual, the bridge as designed by the Nebraska Department of Roads (NDoR) was analyzed. From the dead and live load analyses the positioning of the gages was determined as described below. It was desirable to place gages on the East span because the distance to the ground is only 20' versus nearly 50' on the West span.

STEEL STRAIN SENSORS

Spot-Weldable Vibrating Wire(VW) sensors produced by Slope Indicator CO. of Bothell, WA were used to obtain data involving steel girder strain. The gauge consists of a steel wire held in tension inside a tube. The tube is mounted on a stainless steel flange, which is welded to a structural mem-

ber's surface using specialized equipment. Sensors placed over each gauge read the frequency at which the wire vibrates after the sensor plucks the wire. This frequency varies with the tension in the wire and can therefore be converted to a strain measurement. The reader also contains a thermistor that measures local temperature. An example of this gage can be seen in Figure 2-33. Vibrating wire gages were chosen for this project instead of typical electrical strain gages because of the monitoring duration. An electrical gage could not withstand constant excitation for over two years and reliable readings would be lost. Vibrating wire gages on the other hand have excellent long-term performance and can be expected to perform for many years.

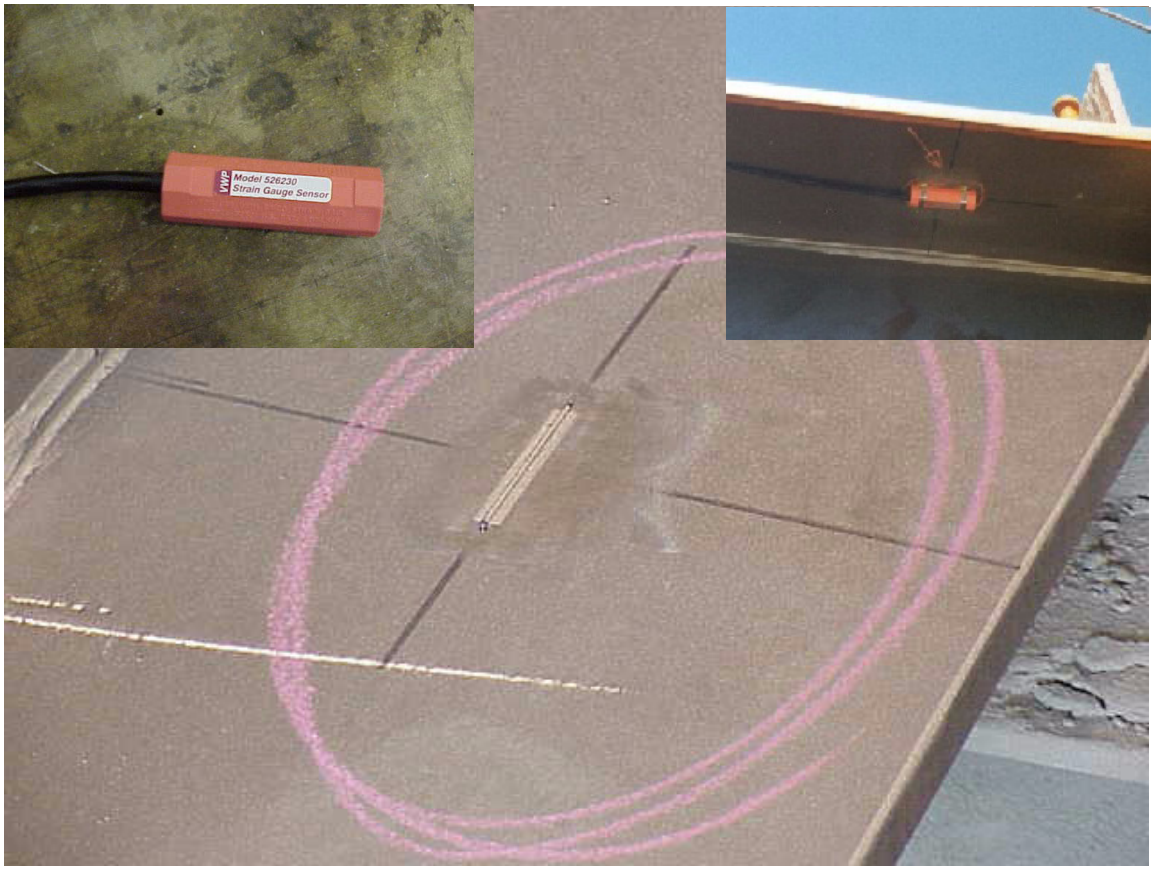

Figure 2-33: Steel strain gage and reader. Clockwise from upper left: reader, gage and reader in place, gage after being placed on reader.

The location of maximum positive bending moment from the Strength I combination was chosen as a gaging location. These strain readings will relate to the bending moment experienced by the girders. To obtain the amount of negative moment carried by girders, strain gages were also placed 2' East of the pier centerline. The gages could not be placed directly at the pier because of the bearing stiffeners there. Finally, spot-weldable gages were placed near the abutments so the amount of end restraint could later be determined and compared to the simple support assumed for design. Strain gages attached to the flanges were centered on the flange at their respective position.

Two cross frames for Phase II were also gaged. These strain readings will indicate how effective cross frames are in transmitting load in the transverse direction as the phases deflect relative to each other. The cross frames chosen to be gaged were the ones closest to the maximum positive moment section (Section 2).

CONCRETE STRAIN SENSORS

Embedment Strain Gauges, model 52630126, produced by Slope Indicator CO. of Bothell, WA were used to obtain the strain in the concrete. The VS Embedment strain gauge is a steel tube with flanges at either end. Inside the body is a steel strap and a magnetic coil. The strap is held in tension between the two flanges, and the coil magnetically “plucks” the steel strap, which then vibrates at a frequency that can then be converted to a strain reading. The gages also contain a thermistor to record local temperature.

The gages are tied to rebar before concrete placement. Figure 2-34 shows two of these gages tied to rebar in the closure region.

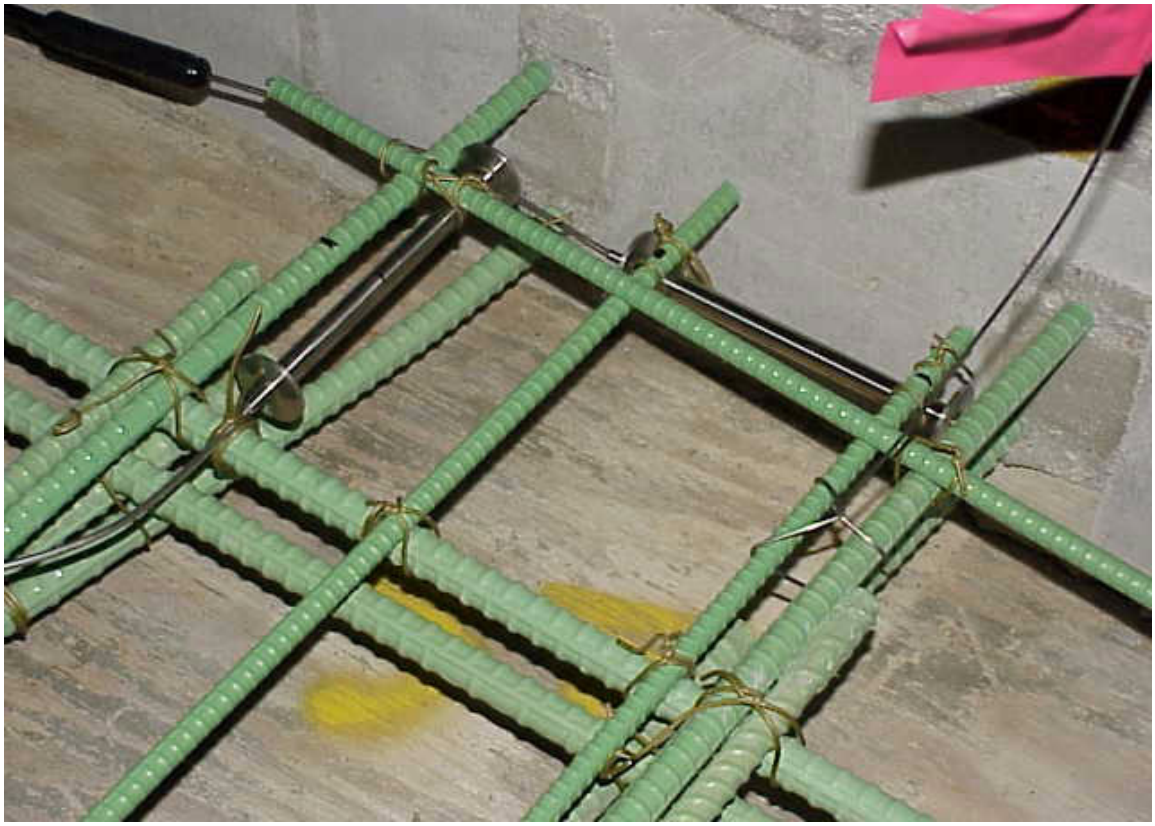

Figure 2-34: Concrete Embedment gage in place. These gages record concrete strain.

To obtain concrete strain data, gages were placed at several locations and orientations in the deck. Additionally, one gage was placed in a control

specimen 7" deep x 6" wide x 18" long, as seen in Figure 2-35, that was placed near the DAS to obtain the concrete's free shrinkage behavior.

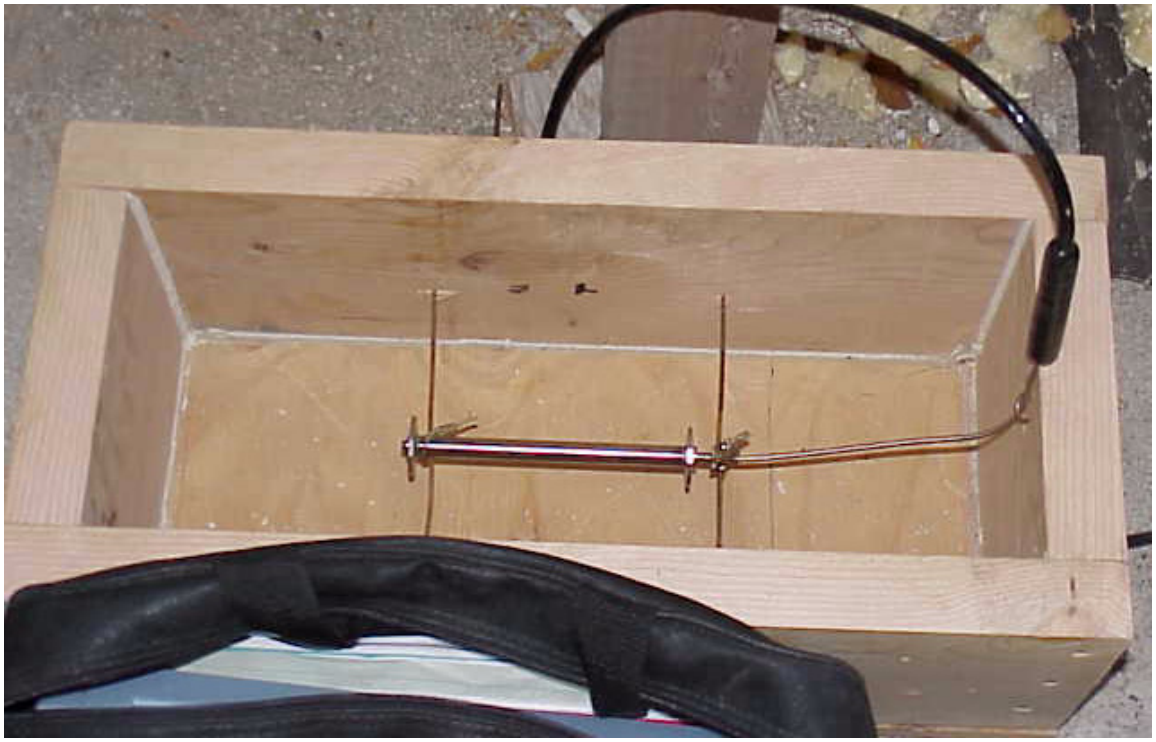

Figure 2-35: Embedment Gage in Free Shrinkage Control Specimen

Gages were placed in the closure pour because it joins the two phases and can carry high strains and crack if differential settlement between the phases occurs. The gages will also provide long-term data on the closure region concrete behavior as it creeps and shrinks.

VERTICAL GIRDER DEFLECTION

The vertical girder deflections were measured using RAYELCO Linear Motion Transducers manufactured by MagneTek of Simi Valley, CA. These gages contain a potentiometer that is connected to a wire spool. A known voltage is sent to the potentiometer and by reading the return voltage the length of stretched wire is computed. The free end of the spooled wire is connected to a fixed point and the potentiometer is fixed to the deflecting structure, or vice-versa. By choosing a datum at an appropriate time the change in deflection can be interpreted from subsequent readings. The

devices were mounted to a piece of steel and then protected from the environment by constructing a covering over them. Care was taken so the covering would not disturb their normal function. The unit in its protective covering clamped to the bridge girder can be seen in Figure 2-36.

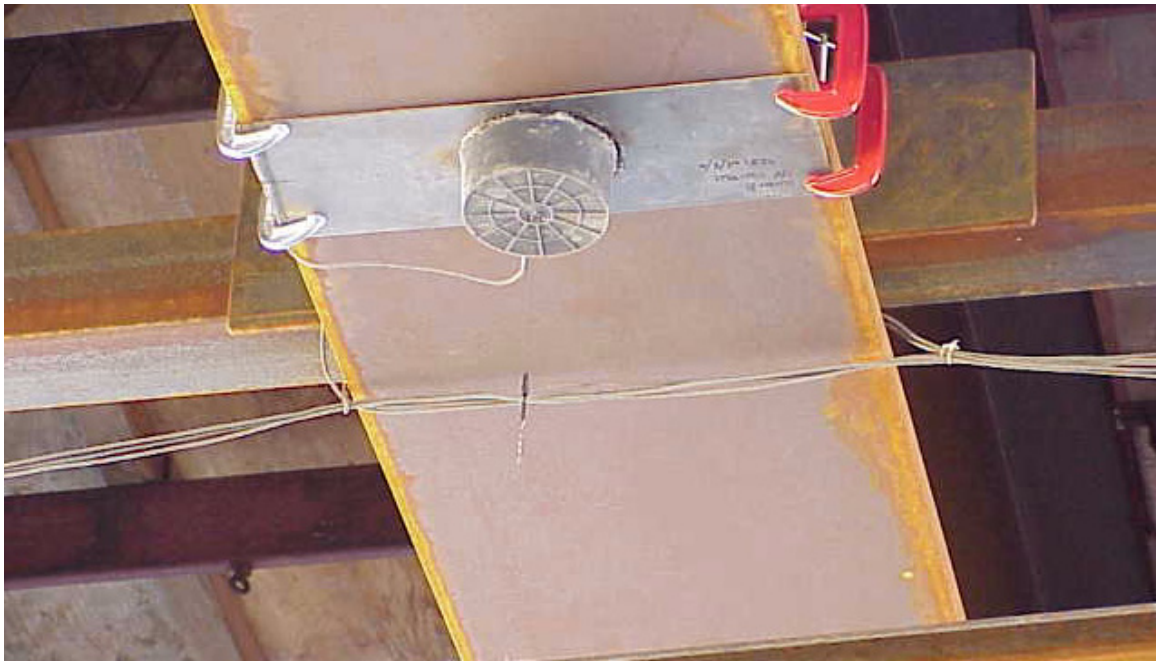

Figure 2-36: Potentiometer connected to the girder and fixed frame.

To obtain meaningful vertical displacement data it is desirable to measure deflection at the predicted location of maximum deflection, 0.4L. Potentiometers (pots) could not be placed exactly at this location because there is a roadway underneath the bridge. Therefore they were placed as close to the roadway as possible while still in a location that would not interfere with construction. The pots are tightly clamped to the underside of the girders while the other end is connected to a rigid test frame, which has its base embedded in concrete at a depth below the frost line. The pots monitor deflection during significant construction events and also long-term behavior. This data will indicate the amount of differential deflection occurring between the phases.

LONGITUDINAL DISPLACEMENTS

Girders D and E were instrumented at each abutment to measure the longitudinal displacement of each phase. These girders were chosen because they are adjacent to the closure pour and should have the most effect on the closure region behavior. This data allows comparisons between the behaviors of the two phases.

Longitudinal girder movements were measured at the abutments using VWP Displacement Transducers (crackmeters) produced by Slope Indicator CO. of Bothell, WA. The device is mounted with one end on the girder's bottom flange and the other on a surface that is assumed not to move, the pile cap in this case. The device operates on the same frequency principle as previously mentioned gages but these instruments relate frequency to displacement. As with the other Slope indicator products, local temperature is also recorded. An example of these units during service can be seen in Figure 2-37. In the figure, note the right end connected to the galvanized

angle that has been screwed into pile cap and the left end which is connected to an angle which has been clamped to girder flange.

Figure 2-37: Crackmeter connected to girder flange

2.4.2 DATA ACQUISITION SYSTEM (DAS)

To acquire the necessary data, a DAS that can perform the essential tasks while remaining flexible to changing needs is essential. These tasks include taking readings from sensors at appropriate intervals, recording the readings in non-volatile memory, and the ability to download data files for analysis. Readings in non-volatile memory are stored such that system power can be lost and previously stored readings are preserved.

The DAS for this task was produced by Slope Indicator CO. and consists of many different modules. The CR10X is the primary module that controls the system and stores the system's instructions. It controls the other modules and dictates when readings are taken and how data is recorded into

memory using the other modules. Gages are connected to the AM416 Relay Multiplexers which excite the gages and read the responses. The AVW100 module switches between multiplexers so the channels are excited in correct order. Power is provided through the PS12LA battery/battery charger. Data is recorded in the CR10X's internal 128k of memory. Finally, the SC32A Optically Isolated RS232 Interface allows the user to interface with the DAS using a computer and a 9-pin connector. The individual modules are manufactured by Campbell Scientific, INC. of Logan, Utah and are assembled by Slope Indicator to meet the project's needs.

Two multiplexers provided adequate resources to acquire data from the 24 vibrating wire gages and 5 potentiometers required for Phase I monitoring. Once Phase II began, the system had to be upgraded. Four additional multiplexers were added providing channels for up to 48 more vibrating wire gages and 16 potentiometers. A COM 100 Cellular Phone Package and a COM 200 Telephone Modem were added so data could be retrieved remotely. A solar panel, manufactured by Solarex of Frederick, MD, was connected to the PS12LA battery/battery charger to provide power during the day and to charge the battery for night usage. Finally a SM4M Storage module was added providing an additional 4 Megabytes of non-volatile

memory allowing for longer intervals between downloading data. Figure 2-38 is a schematic of the final DAS.

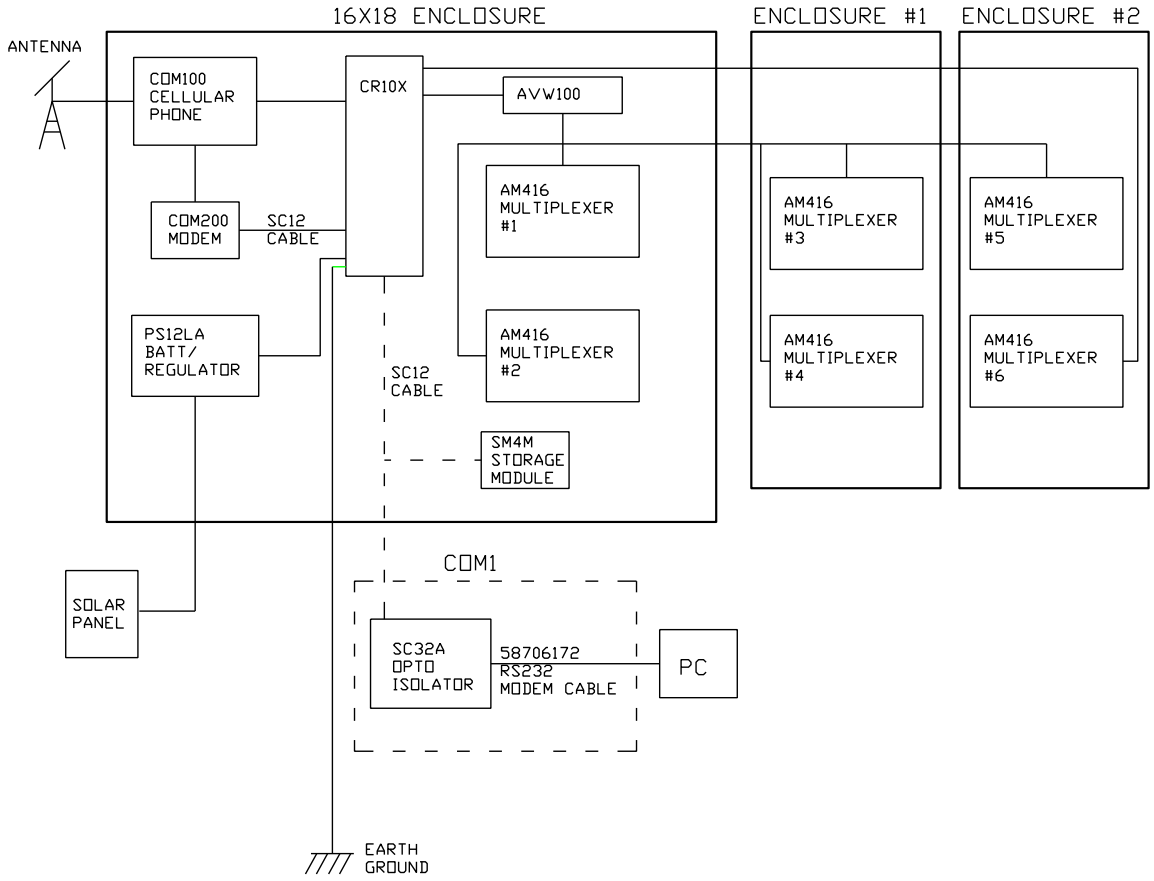

Figure 2-38: Data Acquisition System (DAS) for Dodge Street over I-480

To control, communicate, and access the system's memory, Slope Indicator CO provides a program package, PC208W Datalogger Support Software. The package serves several functions. One is to allow the user to provide the DAS with information concerning gage to channel relationships and at what frequency to excite gages. This information is contained in a program which is uploaded to the CR10X. The program also contains information concerning what data to record into memory so it can be accessed later. Another important function of the package is to download data stored in memory. The user can also set the DAS's clock and instruct it to take readings at set intervals or upon command.

Chapter

3 Long Term Data Reduction

Responses which vary over time due to Seasonal and Daily Temperature Changes

The deflections observed when using phased construction methods can be separated into two main categories. The first category deals with the short term deflection concerns, which are present shortly after the bridge is built and completely opened to traffic. The other is concerned with the long term performance of the structure, which happens during its life time, when the two phases have already suffered initial deflections due to creep and shrinkage and have "settled in" being one monolithic system.

Short term deflection prediction, including creep and shrinkage, is treated profoundly in the report *Development of a Design Guideline for Phase Construction of Steel Girder Bridges*. The present report focuses on long term deflections, due mainly to temperature.

3.1 Deflection Mechanisms

Sun light strikes the bridge heating the deck while the shaded girders below remain at the ambient air temperature. This thermal gradient results in an uneven expansion of the bridge through the depth. Since the top of the bridge expands, or elongates, more than the bottom, the result is an upward bending of the bridge. This effect is illustrated in Figure 3-1.

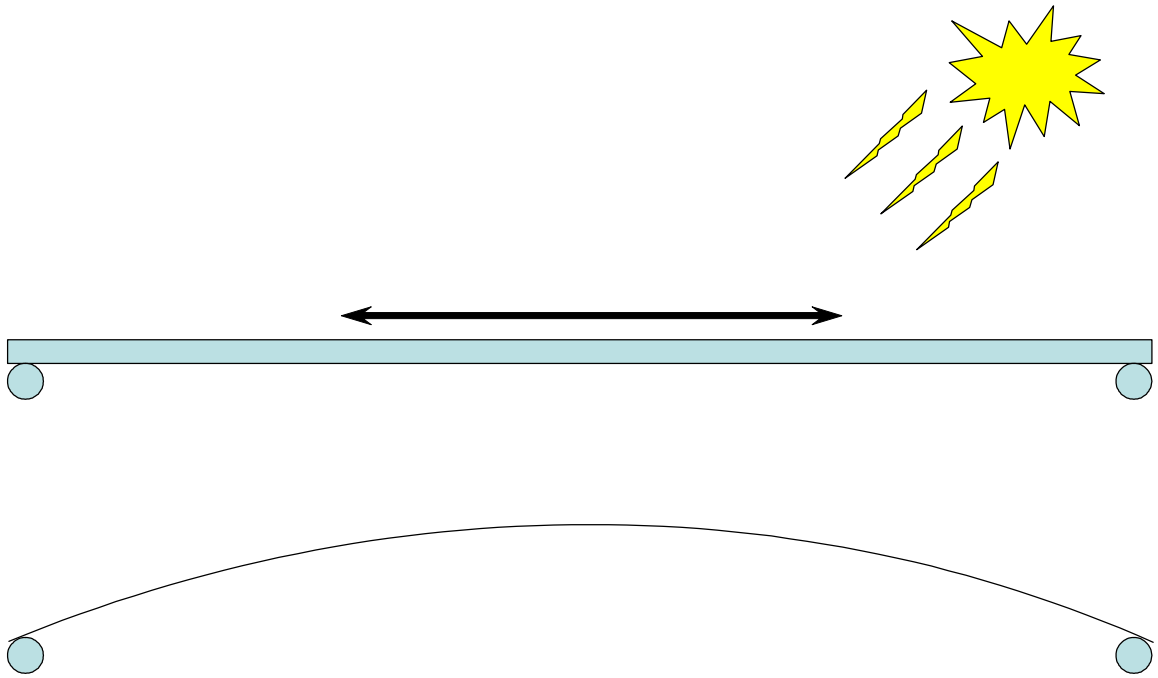

Figure 3-1: Deflection due to Thermal Gradient

In addition to deflection due to thermal gradient, deflection can also be in response to a change in ambient temperature. Two potential mechanisms have been identified which explain this occurrence.

The first explanation is the different coefficients of thermal expansion for steel and concrete. The values are 6.5×10^{-6} and 5.5×10^{-6} in/in/°F for steel and concrete respectively. Therefore, the steel elongates 1.0×10^{-6} in/in/°F more than the concrete. Since the steel is on the bottom of the structure, the bottom of the bridge elongates more than the top and the bridge deflects downwards. Note that this is in the opposite direction as the

movement due to temperature gradient. This phenomenon is illustrated in Figure 3-2.

The second mechanism requires the presence of at least partial end restraint at the end of the girders which acts eccentric to the girder centroid as shown in Figure 3-3. If the restraint is assumed to act in line with the deck, then as the girder expands, the deck is restrained from expansion while the steel girder is not. Therefore, the bottom of the bridge is free to elongate more than the top. Again, the bridge deflection is downwards.

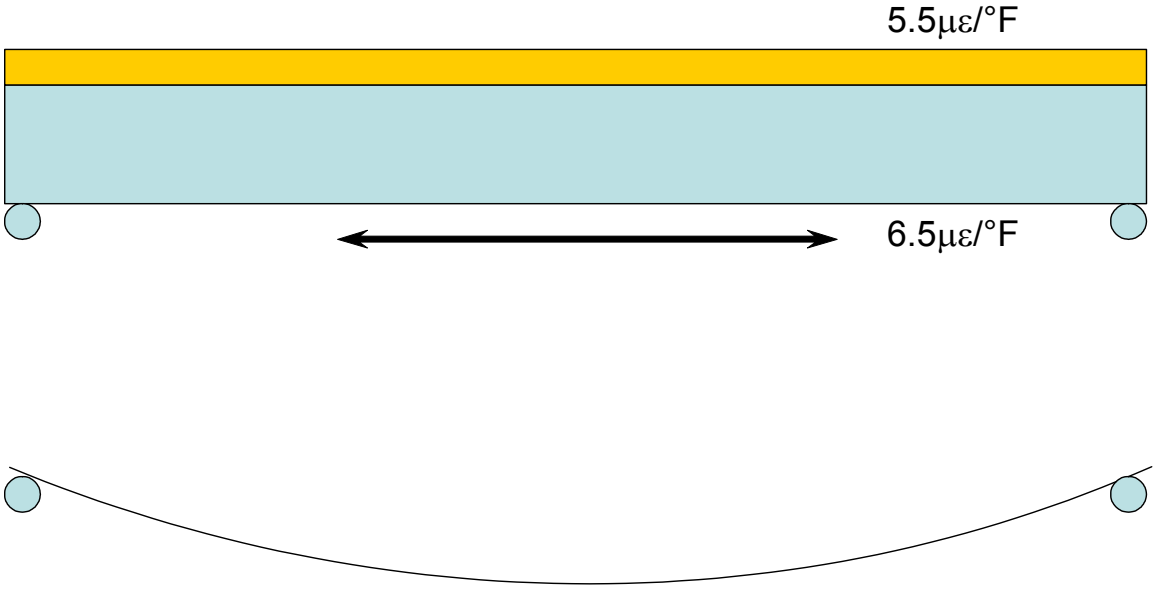

Figure 3-2: Deflection due to Uniform Temperature (Different Expansion Coefficient)

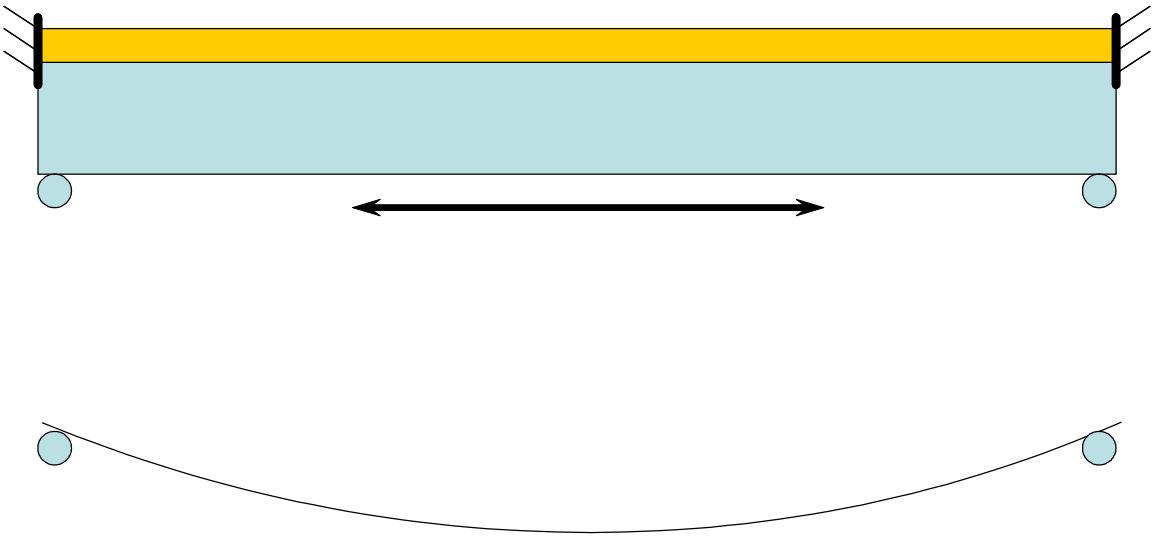

Figure 3-3: Deflection due to Uniform Temperature (End Restraint))

3.2 Observed Movement

3.2.1 One Week Analysis

The temperature during a sunny summer day can be seen in Figure 3-4. The data in Figure 3-4 is from an interior girder taken around June 23, 2000. The numbers along the x-axis are the number of days since the beginning of the project with midnight falling on the whole numbers. It can be seen from the figure that the temperature in the slab can be a great deal higher than the temperature of the steel. This is due to solar heating. The temperature of the bottom flange follows very closely the ambient temperature. Further, due to conductive heating of the steel by the slab, the top flange temperature remains higher than the bottom flange. Finally, note that the temperature of the slab remains well above the temperature of the steel even into the morning hours. The entire system generally reaches a uniform temperature around 4:00 am.

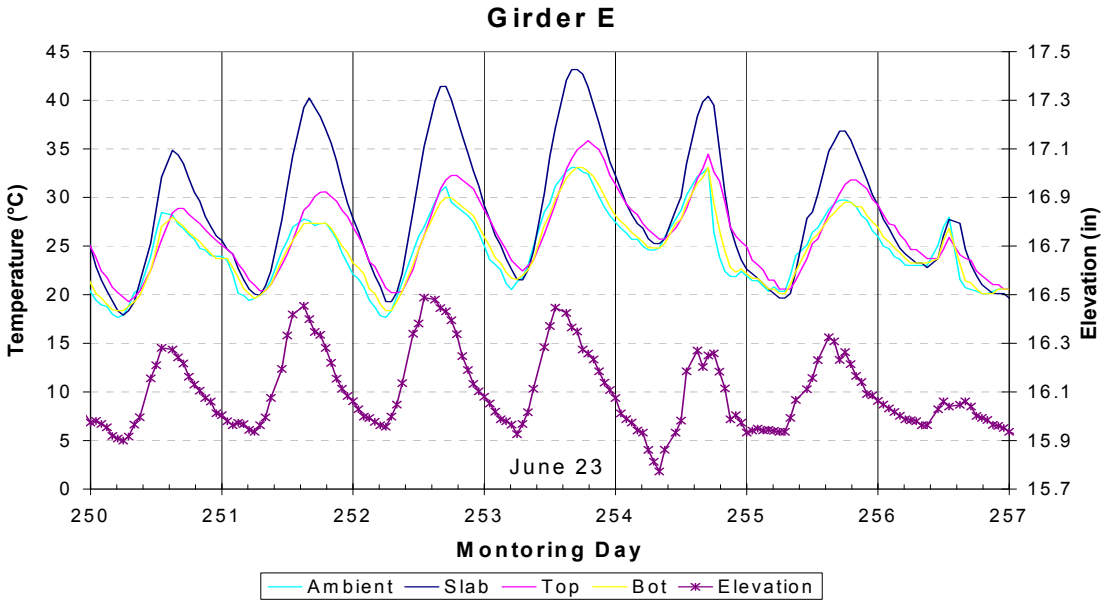

Figure 3-4: Vertical Movement due to daily temperature fluctuation

Figure 3-5 illustrates the gradient through the depth of the girder at 5:00pm on June 23, 2000. Also shown in the figure is the thermal gradient specified by the AASHTO LRFD Specification. Instrumentation was not provided to obtain the temperature through the entire depth of the slab, however, the temperature obtained at mid-depth does coincide well with the prescribed value. The predicted value at the top flange is well below the observed value. The higher temperature of the top flange is due to the conductive heating of the steel. It is assumed that the zone of elevated temperature is small and is therefore ignored by the predictive equations.

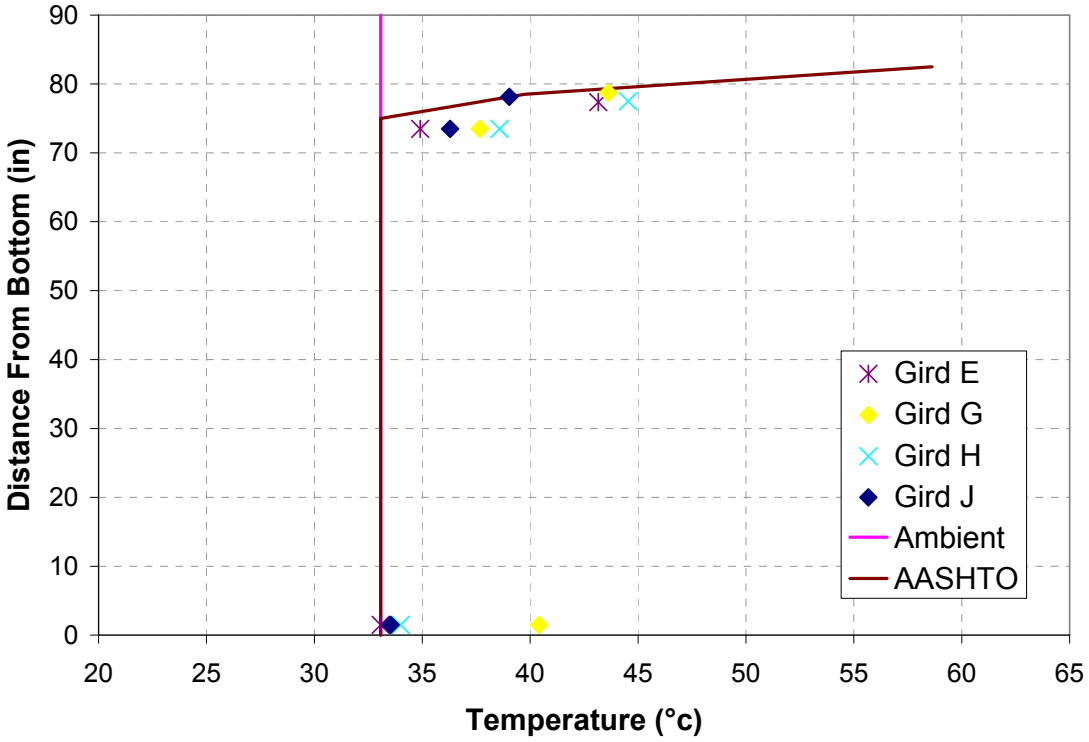

Figure 3-5: Gradient through depth of girder

The elevation of Girder E has also been shown in Figure 3-4. The values along the right y-axis are the elevation in inches as measured from an arbitrary reference height. It can be seen that both the temperature gradient and deflection peak around 5:00 in the afternoon. The elevation increases over the course of the afternoon meaning the bridge deflects upwards.

It is of particular interest to observe the elevation of the girder at the time when the temperature is uniform over the depth of the girder. During the week presented in Figure 3-4 the early morning uniform temperature on most days was around 68˚ Fahrenheit. At that same time the elevation of the girder was around 15.95 inches. However, on the morning of the 24th the uniform temperature was found to be 9˚ higher at 77˚ F. On this day the elevation was at 15.75 inches. This demonstrates that as the uniform temperature increases the bridge deflects downwards.

The week of data presented in Figure 3-4 demonstrates well the primary deflection modes in response to temperature. It should be emphasized that the movement due to an increase in temperature gradient is in the opposite direction as the movement due to an increase in the uniform temperature. During the course of a typical day both the ambient temperature and temperature gradient increase during the afternoon and decrease during the evening resulting in opposing deflections. In a practical sense this is a good thing since the two effects oppose each other lessening the overall movement due to temperature. However, this situation is difficult to account for in analyzing the data obtained from the field testing.

3.2.2 Proposed Methods to Handle Temperature Effects

Three general methods were proposed for dealing with the temperature effects. The first was to fully account for all thermal effects utilizing simulation and analysis techniques. It was determined that, due to the complex interaction between the various factors including additional meteorological factors not yet mentioned such as humidity, drought and precipitation, this alternative was too costly given the ultimate objectives of the project.

The second alternative was to ignore the presence of the thermal gradient and deal solely with the average ambient temperature at the time of a reading. As was shown in the preceding section, during the afternoon as the average ambient temperature is increasing thus forcing the bridge downwards, the thermal gradient is increasing thus forcing the bridge upwards. It is quite apparent from Figure 3-4 that the thermal gradient effects are much greater than the ambient temperature effects on a day to day basis. On a good sunny day one can expect to see an approximate upwards deflection of 0.6 inches. However the approximate change in elevation observed through the seasonal thermal change is 0.5 inches. Therefore, since the magnitude of movement is the same for the two effects it would be incorrect to ignore either.

The third alternative was to consider the effects separately. Studying the effect of thermal gradient can be done by examining the data obtained from individual days. The goal in particular is to find a sunny day during which the ambient temperature remains relatively constant. This minimizes the effects of change in ambient temperature while exposing the response of the bridge to thermal gradient. The procedure for isolation of the bridge response to ambient temperature in absence of thermal gradient is less straight forward and will be discussed in the following section.

3.3 Removal of Thermal Gradient

After completion of the second phase there were 75 sensors capable of indicating temperature however the results from each and every gage are not necessarily accurate. Looking at a two week period of time in Figure 3-6 one can see that the temperature data can be quite noisy. This noise can come from a number of sources including but not limited to communication problems, interference, faulty gages, loads and vibration, and moisture in the wiring.

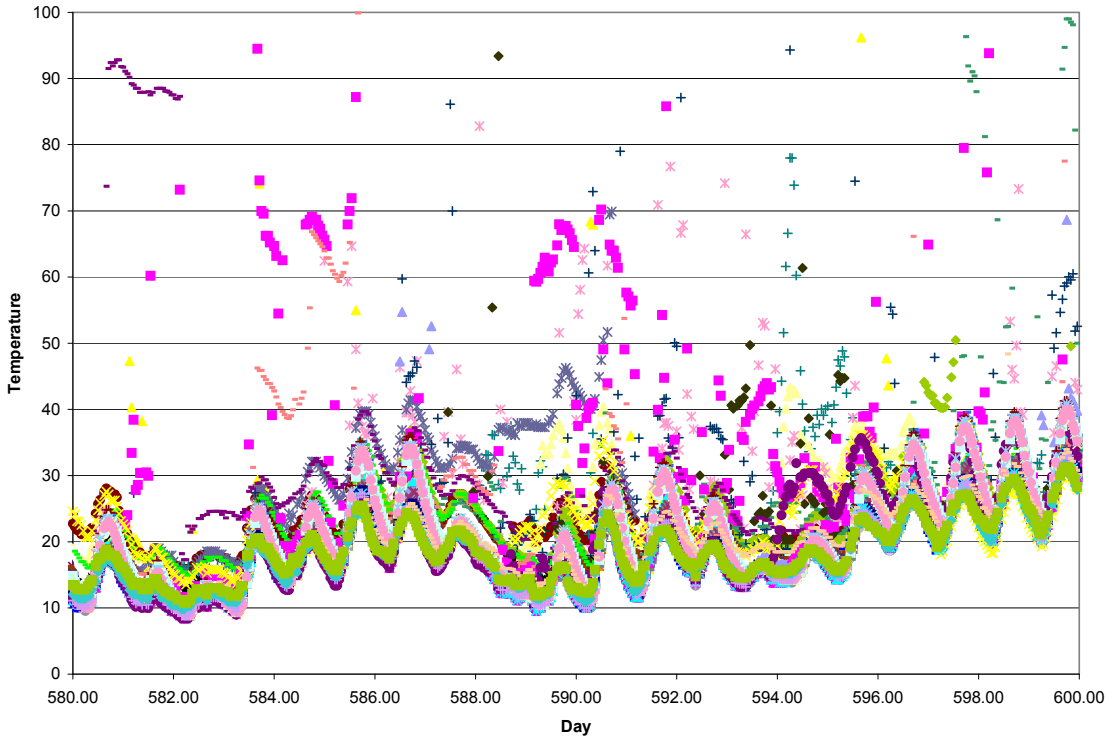

Figure 3-6: Raw Temperature Data

It was seen in the previous section that there is a short period of time during which the thermal gradient is at a minimum each day. The goal of filtering is to isolate that period of time and obtain the temperature and bridge response corresponding to a constant uniform temperature for each day. It would also be desirable to reduce the overall volume of data.

The first step in filtering the temperature data is to limit the time period used in the analysis. The time period chosen is from 4:00 am to 10:00 am resulting in seven readings for each day. The plots such as Figure 3-7 which shows all gages over a one day period indicate that the temperature is most stable during this period of time with the gages showing a small spread in values.

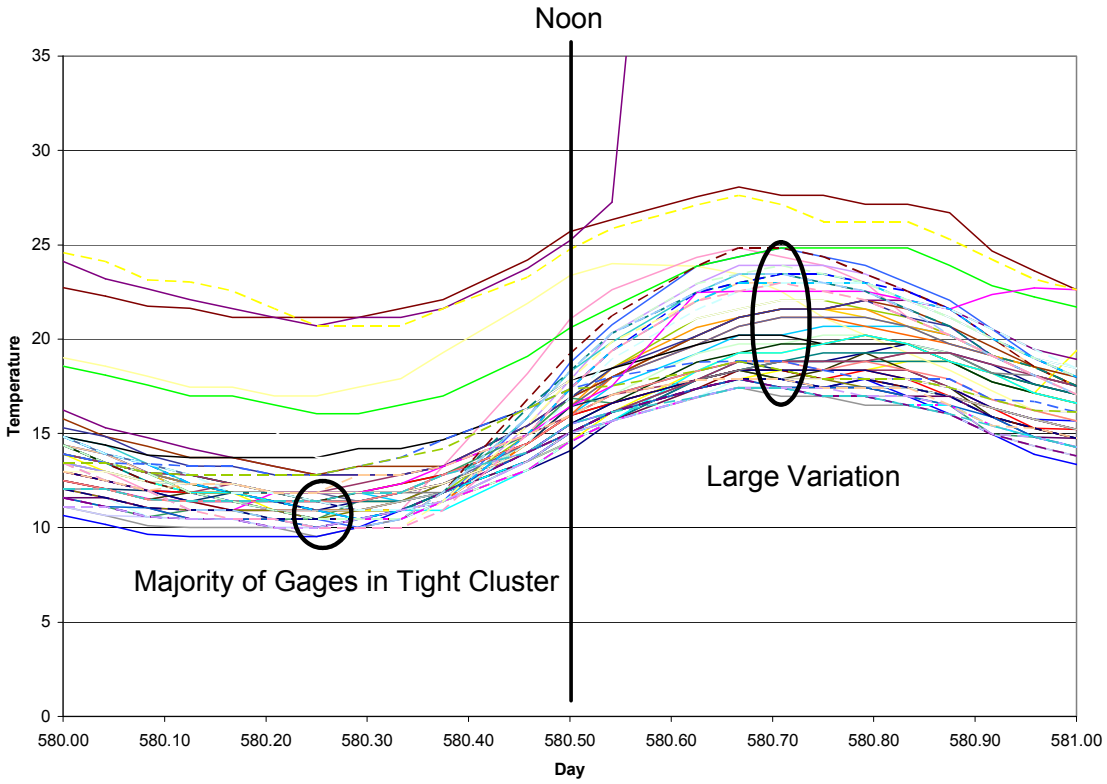

Figure 3-7: Variation in Temperature During Day

The next step is to eliminate the obvious outliers. These are the values which are so far out of range that they are obviously due to systemic error. Since future filtering steps will further eliminate outlier points the limits at this point can be very generous. These limit points have been chosen to be -30 and 60 degrees Celsius (-22˚ and 140˚ F). Any reading which falls outside these limits is eliminated from the data set. Figure 3-8 shows the same twenty days displayed in Figure 3-9 after imposing the time and extreme value limits.

The next step is to further refine the elimination of outlier data points. This step is based on the following premise. If the temperature is constant, and has been for some time, one would expect all 75 gages to give approximately the same value. Based on this, the average value and standard deviation is calculated for each reading. If the standard deviation is less than

3˚ C (5.4˚ F) then the reading is acceptable. However, if the standard deviation is over 3˚ C (5.4˚ F) then the individual gage reading which is furthest from the mean is eliminated and the mean and standard deviation is recalculated. This is repeated until the three degree standard deviation criterion is satisfied. At this point if there are at least five gages remaining in the data set then the average value from the remaining gages is determined to be the average uniform temperature of the structure for the time of that reading. This is then repeated for each hour such that a single temperature is obtained for each hour. Figure 3-8 shows the results of this filter for the twenty days referenced previously. Since the outliers have been removed the data falls in a much tighter band and the limits in the plot have been adjusted accordingly to provide more detail.

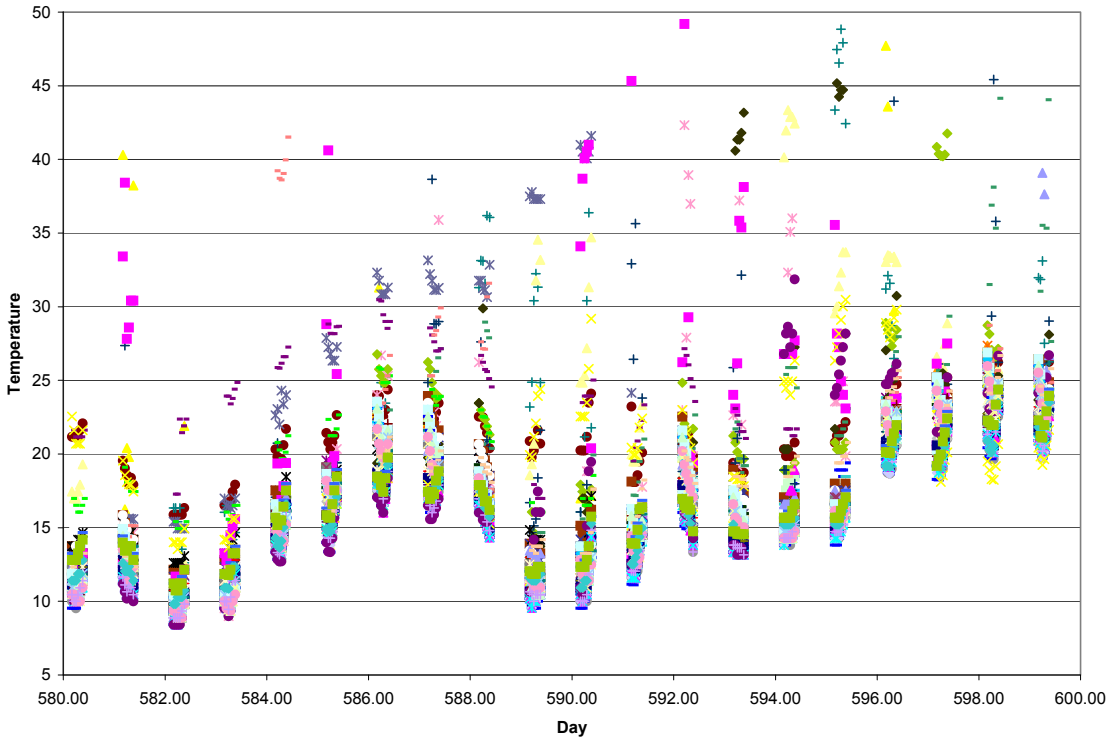

Figure 3-8: Temperature Data after elimination of obvious outliers

The next step in the filtering process is to reduce to data down to a single temperature reading per day. The criteria for this operation are that the temperature range during the day must not exceed 3˚ C (5.4˚ F) and the

number of hourly reading remaining during that day be greater than or equal to two. The first criterion assures that the temperature is not changing too rapidly during the period of time. This is because the steel changes temperature quickly and closely follows the ambient temperature while the concrete slab has more thermal inertia requiring more time to respond to rapidly changing temperatures. The second criterion requires that there are a sufficient number of readings available to provide a statistically relevant result. If the specified criteria are met then a centrally weighted average is performed with the resulting temperature being the temperature for that day. These temperatures are shown in Figure 3-10 for the twenty days being examined. The days in Figure 3-10 without a large marker indicating the final daily temperature are those days which violated the prescribed crieria.

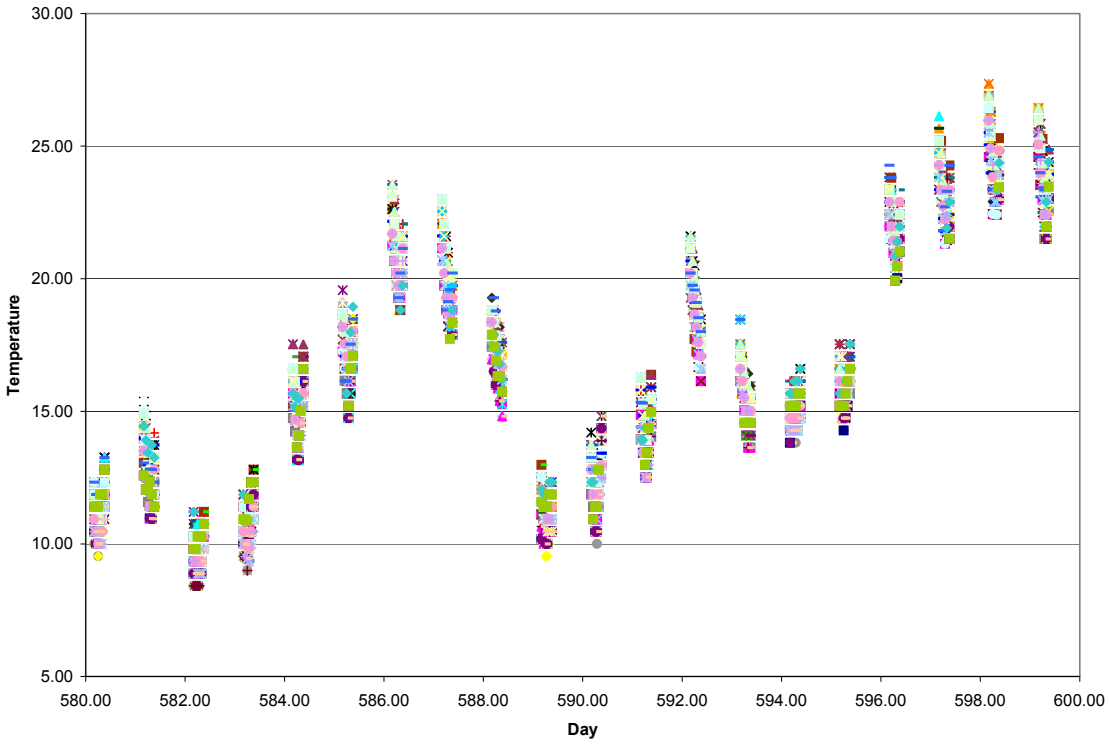

Figure 3-9: Temperature Data after filtering

The final step in the temperature filtering process is to obtain daily values for the bridge response variables such as deflection, and strain. Minimal filtering is performed on the response variables. For each gage generous extreme outlier limits have been specified and the excessive values eliminated from the data set. Once the extreme values have been removed a centrally weighted average is performed on the admissible hourly reading values for each day. The resulting value is the response variable value for that day.

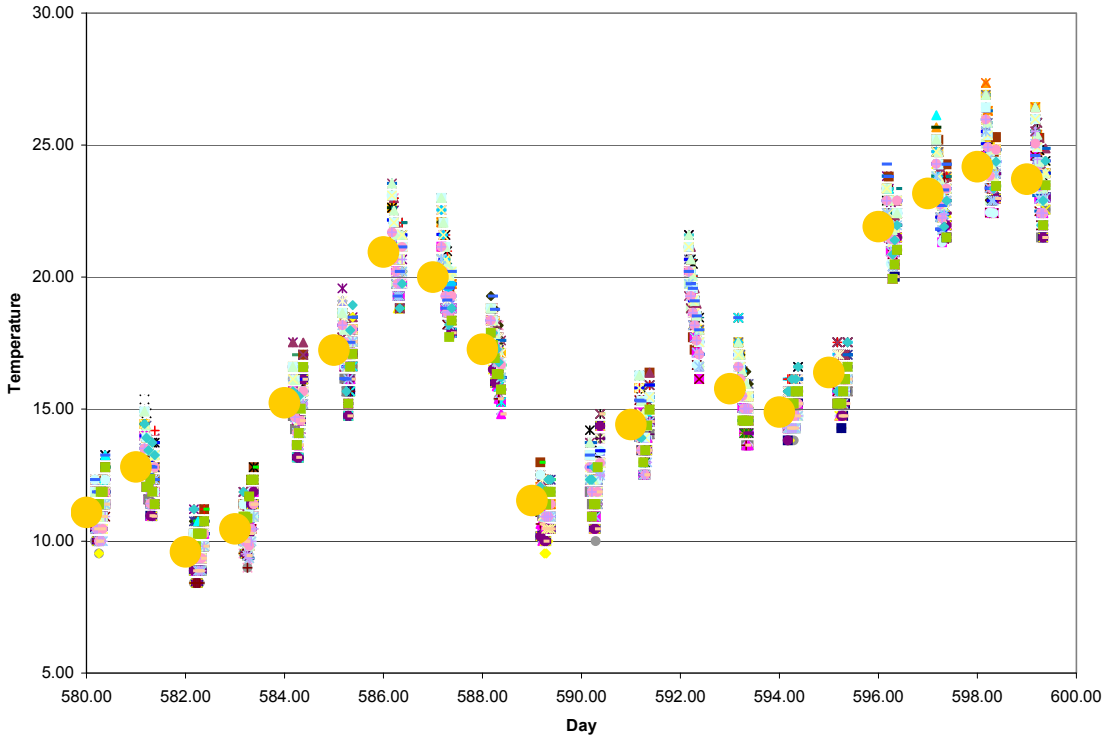

Figure 3-10: Temperature Data after Averaging Process

The result of temperature filtering has thus reduced the full data set into a single temperature and the corresponding response data for each day. The values are from a period each day when the thermal gradient through the depth is at a minimum. Days during which the temperature is changing rapidly have been discarded and central averaging has been utilized to further reduce the effect of variability in the response variables.

Chapter

4 Longitudinal Deformation

LONGITUDINAL RESPONSE DUE TO UNIFORM TEMPERATURE CHANGE

Once the effects of thermal gradient had been removed using the procedure described in the preceding chapter, one could begin investigating the movements which could be attributable to a uniform change in temperature.

4.1 DEFORMATION BEHAVIOR

There are four gages capable of monitoring the longitudinal deformation. One gage is placed at each end of girders E and D. A more detailed description of the instrumentation is given in Chapter 2 . To begin examining the influence of temperature on longitudinal movement, the longitudinal position has been plotted versus daily temperature for all data collected in Figure 4-1. The zero position for each gage is the arbitrarily chosen initial

position when the gage was installed. This serves to separate the data and make each gage distinguishable from the other.

Inspecting Figure 4-1, one should notice an apparent linear relation for each of the gages. Further, a pairing of the data is observed with respect to which end of girder the gages are on. Figures 4-2 and 4-3 separate the pairs for the west abutment and east abutment respectively.

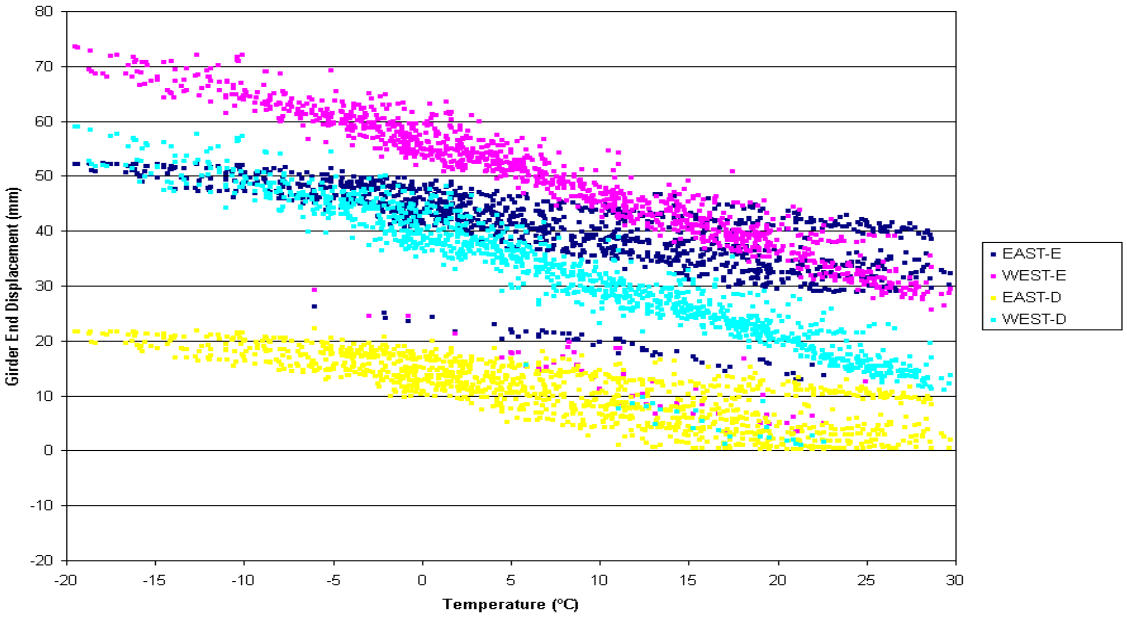

Figure 4-1: Longitudinal Movement versus Temperature

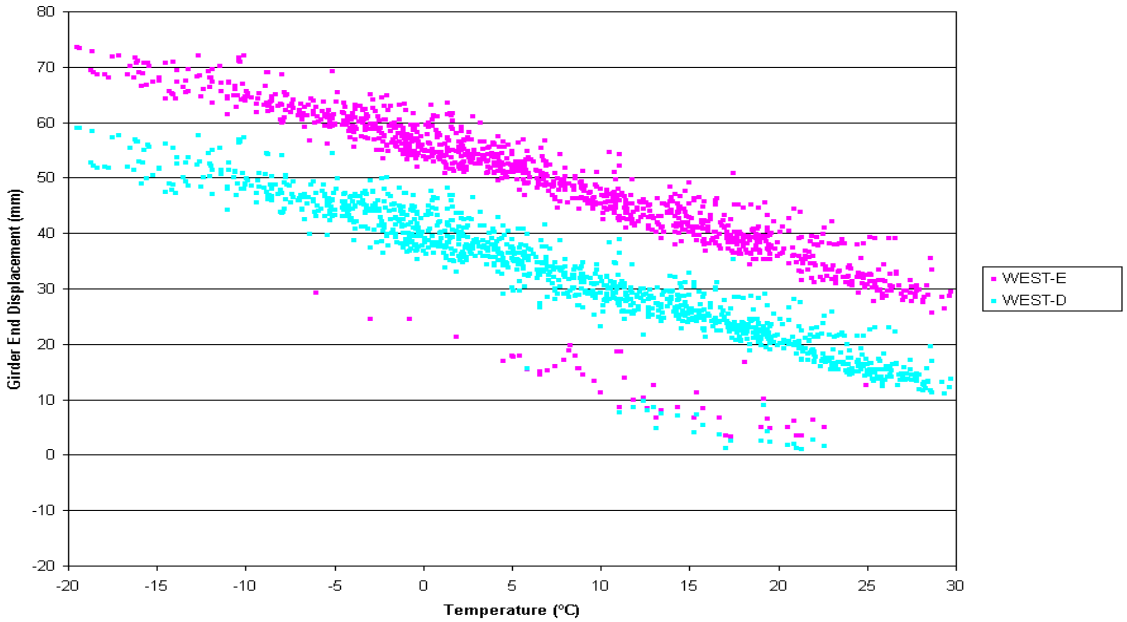

Figure 4-2: Longitudinal Movement versus Temperature (West End)

From inspection of the two previous figures one observes the deflection of the west end of the bridge caused by a change in temperature is larger than the deflection of the east end of the bridge subjected to the same temperature change. While there is insufficient instrumentation to verify, one hypothesis is that the difference in behavior between the two ends of the bridge is due to the vertical curve of the roadway as depicted in Figure 4-4. The supposition is that the lower end provides a rigid base off of which the rest of the bridge pushes off of. This is similar to a vertical metal rod resting on a table and subjected to a temperature change. The bottom remains fixed while the top of the bar experiences all the deformation.

Of greater significance than which end deforms more or less than the other is the total elongation or contraction of the bridge in response to temperature fluctuations. To obtain this value, the deformation from the west end has been added to the deformation of the east end. The resulting data versus the average daily temperature has been plotted in Figure 4-5 for girders D and E. As was done with the position data, the reference point for

zero deformation is arbitrary which separates the two data series on the same plot.

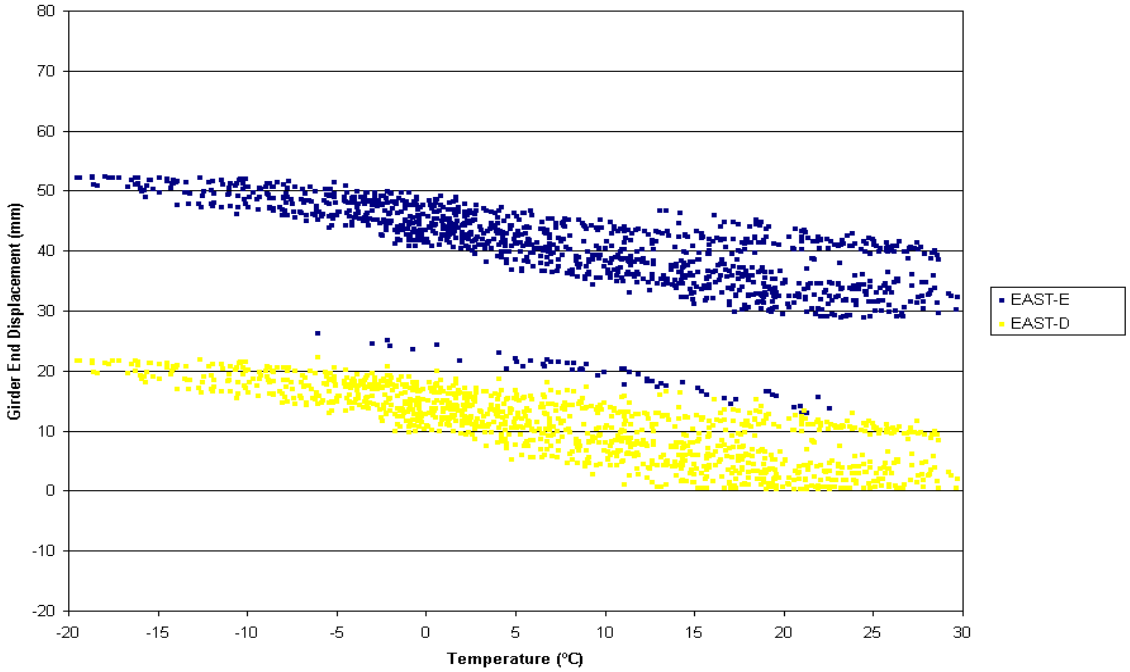

Figure 4-3: Longitudinal Movement versus Temperature (East End)

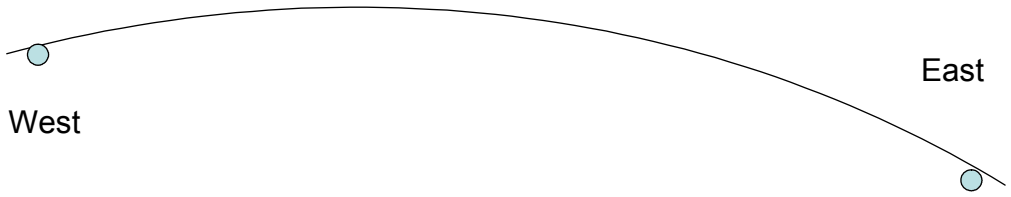

Figure 4-4: Bridge Vertical Alignment

4.2 Predicted and Real Displacement

A linear regression for the girder contraction versus temperature data from Girders E is shown in Figure 4-5. As the intercept is arbitrary the slope is of interest. Equation 4-1 gives an approximation for the longitudinal movement due to a change in temperature, which is used by most designers to approximate longitudinal movement.

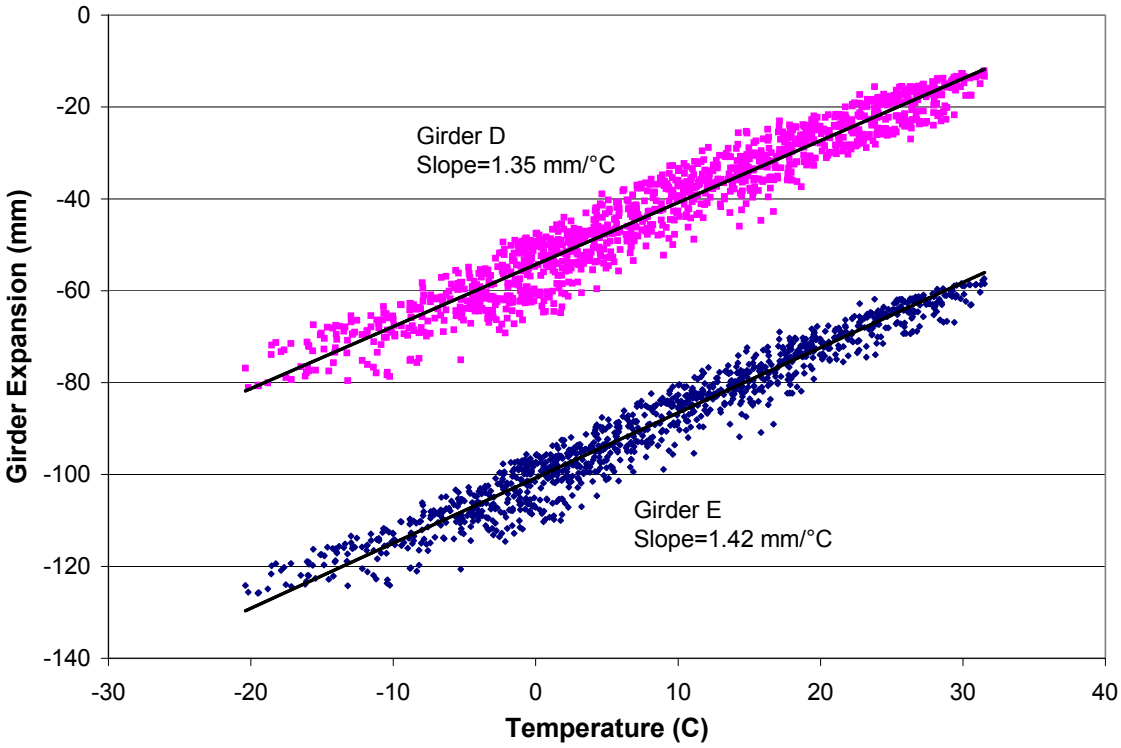

Figure 4-5: Girder Shortening versus Temperature

$$\delta = \Delta_T \alpha L \tag{4-1}$$

Where

δ = Longitudinal movement due to temperature change

Δ_T = Change in temperature

α = Coefficient of thermal expansion

L = Length of girder

The coefficient of thermal expansion of steel is 11.7×10^{-6} mm per mm per degree Celsius (6.5×10^{-6} in/in/˚F). Multiplying this value by the total bridge length of 144,180 mm (473 ft) gives the rate of deformation with respect to change in temperature. Comparing the resulting value of 1.69 mm/˚C (0.0369 in/˚F) to the slope of the line in Fig. 9, 1.42 mm/˚C (0.0311 in/˚F) it

can be seen that the predicted rate of deformation with respect to temperature change is very close to the measured value.

The bridge is located within the Cold Climate region as specified in the AASHTO Specifications. The assumed temperature extremes used for design is from -35˚ C to 50˚ C (-30˚ to 120˚ F) for a range of 83.3˚ C (150˚ F). Therefore, the full predicted deformation for design would be 141 mm (5.55 in) while the actual deformation of the bridge due to the specified temperature variation over five years is 118 mm (4.65 in).

Chapter

5 Vertical Deformation

VERTICAL RESPONSE DUE TO TEMPERATURE CHANGE

In the previous chapter it was found that the longitudinal deformation correlated well with the change in average daily temperature and matched well with the theoretical prediction.This same exercise was also performed with respect to vertical midspan deflection.

5.1 DEFORMATION BEHAVIOR

Vertical deflection of each of the eight girders is measured near 0.4L in the East span using potentiometers. Figure 5-1 plots the vertical deflection at midspan versus time from the end of construction up to May 23, 2005. The deflection trends from all girders are similar. However, due to various factors such as wire splice corrosion and sensor malfunction, the signals become increasingly noisy. Therefore, to minimize clutter, only two gages, G and H, are shown in the Figure 5-2.

As noted in Figure 5-2, despite the obvious seasonal deflection trend, the deformation peaks do not correspond with the observed peaks in temperature. In fact, the deformation appears to peak approximately one month after the temperature. When the vertical deflection is plotted versus the daily average temperature as shown in Figure 5-3, one can see that there is no apparent relationship.

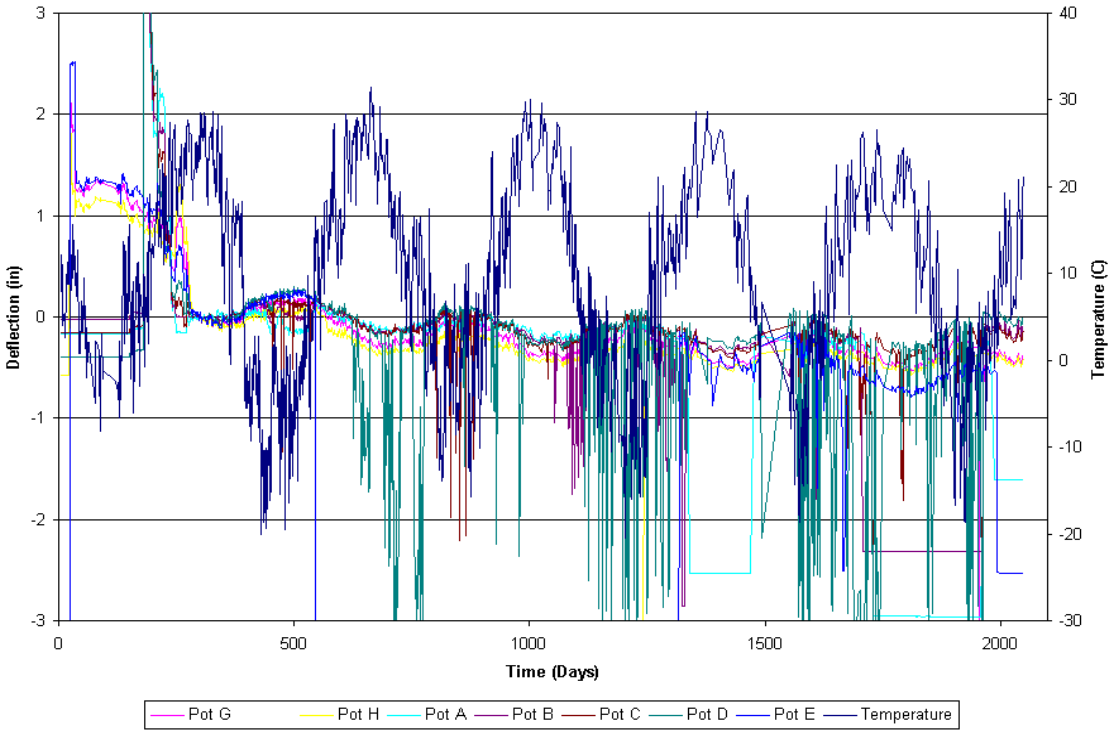

Figure 5-1: Vertical Movement over Time

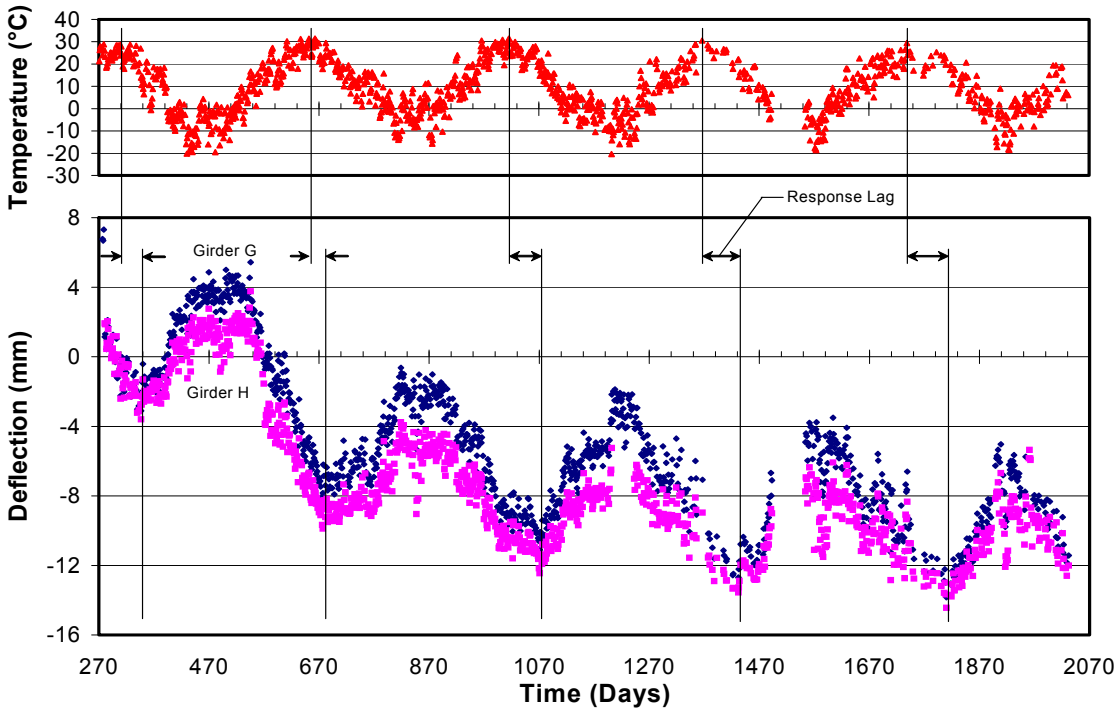

Figure 5-2: Vertical Movement Gages G and H Only

The conclusion which the data suggests is that temperature is not the only factor driving the seasonal variation in vertical deflection. It is quite evident that there is seasonal variation in the deflection history. Therefore, it is suggested that an additional parameter also varies seasonally and operates in conjunction with the temperature to drive the deflection changes.

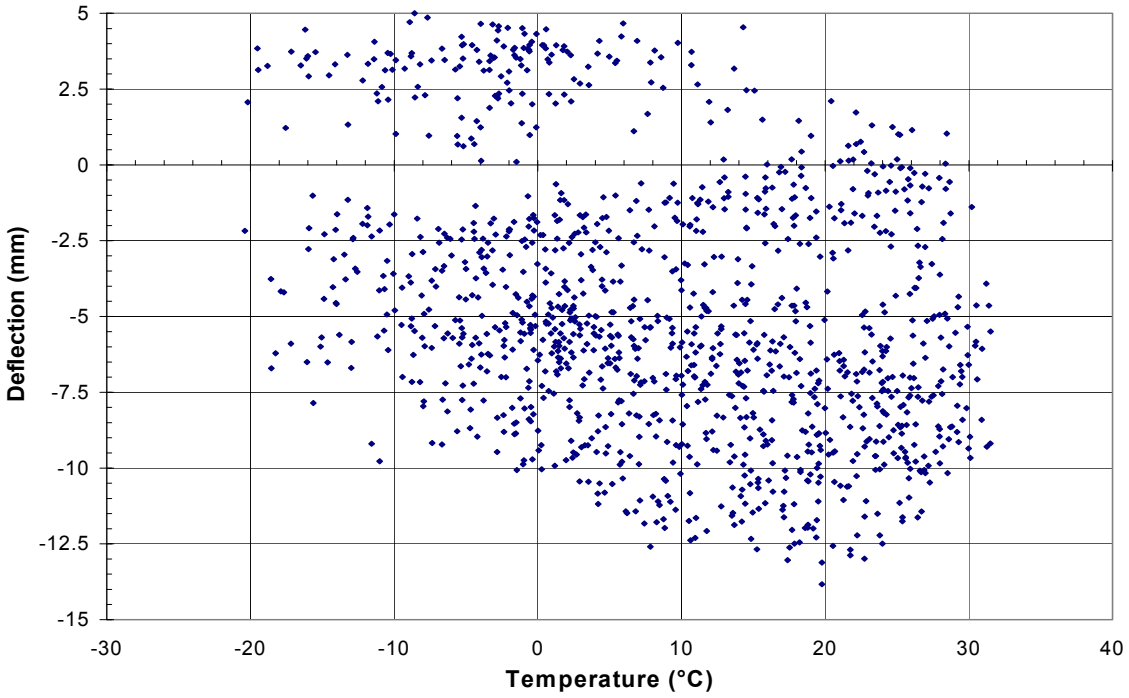

Figure 5-3: Vertical Movement Girder G versus Temperature

5.2 Other Meteorological Effects

The meteorological parameters which keep arising as likely culprits are humidity and precipitation. Just as shrinkage occurs when concrete cures and loses moisture, exposing dry cured concrete to humidity can result in a re-expansion. Humidity, like temperature, fluctuates with the seasons. The summers are humid and moist and the winters dry. It would be expected, however that, as the concrete deck expanded during the moist summer months, the vertical deflection would tend upwards. It is seen in Figure 5-2 that during the summer months the bridge actually moves downwards. This could suggest that temperature is still the predominant factor with humidity being of lesser importance yet significant enough to force a shift in the peak deflection.

Chapter

6 Conclusion

Final Observations

Construction of the Dodge Street Bridge over I-480 in Omaha, Nebraska provided an opportunity to monitor a bridge constructed using phased construction both during construction and beyond. The bridge was monitored between September 1999 and May 2005. During construction, the majority of monitored deflections were predictable and attributable to discreet events. These results are found in the previous report, *Development of a Design Guideline for Phase Construction of Steel Girder Bridges*.

Long term monitoring of the bridge showed that the full actual deformation due to temperature variation is safely within the design limits. It also shows that the longitudinal movements are strongly correlated to the ambient temperature. However, vertical deflection, although varying seasonally, does not appear to directly correlate to temperature since the peak in response lags behind the peak in temperature by approximately one

month. Identification of the underlying mechanism driving the seasonal deformation is a topic for future research.

References

[1] AASHTO (1998). *AASHTO LRFD Bridge Design Specifications* - 1994, American Association of State Highway and Transportation Officials, Inc., Washington D.C.

[2] ACI Committee 209, Subcommittee II, "Prediction of Creep, Shrinkage and Temperature Effect, 2", *Draft Report*, Detroit, October 1978, 98 pp.

[3] Gilbert, R.I. (1988). *Time Effects in Concrete Structures*, Elsevier Science Publishers, New York.

[4] Stallings, J.M. and Yoo, C.H. (1993), "Tests and Ratings of Short-Span Steel Bridges," *Journal of the Structural Division*, ASCE, 119, ST7 (July 1993).

[5] Swendroski, J.P. (2001), *Field Monitoring of a Staged Construction Bridge Project,* M.S. thesis, University of Nebraska, Lincoln, NE, 626 pp.

Appendix

A Sensor Data

CHARTS WITH DATA FROM GAGES INSTALLED ON THE BRIDGE

This appendix contains all of the data obtained from the monitoring project. Both the raw data and filtered data is presented. Note that the data obtained from obviously bad gages have been included as well. This is simply to maintain correspondence with the instumentation descriptions and eliminate question as to whether a gage was inadvertantly omitted.

To conserve space, a compromise had to be reached that balanced the volume of data with its value. Therefore, some of the plots in this Appendix may be somewhat small. However, the general trends they convey is still discernable. Additionally, the electronic versions of this report contain high resolution eps files that may be viewed or printed at any level of detail desired.

A.1 Raw Data

The following figures contain raw data from instrumentation used in the project. This is the original raw signal obtained from the sensors. Data which has been through minimal filtering can be found in Section A.2.

This information is being presented to show the spread, variability, and long term trends in the complete raw data set. Therefore, it is shown in a condensed format. The filtered data is presented in a larger format. A file containing full page versions for each of the gages is included on the report CD.

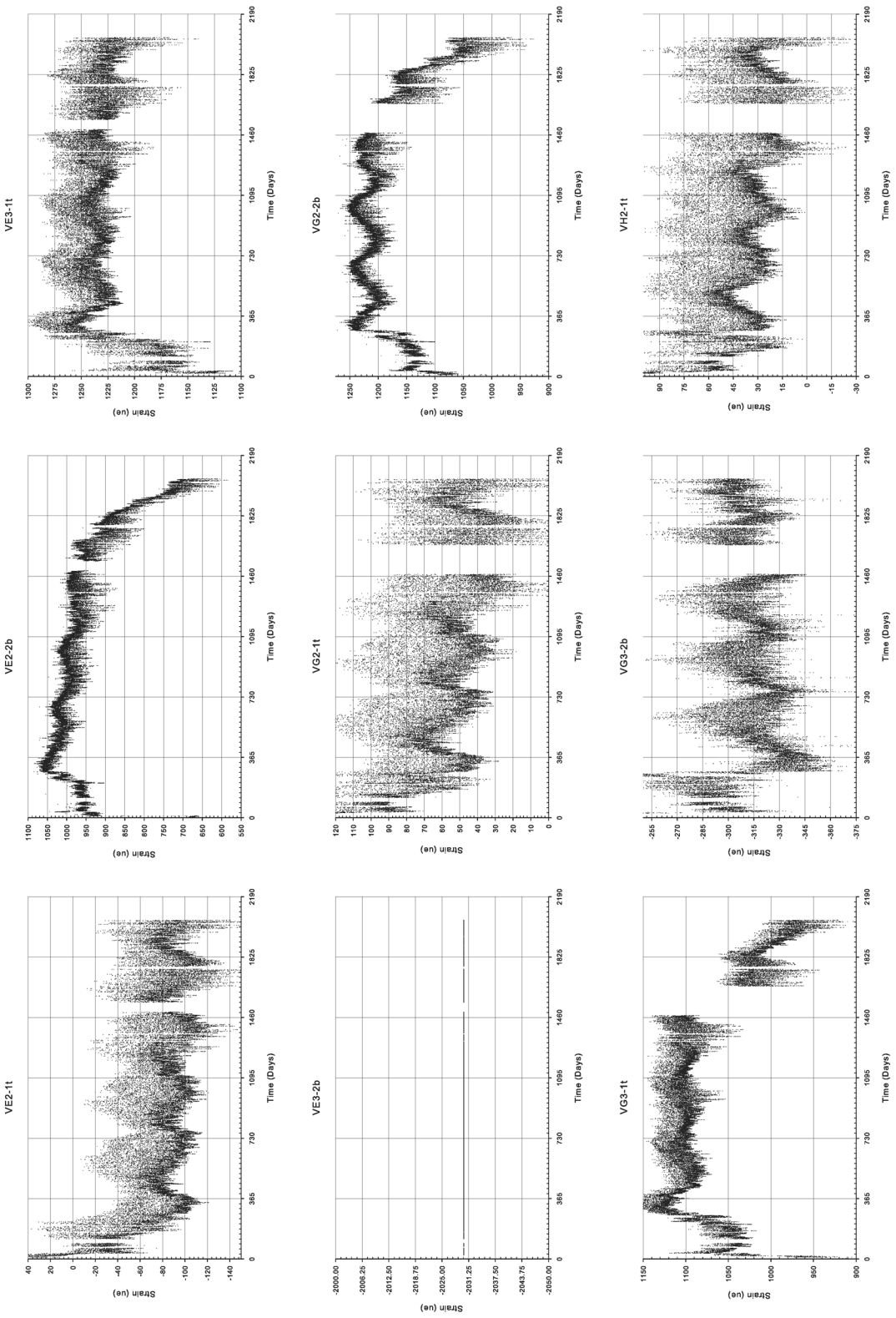

Figure A-1: Raw Sensor Data

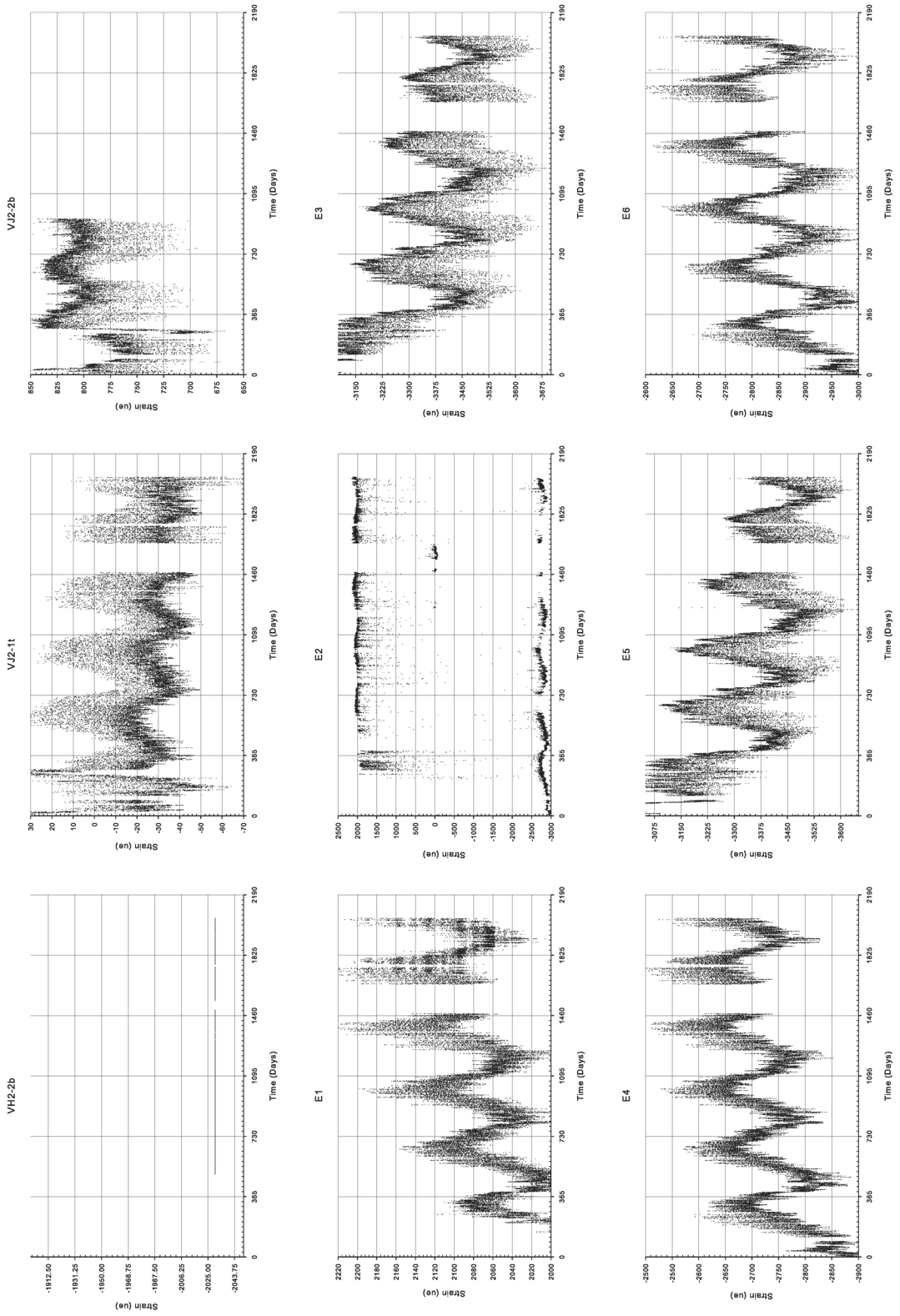

Figure A-2: Raw Sensor Data

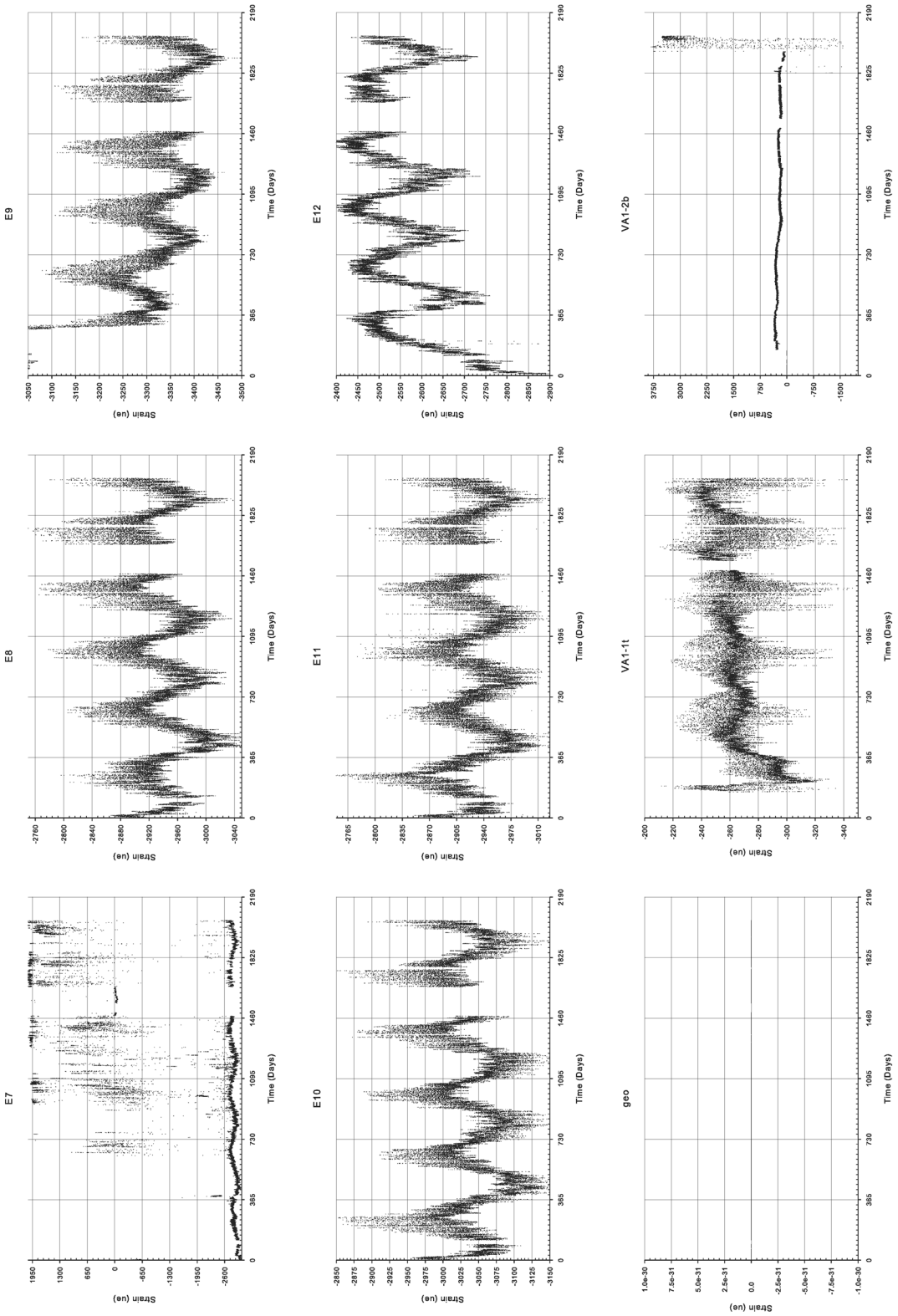

Figure A-3: Raw Sensor Data

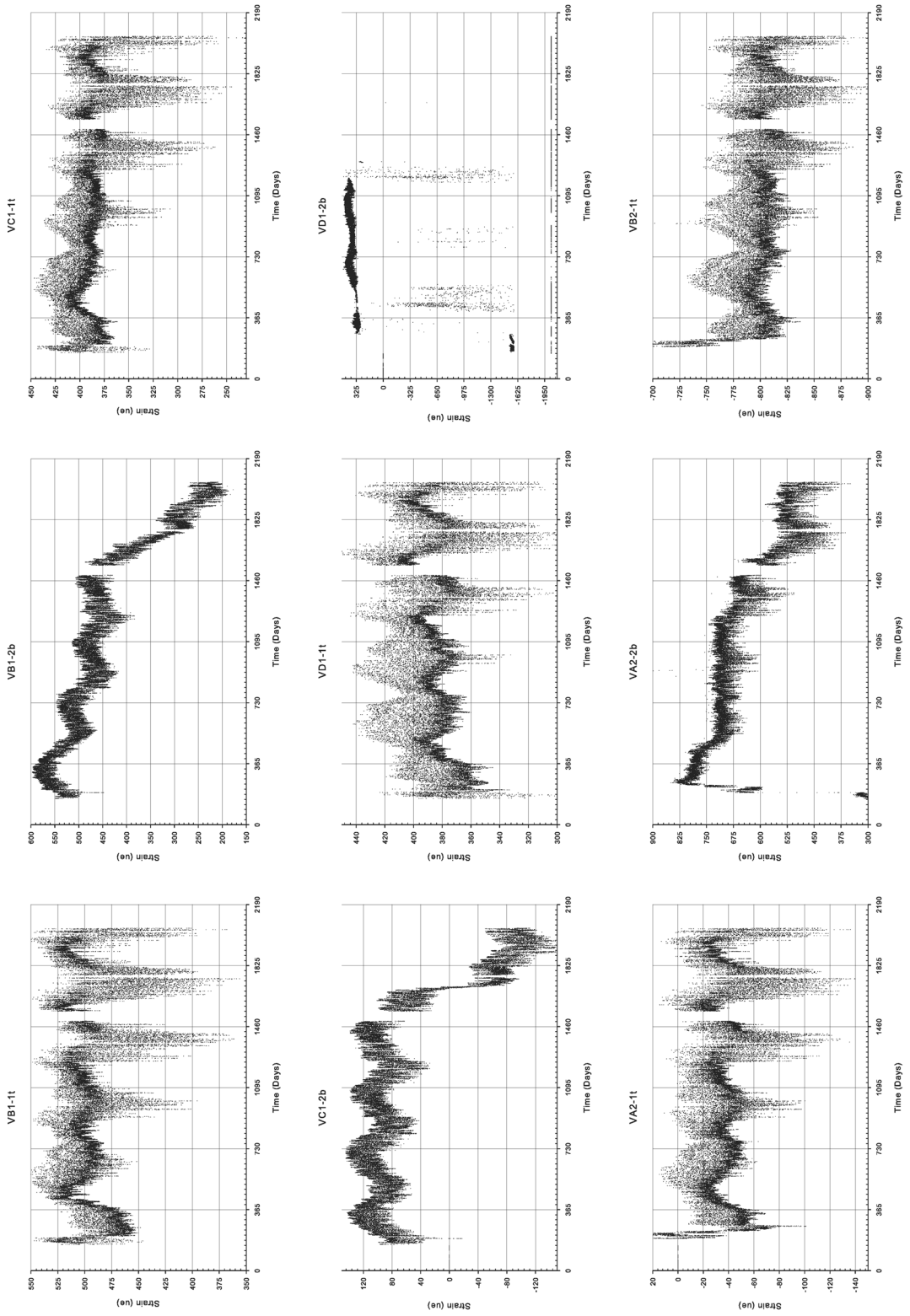

Figure A-4: Raw Sensor Data

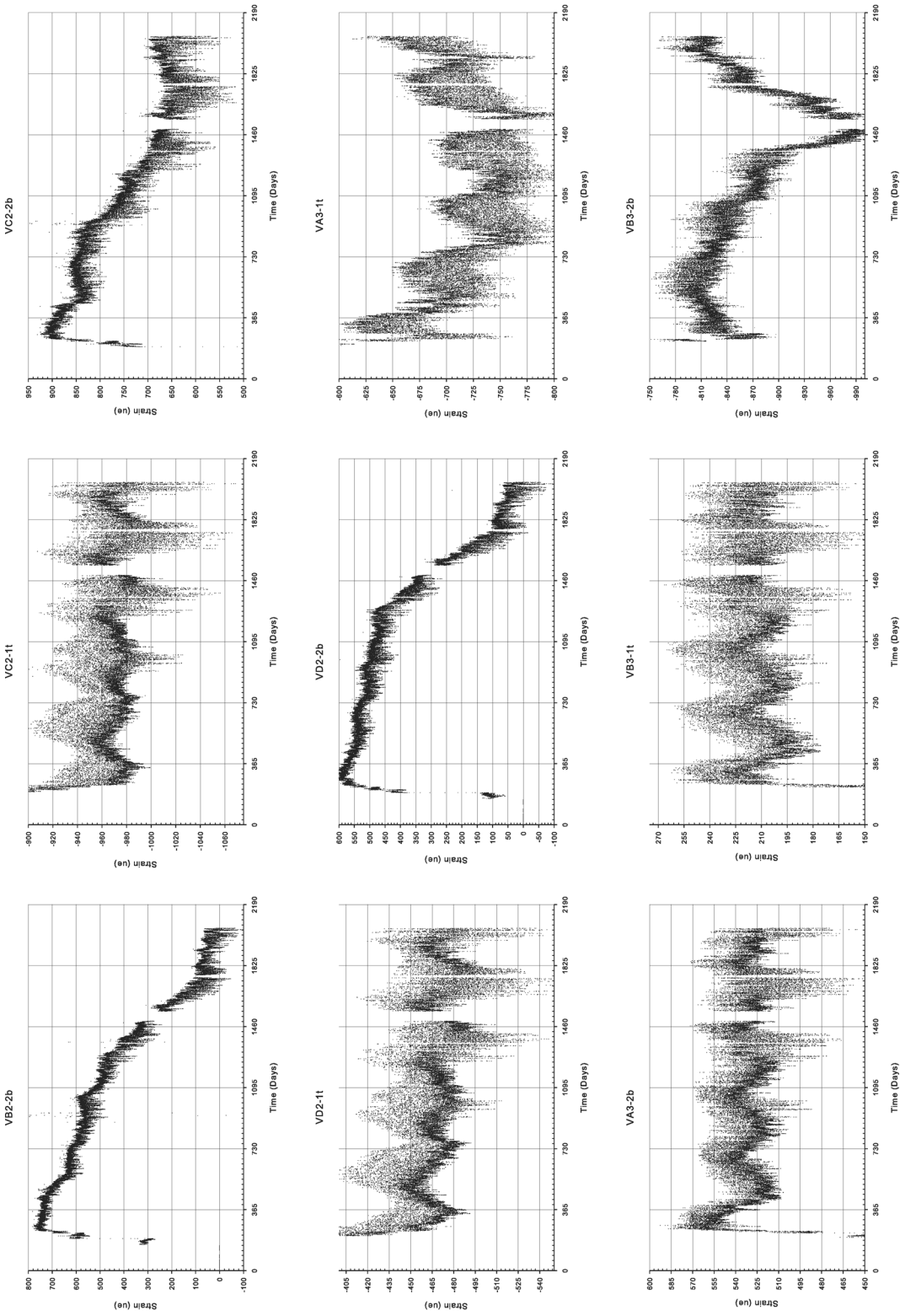

Figure A-5: Raw Sensor Data

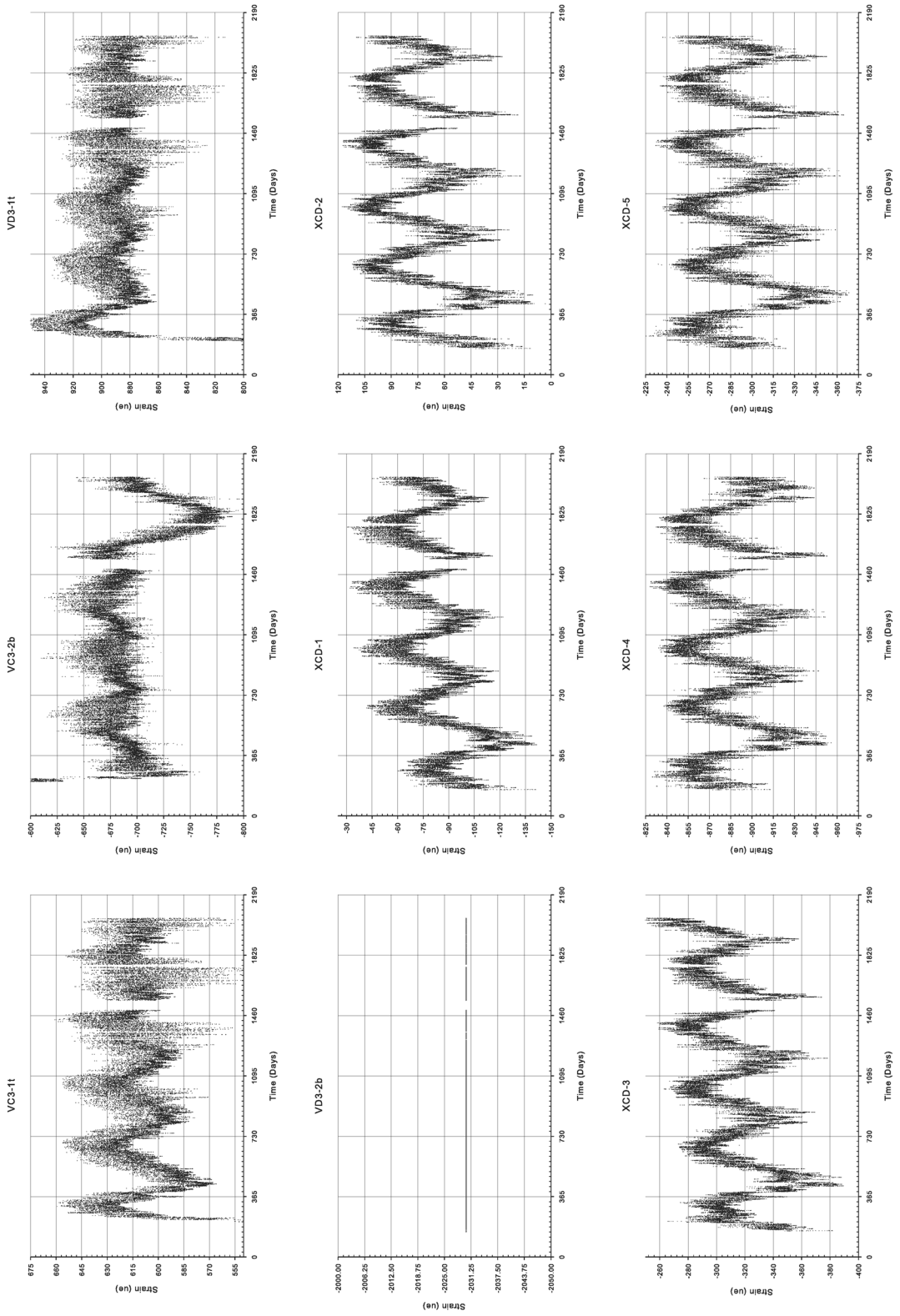

Figure A-6: Raw Sensor Data

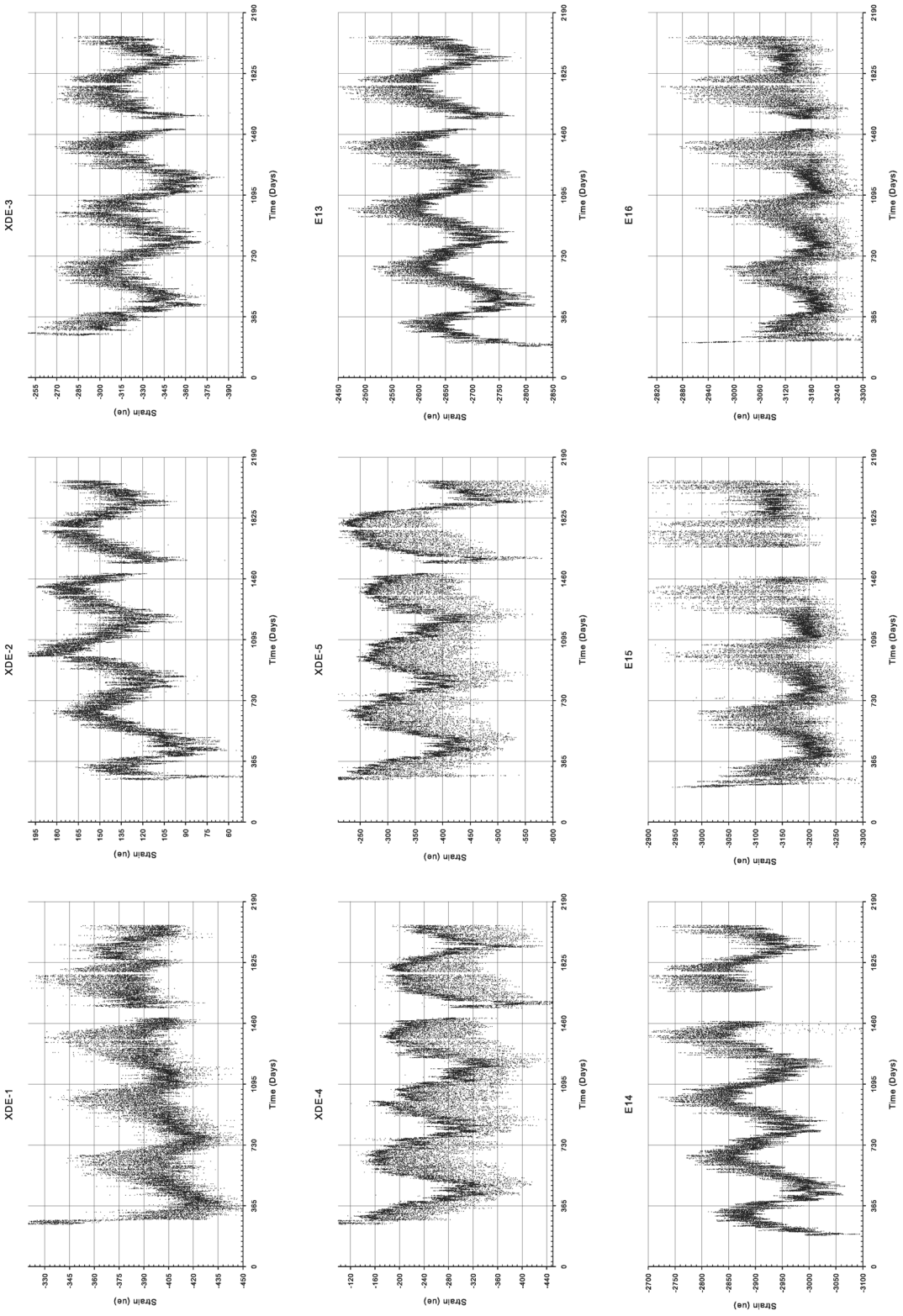

Figure A-7: Raw Sensor Data

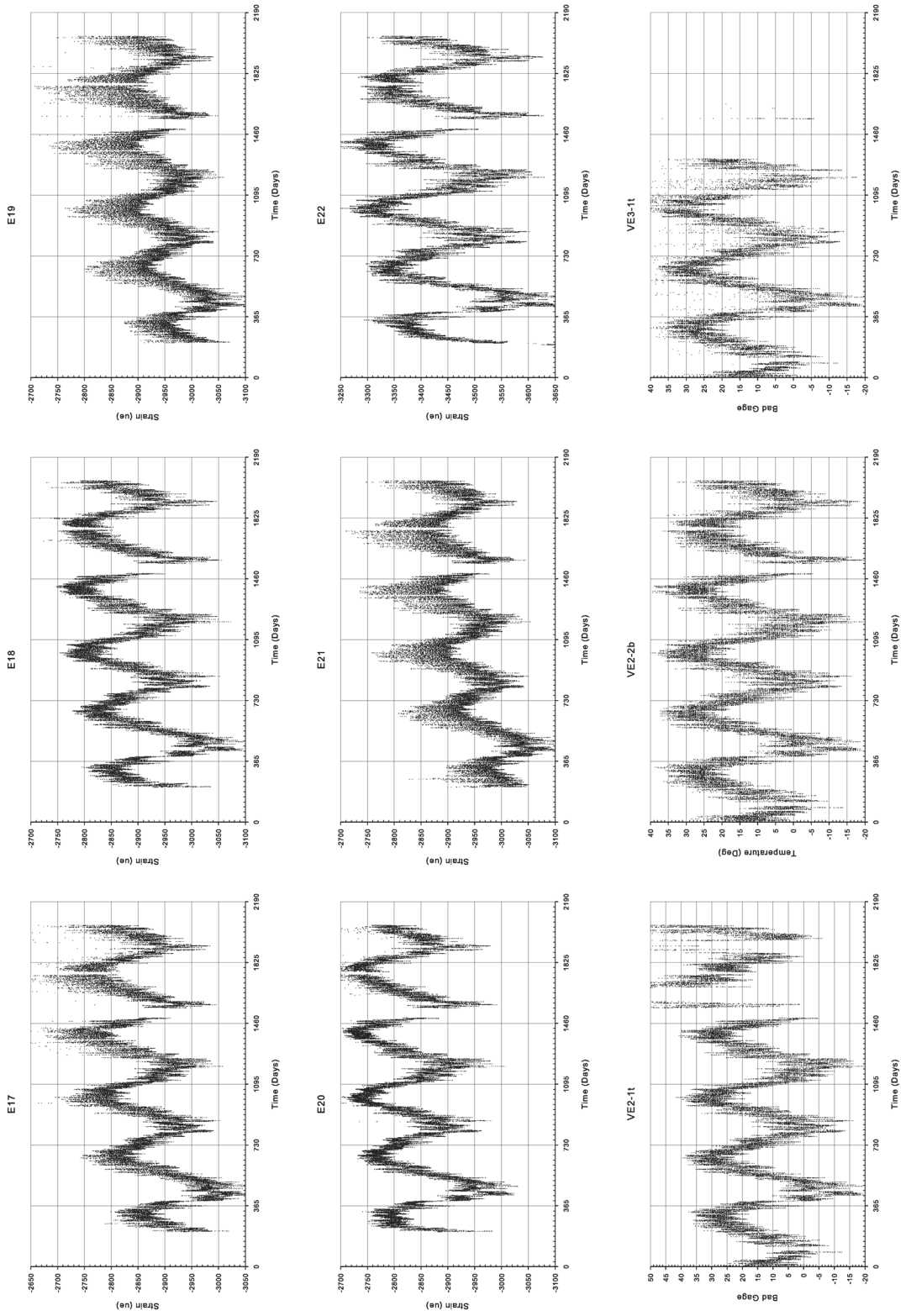

Figure A-8: Raw Sensor Data

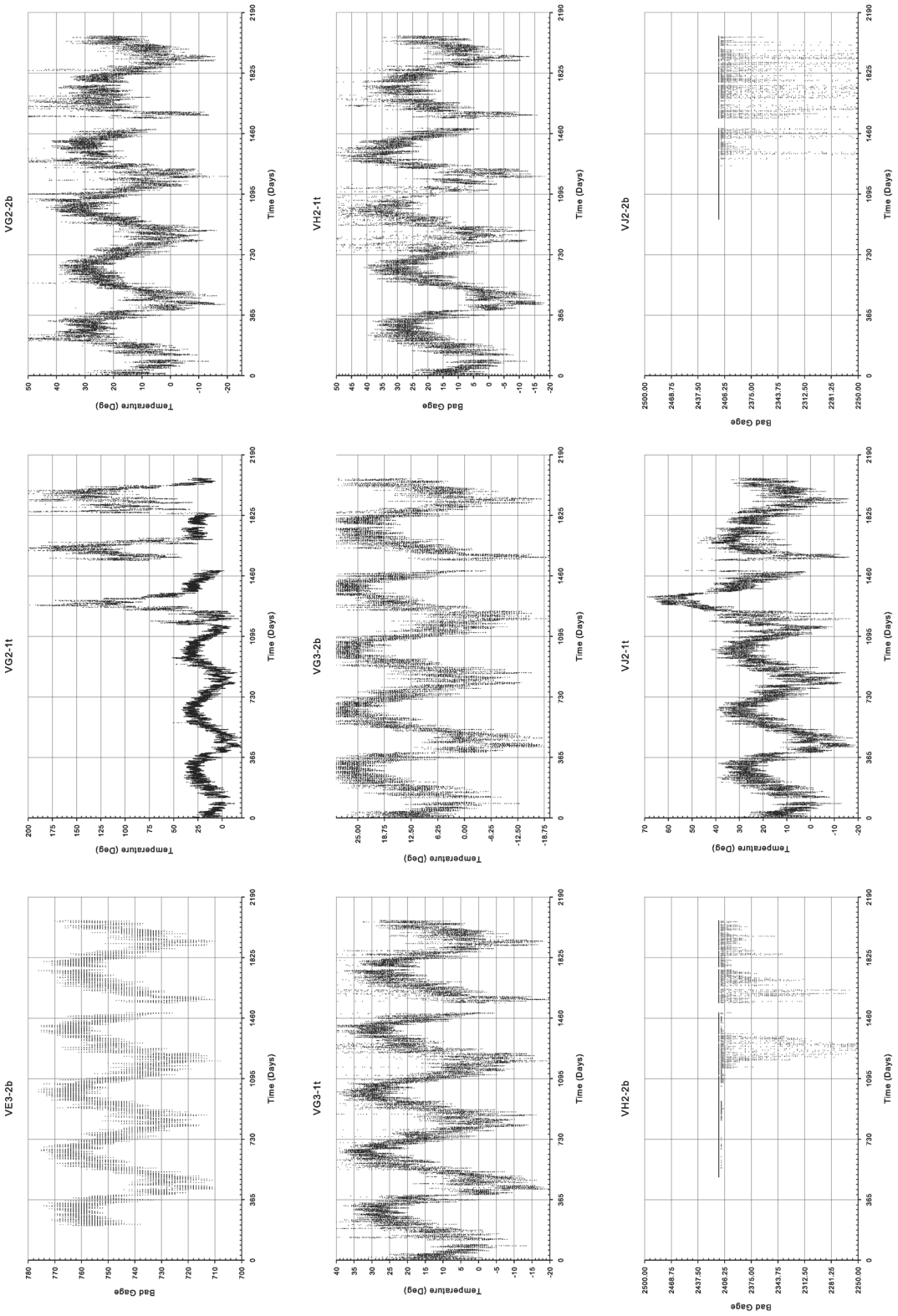

Figure A-9: Raw Sensor Data

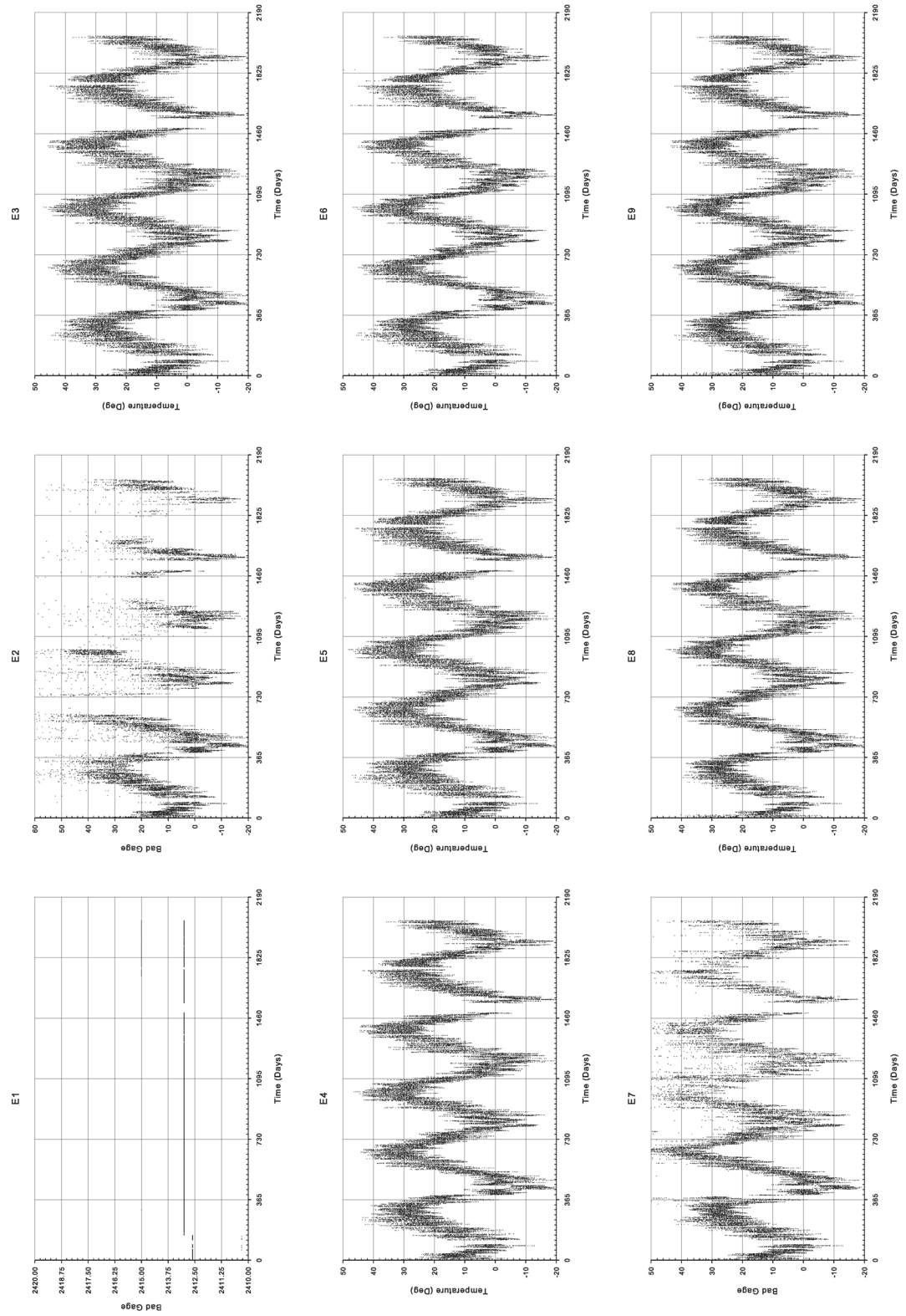

Figure A-10: Raw Sensor Data

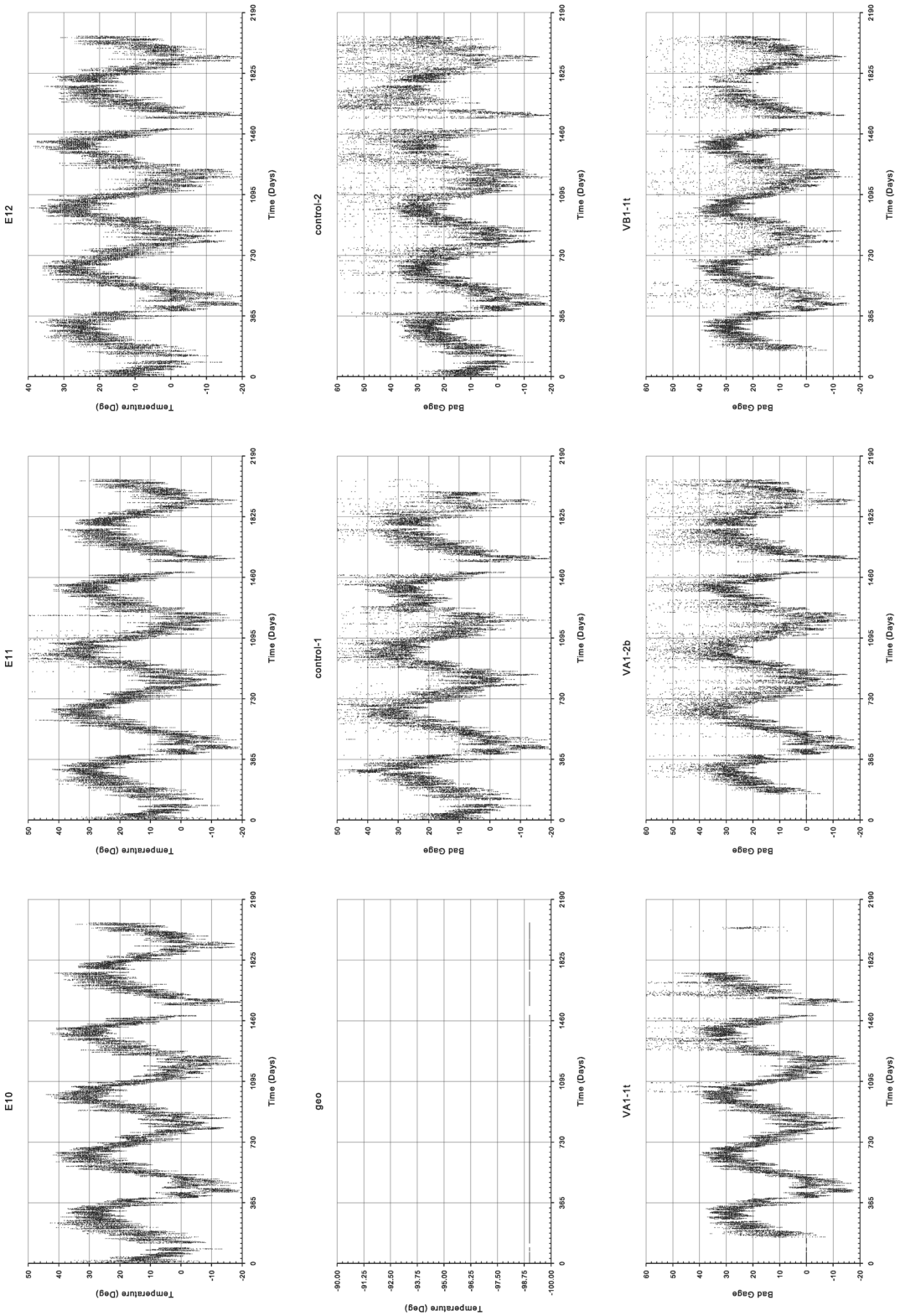

Figure A-11: Raw Sensor Data

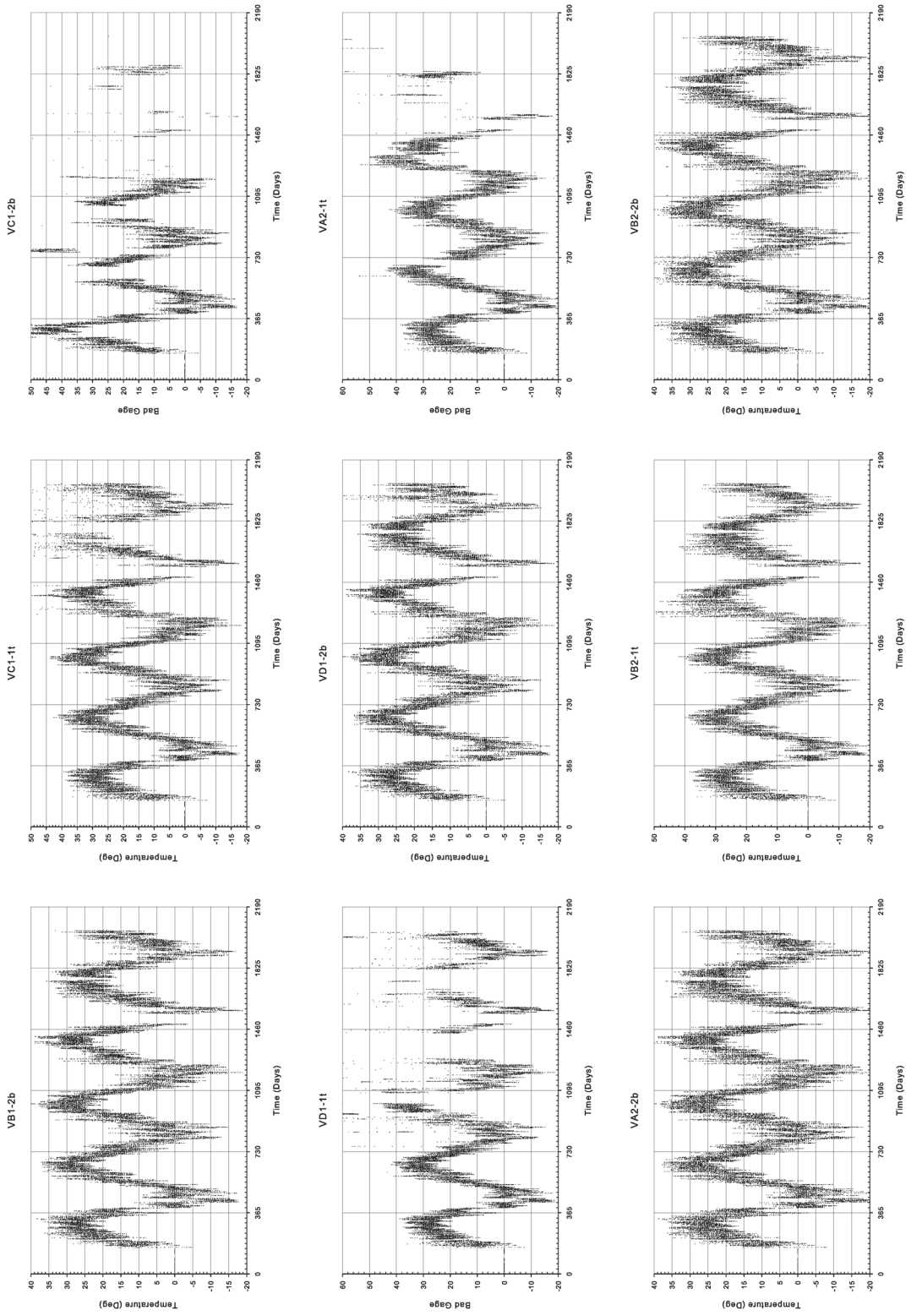

Figure A-12: Raw Sensor Data

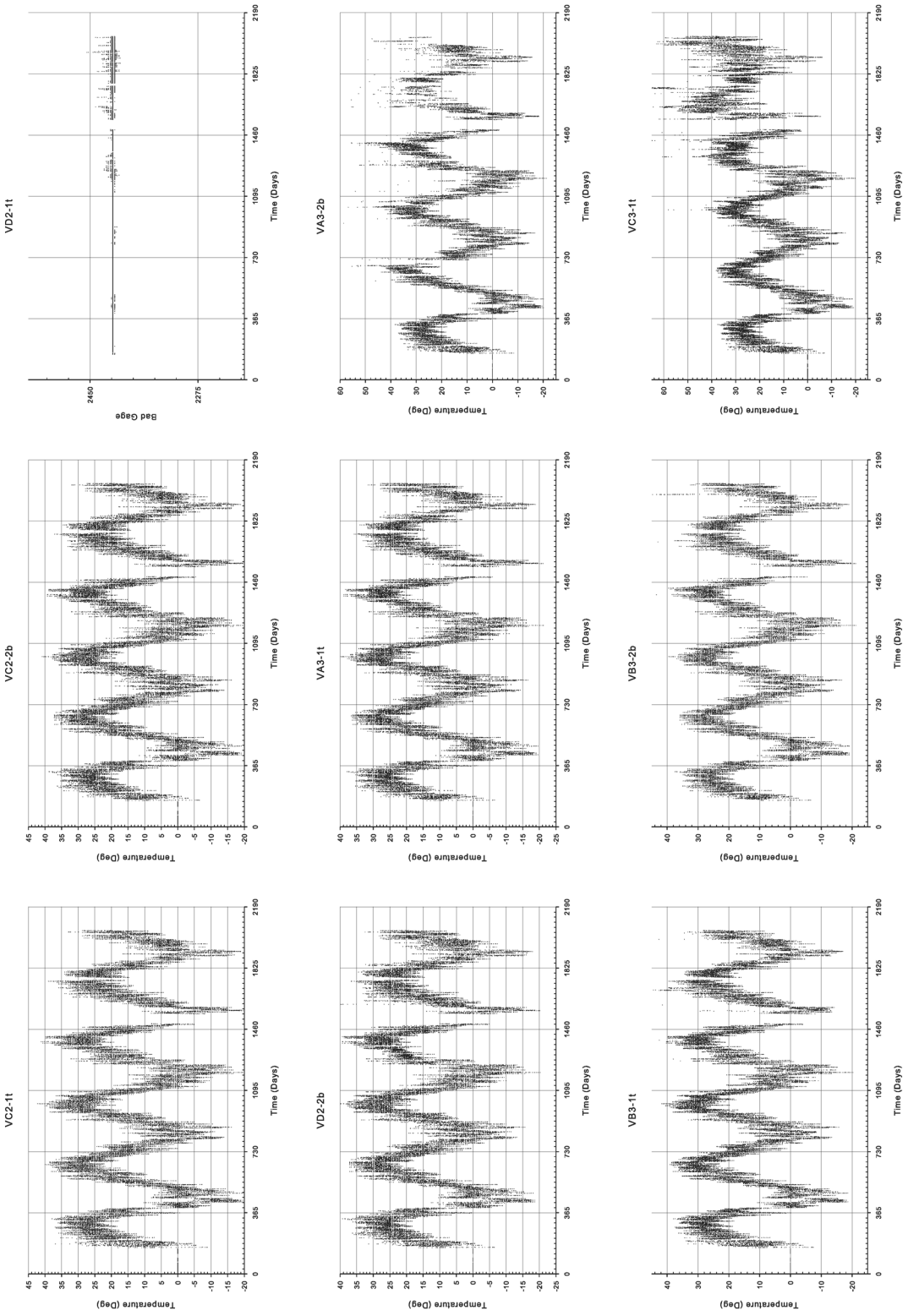

Figure A-13: Raw Sensor Data

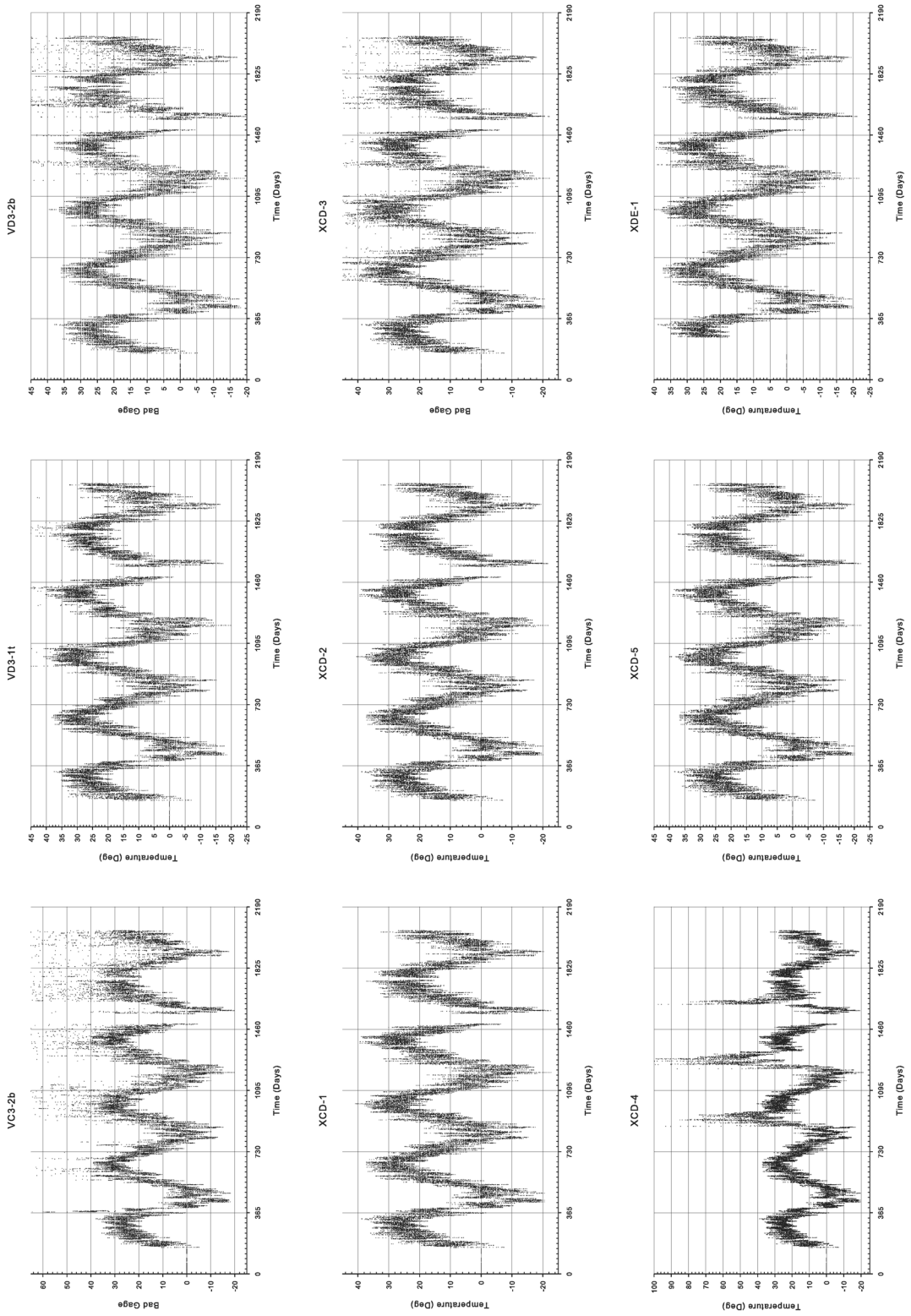

Figure A-14: Raw Sensor Data

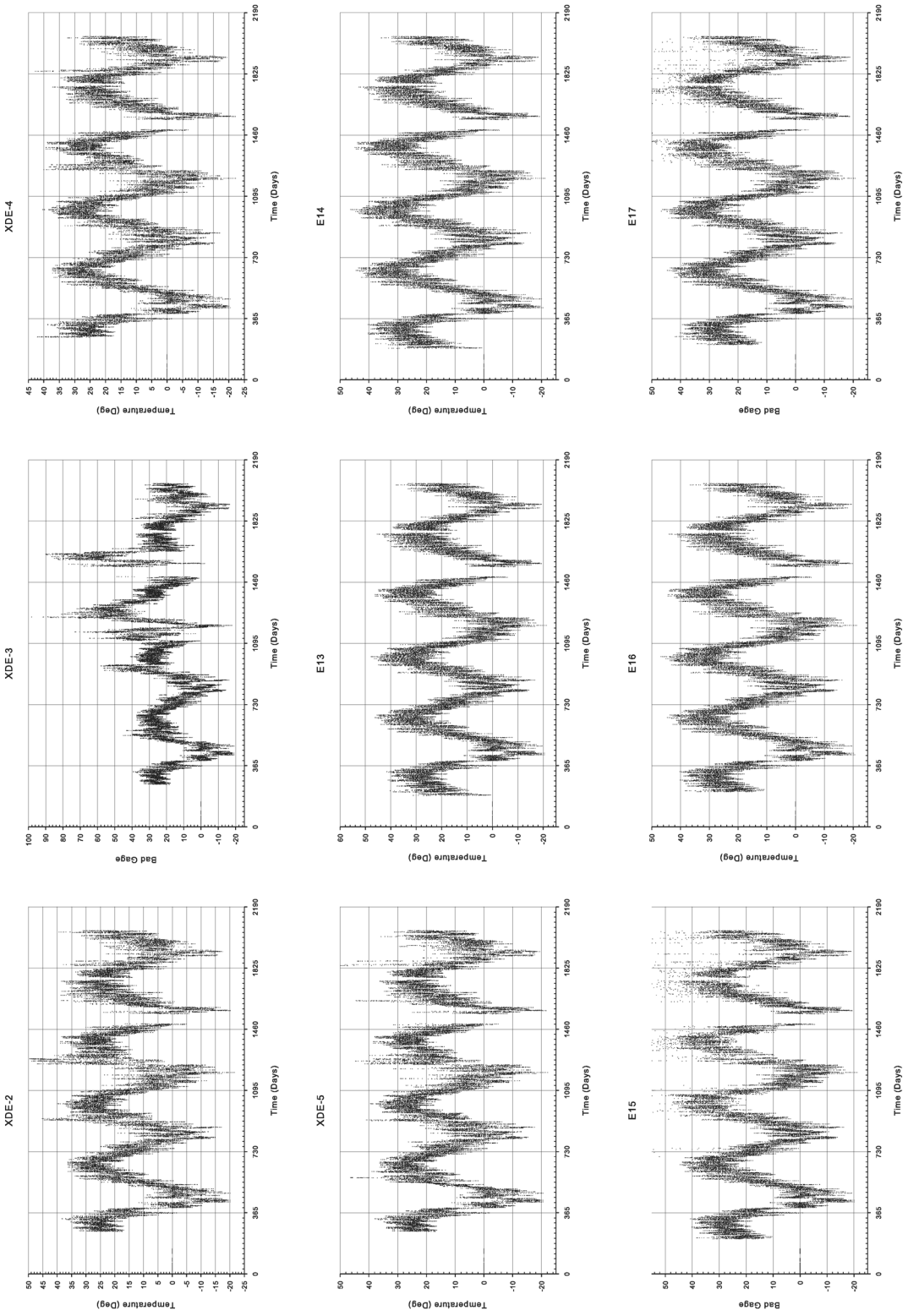

Figure A-15: Raw Sensor Data

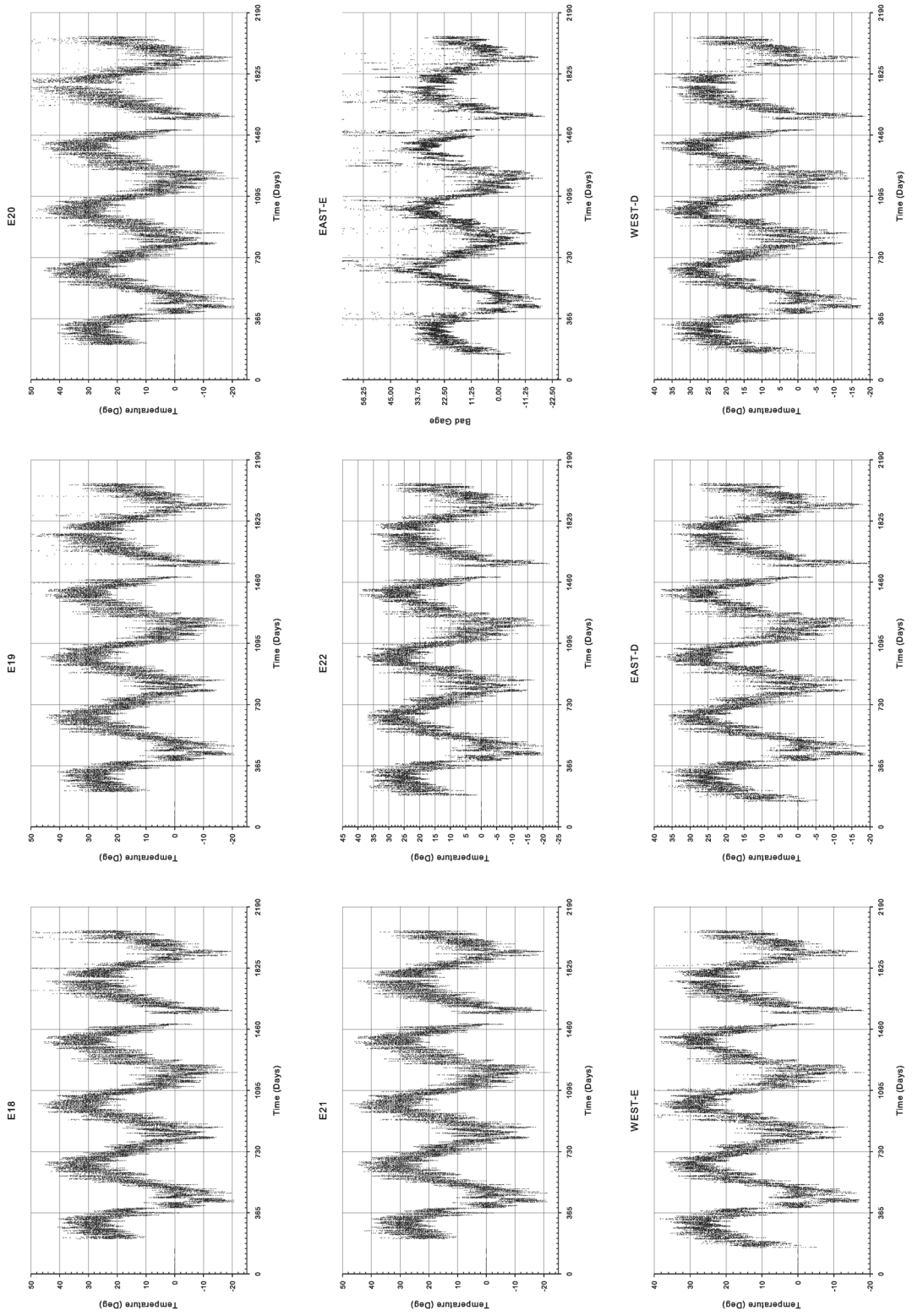

Figure A-16: Raw Sensor Data

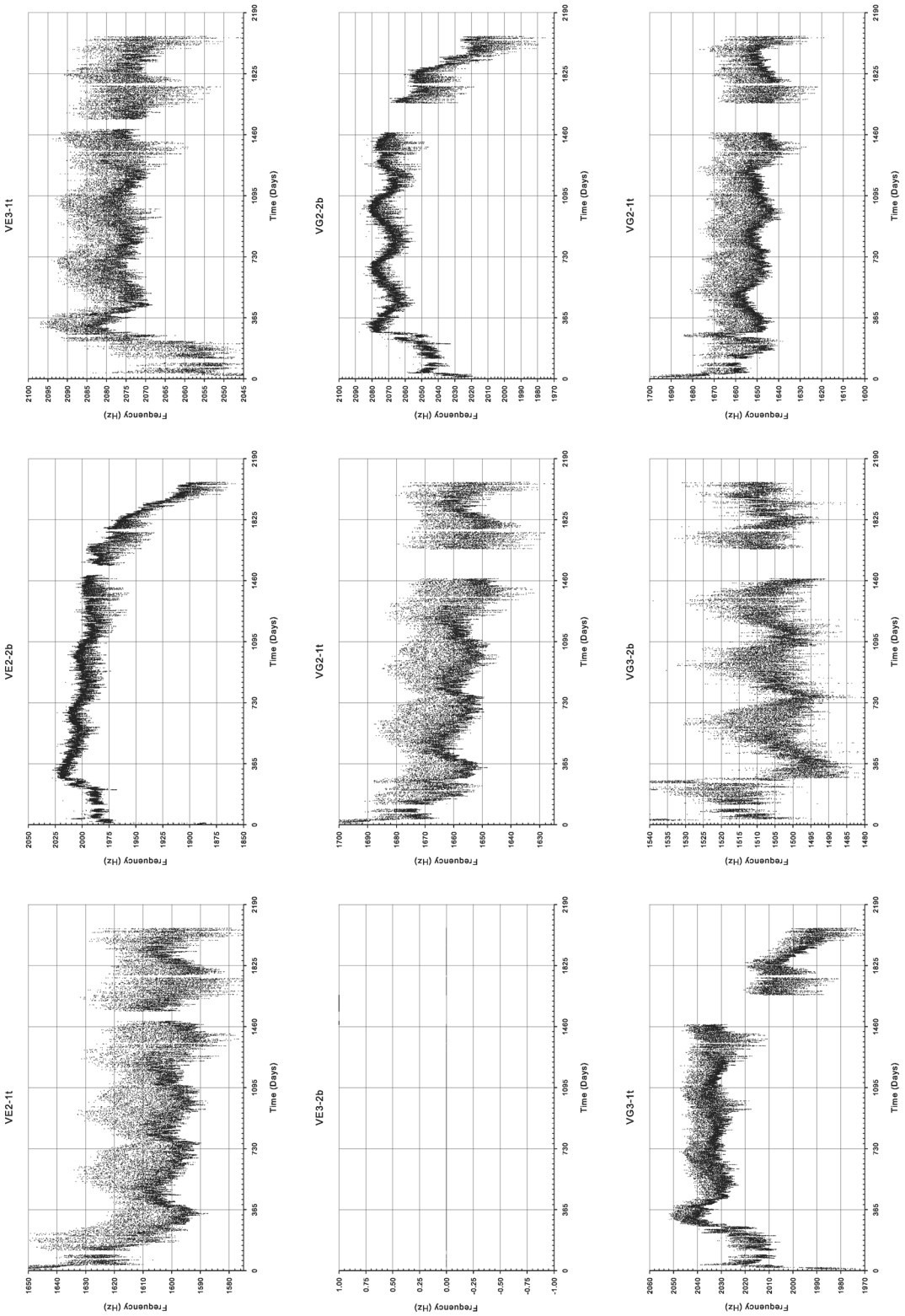

Figure A-17: Raw Sensor Data

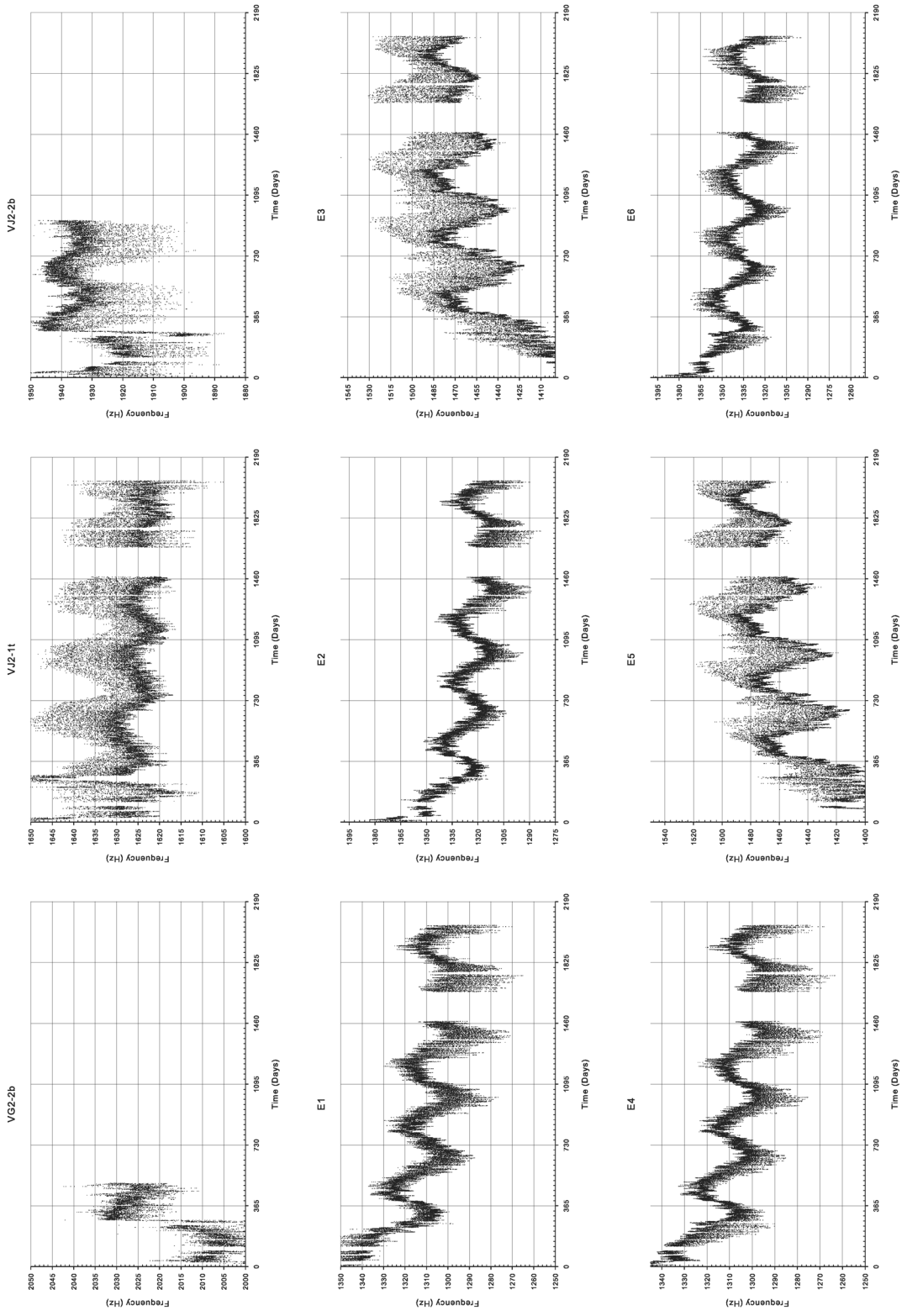

Figure A-18: Raw Sensor Data

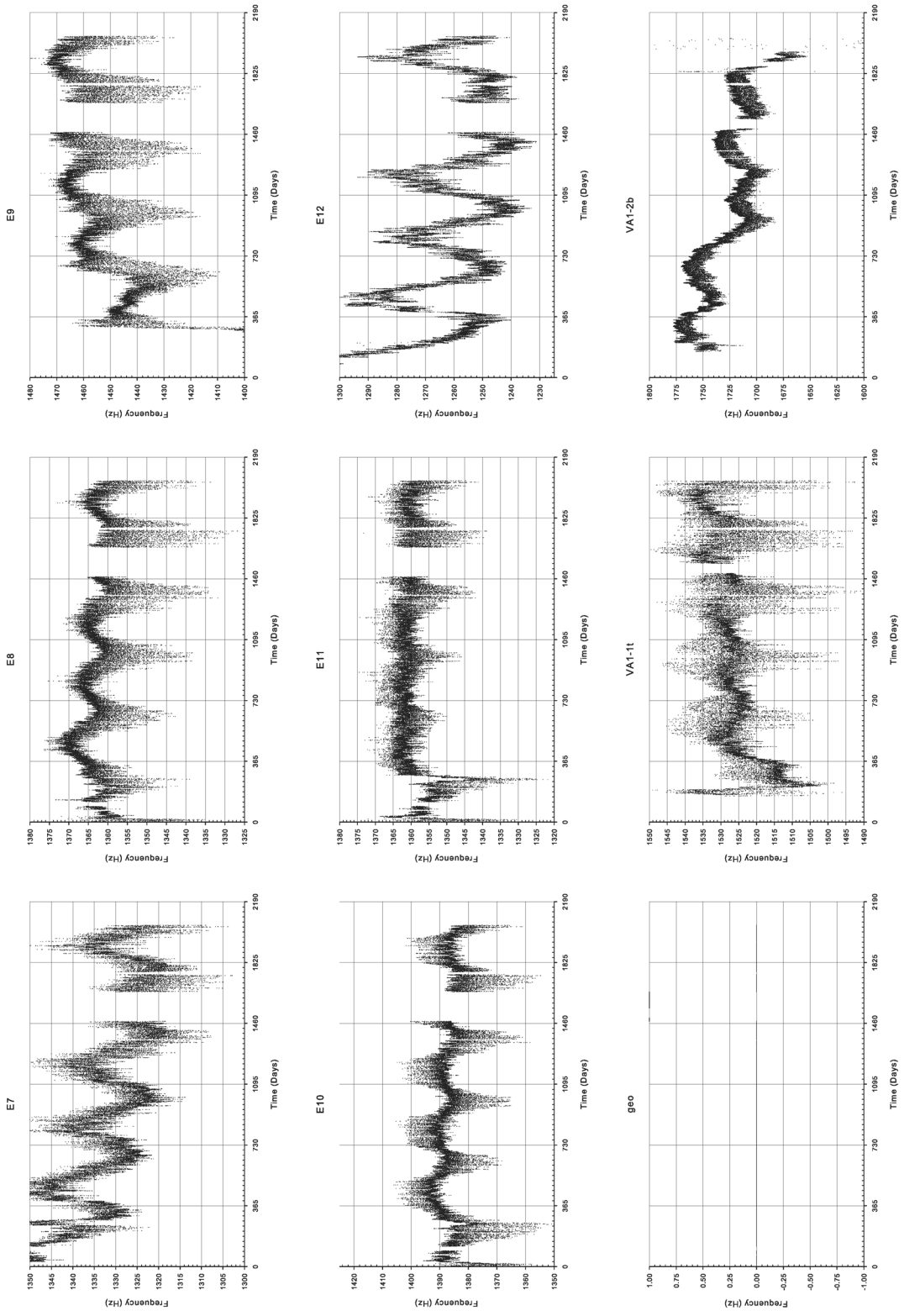

Figure A-19: Raw Sensor Data

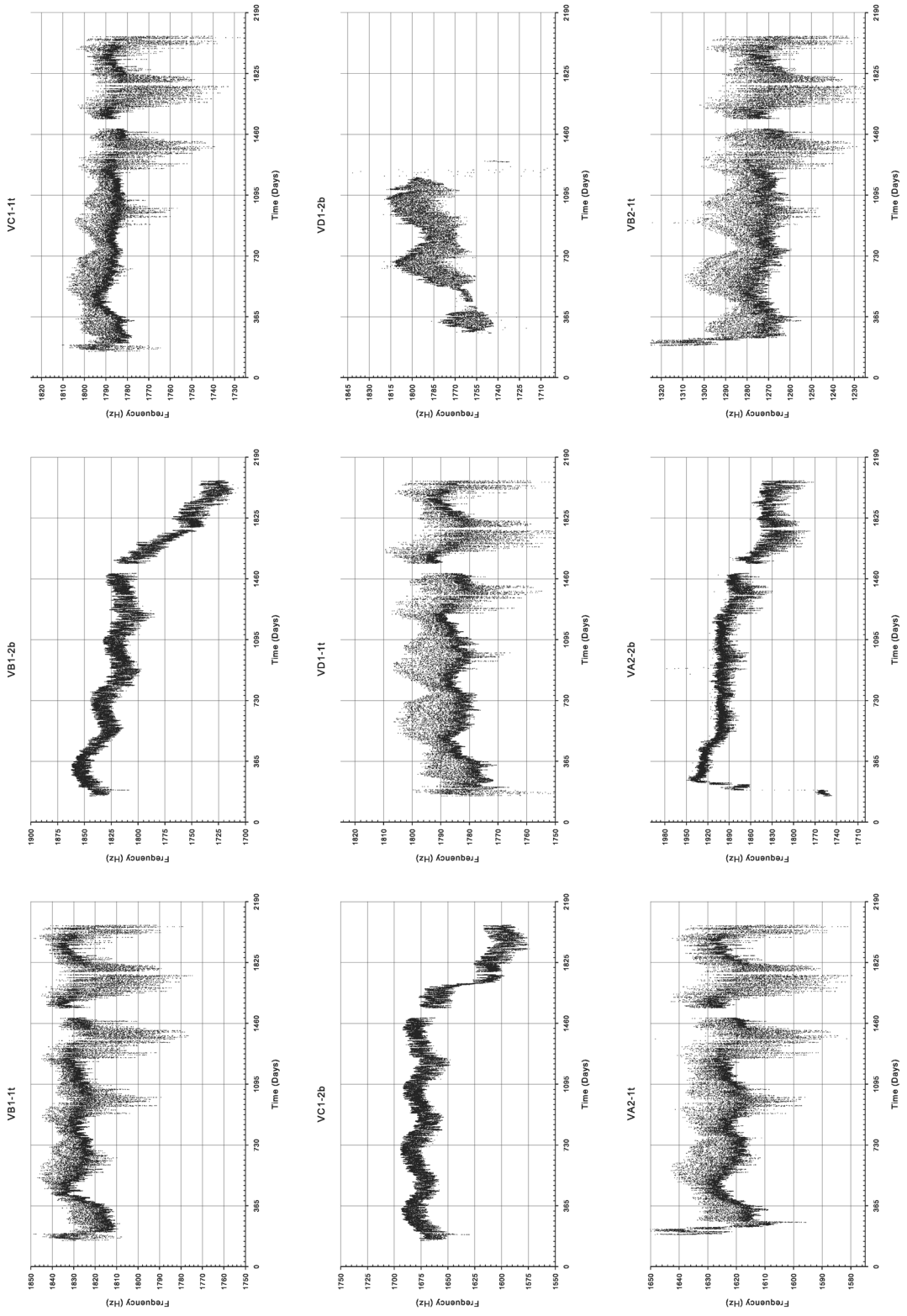

Figure A-20: Raw Sensor Data

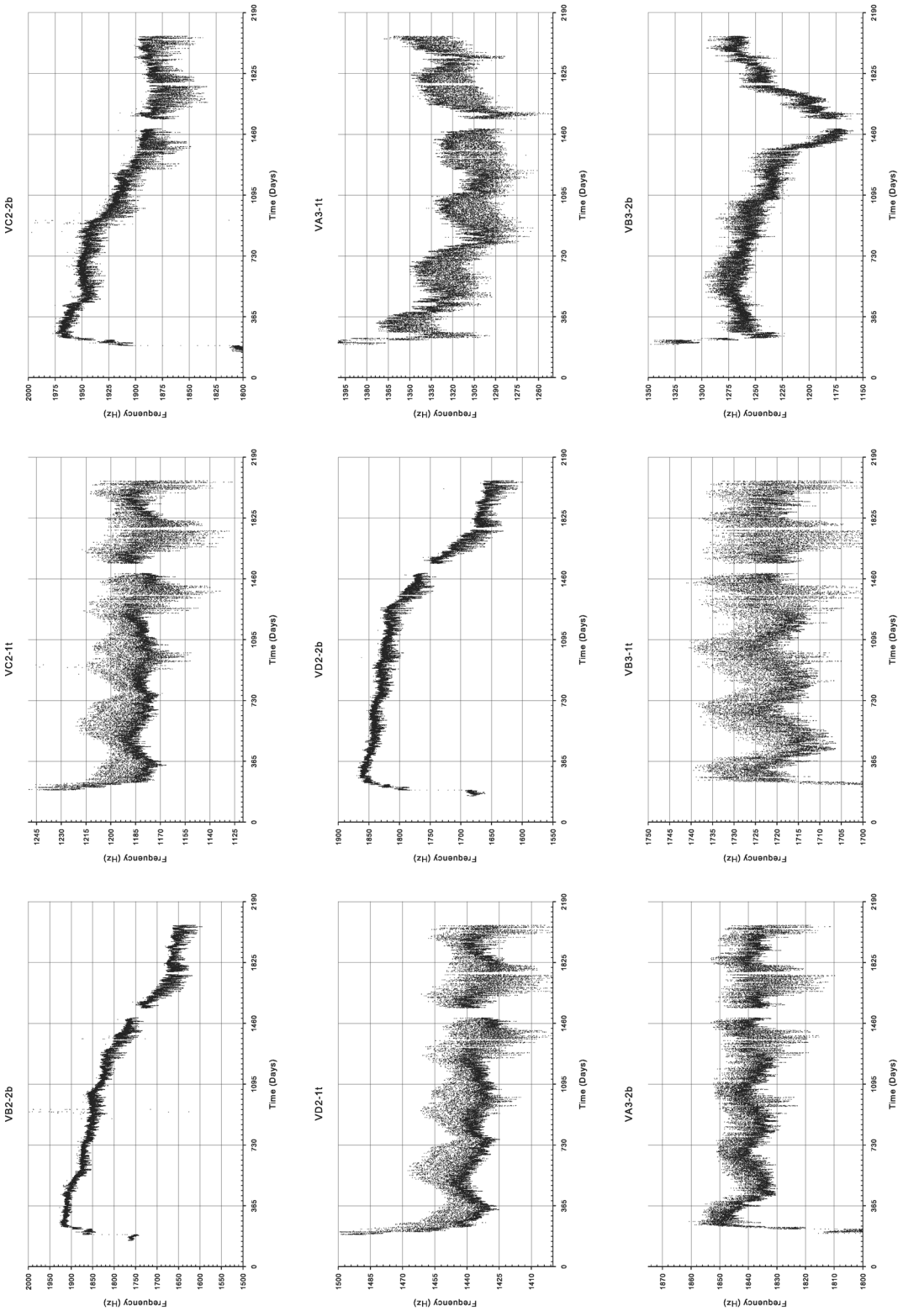

Figure A-21: Raw Sensor Data

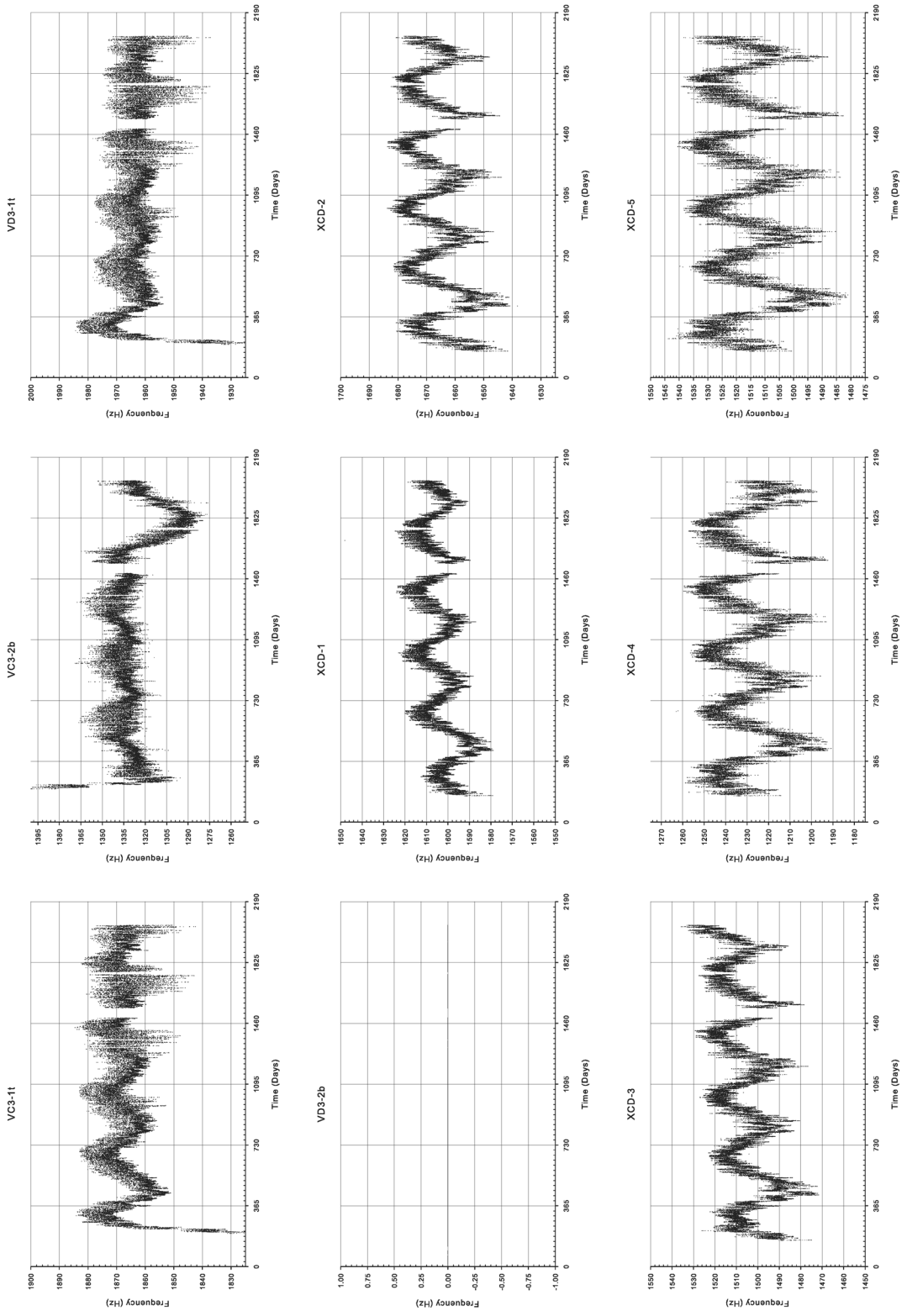

Figure A-22: Raw Sensor Data

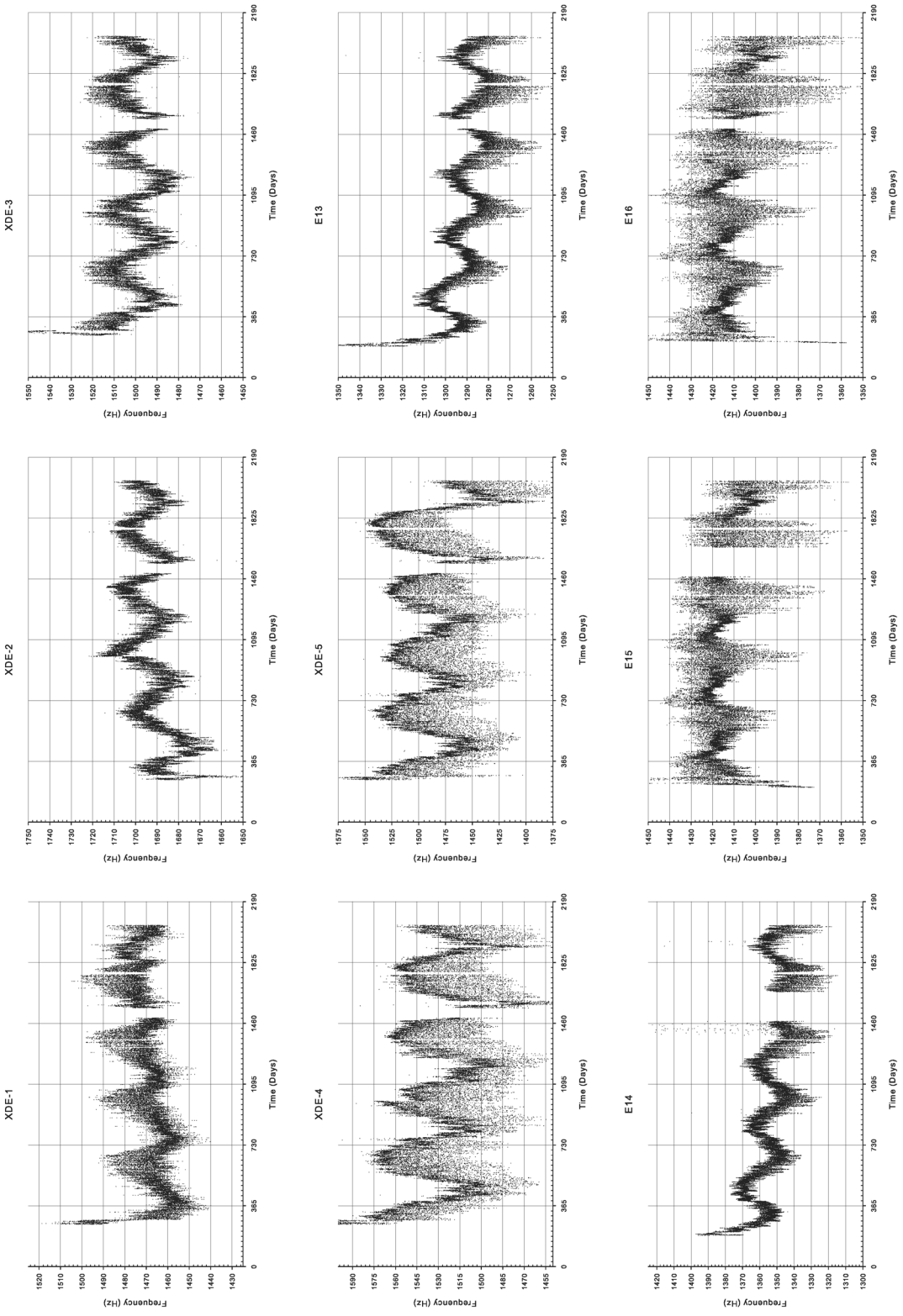

Figure A-23: Raw Sensor Data

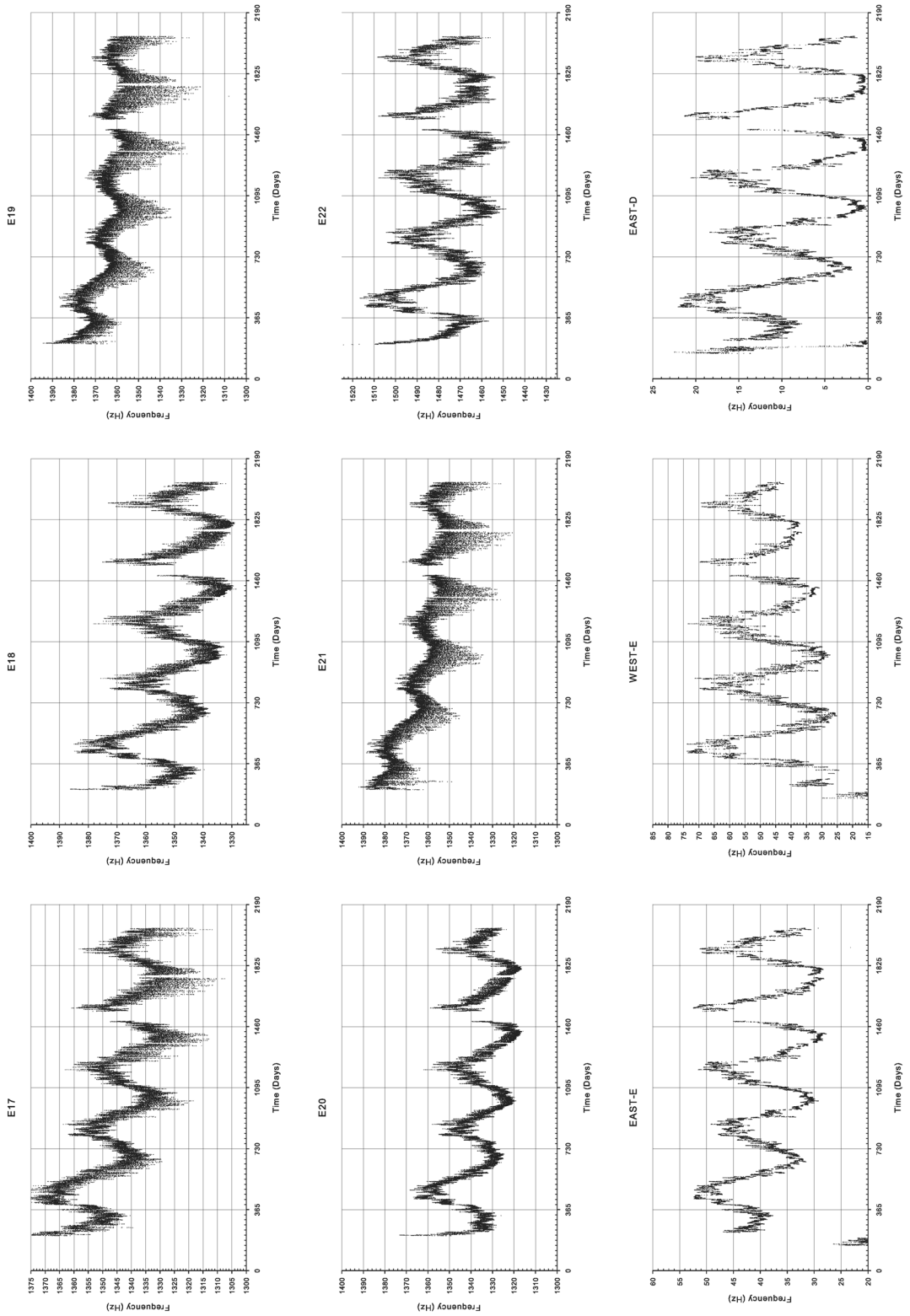

Figure A-24: Raw Sensor Data

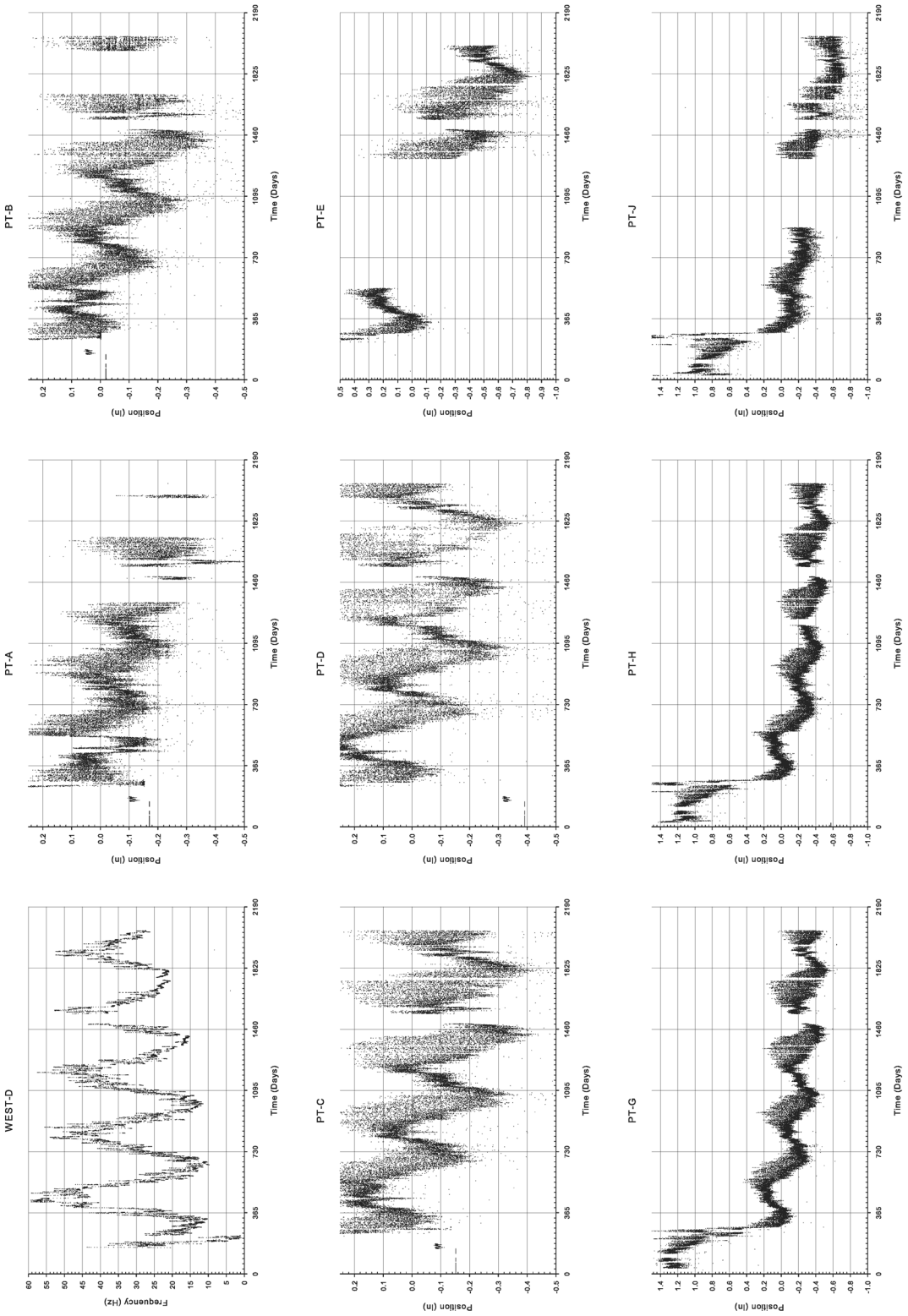

Figure A-25: Raw Sensor Data

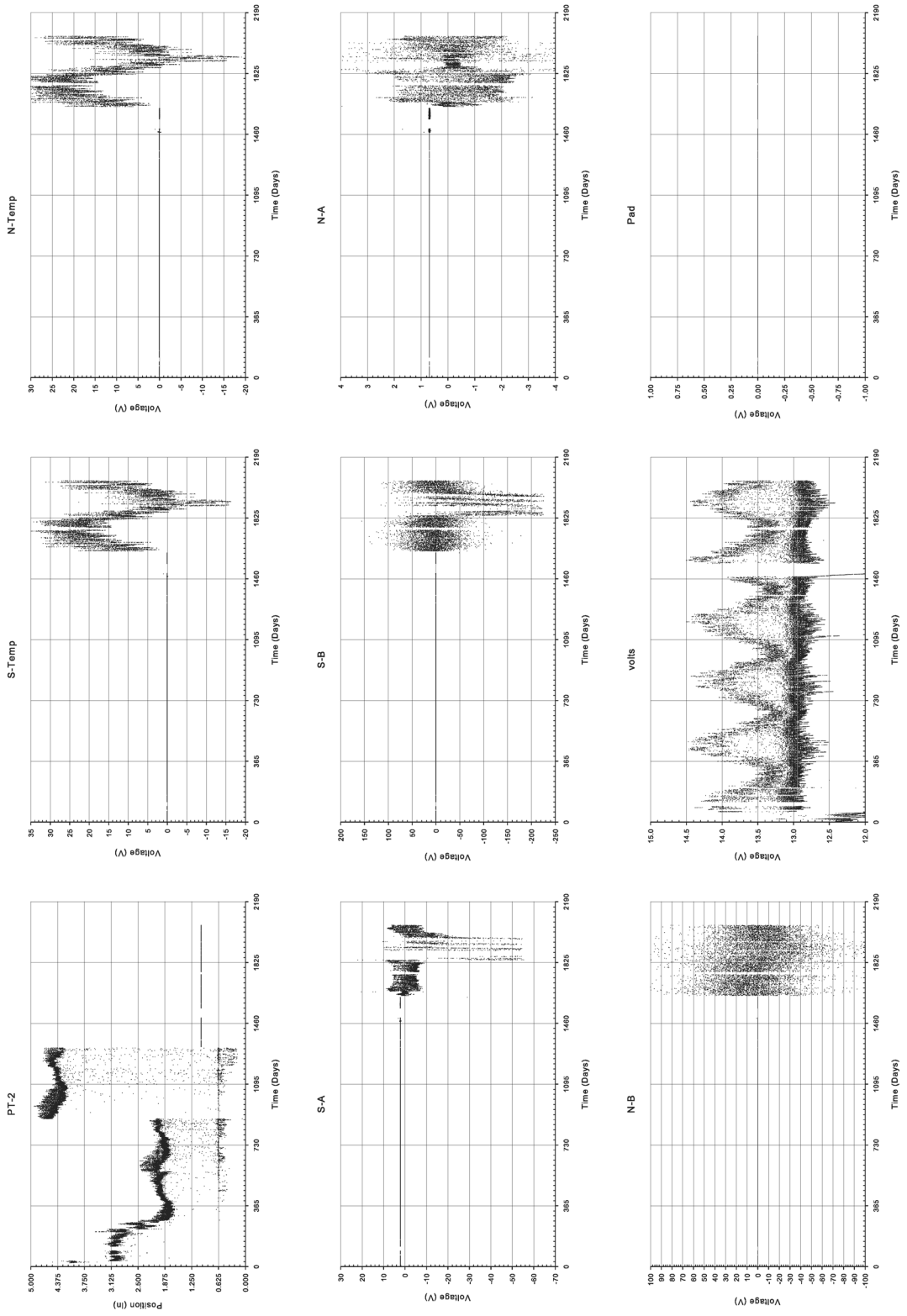

Figure A-26: Raw Sensor Data

A.2 Filtered Data

The following figures contain daily filtered data from instrumentation used in the project.

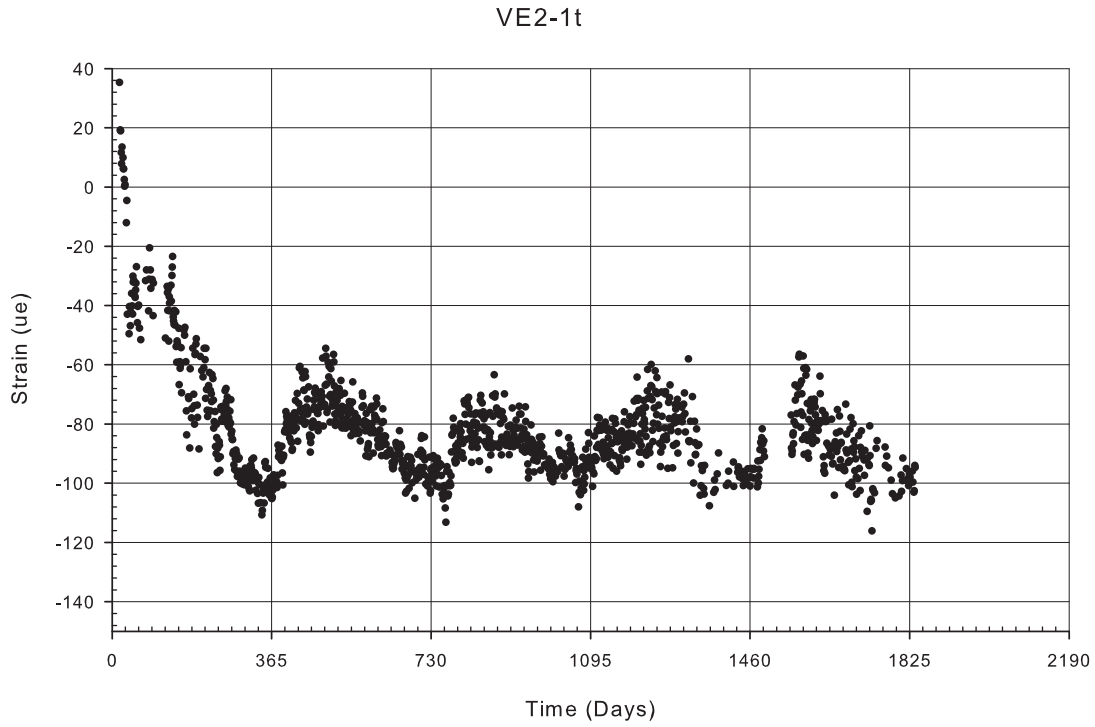

Figure A-27: Gage VE2-1t filtered strain data

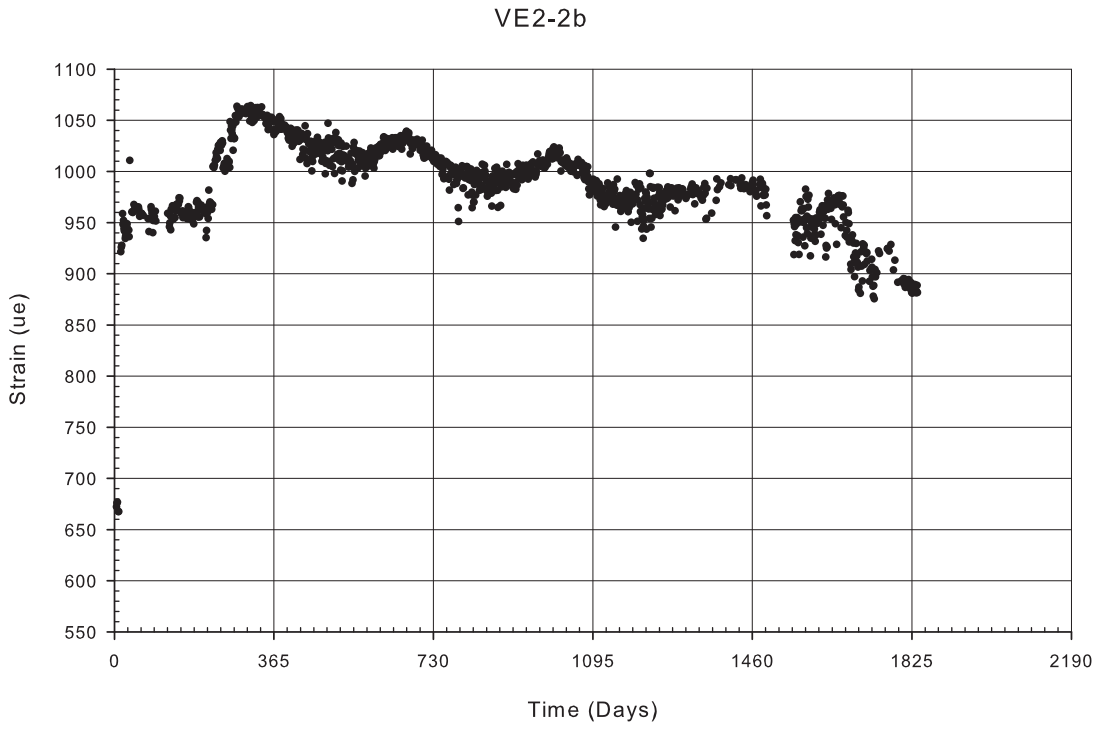

Figure A-28: Gage VE2-2b filtered strain data

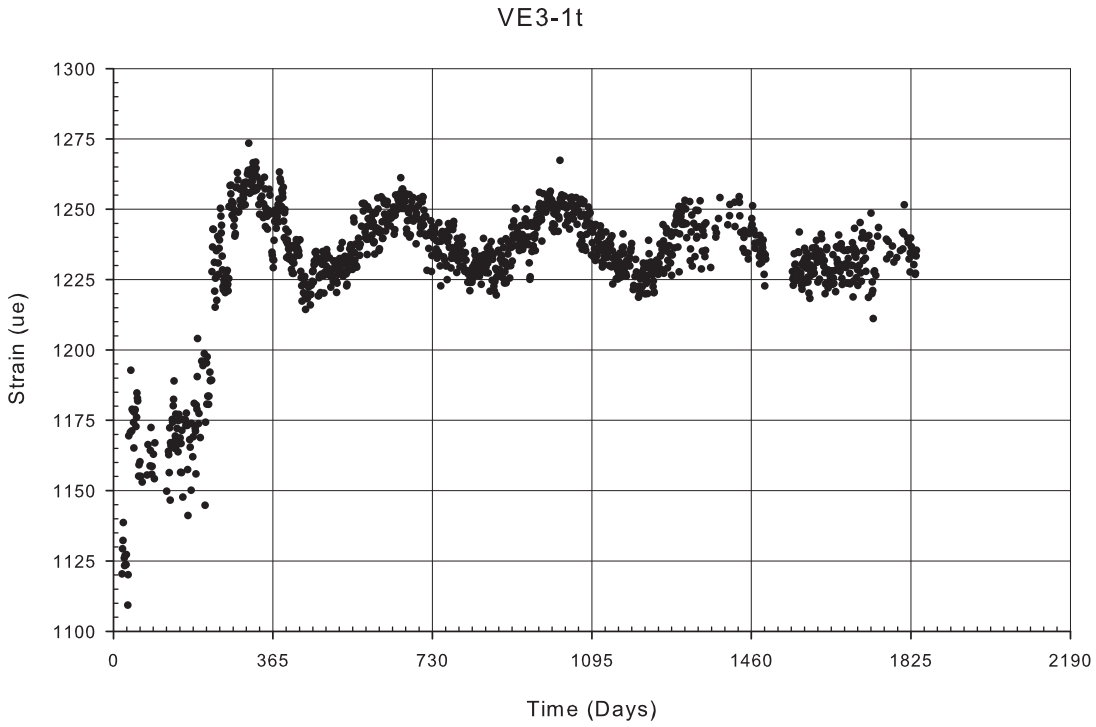

Figure A-29: Gage VE3-1t filtered strain data

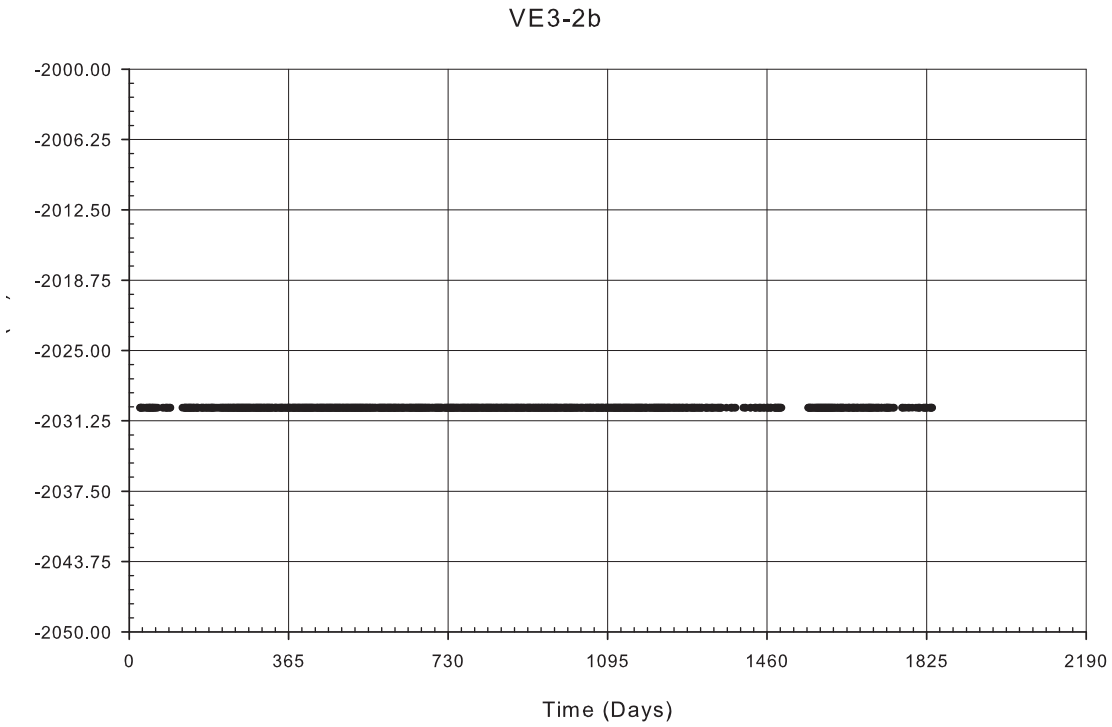

Figure A-30: Gage VE3-2b filtered strain data

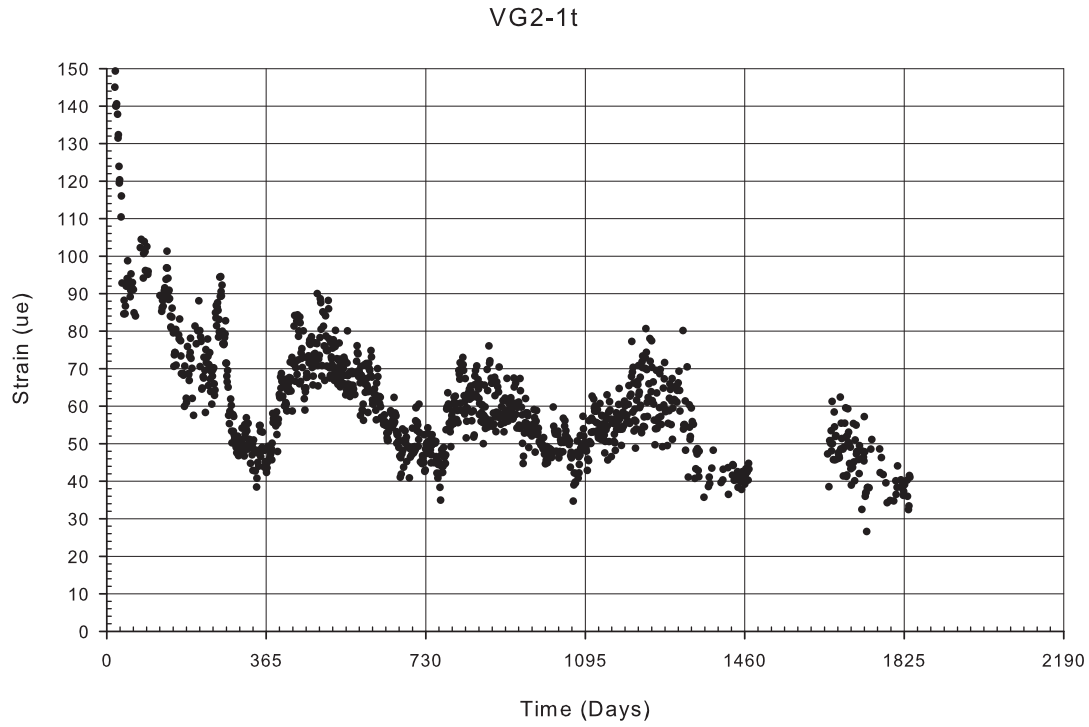

Figure A-31: Gage VG2-1t filtered strain data

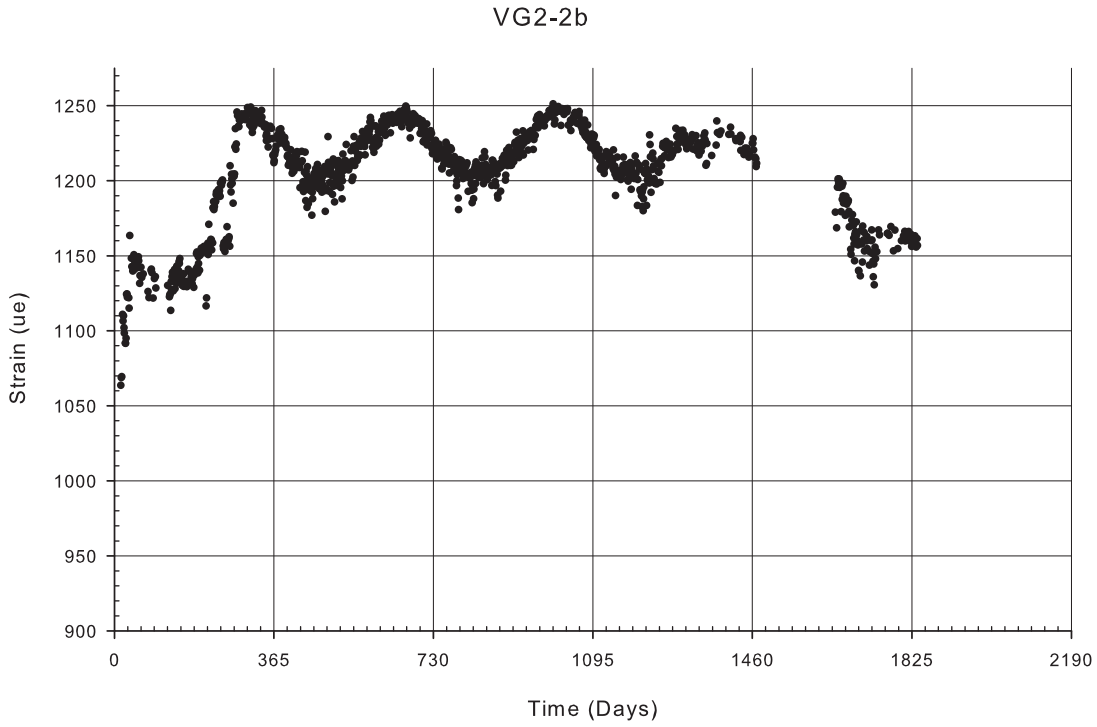

Figure A-32: Gage VG2-2b filtered strain data

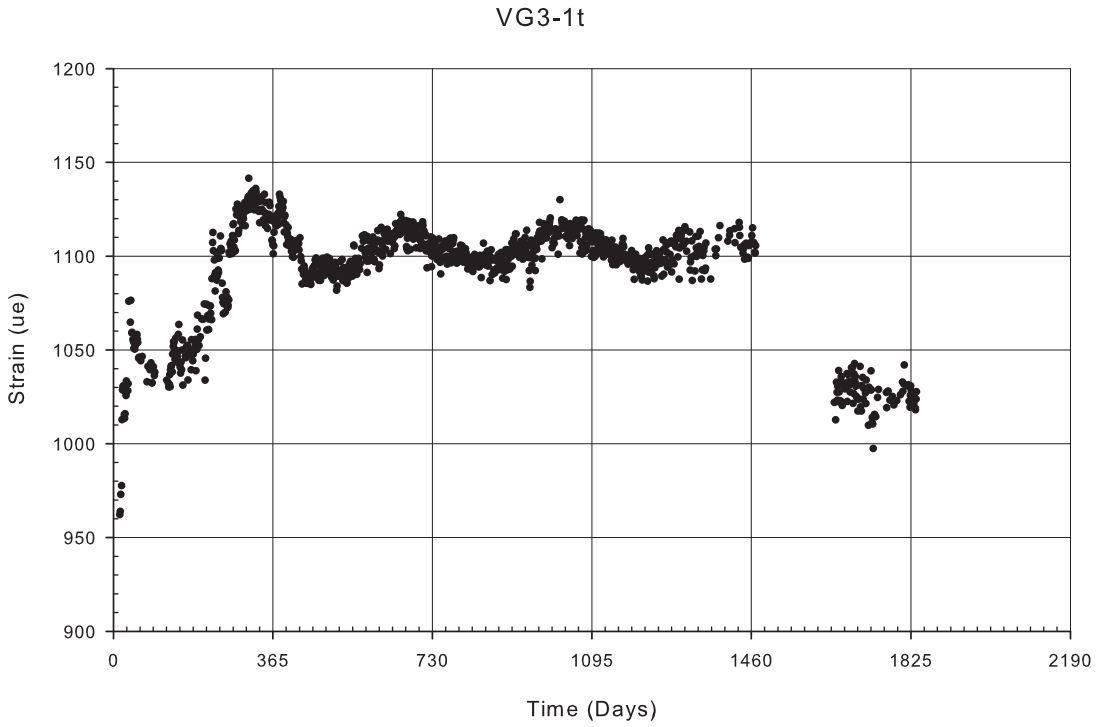

Figure A-33: Gage VG3-1t filtered strain data

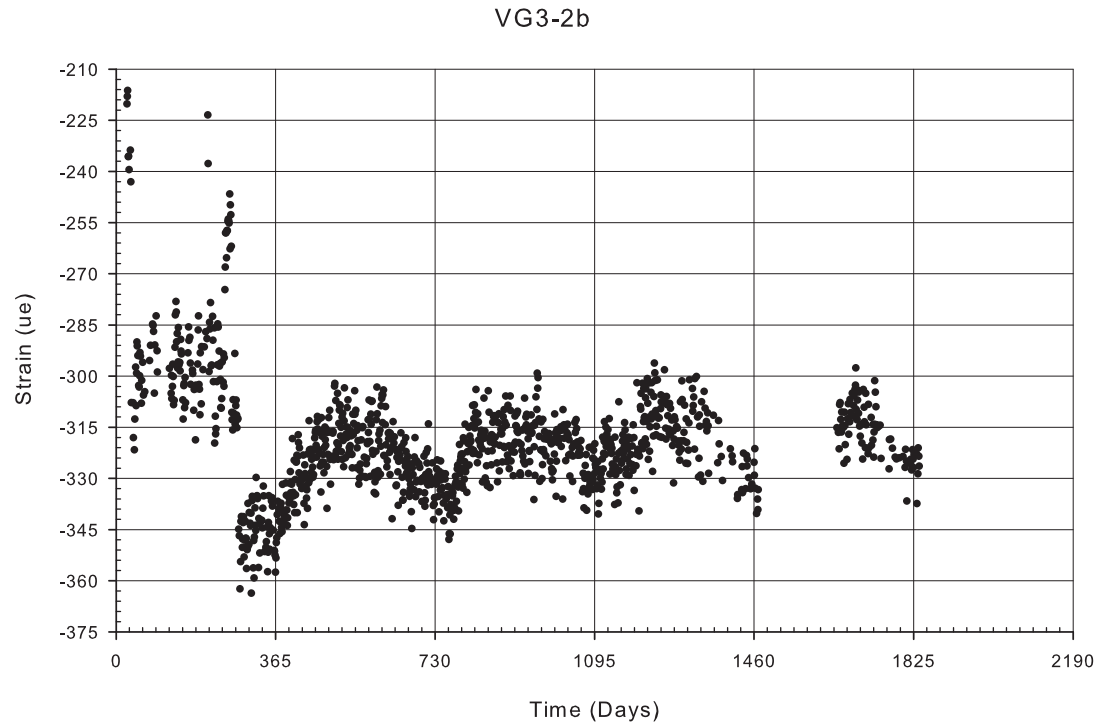

Figure A-34: Gage VG3-2b filtered strain data

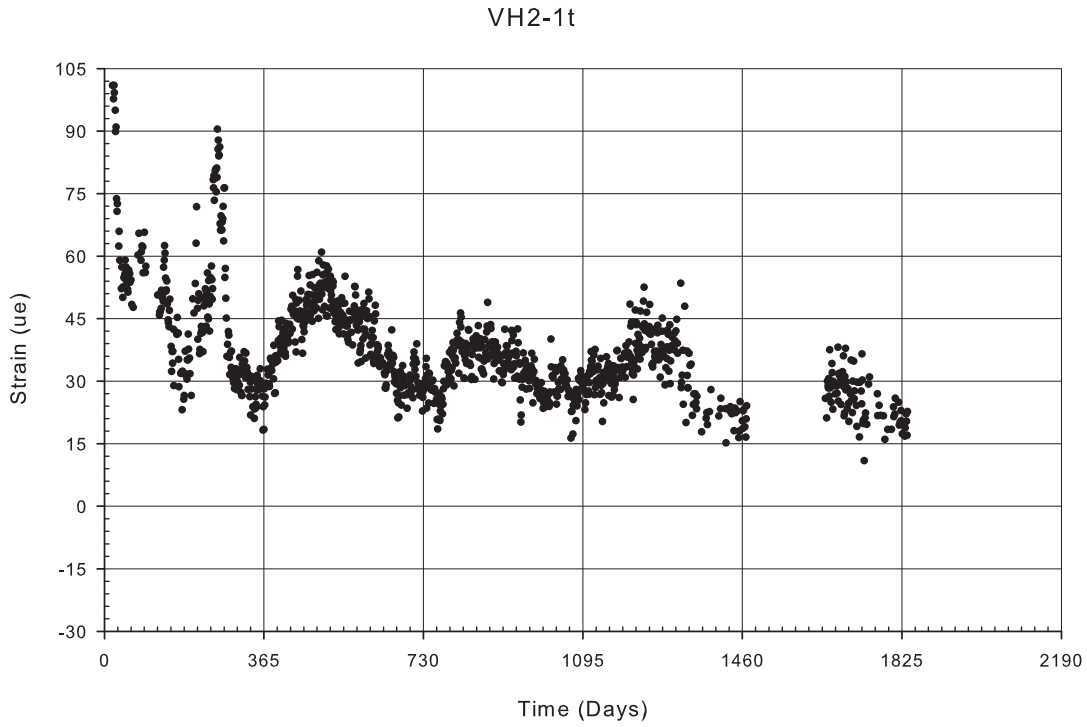

Figure A-35: Gage VH2-1t filtered strain data

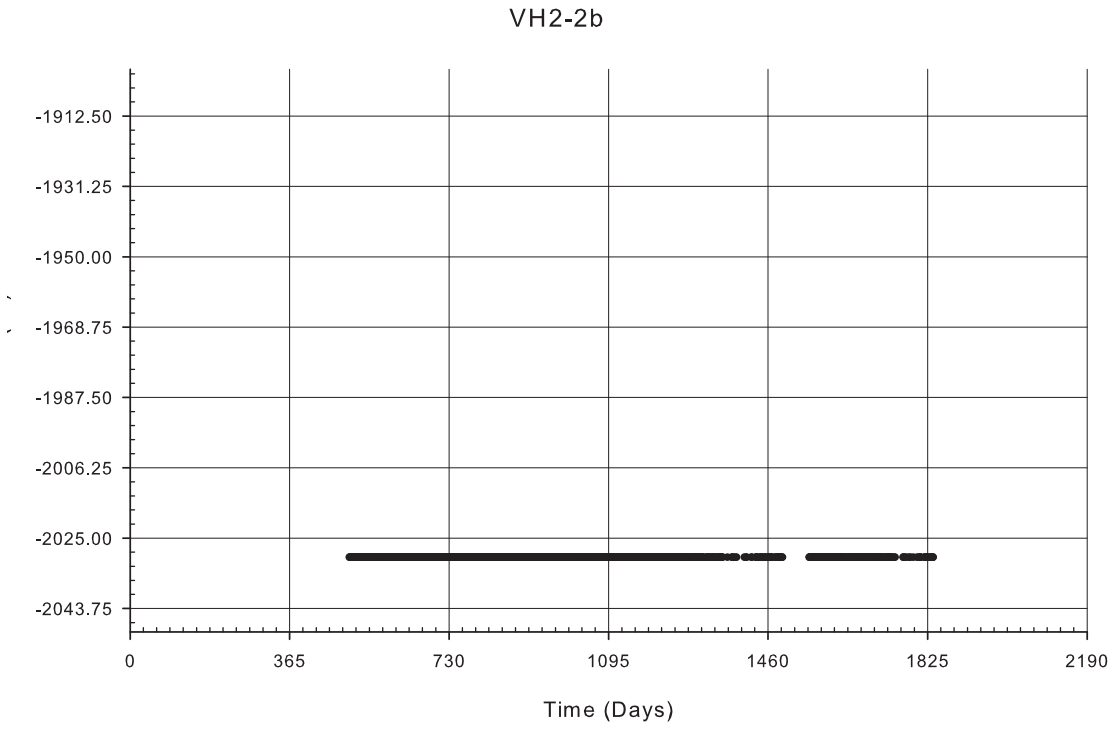

Figure A-36: Gage VH2-2b filtered strain data

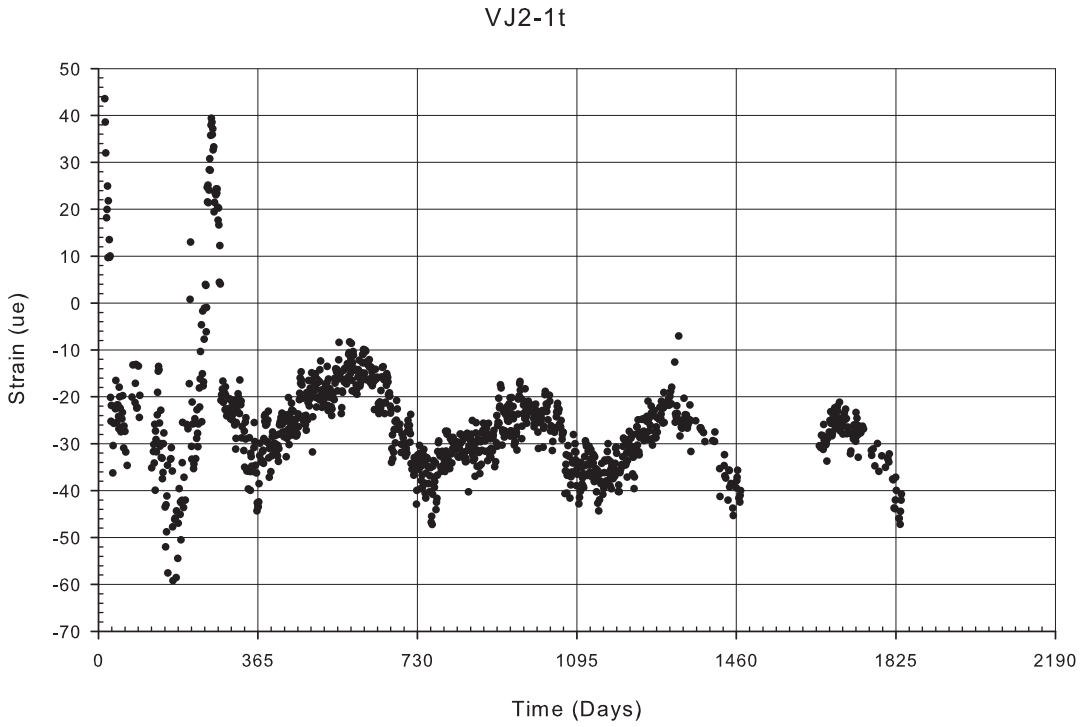

Figure A-37: Gage VJ2-1t filtered strain data

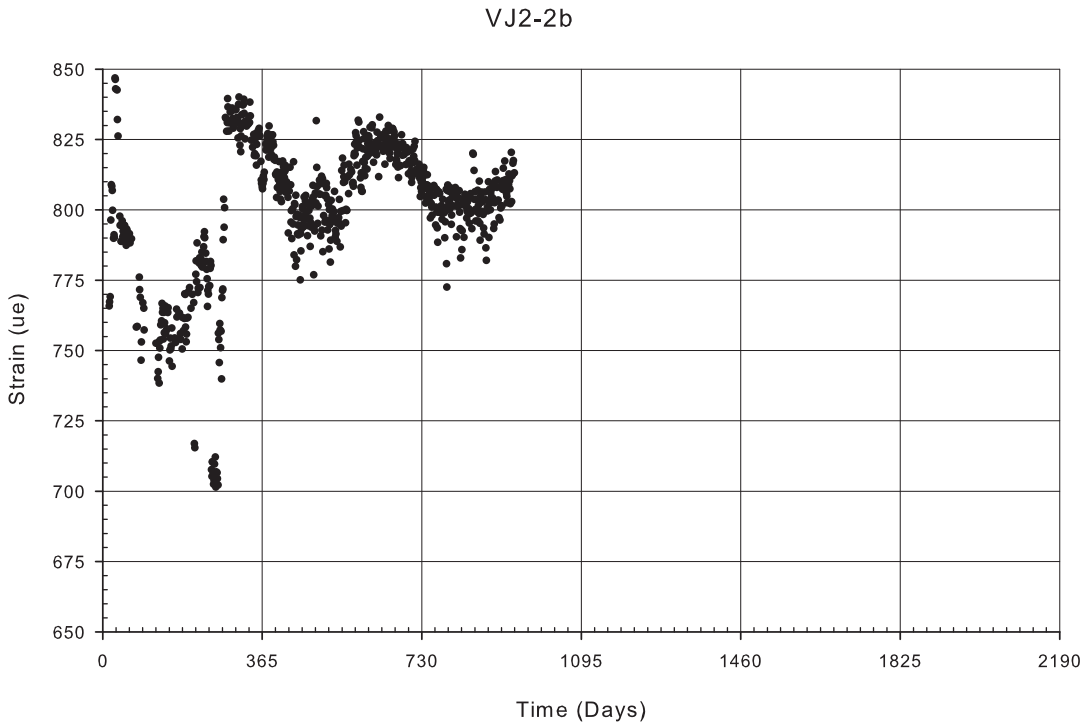

Figure A-38: Gage VJ2-2b filtered strain data

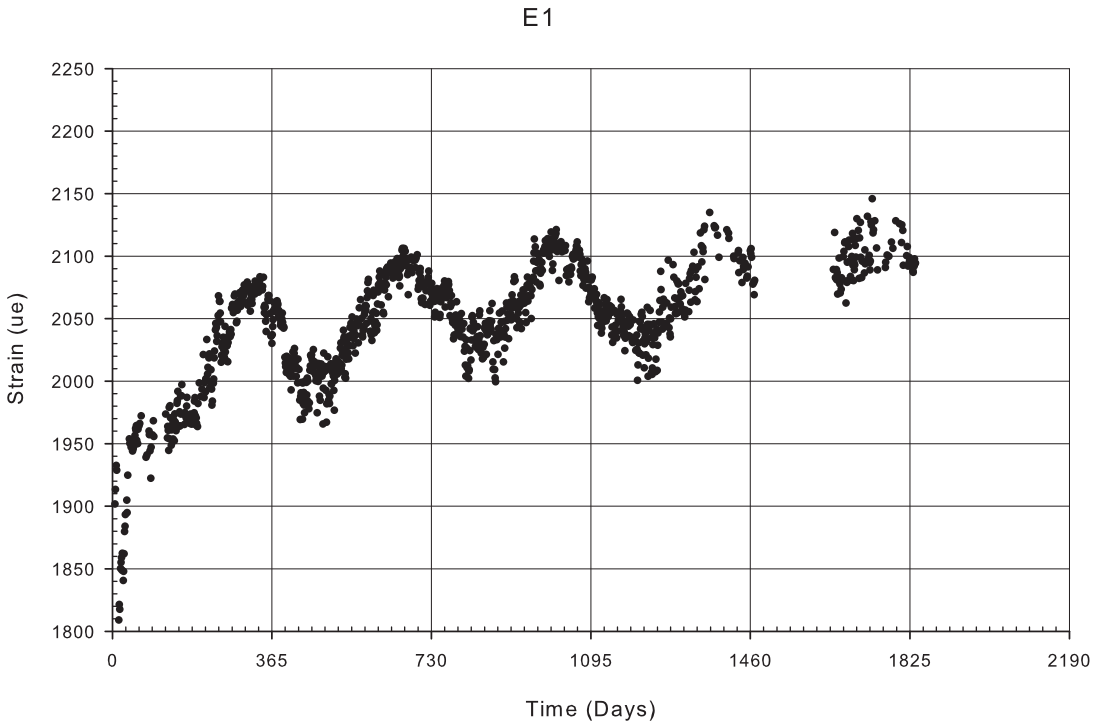

Figure A-39: Gage E1 filtered strain data

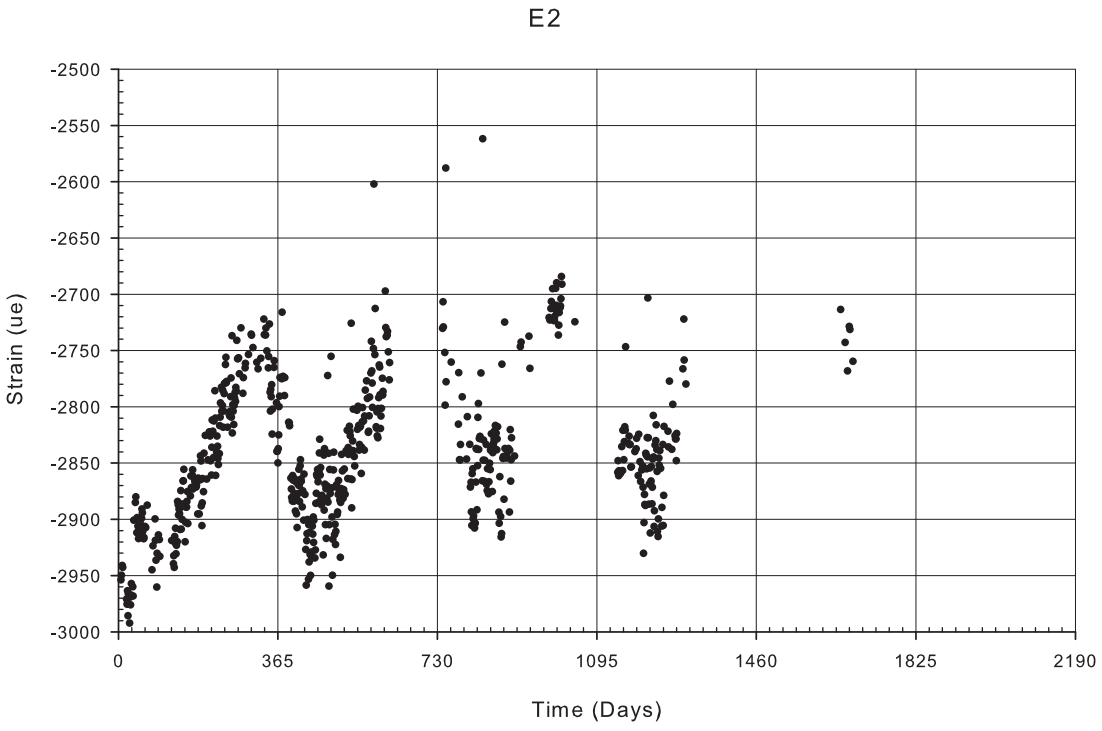

Figure A-40: Gage E2 filtered strain data

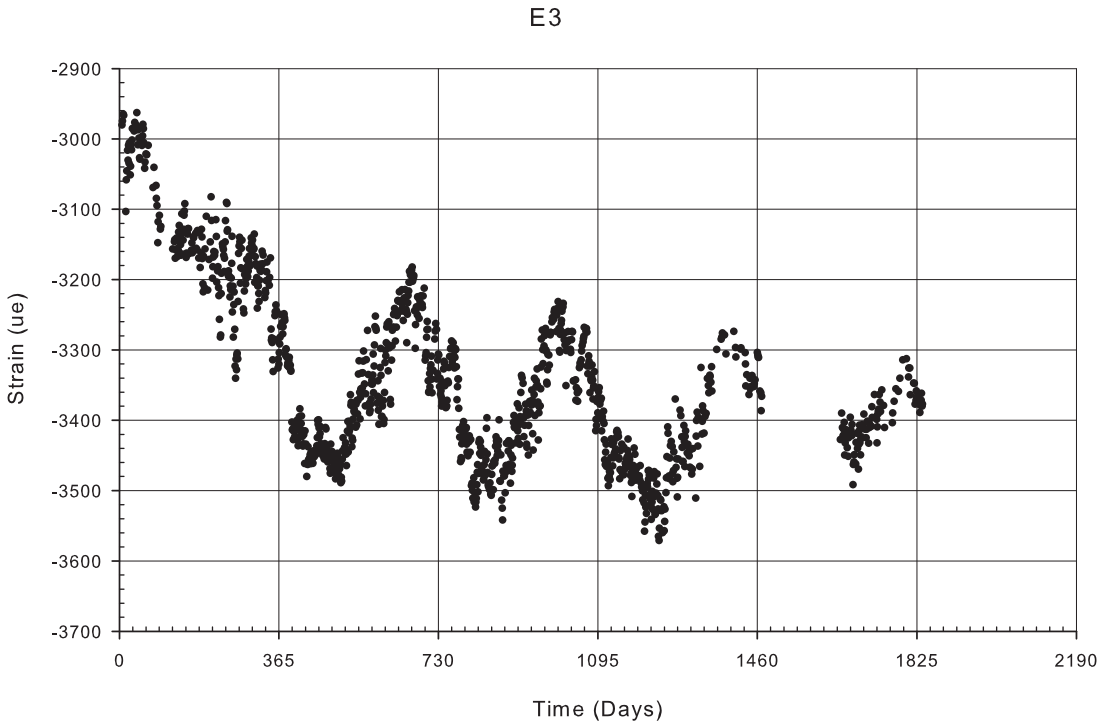

Figure A-41: Gage E3 filtered strain data

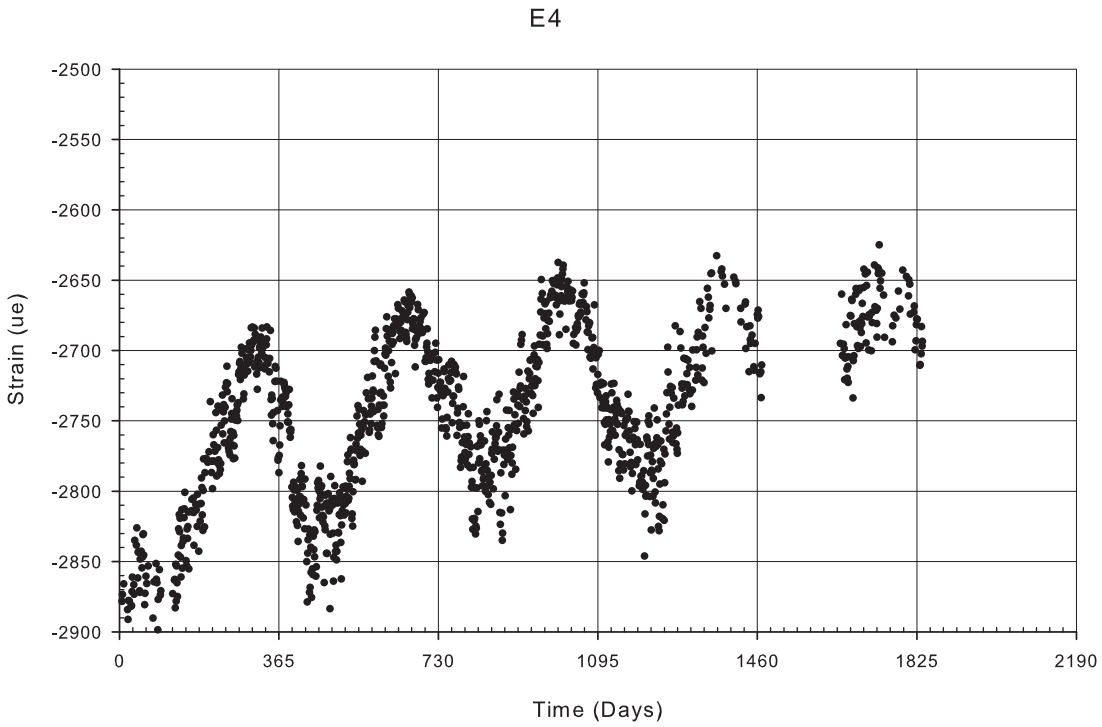

Figure A-42: Gage E4 filtered strain data

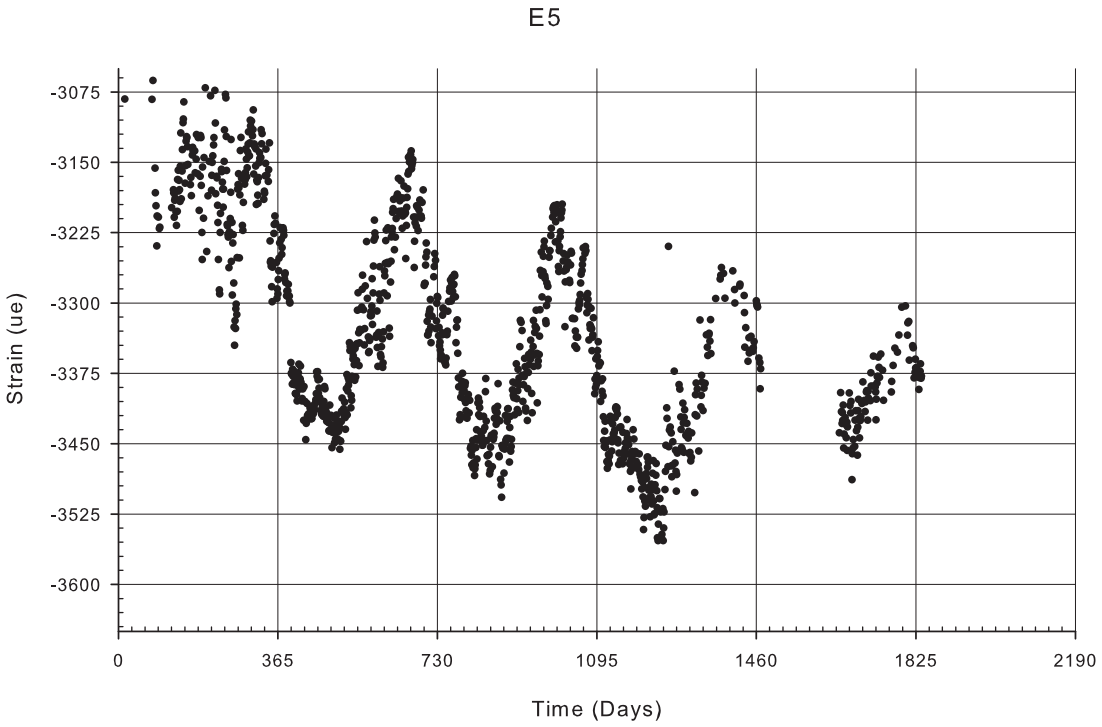

Figure A-43: Gage E5 filtered strain data

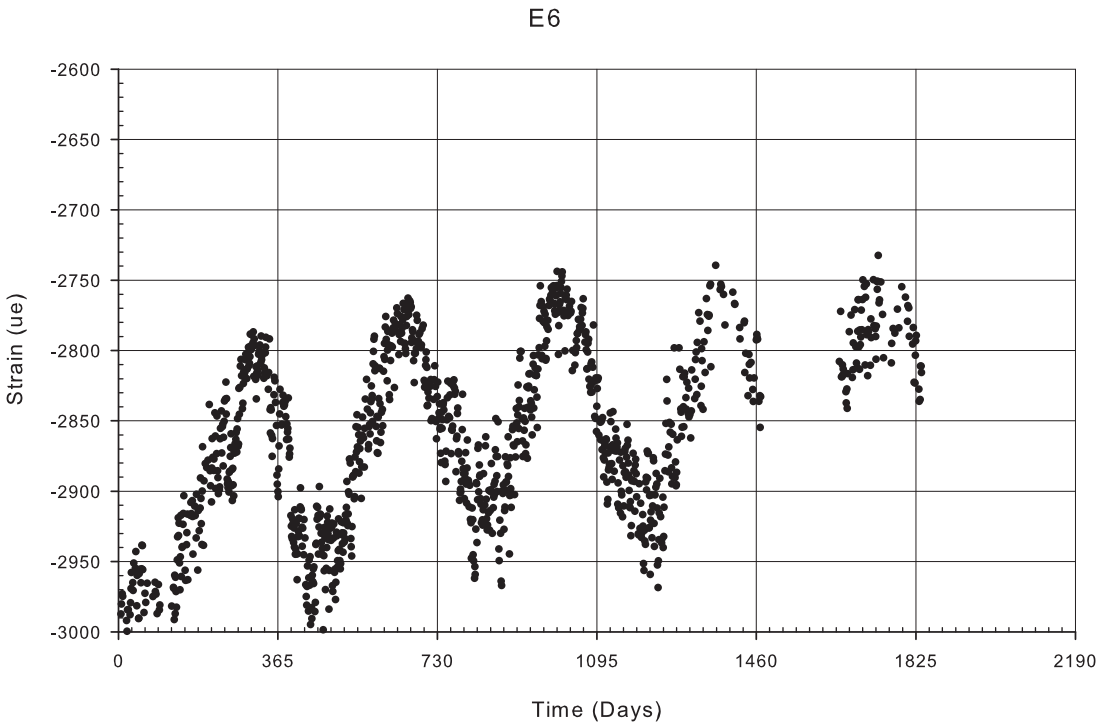

Figure A-44: Gage E6 filtered strain data

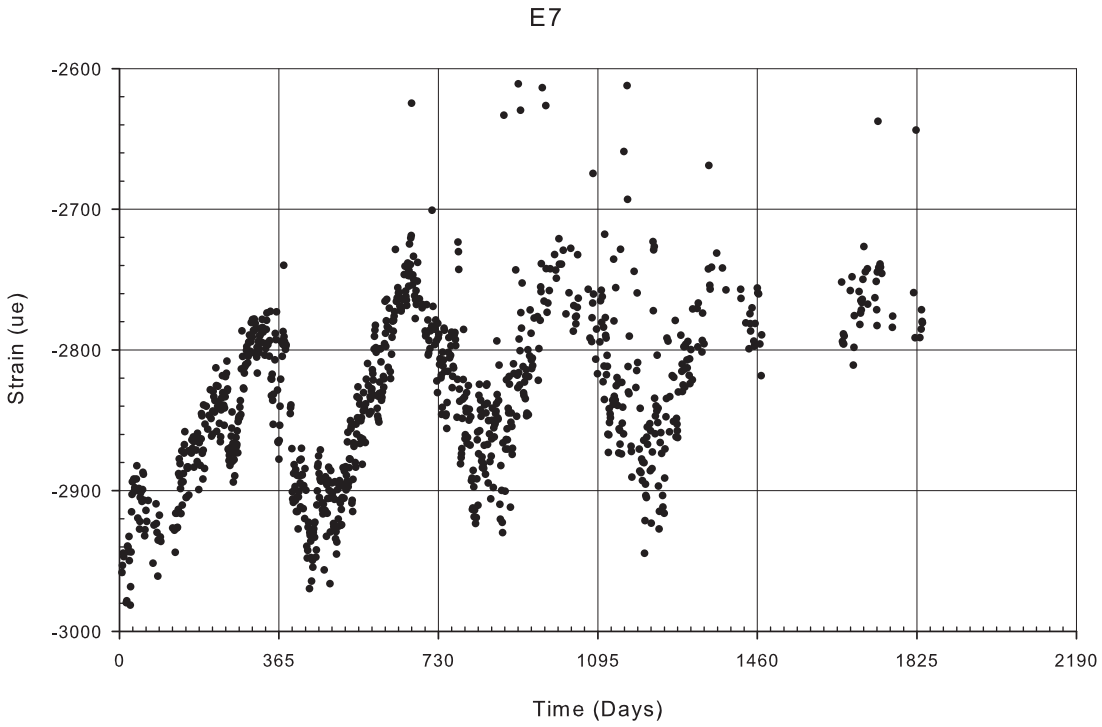

Figure A-45: Gage E7 filtered strain data

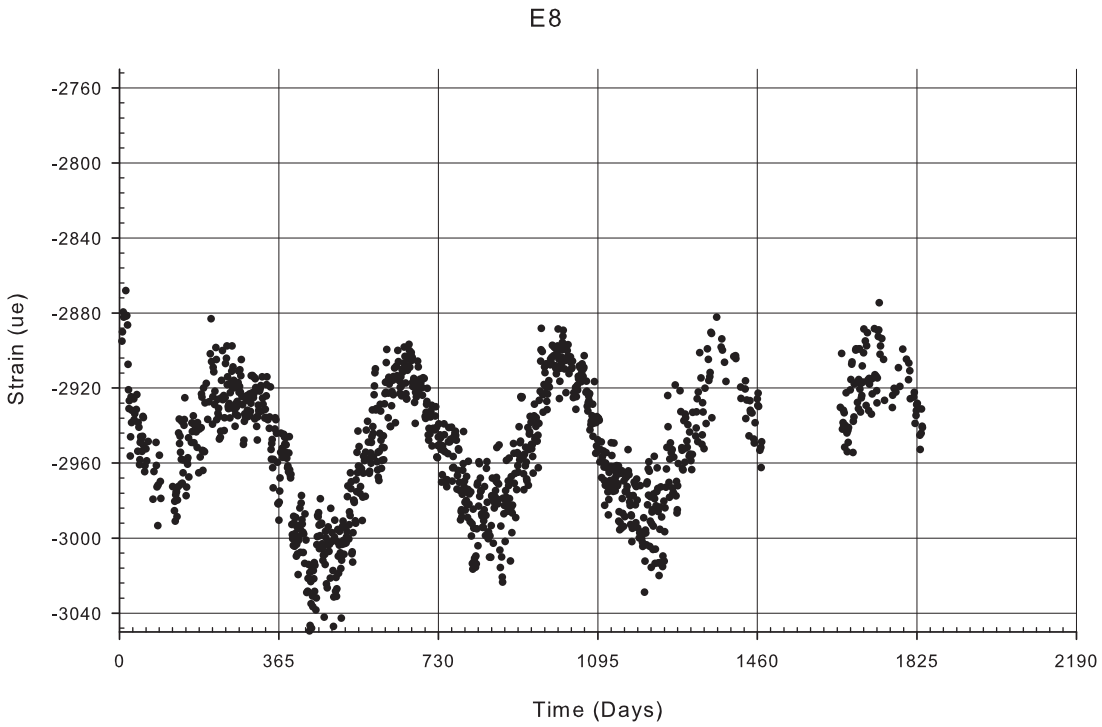

Figure A-46: Gage E8 filtered strain data

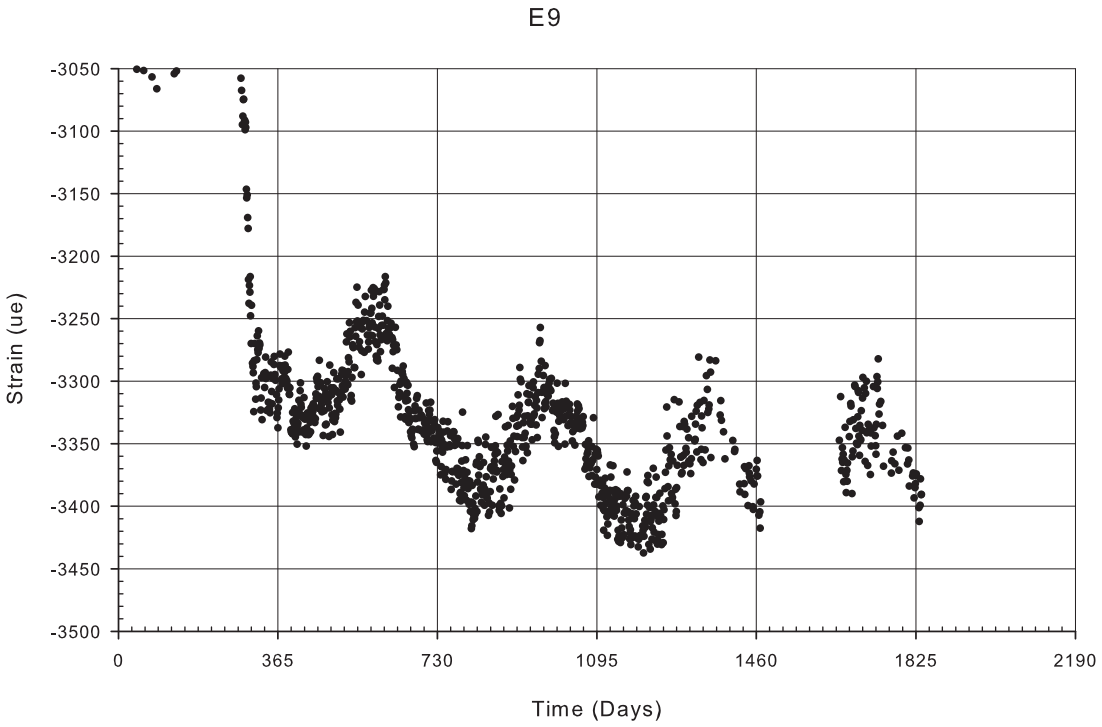

Figure A-47: Gage E9 filtered strain data

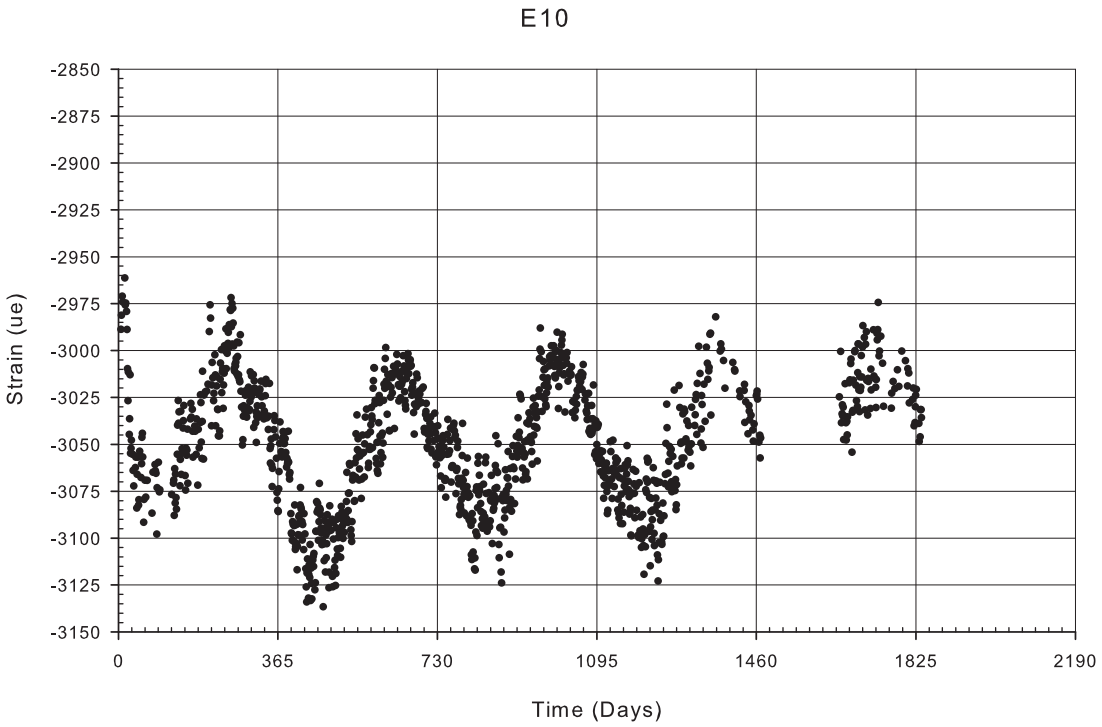

Figure A-48: Gage E10 filtered strain data

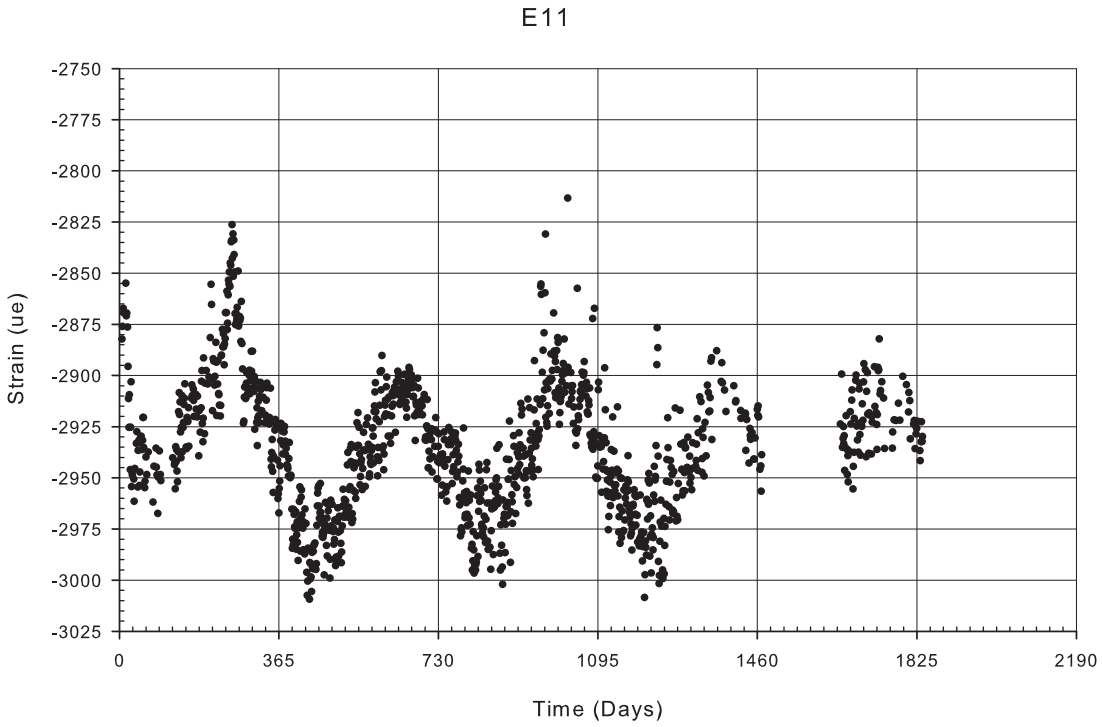

Figure A-49: Gage E11 filtered strain data

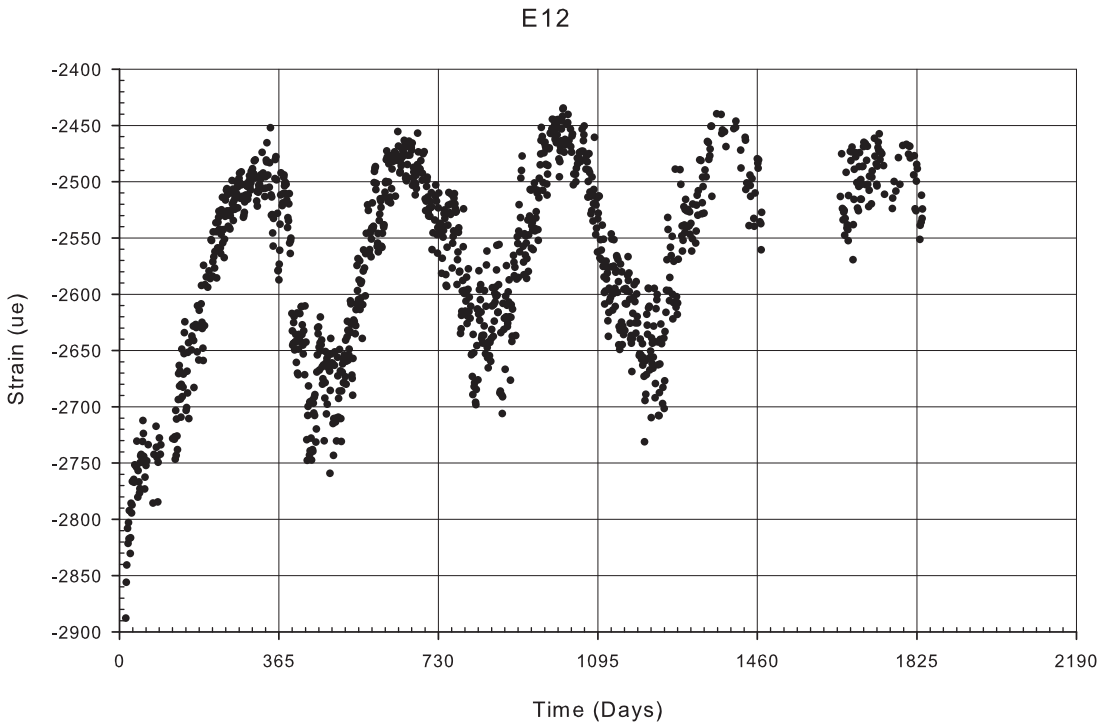

Figure A-50: Gage E12 filtered strain data

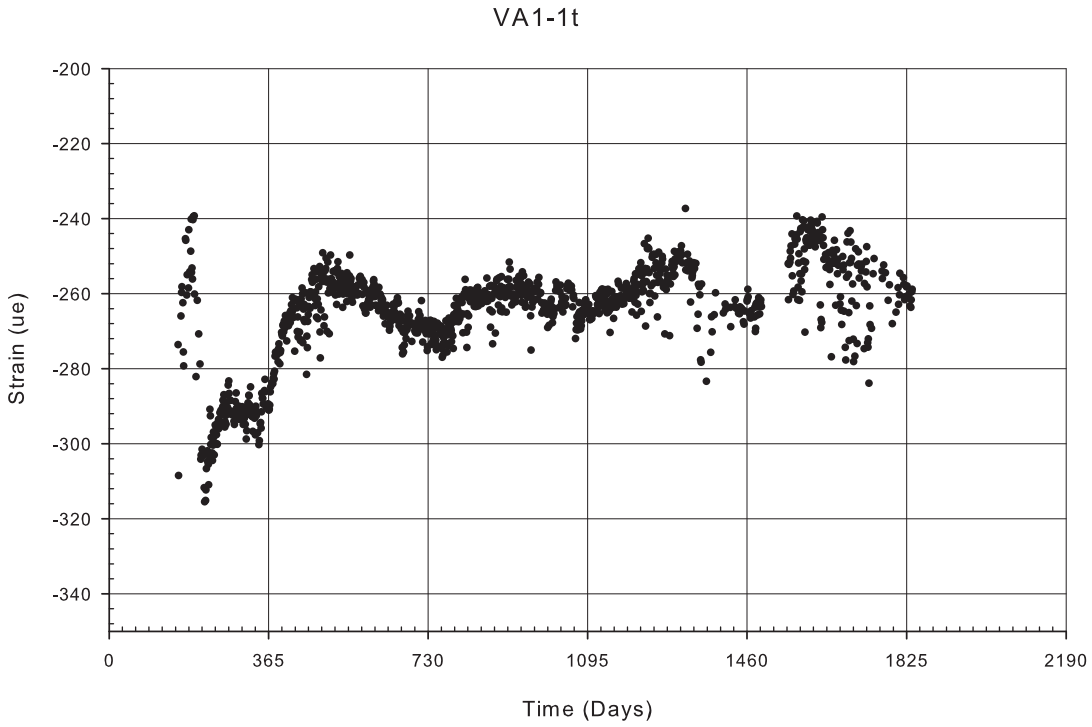

Figure A-51: Gage VA1-1t filtered strain data

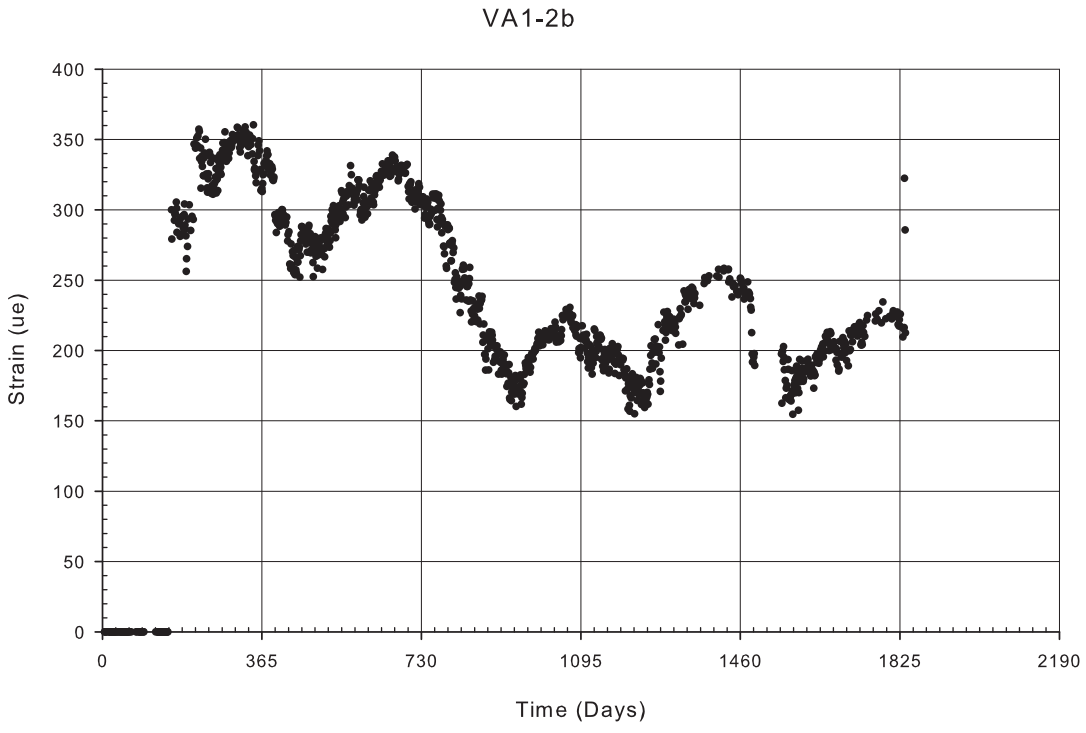

Figure A-52: Gage VA1-2b filtered strain data

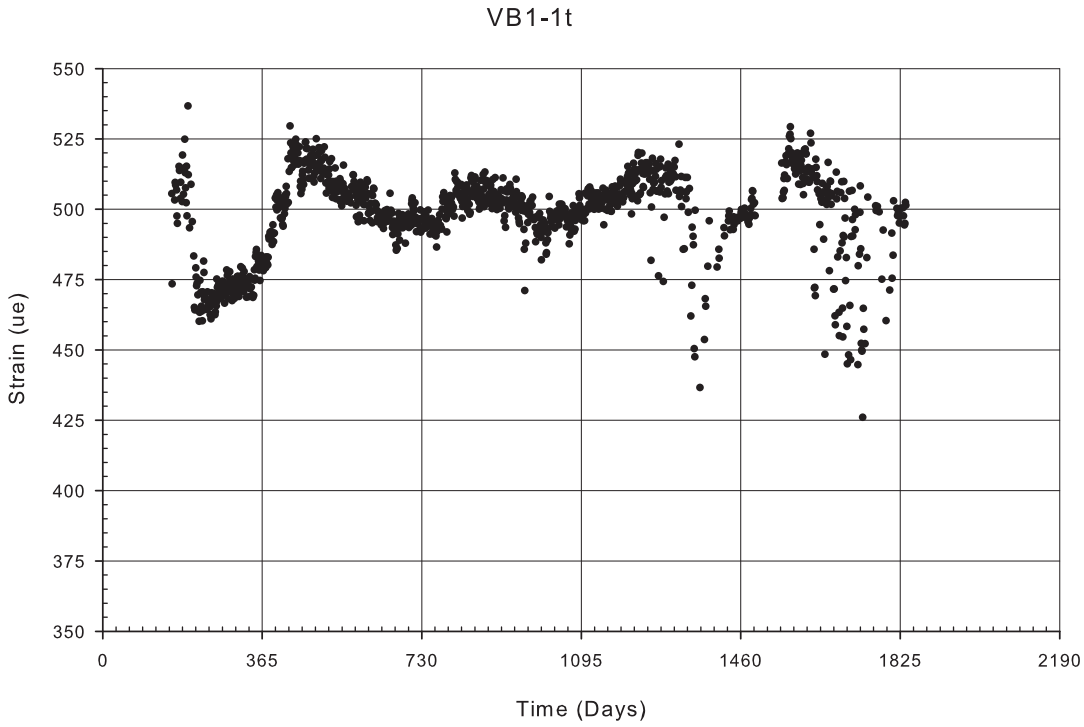

Figure A-53: Gage VB1-1t filtered strain data

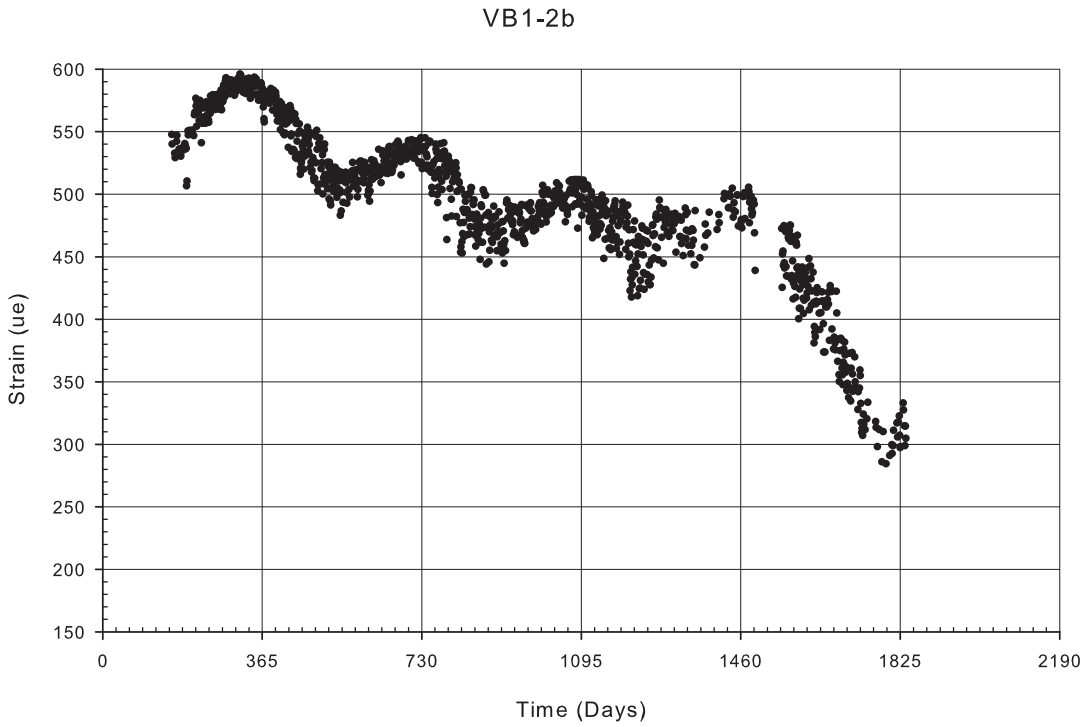

Figure A-54: Gage VB1-2b filtered strain data

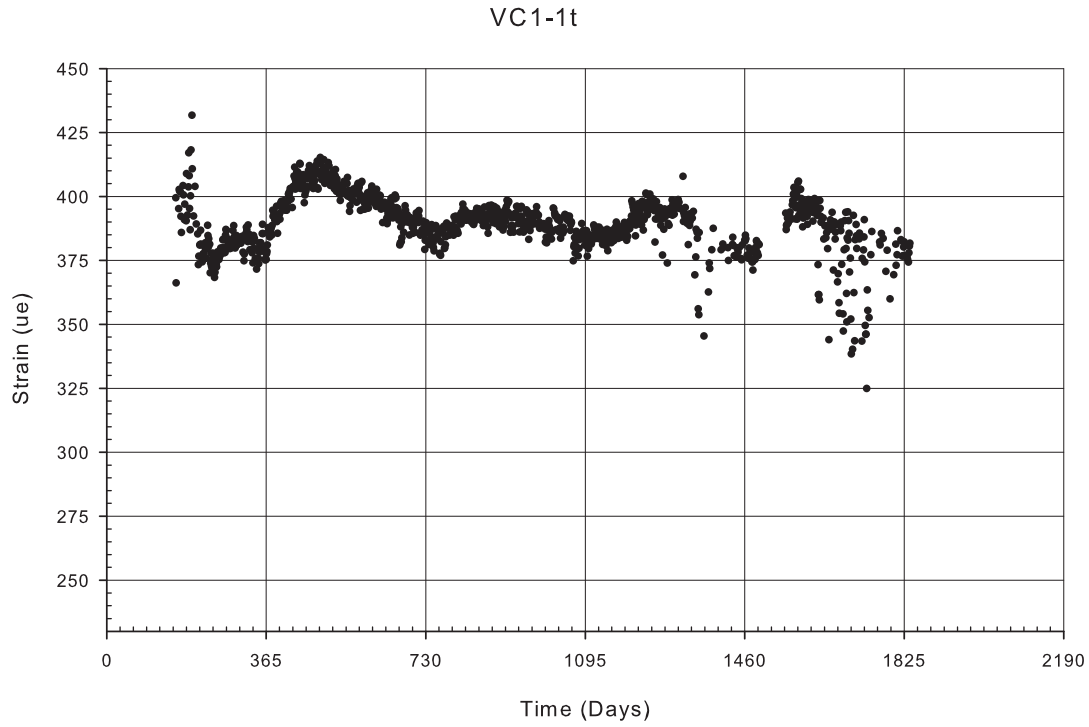

Figure A-55: Gage VC1-1t filtered strain data

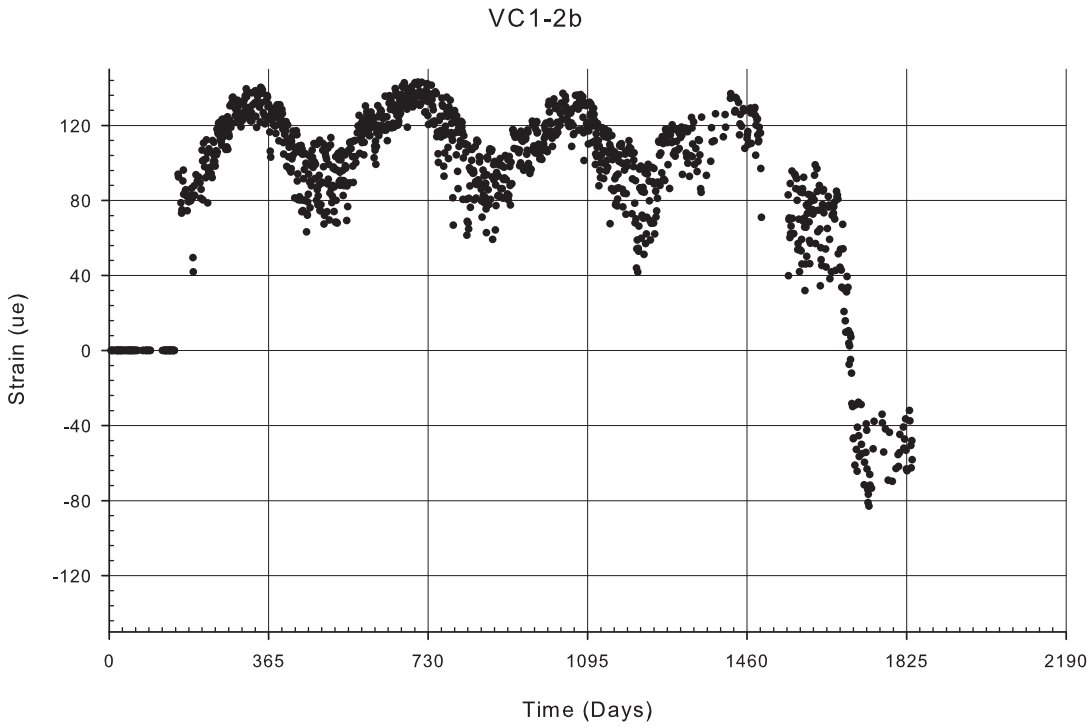

Figure A-56: Gage VC1-2b filtered strain data

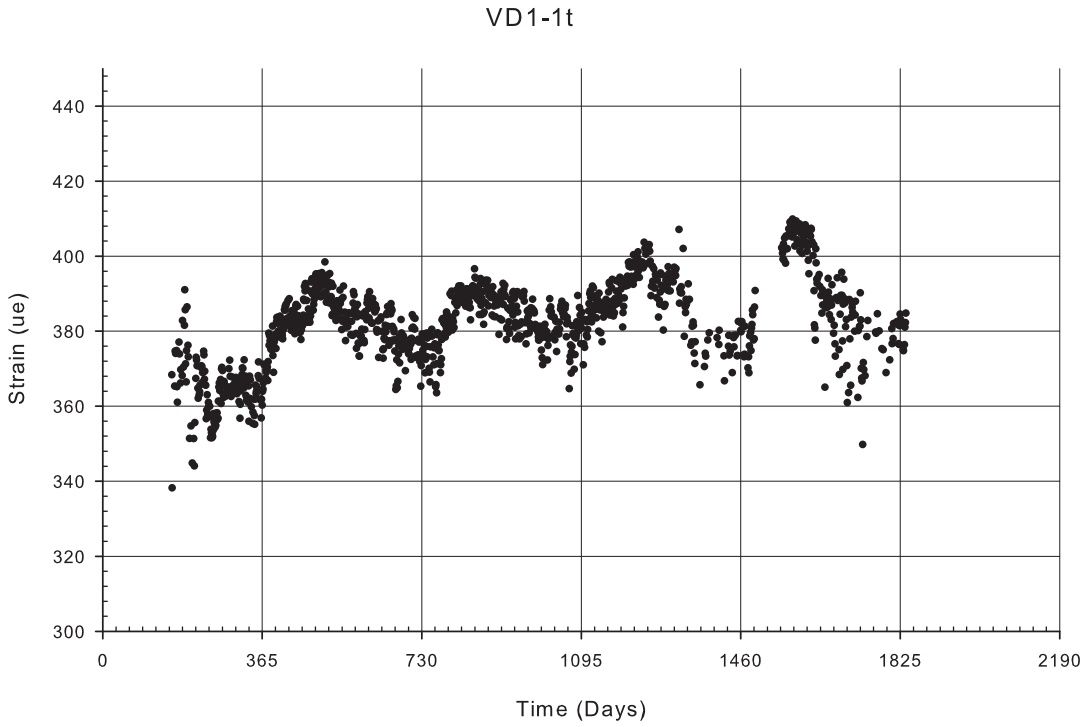

Figure A-57: Gage VD1-1t filtered strain data

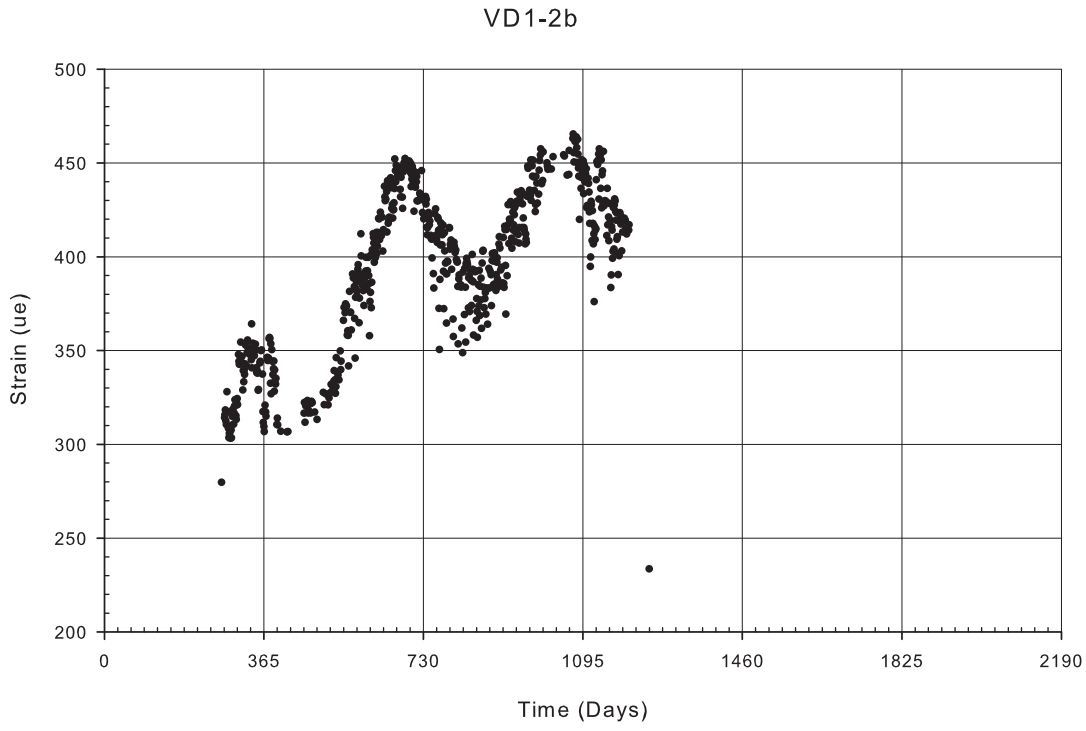

Figure A-58: Gage VD1-2b filtered strain data

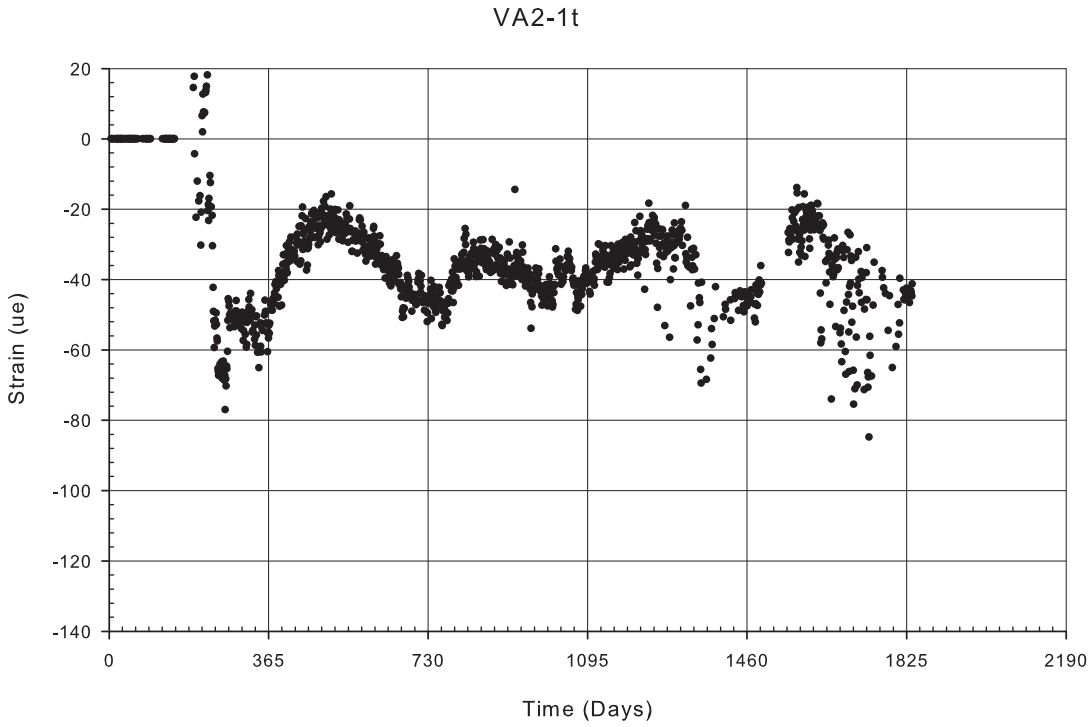

Figure A-59: Gage VA2-1t filtered strain data

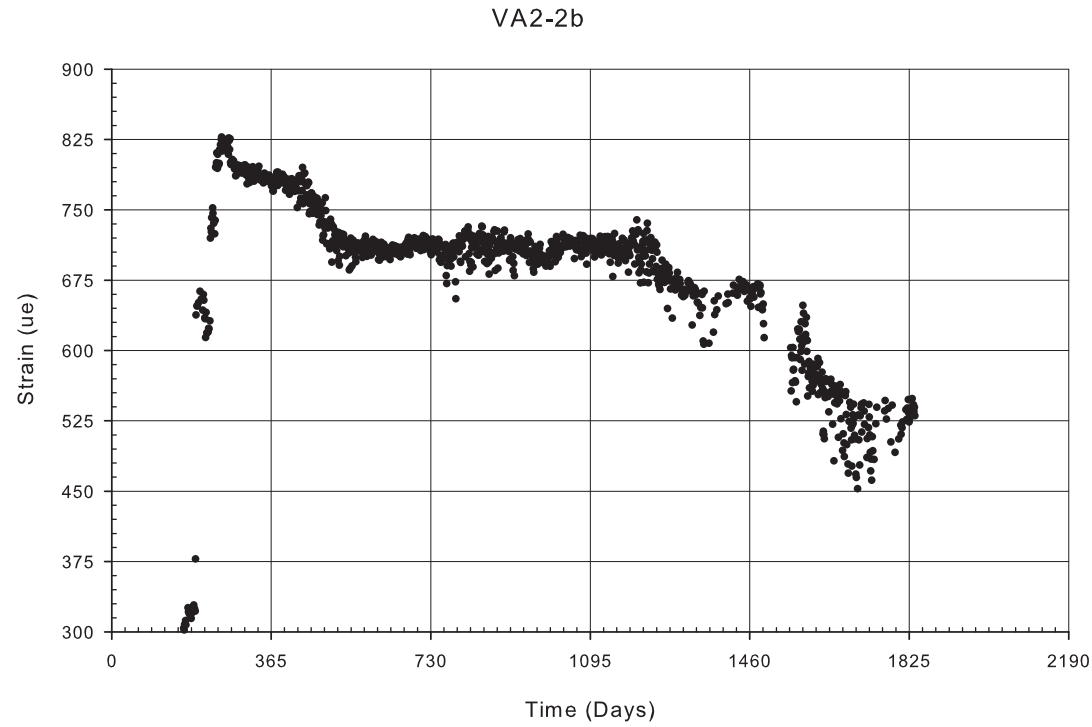

Figure A-60: Gage VA2-2b filtered strain data

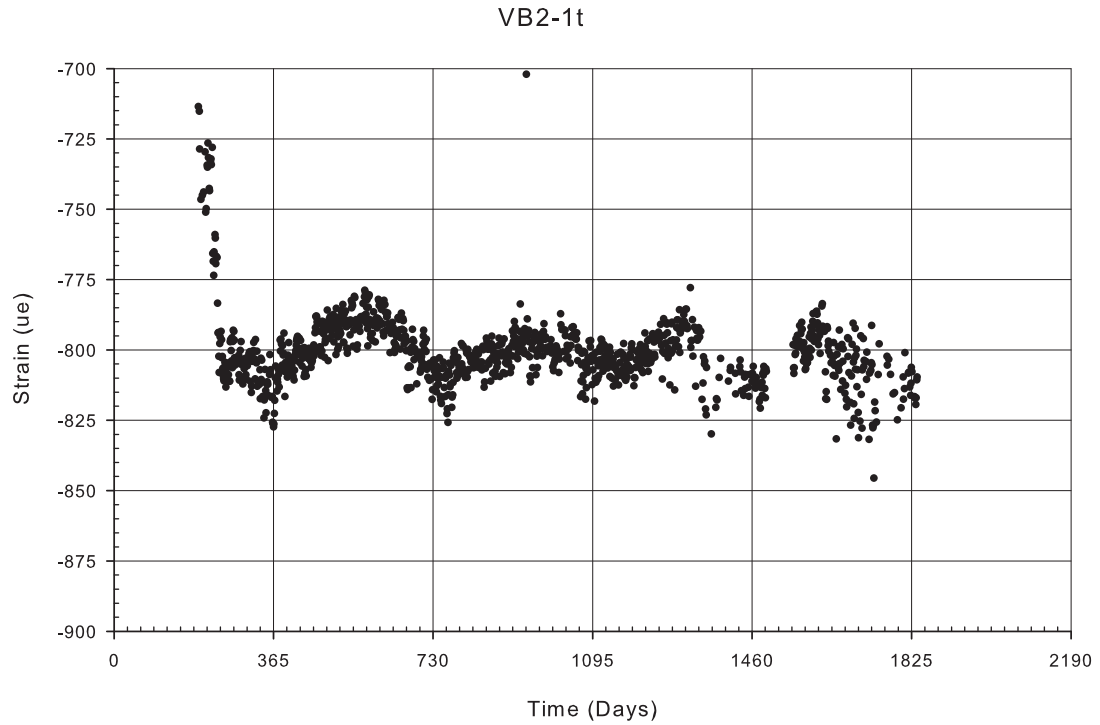

Figure A-61: Gage VB2-1t filtered strain data

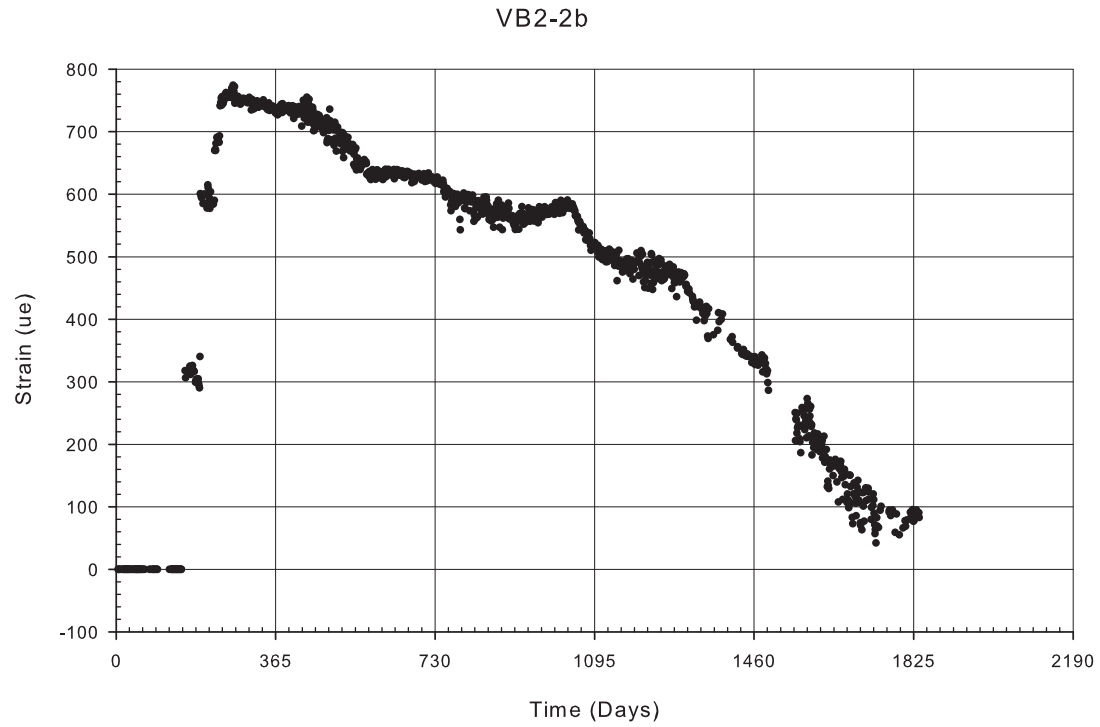

Figure A-62: Gage VB2-2b filtered strain data

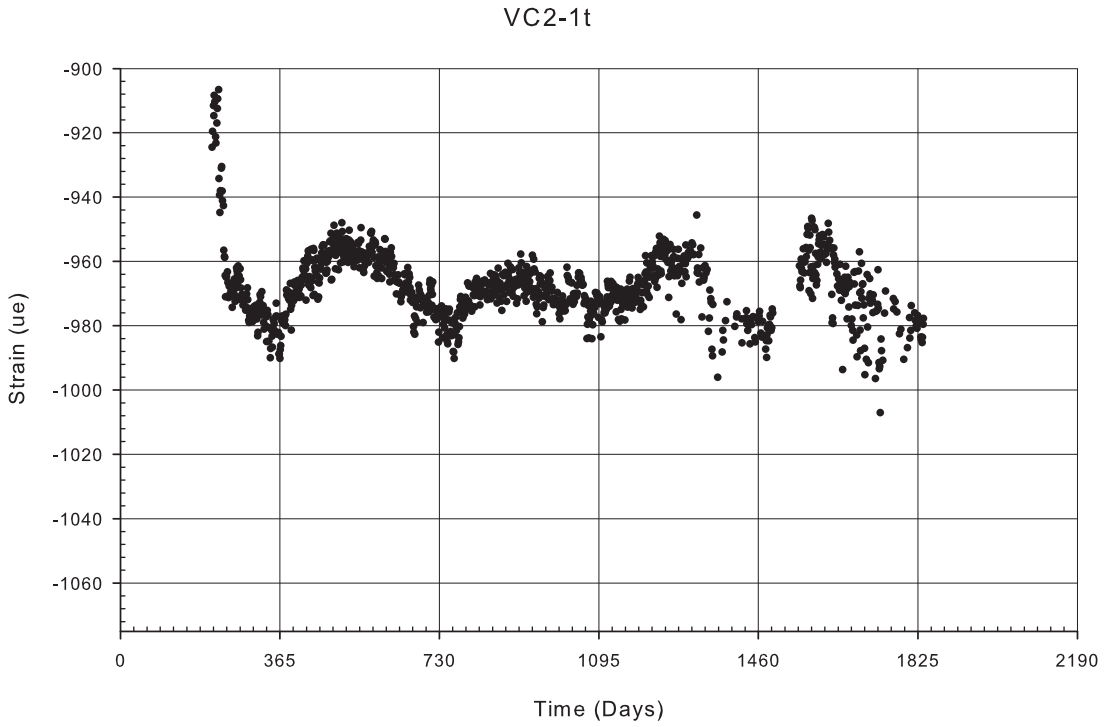

Figure A-63: Gage VC2-1t filtered strain data

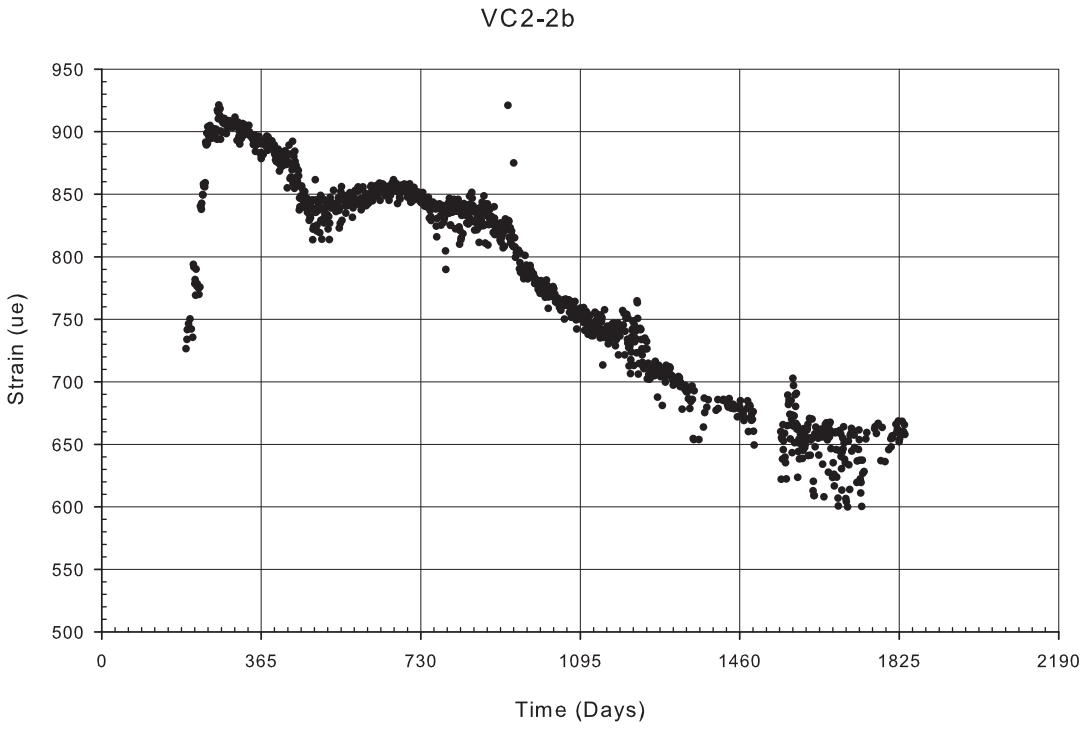

Figure A-64: Gage VC2-2b filtered strain data

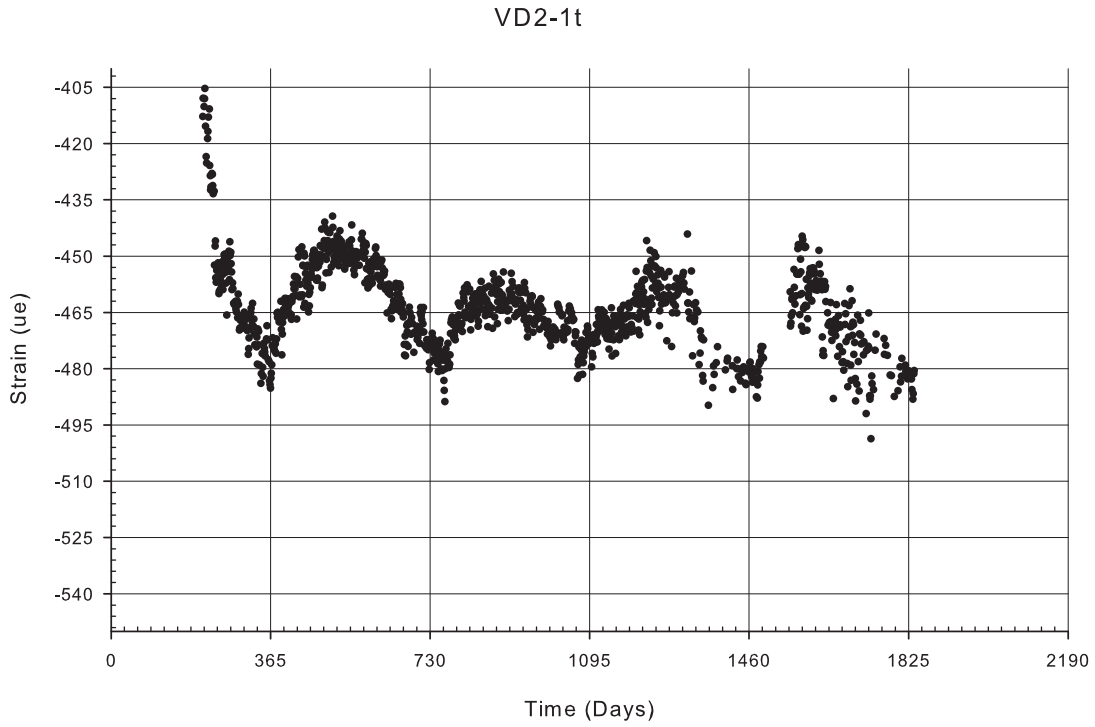

Figure A-65: Gage VD2-1t filtered strain data

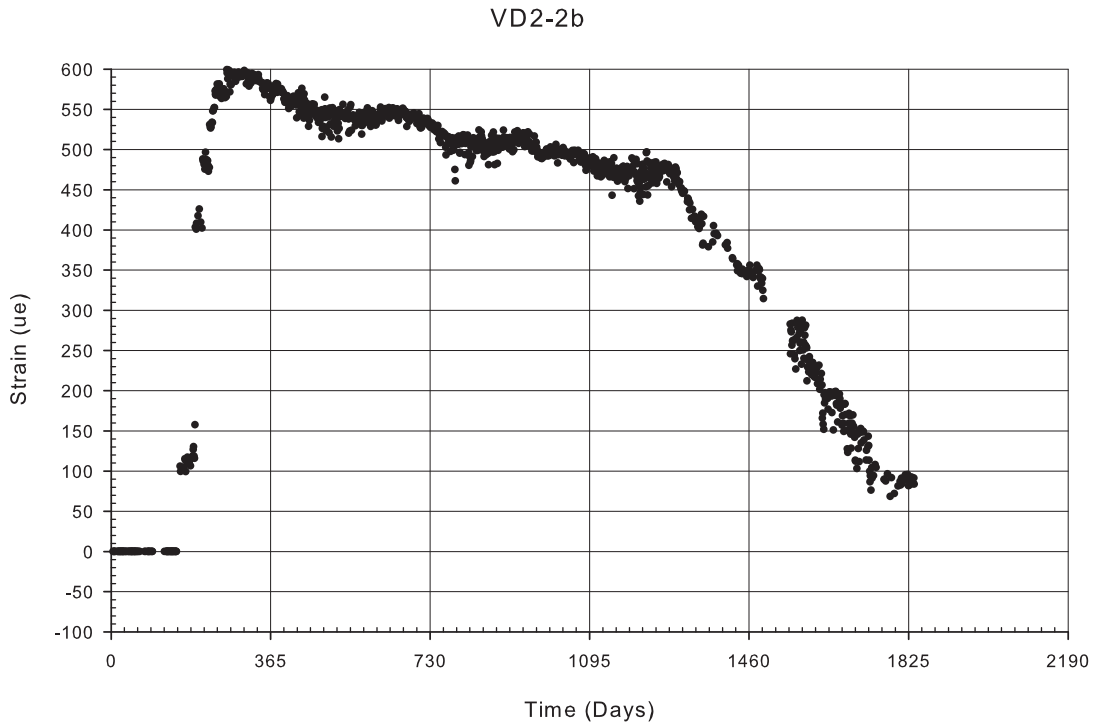

Figure A-66: Gage VD2-2b filtered strain data

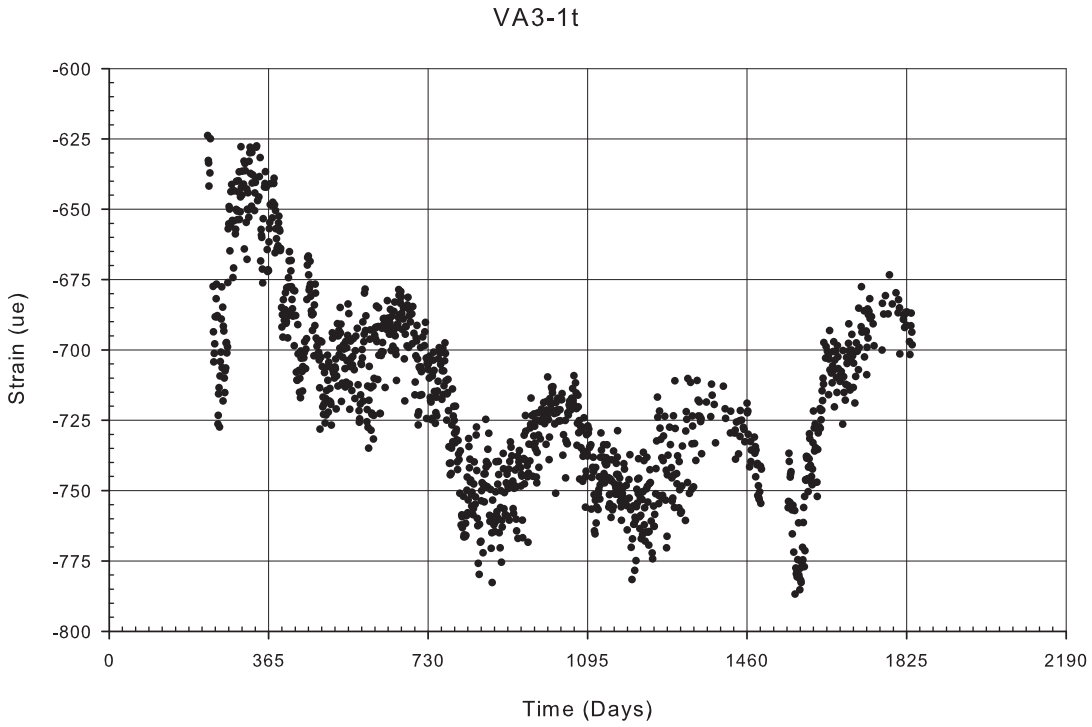

Figure A-67: Gage VA3-1t filtered strain data

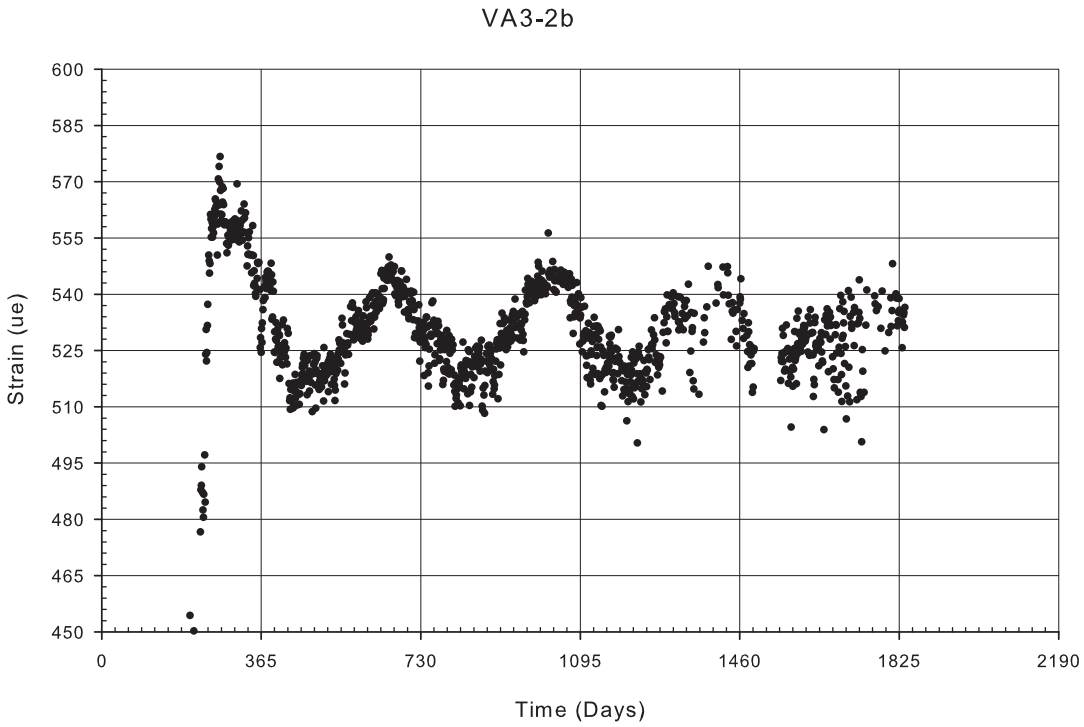

Figure A-68: Gage VA3-2b filtered strain data

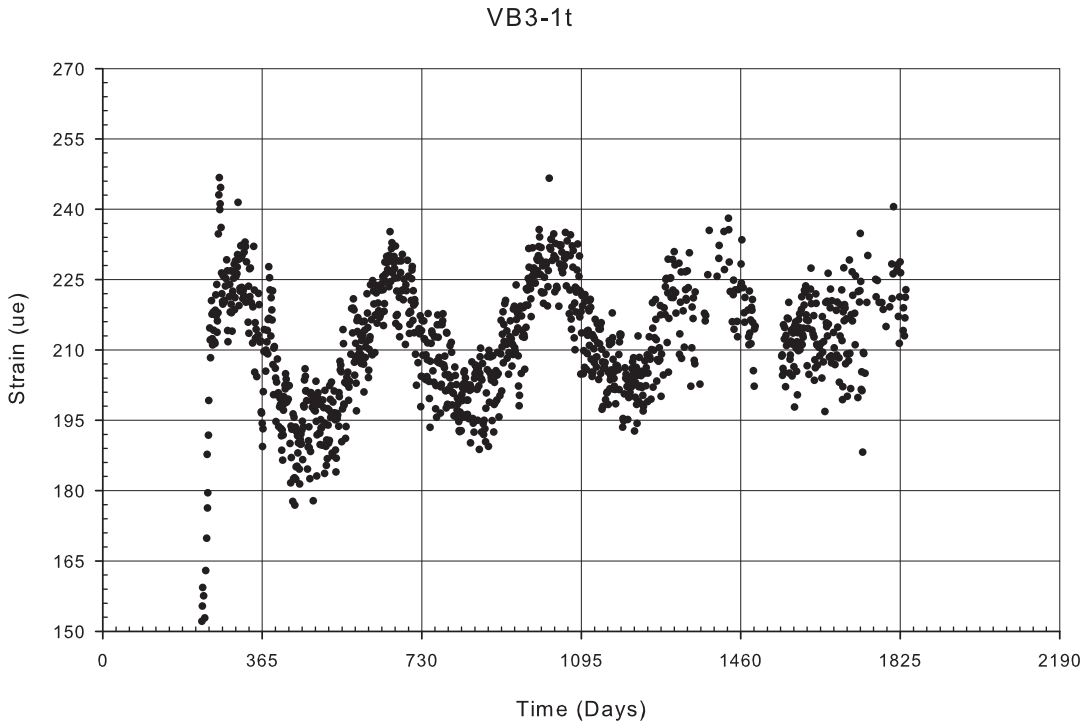

Figure A-69: Gage VB3-1t filtered strain data

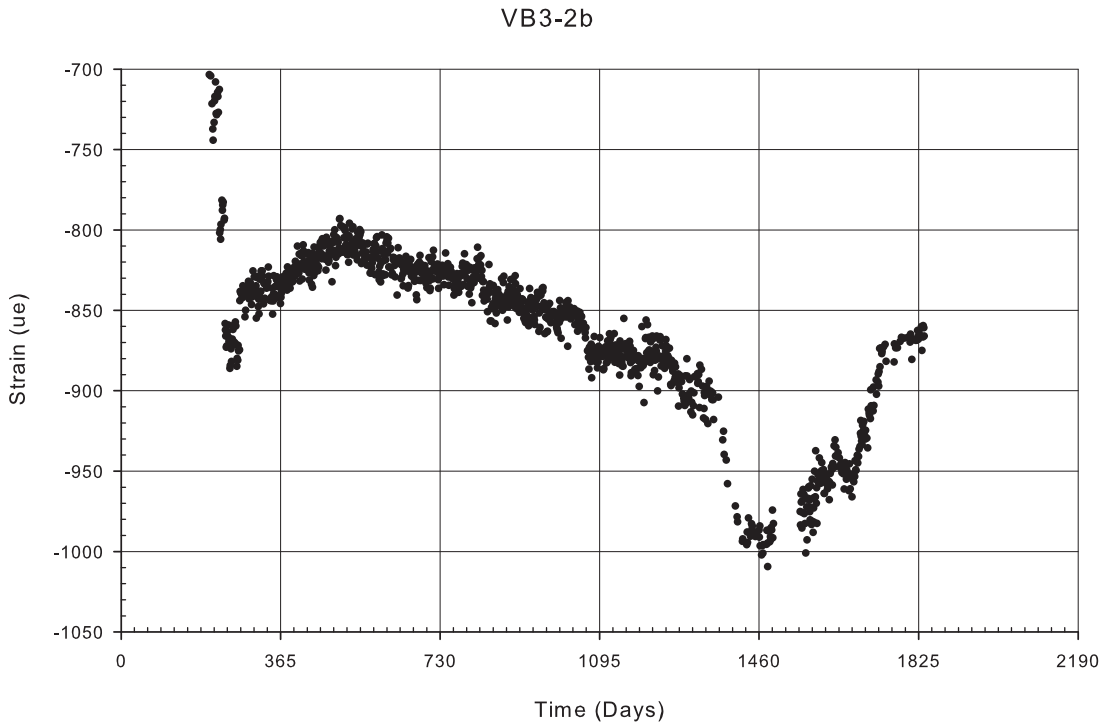

Figure A-70: Gage VB3-2b filtered strain data

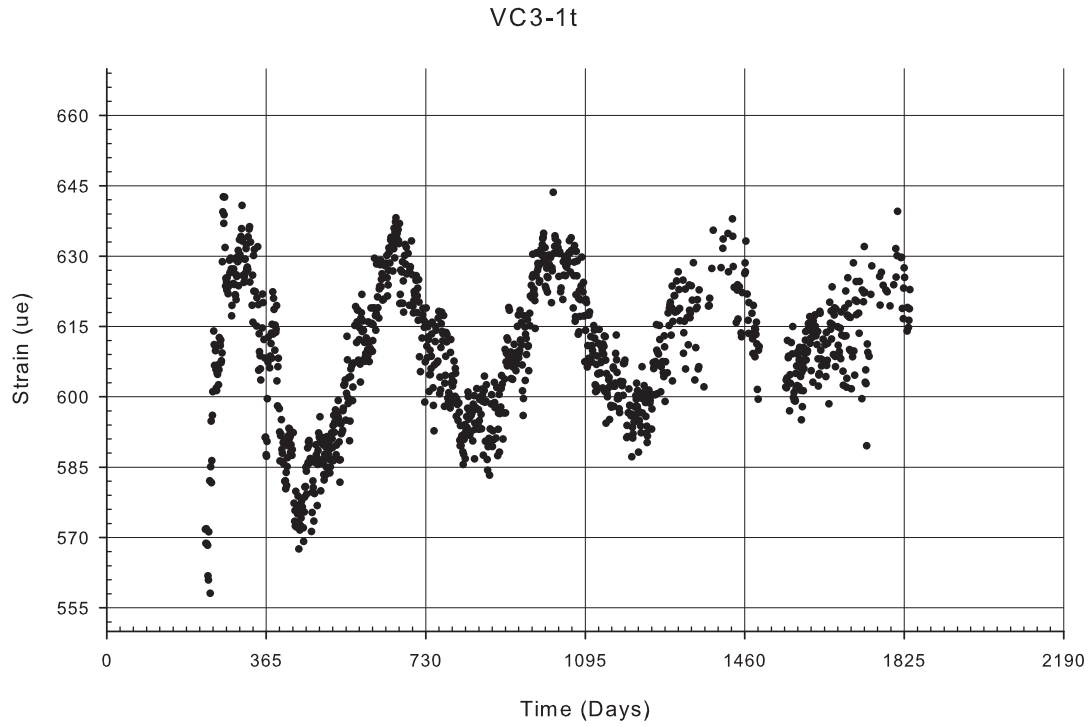

Figure A-71: Gage VC3-1t filtered strain data

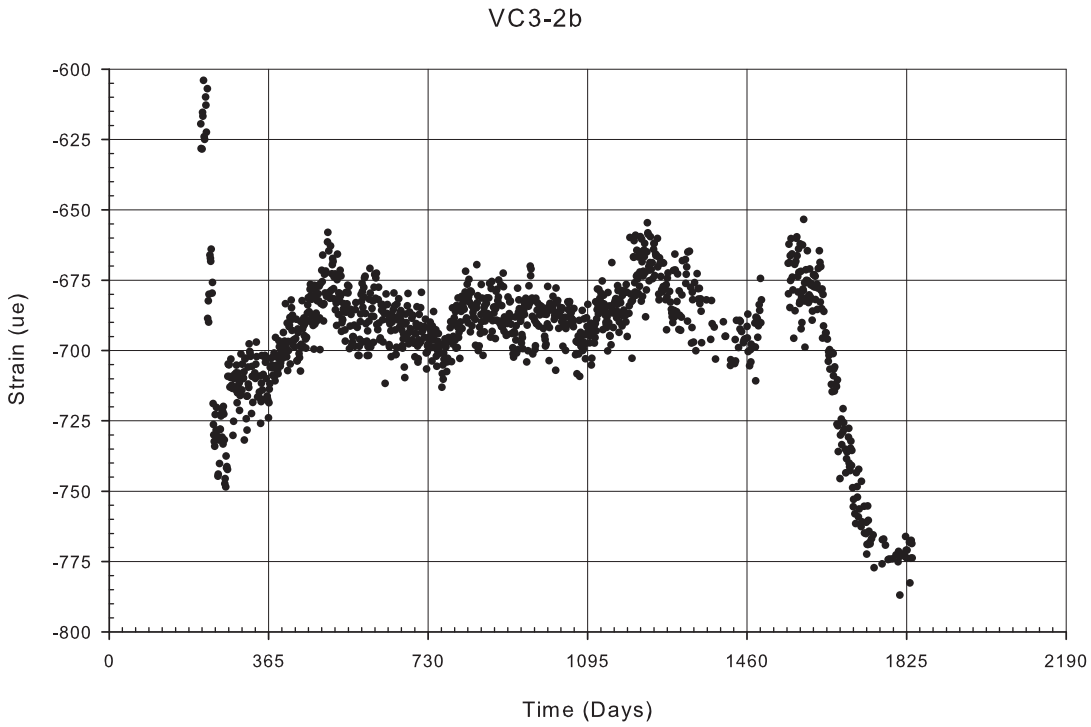

Figure A-72: Gage VC3-2b filtered strain data

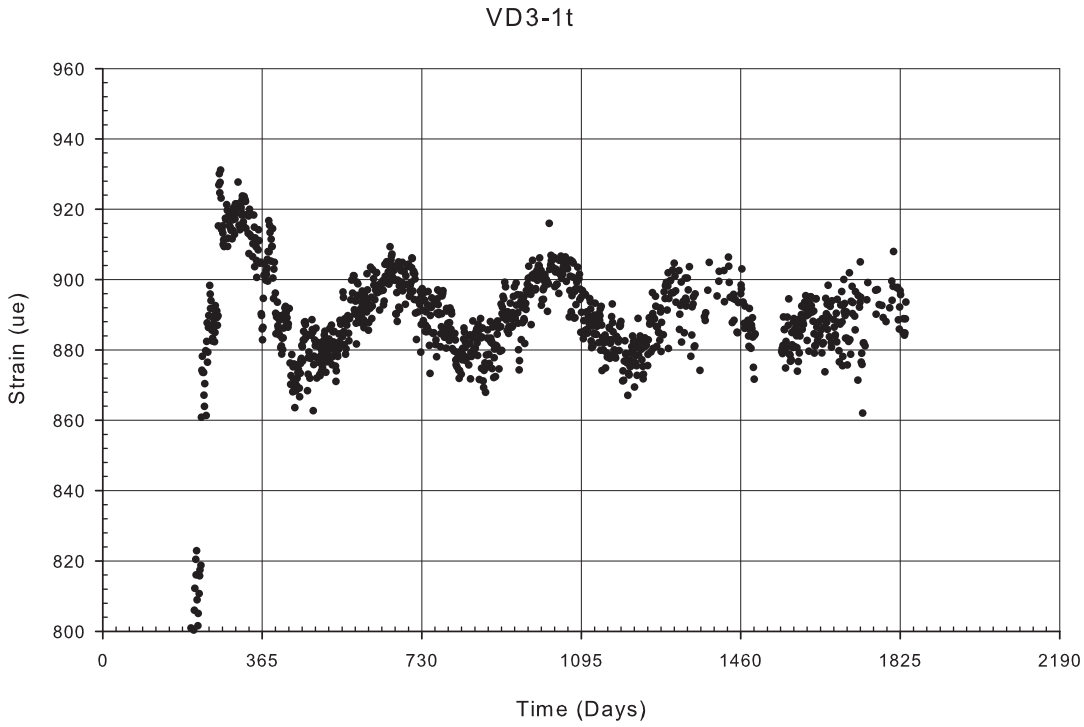

Figure A-73: Gage VD3-1t filtered strain data

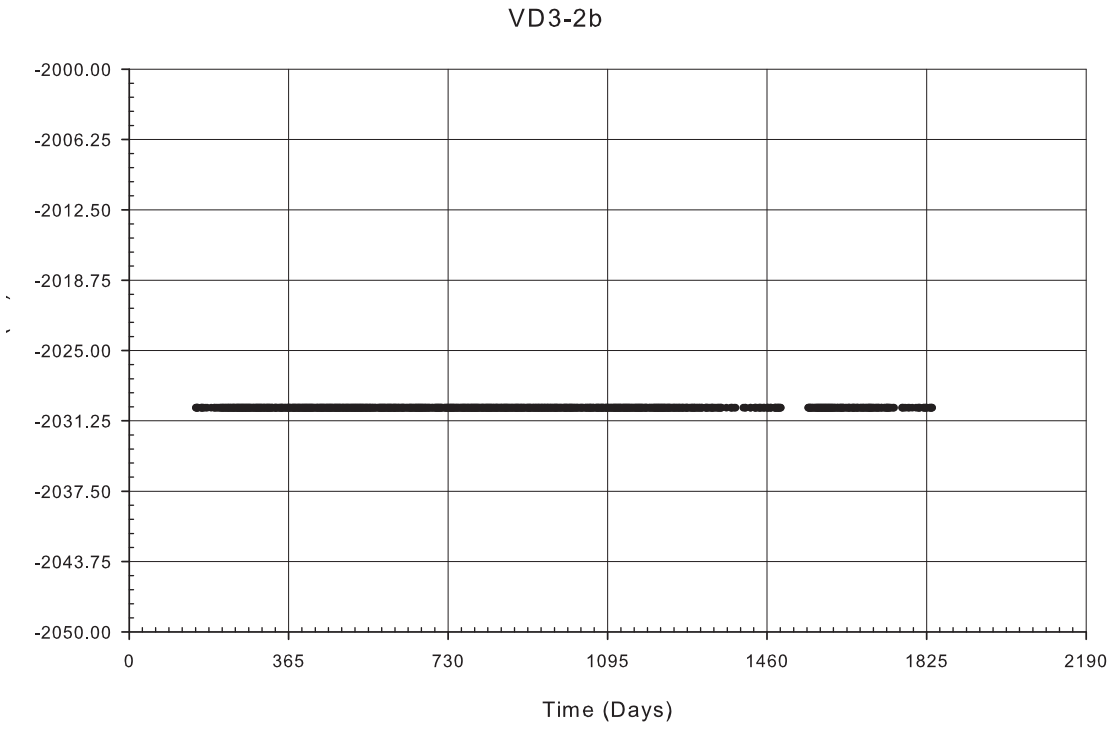

Figure A-74: Gage VD3-2b filtered strain data

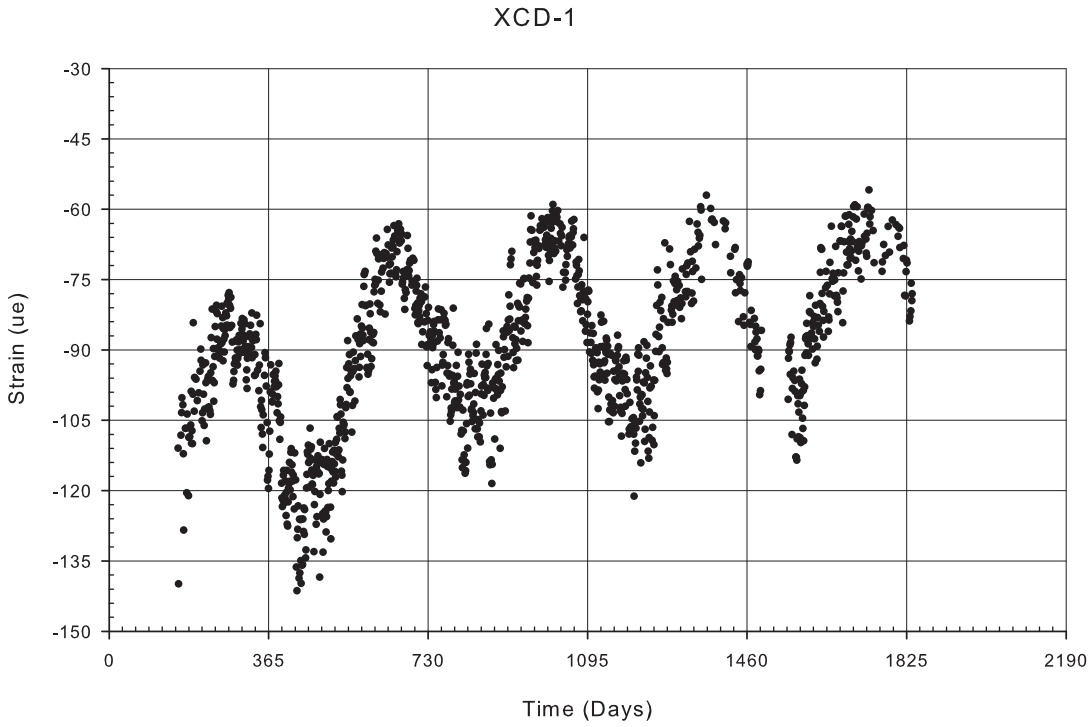

Figure A-75: Gage XCD-1 filtered strain data

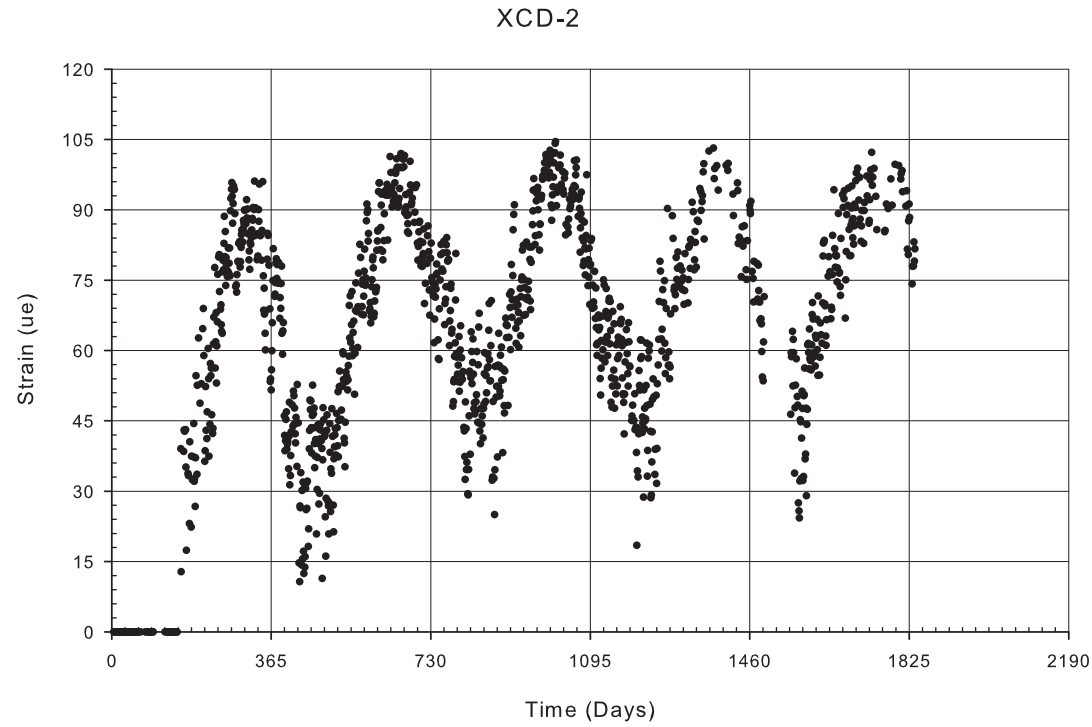

Figure A-76: Gage XCD-2 filtered strain data

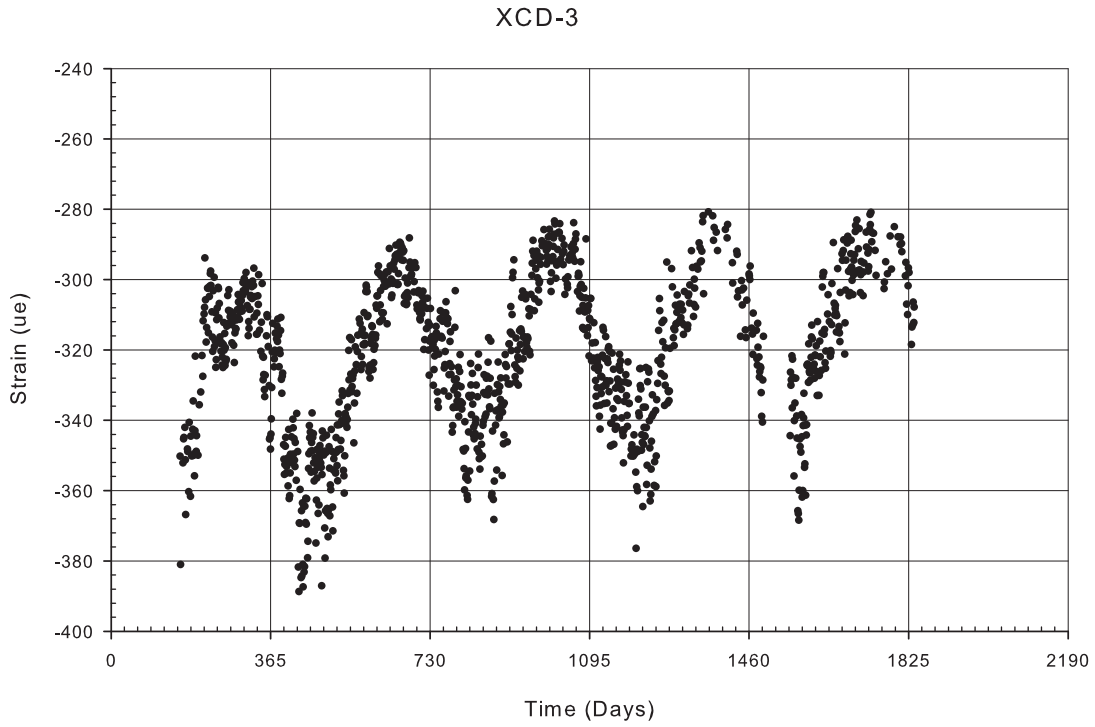

Figure A-77: Gage XCD-3 filtered strain data

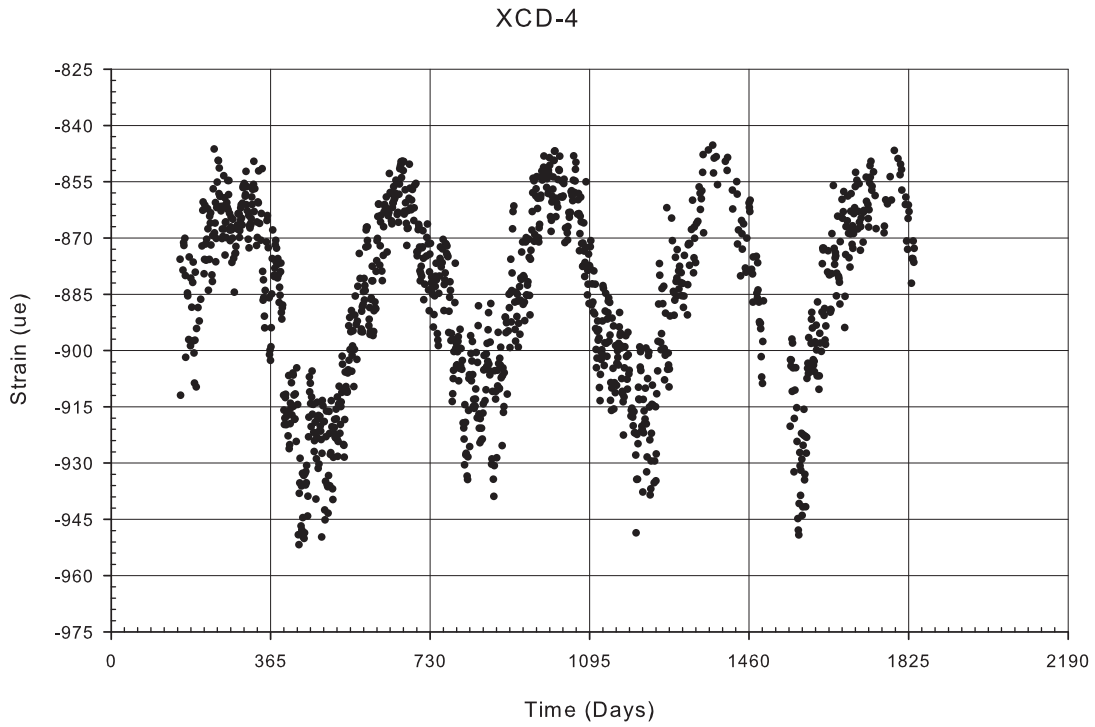

Figure A-78: Gage XCD-4 filtered strain data

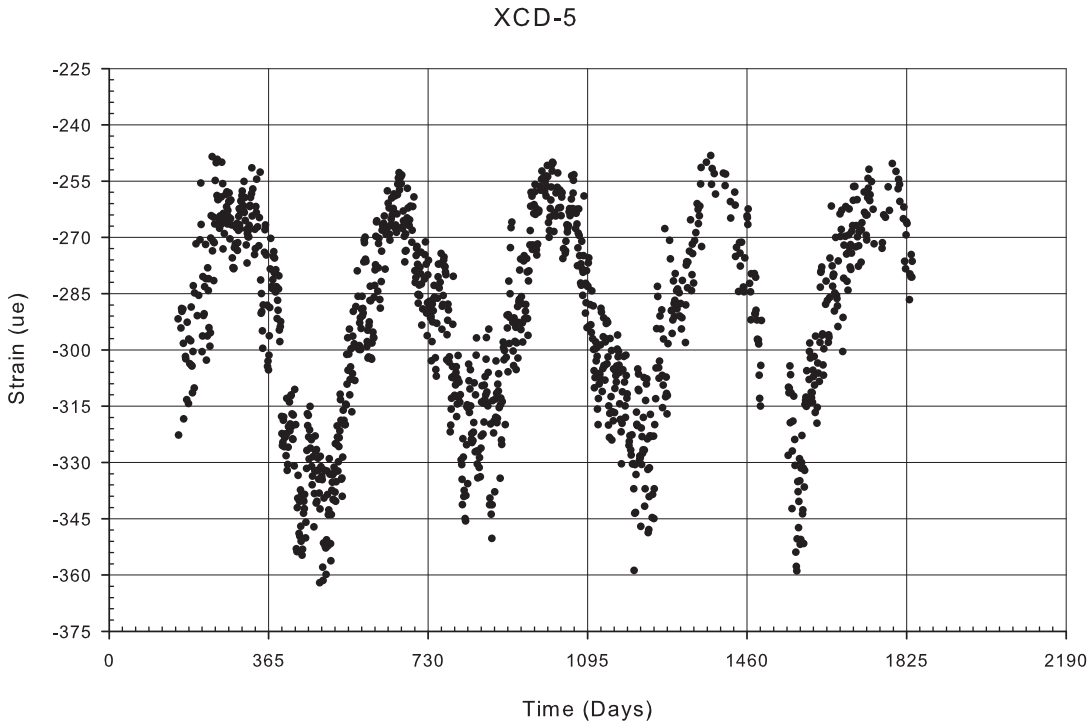

Figure A-79: Gage XCD-5 filtered strain data

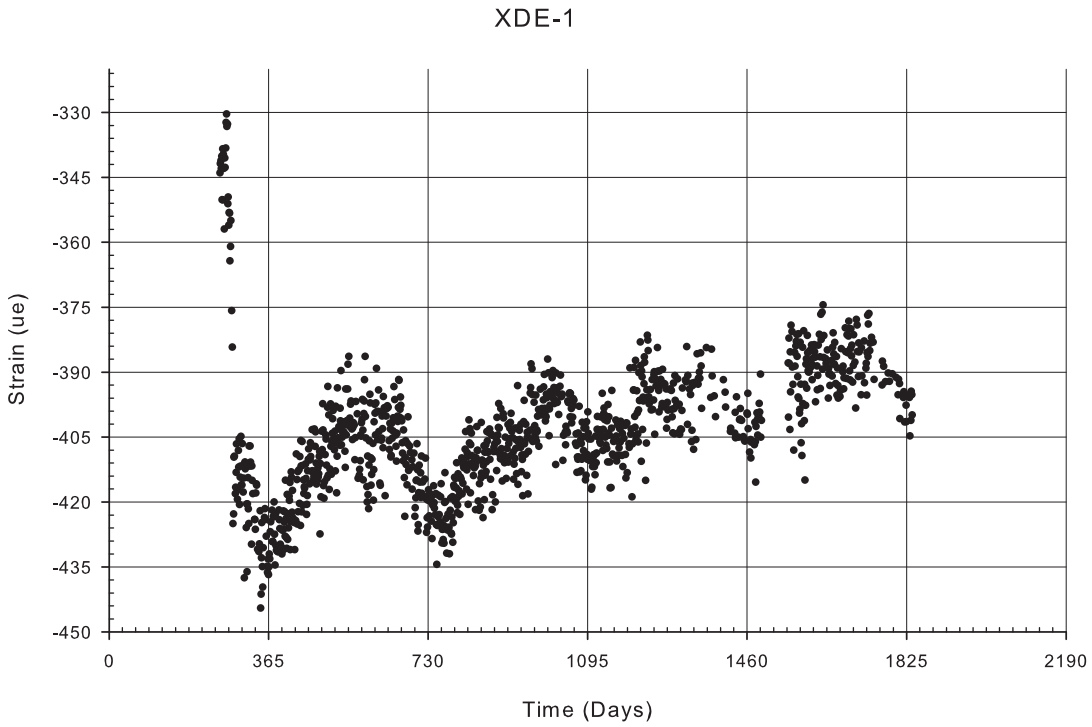

Figure A-80: Gage XDE-1 filtered strain data

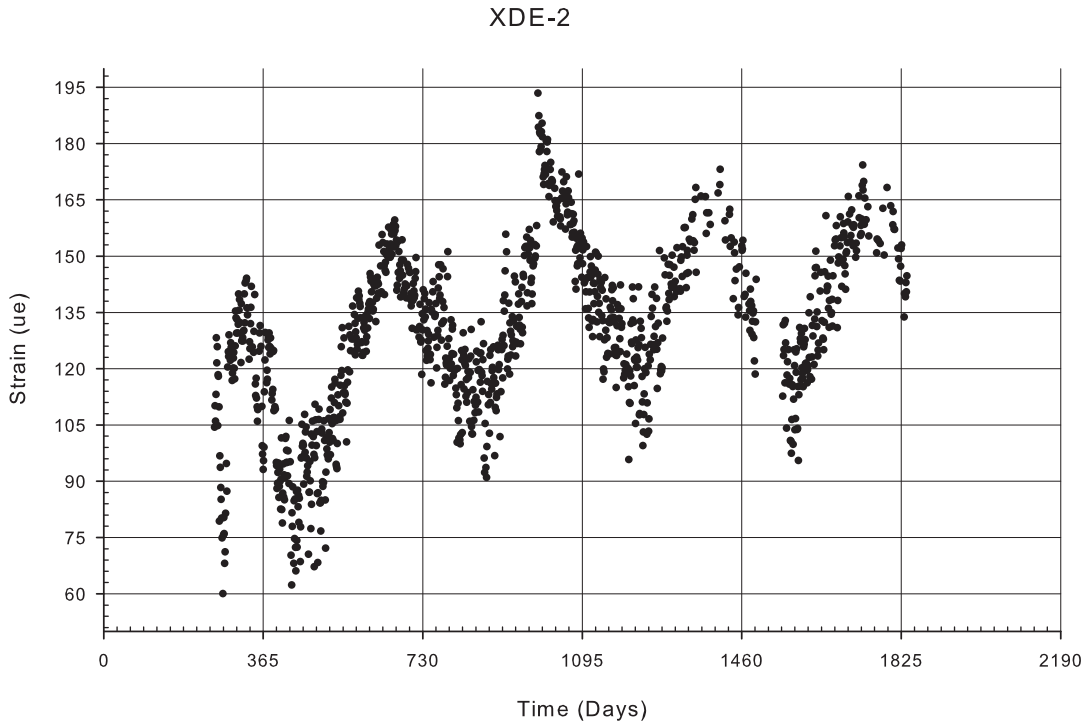

Figure A-81: Gage XDE-2 filtered strain data

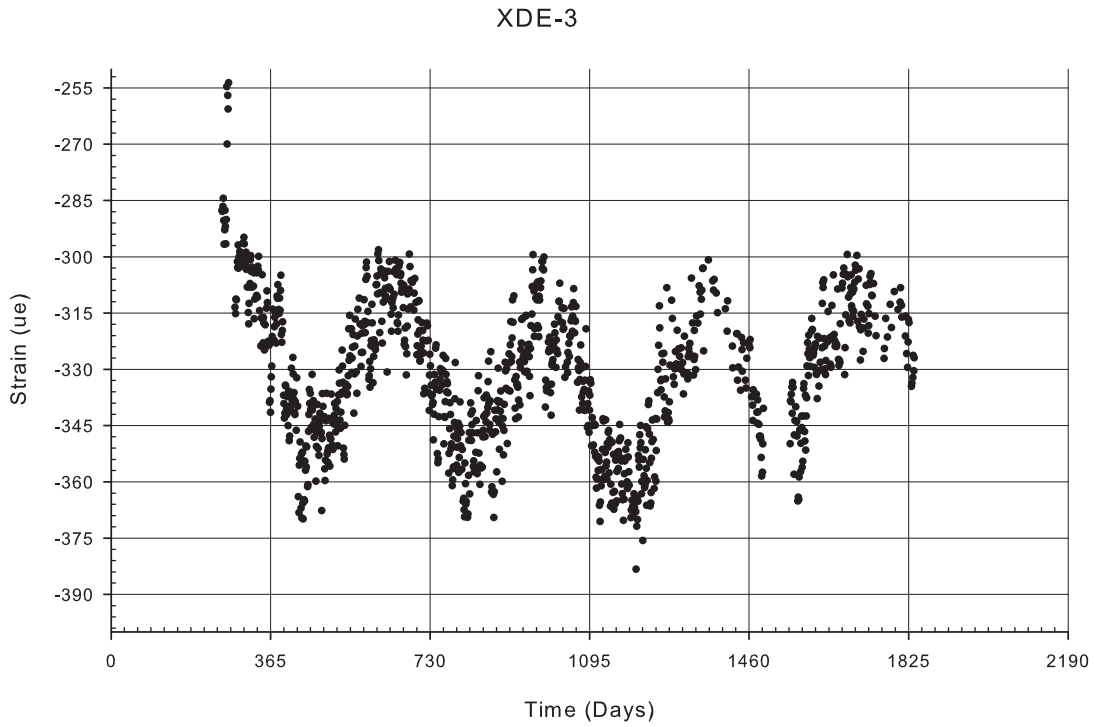

Figure A-82: Gage XDE-3 filtered strain data

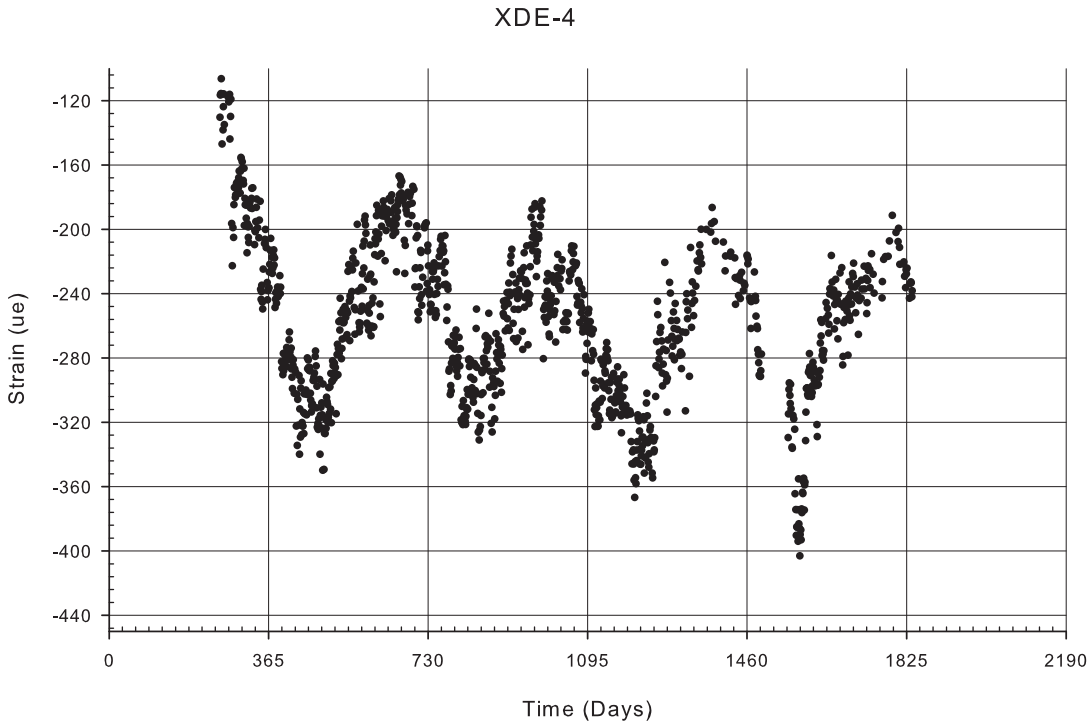

Figure A-83: Gage XDE-4 filtered strain data

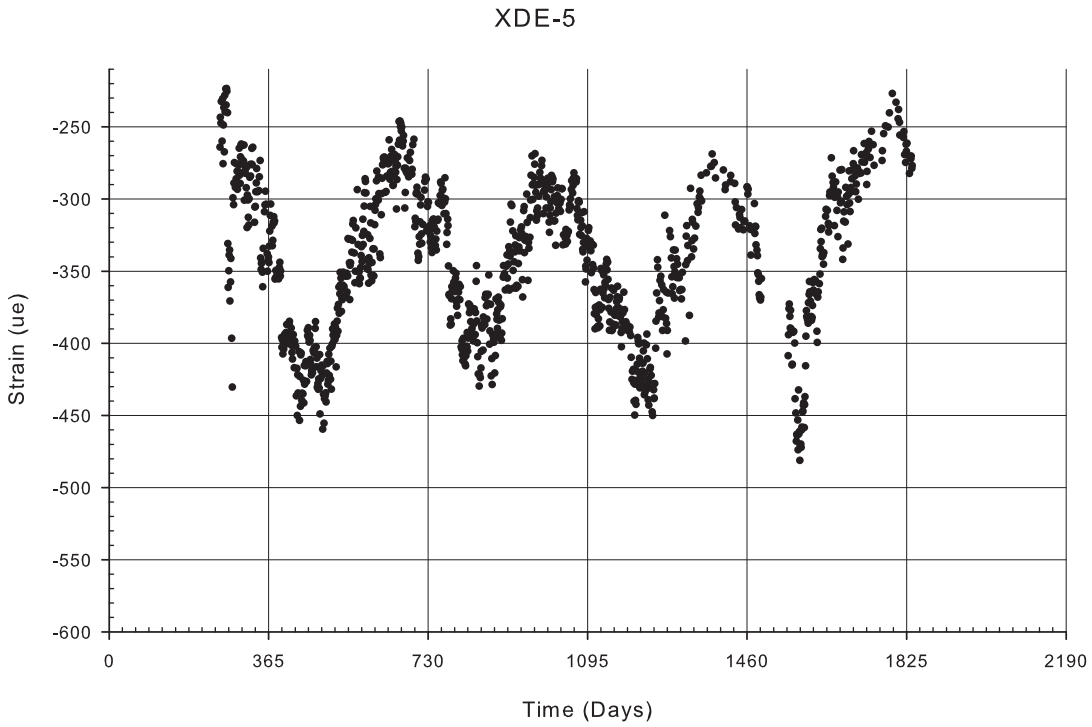

Figure A-84: Gage XDE-5 filtered strain data

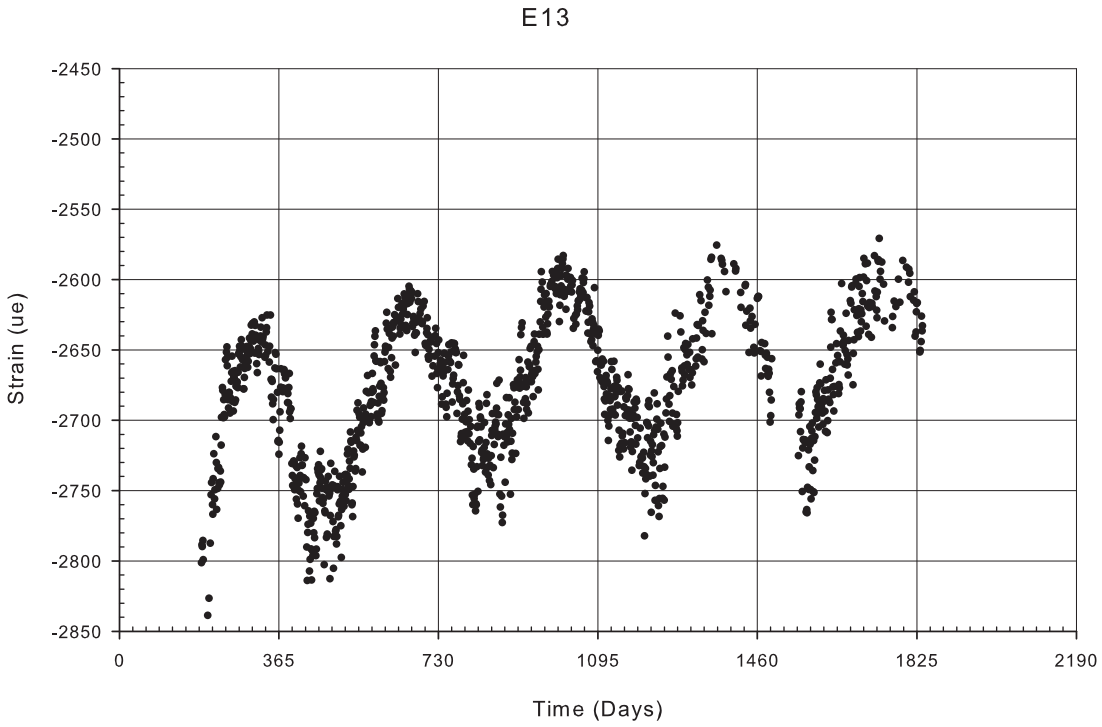

Figure A-85: Gage E13 filtered strain data

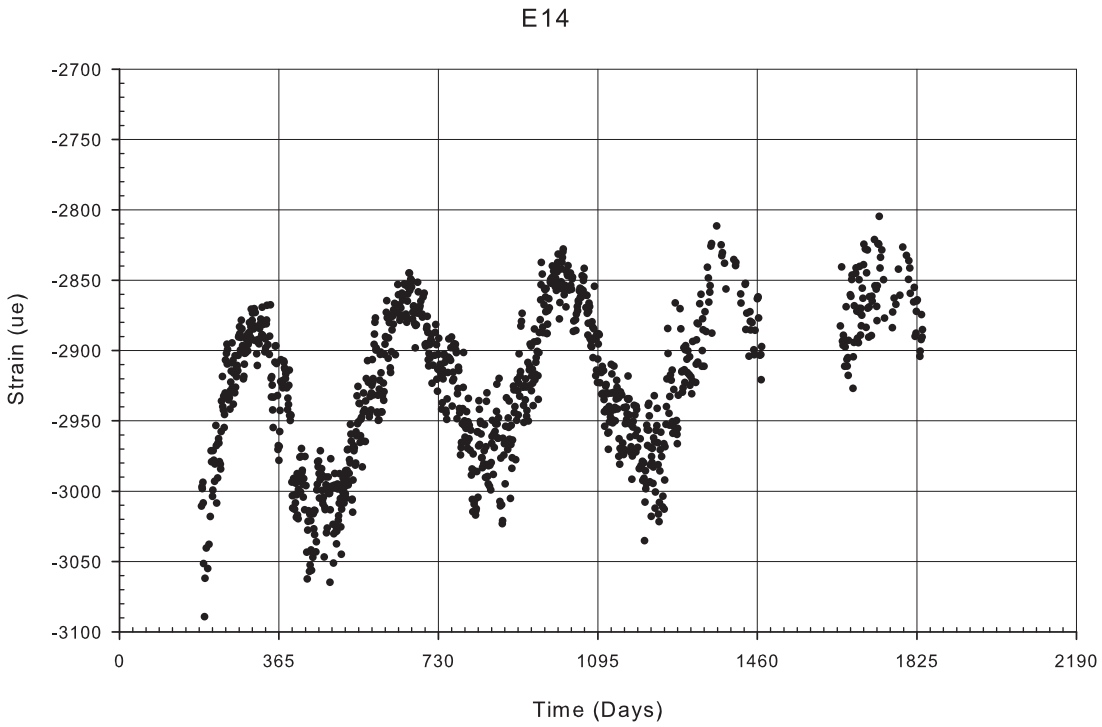

Figure A-86: Gage E14 filtered strain data

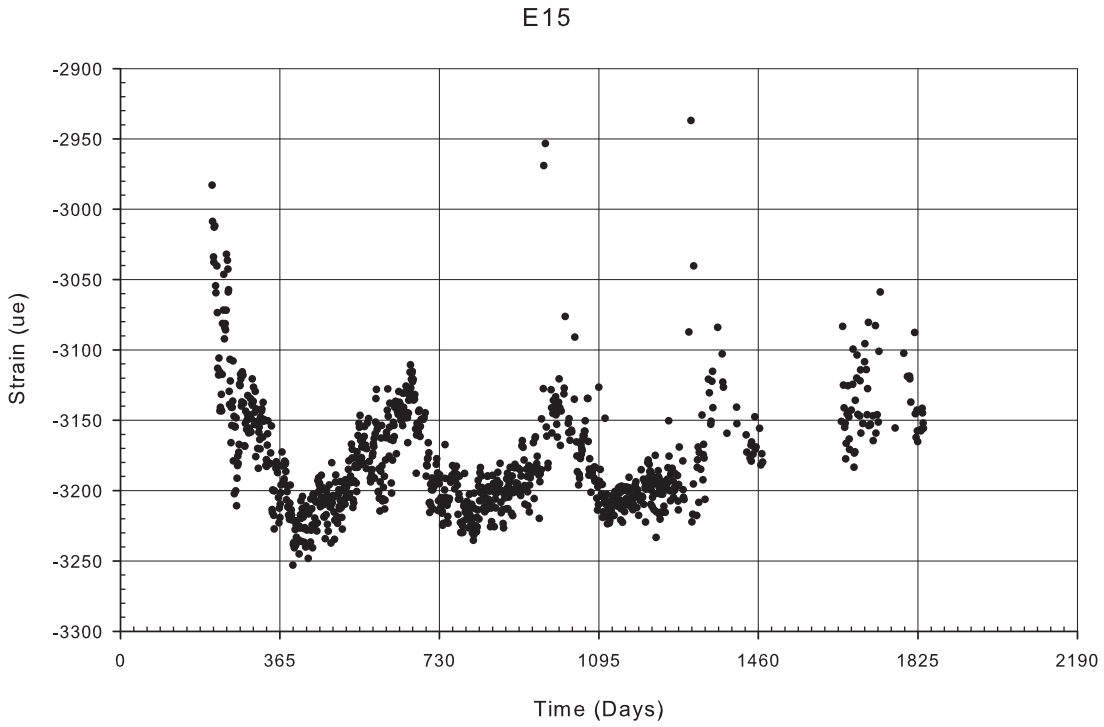

Figure A-87: Gage E15 filtered strain data

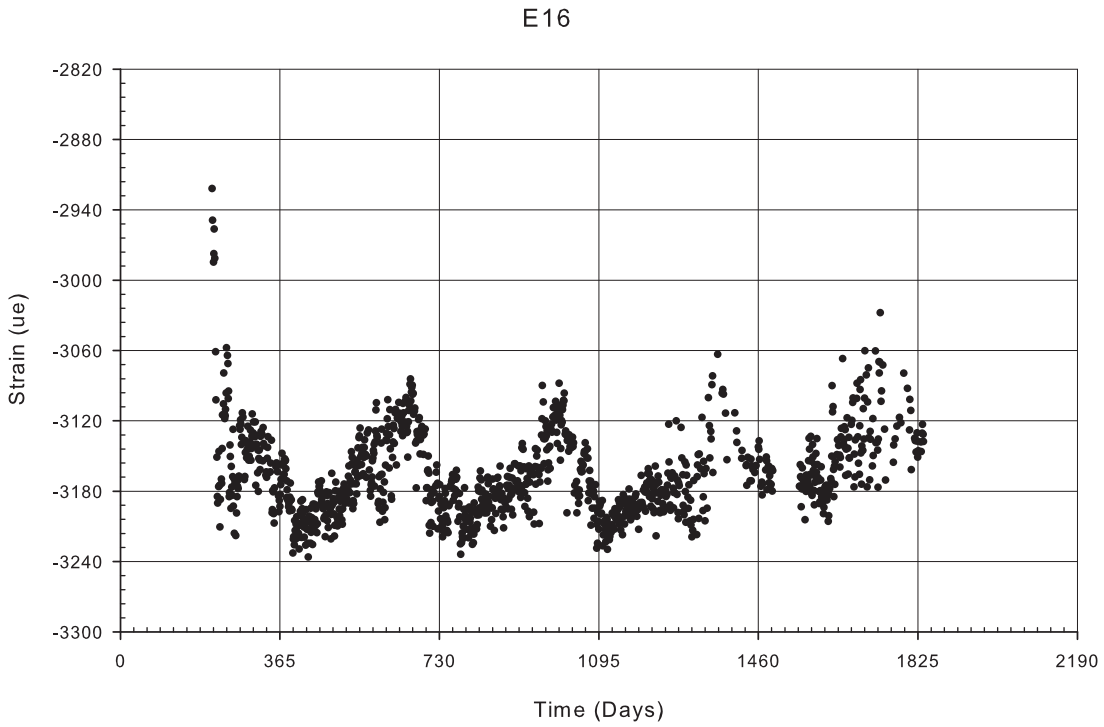

Figure A-88: Gage E16 filtered strain data

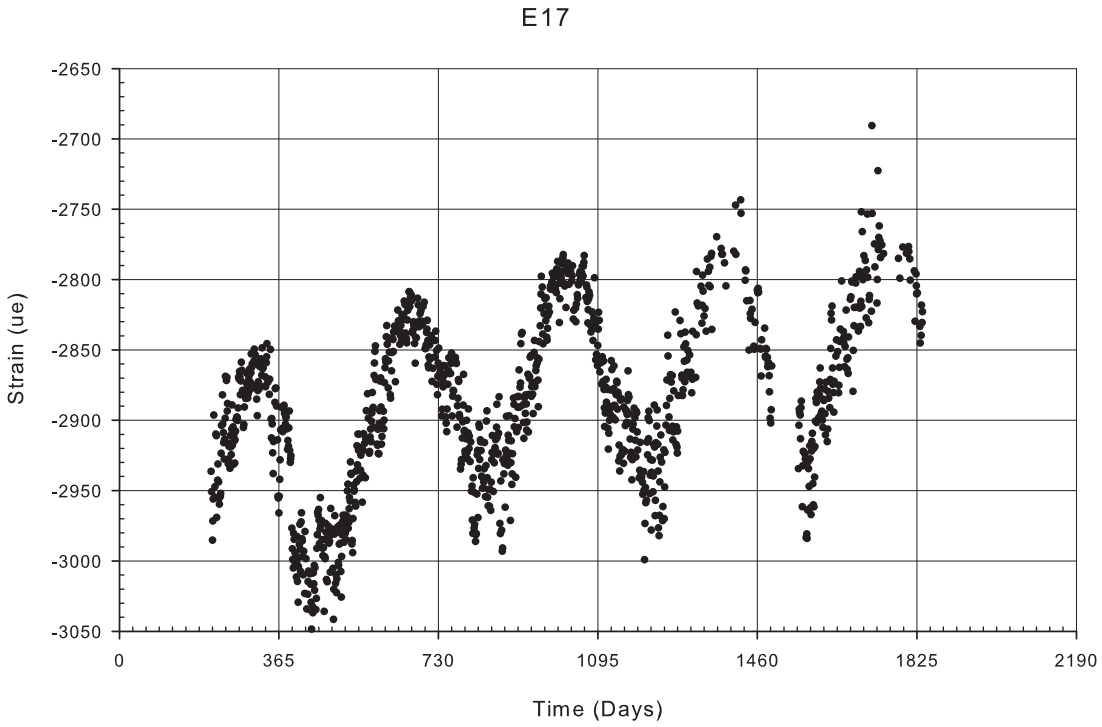

Figure A-89: Gage E17 filtered strain data

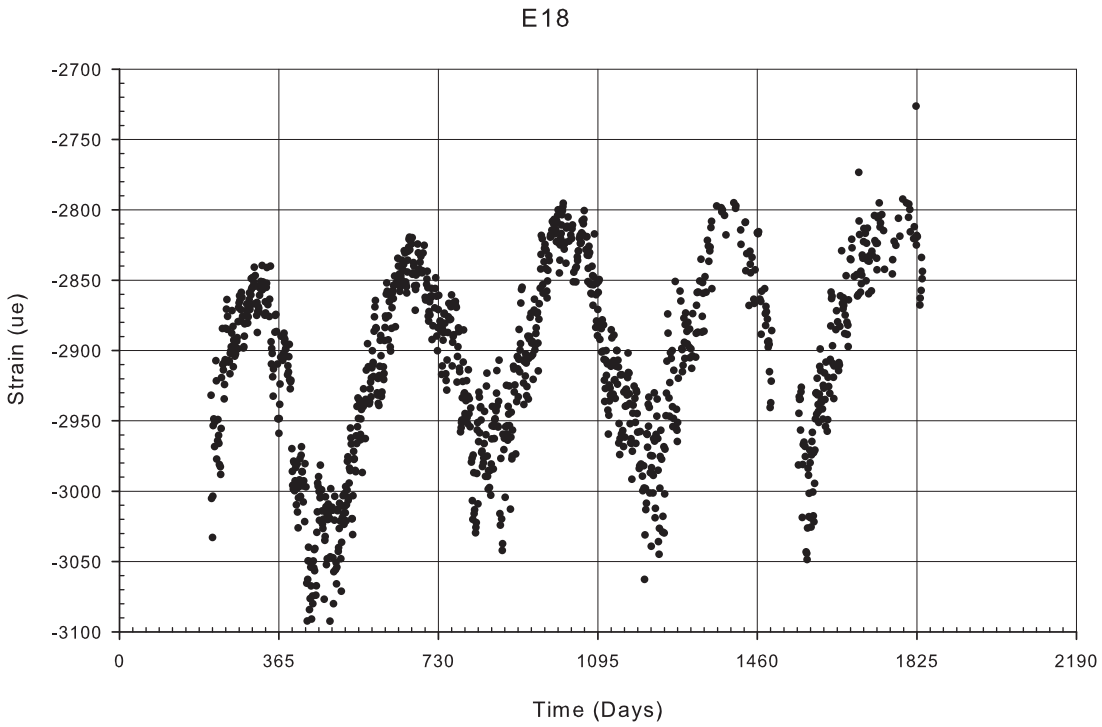

Figure A-90: Gage E18 filtered strain data

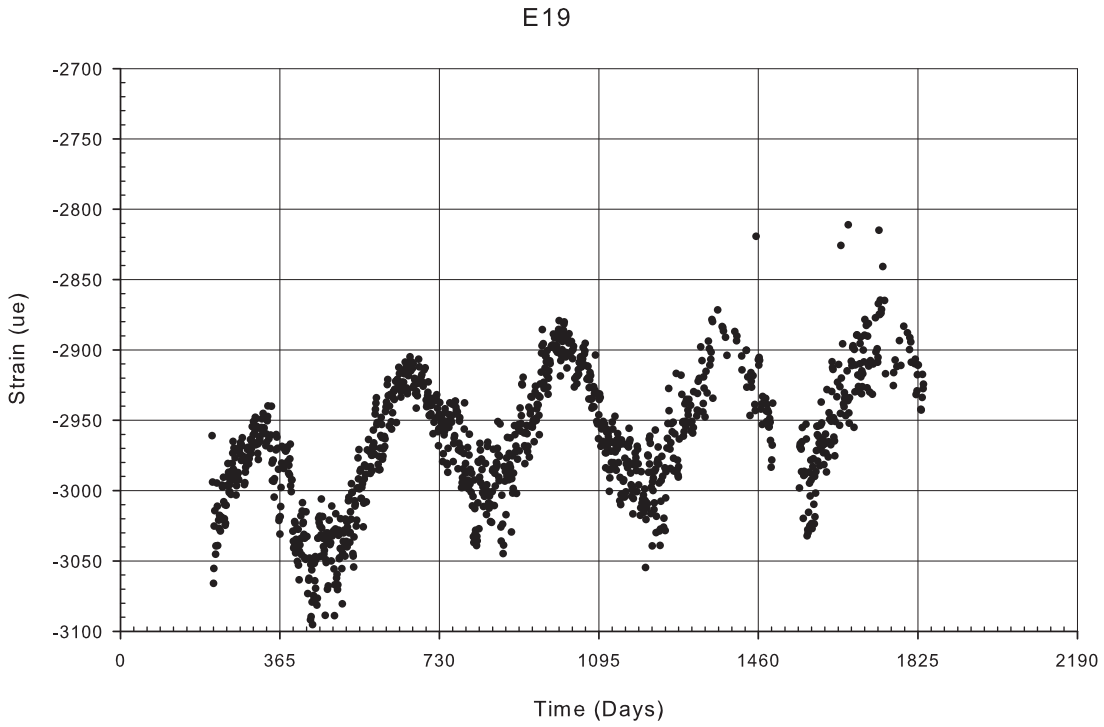

Figure A-91: Gage E19 filtered strain data

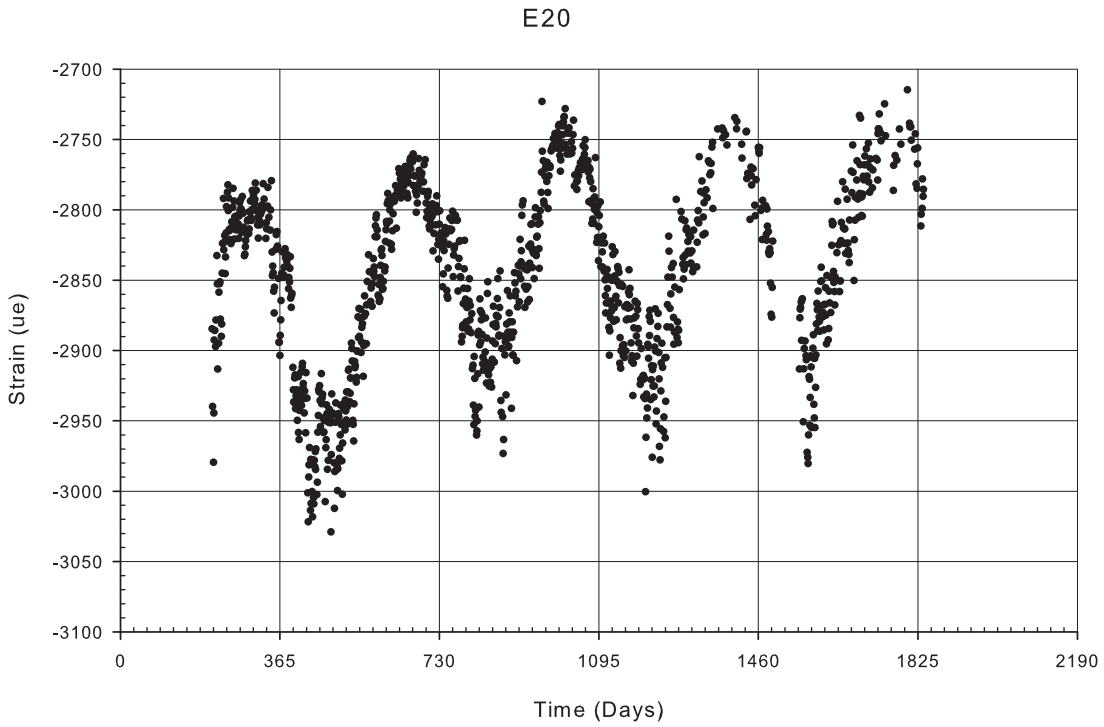

Figure A-92: Gage E20 filtered strain data

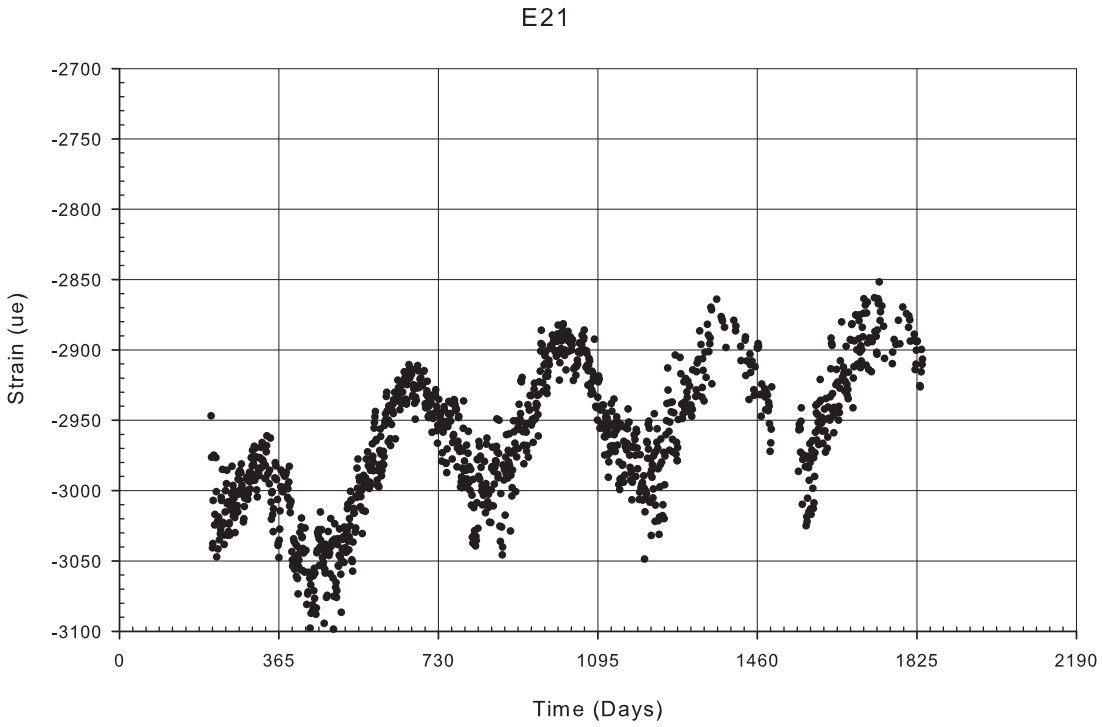

Figure A-93: Gage E21 filtered strain data

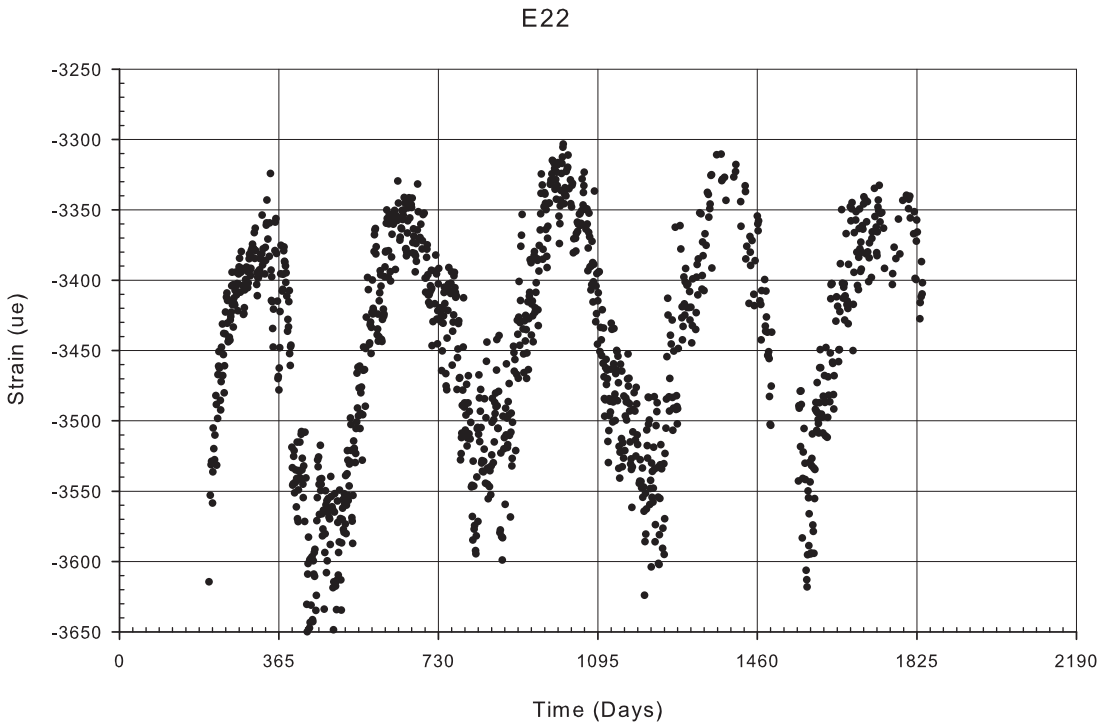

Figure A-94: Gage E22 filtered strain data

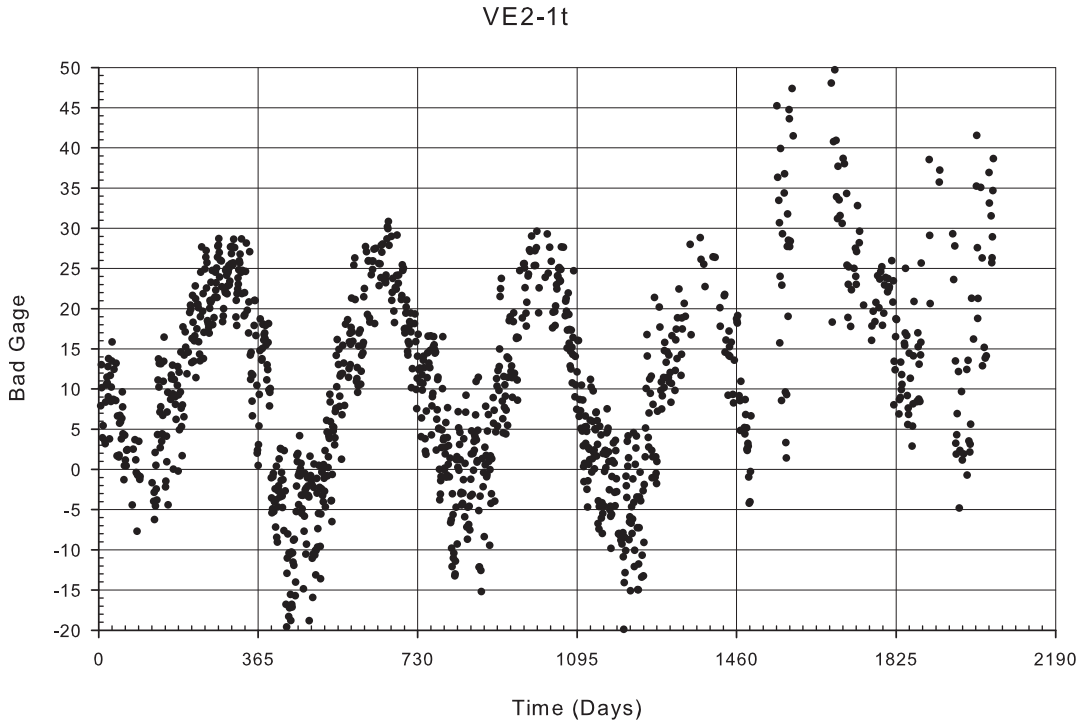

Figure A-95: Gage VE2-1t filtered temperature data

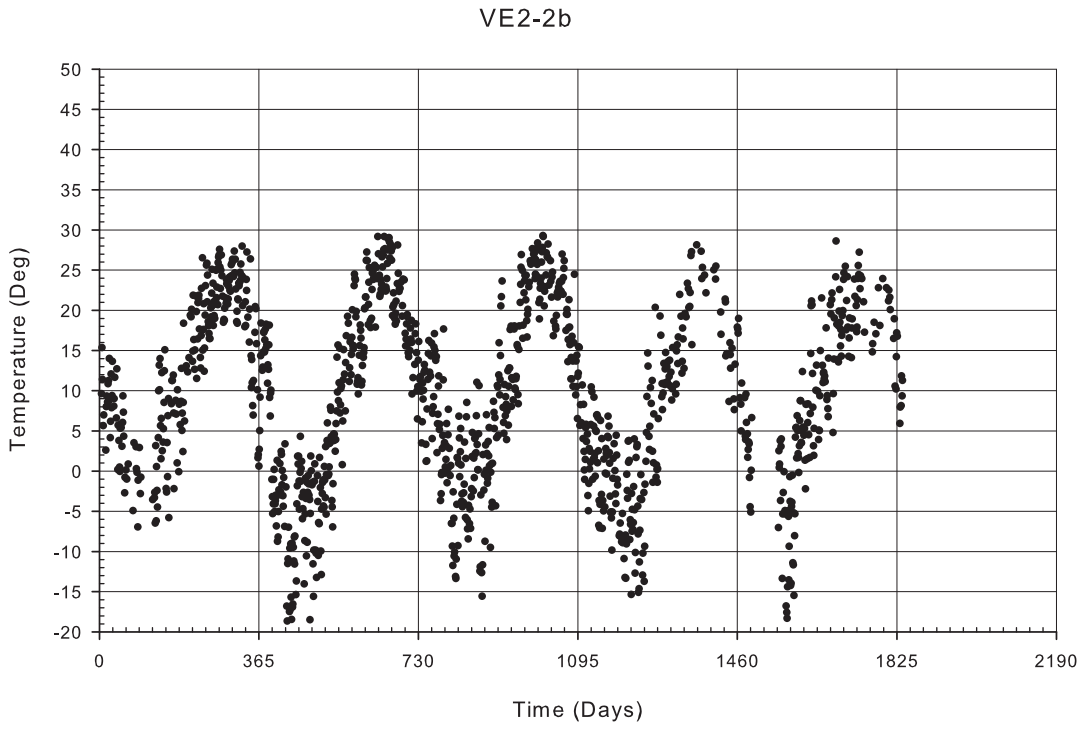

Figure A-96: Gage VE2-2b filtered temperature data

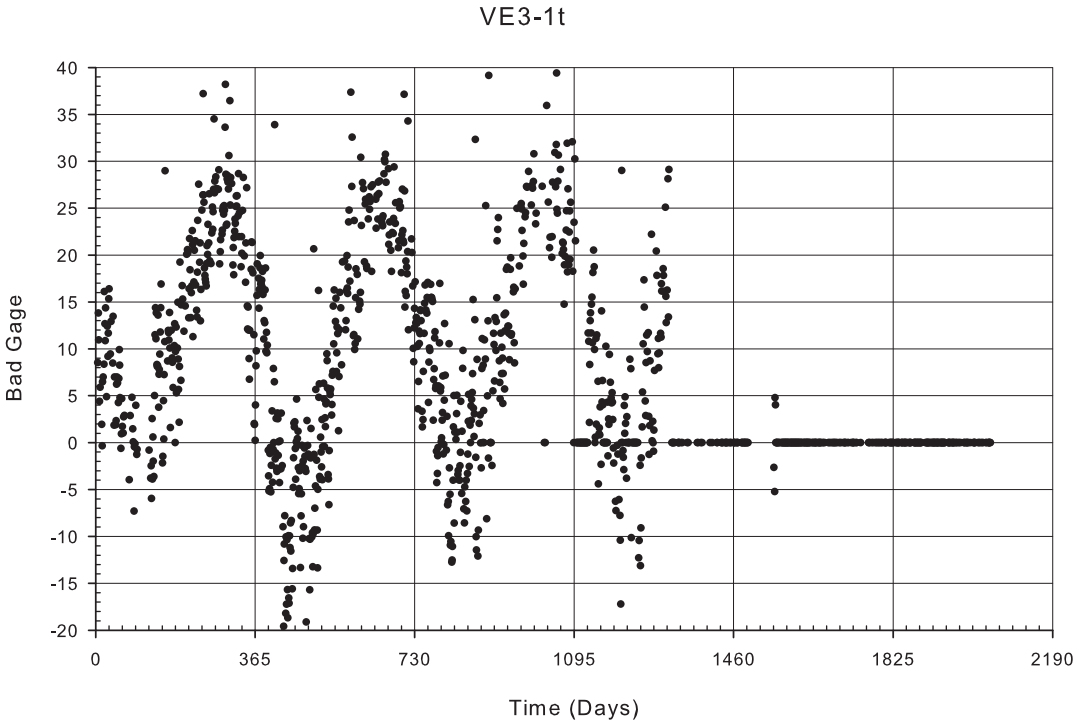

Figure A-97: Gage VE3-1t filtered temperature data

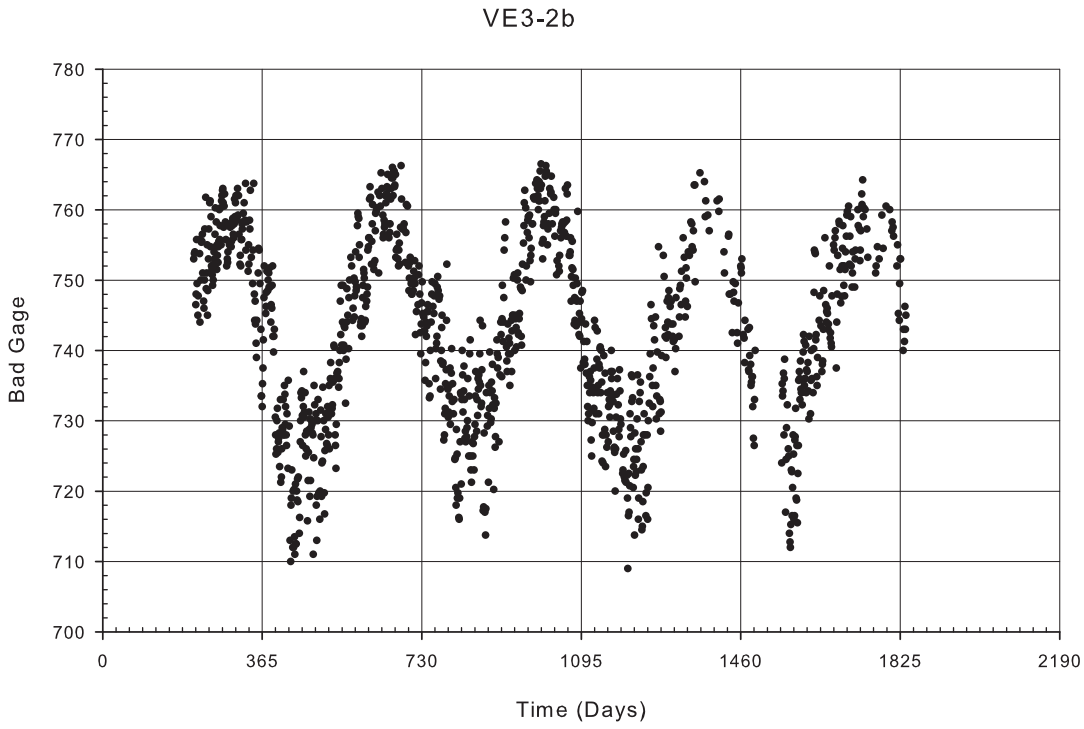

Figure A-98: Gage VE3-2b filtered temperature data

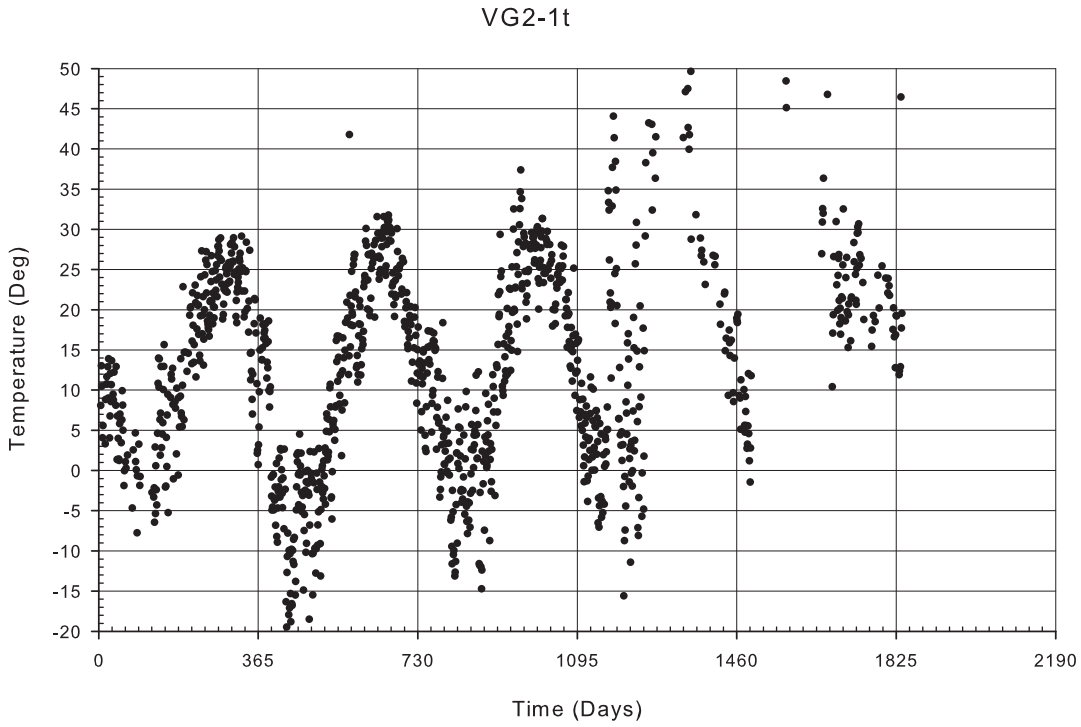

Figure A-99: Gage VG2-1t filtered temperature data

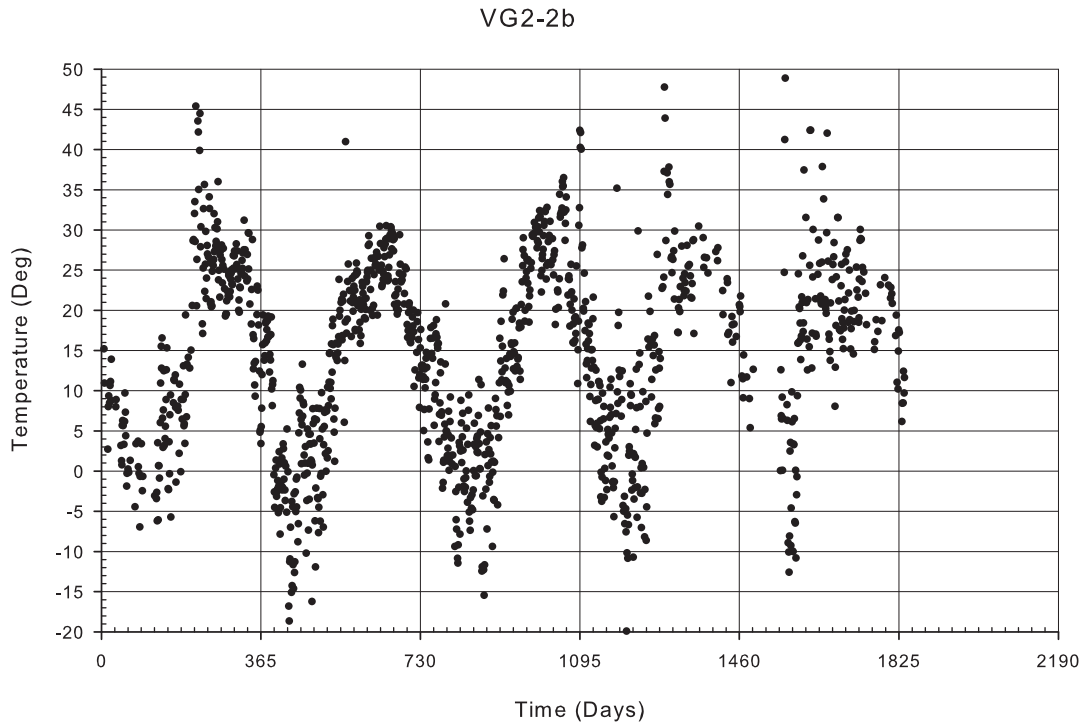

Figure A-100: Gage VG2-2b filtered temperature data

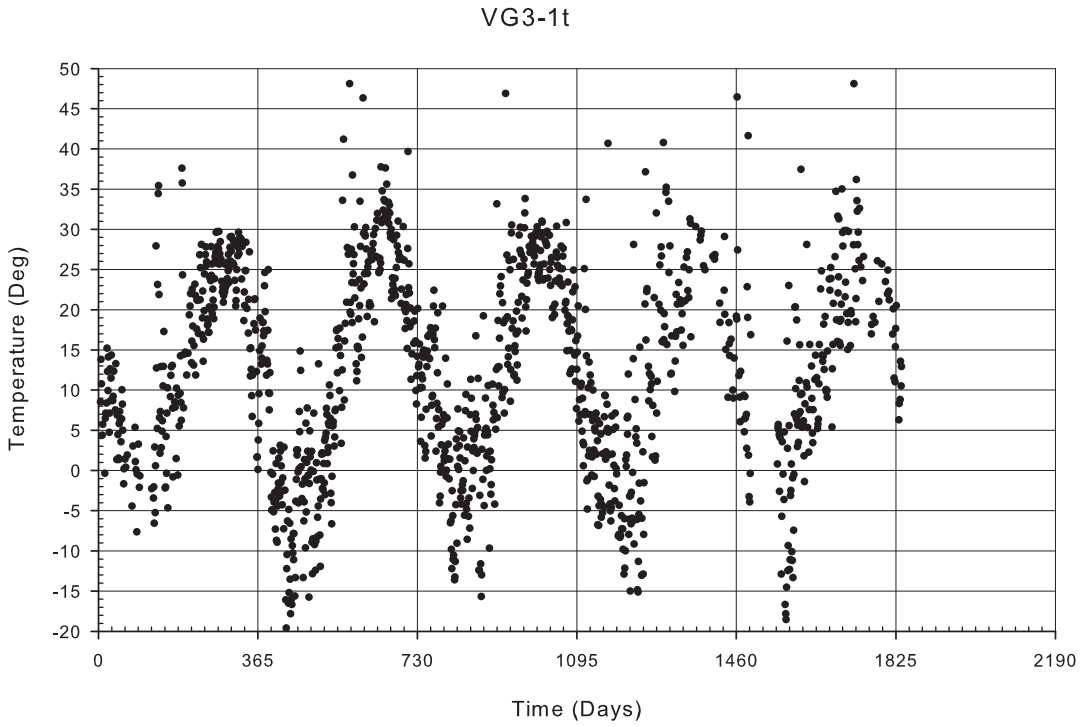

Figure A-101: Gage VG3-1t filtered temperature data

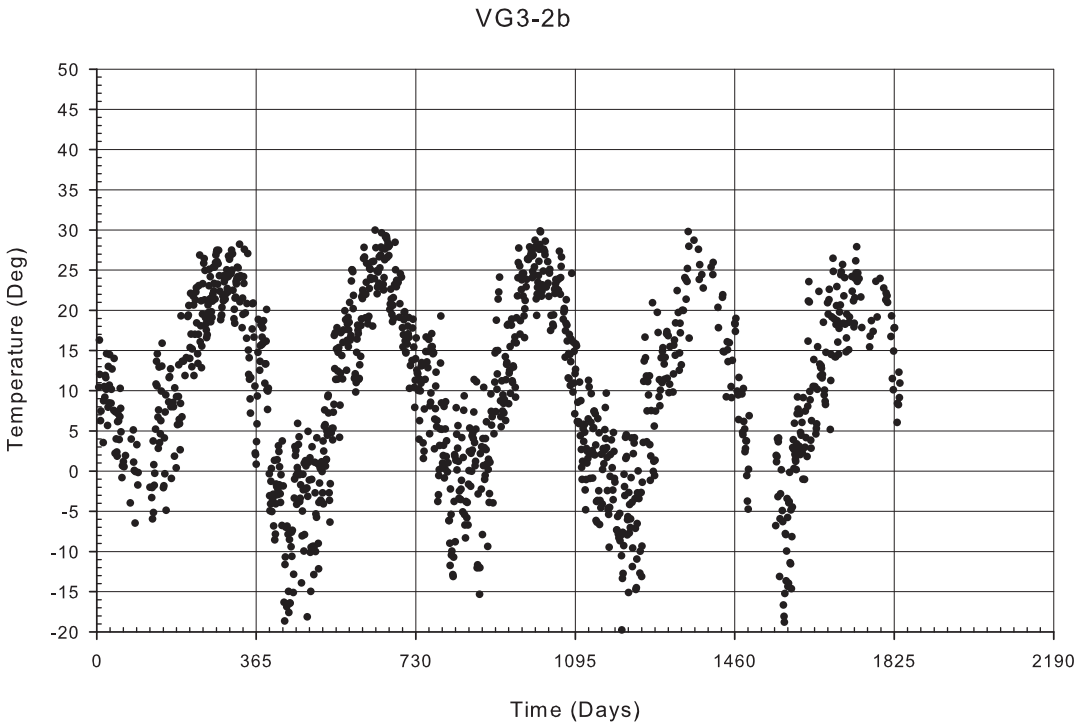

Figure A-102: Gage VG3-2b filtered temperature data

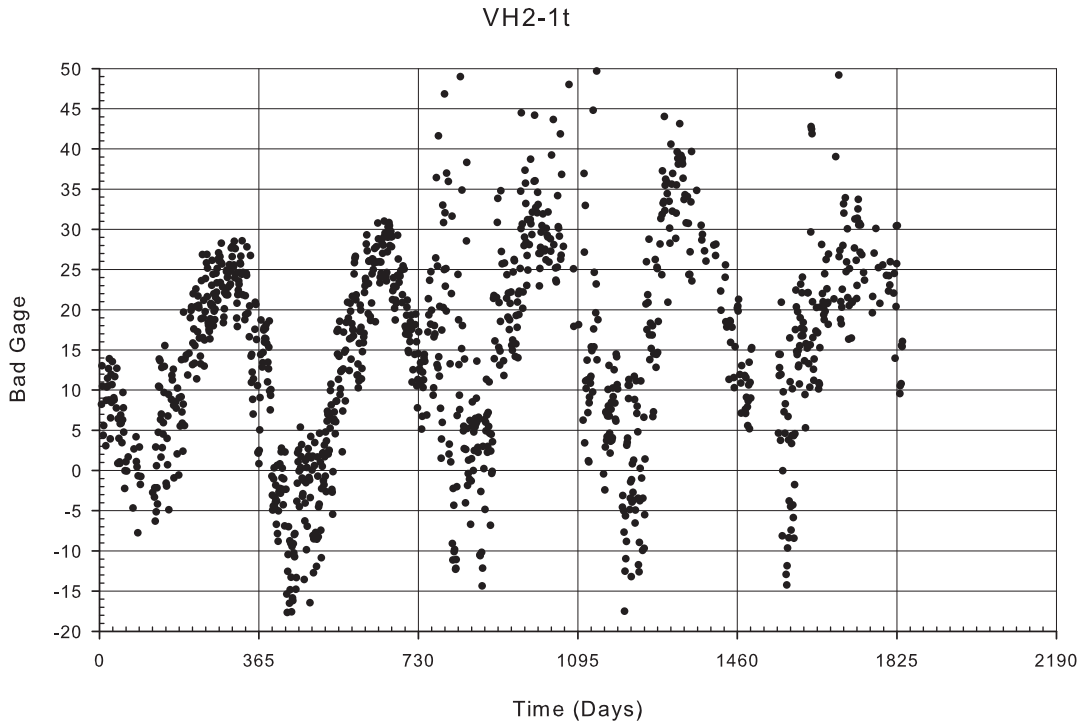

Figure A-103: Gage VH2-1t filtered temperature data

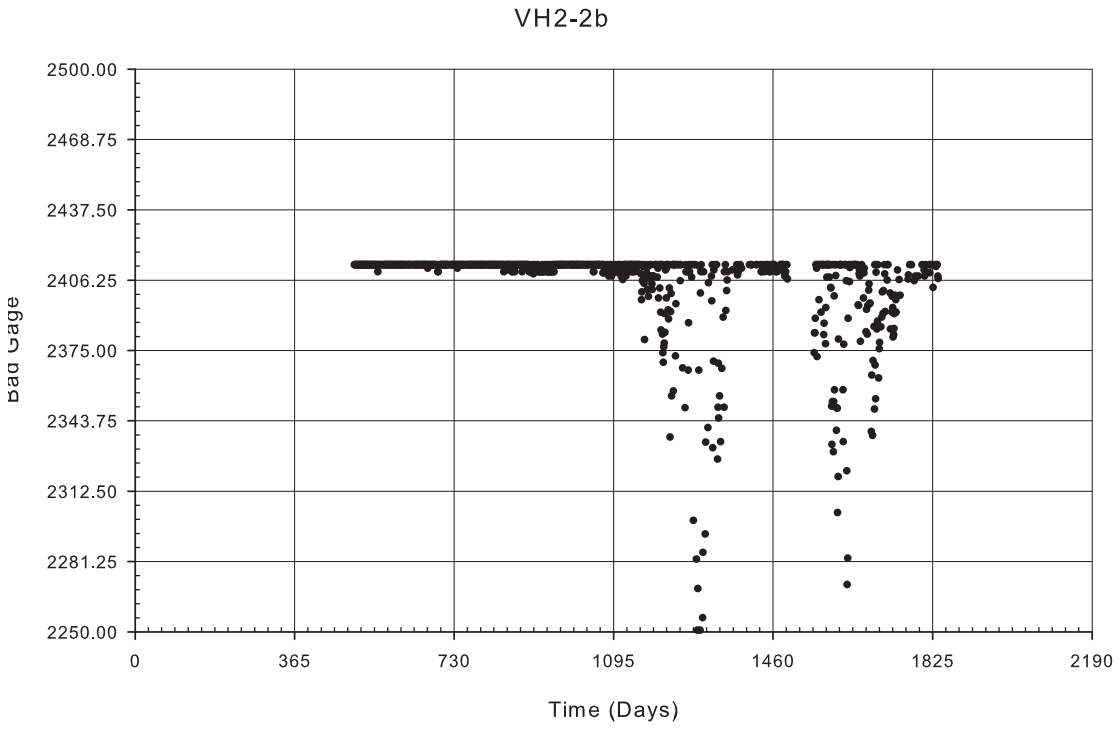

Figure A-104: Gage VH2-2b filtered temperature data

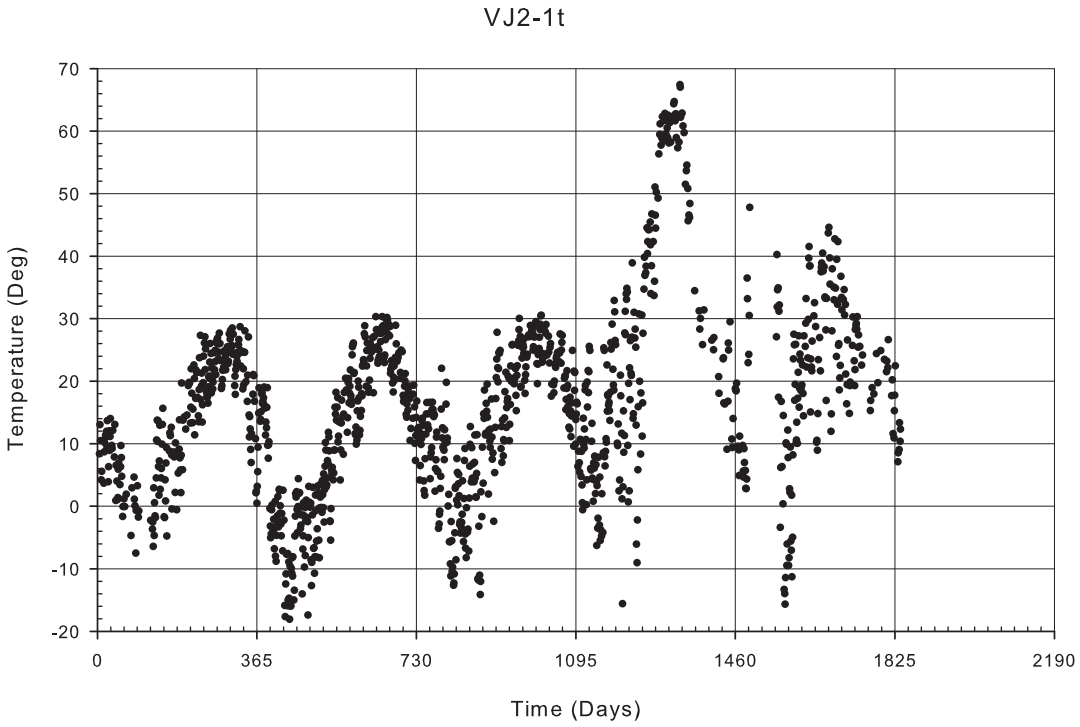

Figure A-105: Gage VJ2-1t filtered temperature data

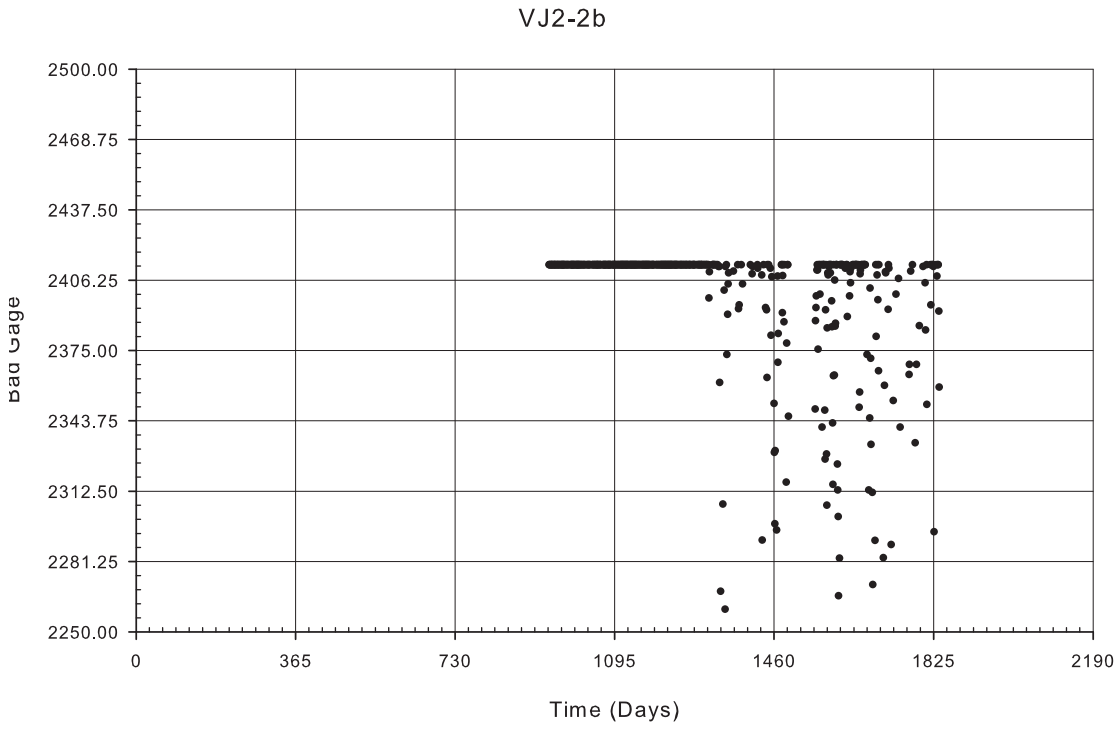

Figure A-106: Gage VJ2-2b filtered temperature data

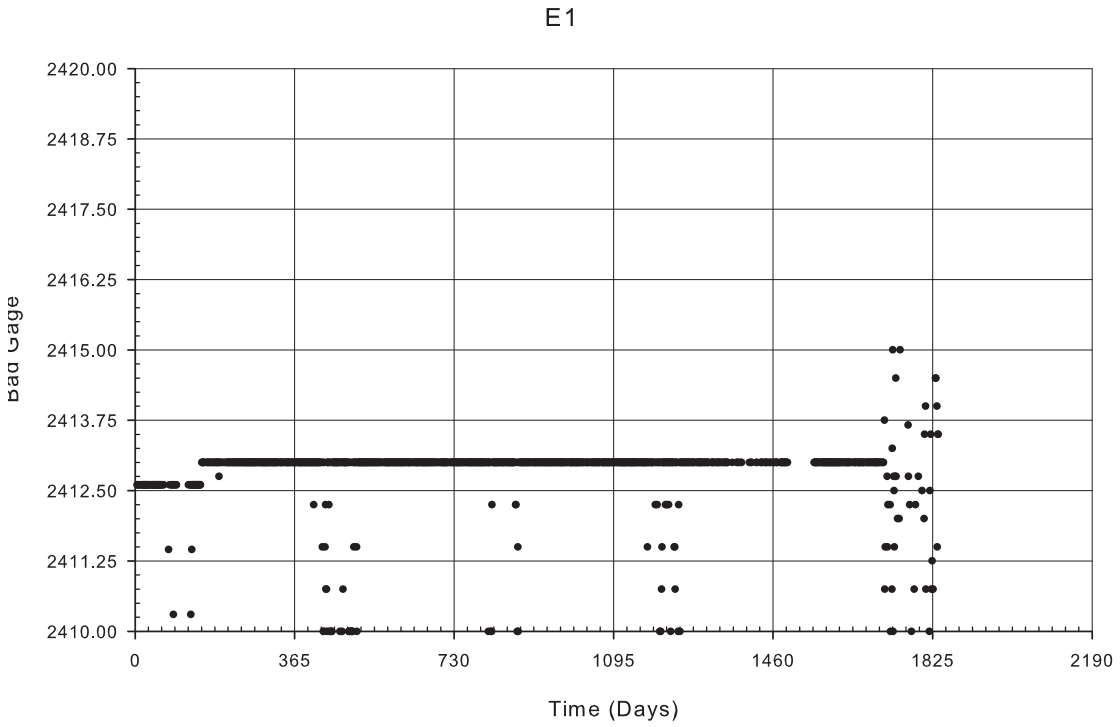

Figure A-107: Gage E1 filtered temperature data

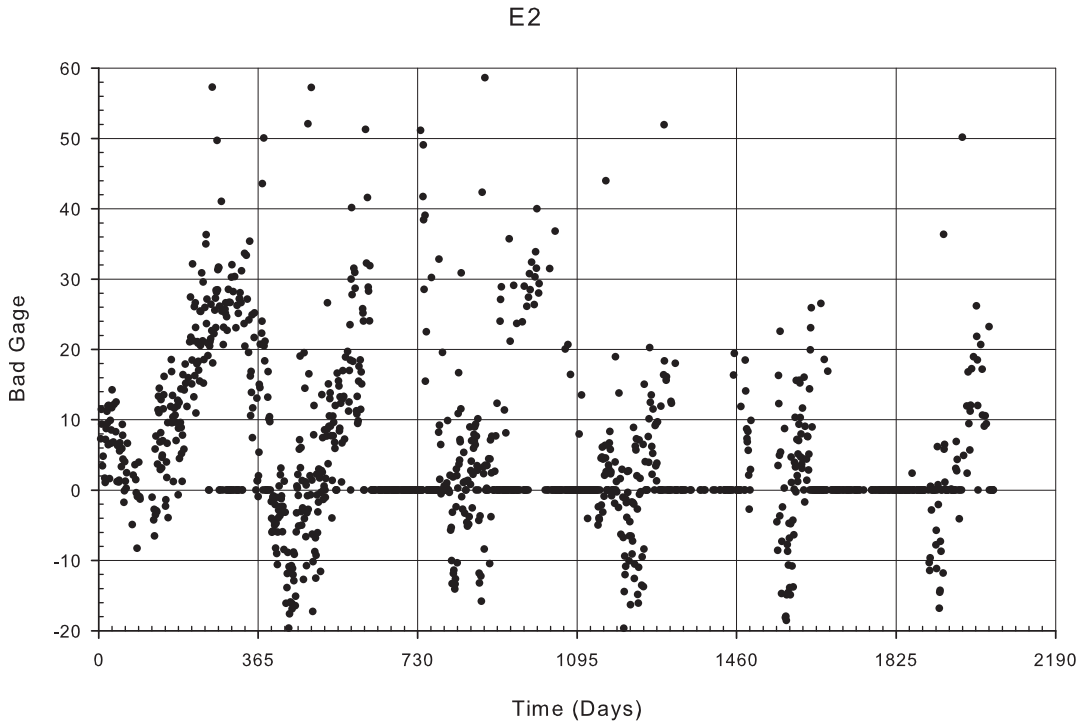

Figure A-108: Gage E2 filtered temperature data

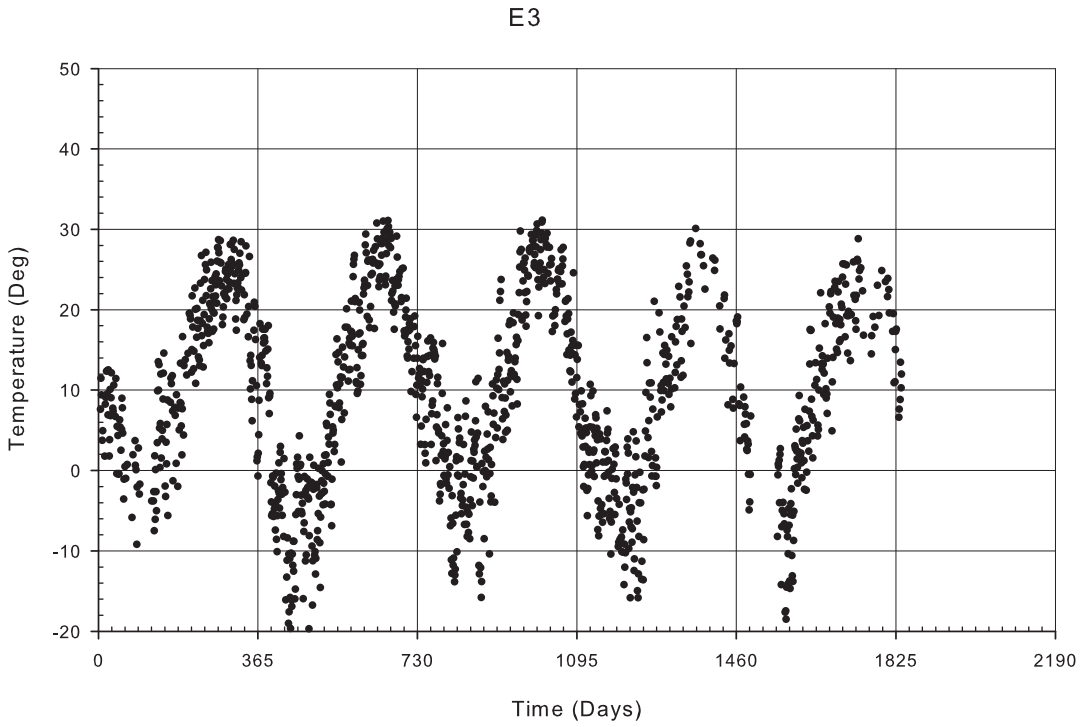

Figure A-109: Gage E3 filtered temperature data

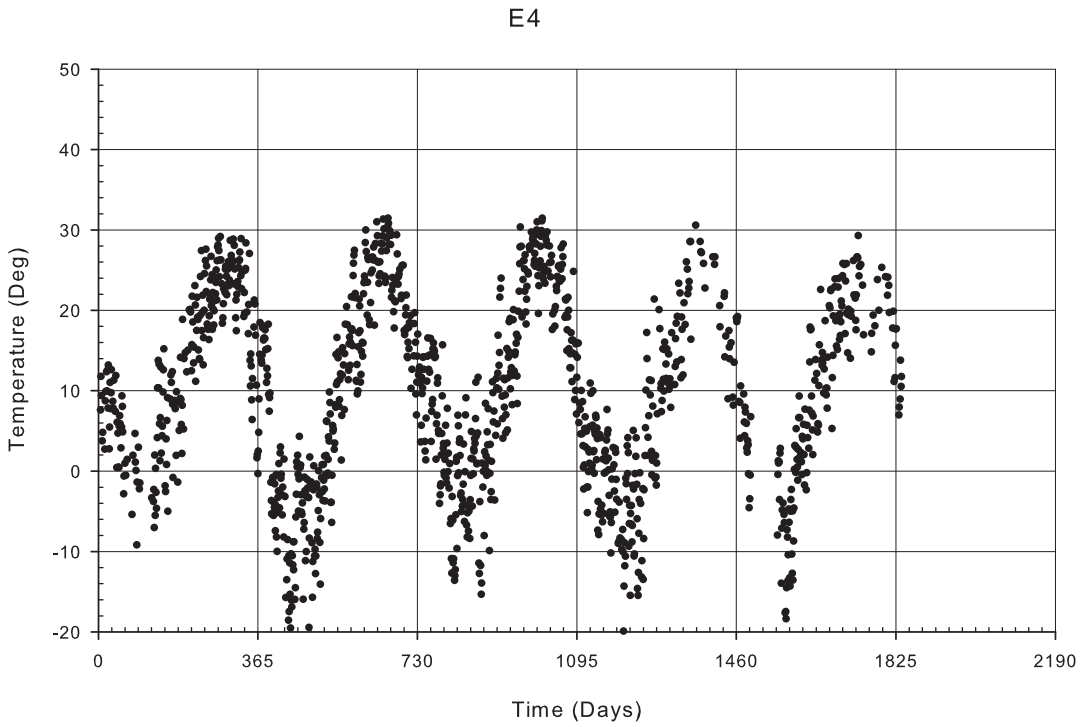

Figure A-110: Gage E4 filtered temperature data

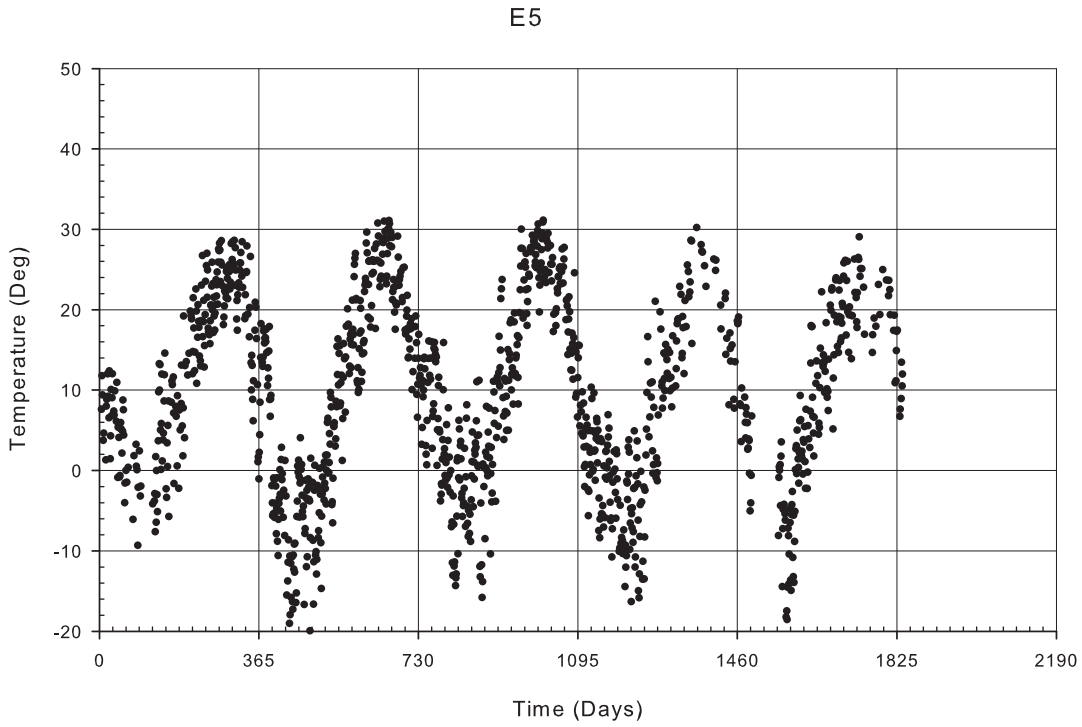

Figure A-111: Gage E5 filtered temperature data

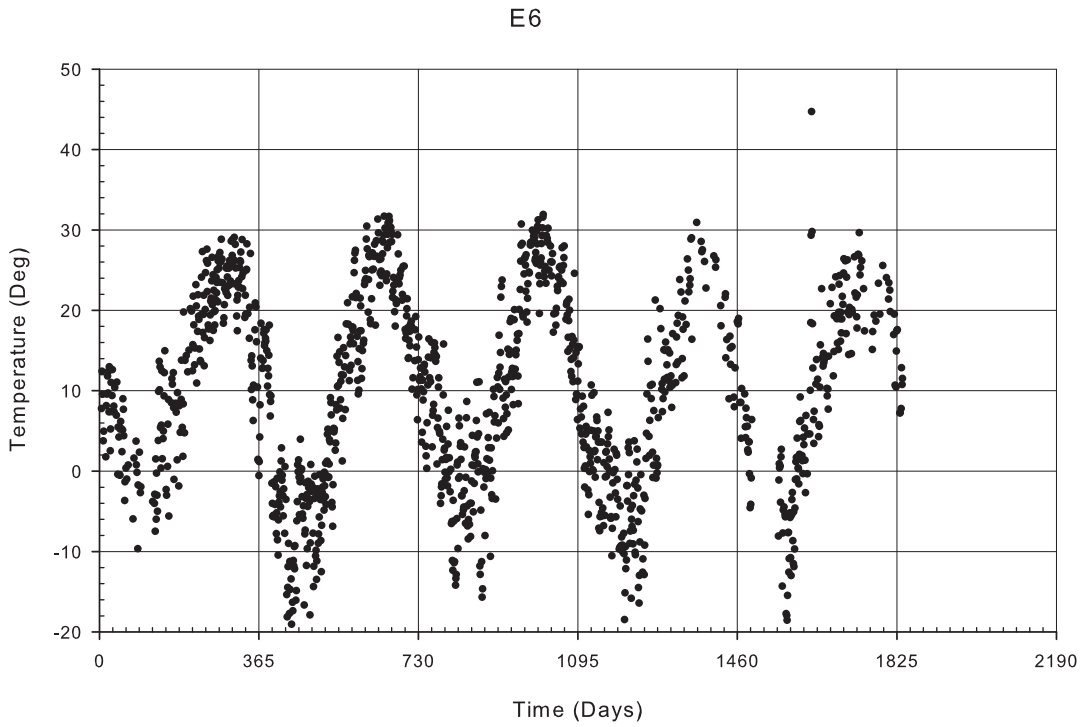

Figure A-112: Gage E6 filtered temperature data

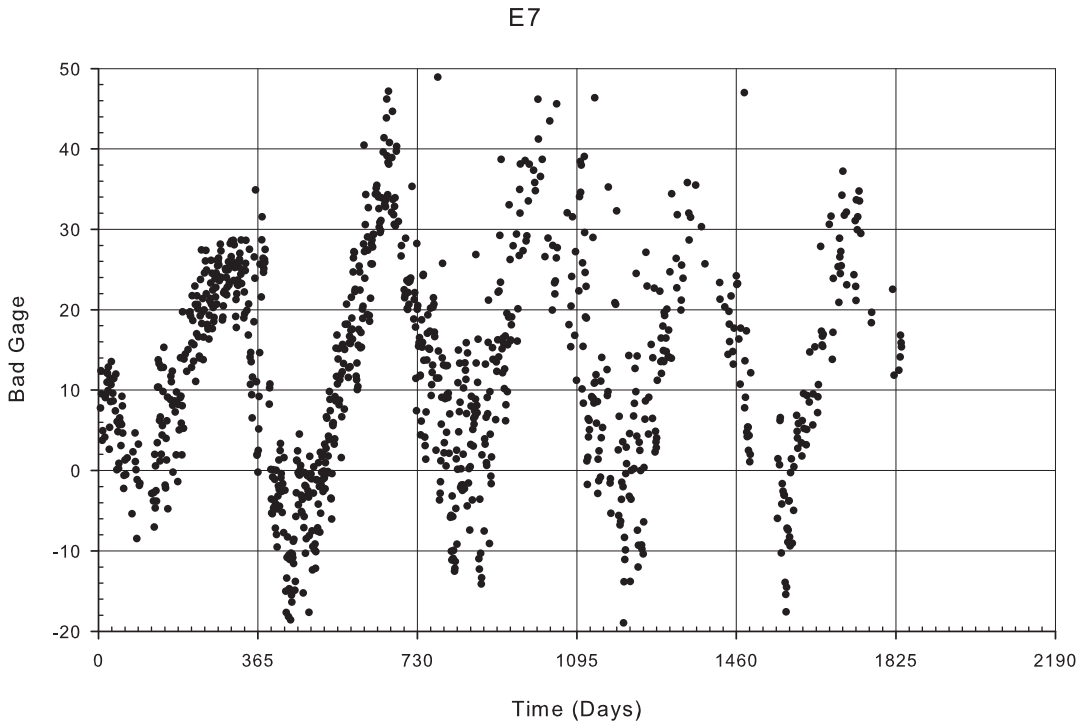

Figure A-113: Gage E7 filtered temperature data

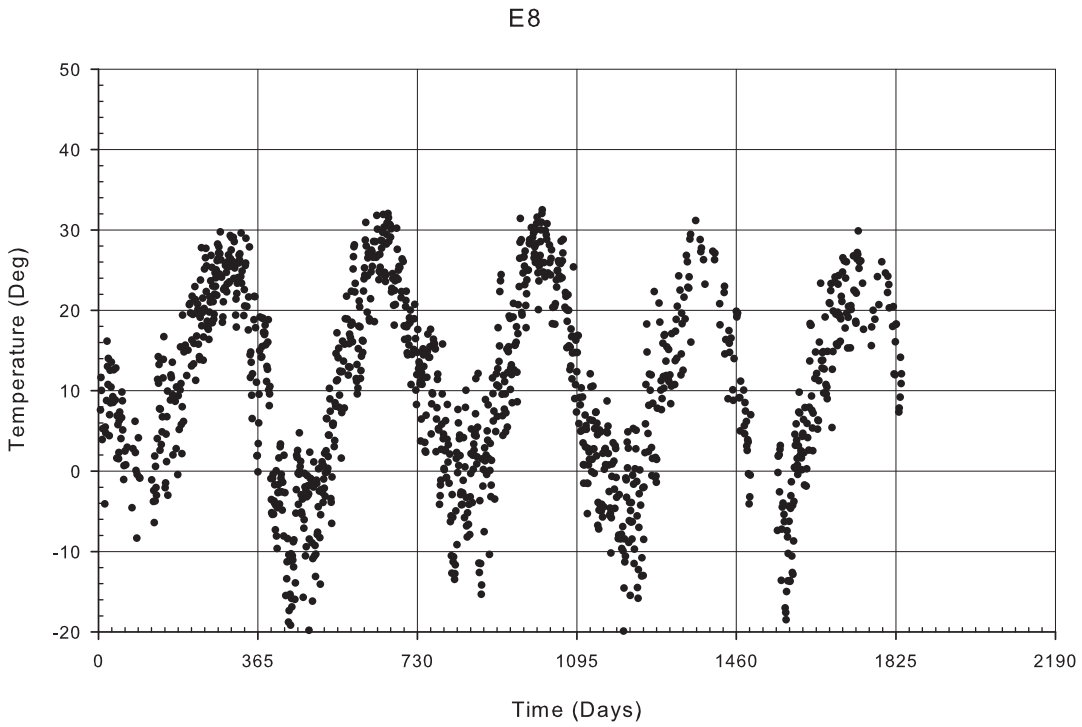

Figure A-114: Gage E8 filtered temperature data

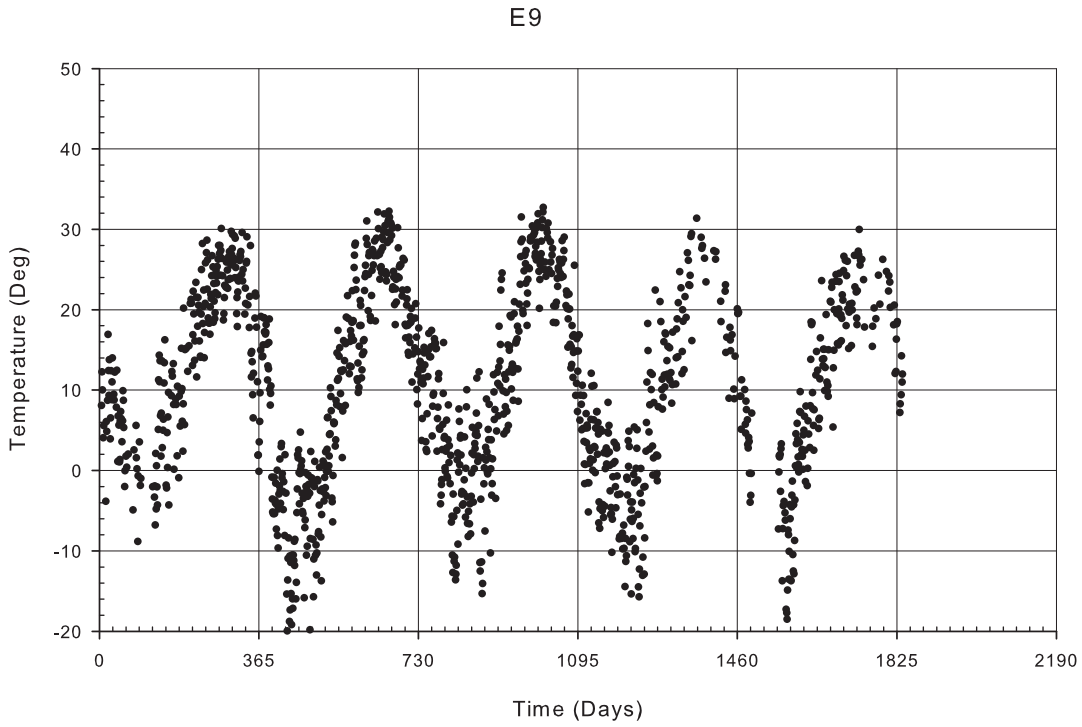

Figure A-115: Gage E9 filtered temperature data

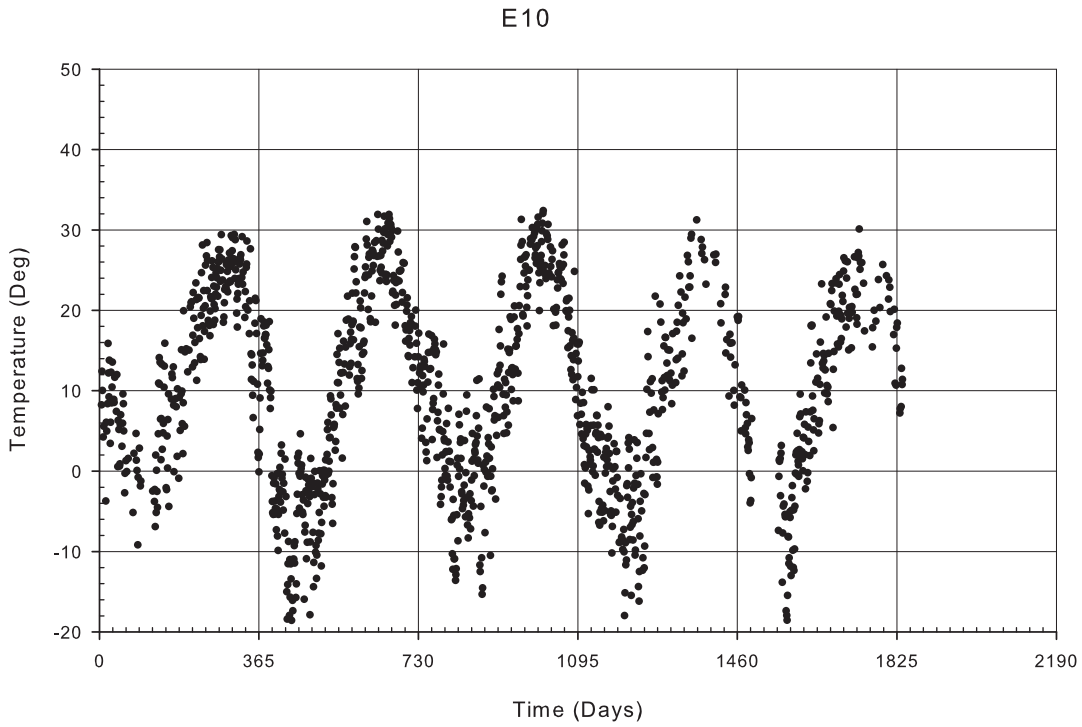

Figure A-116: Gage E10 filtered temperature data

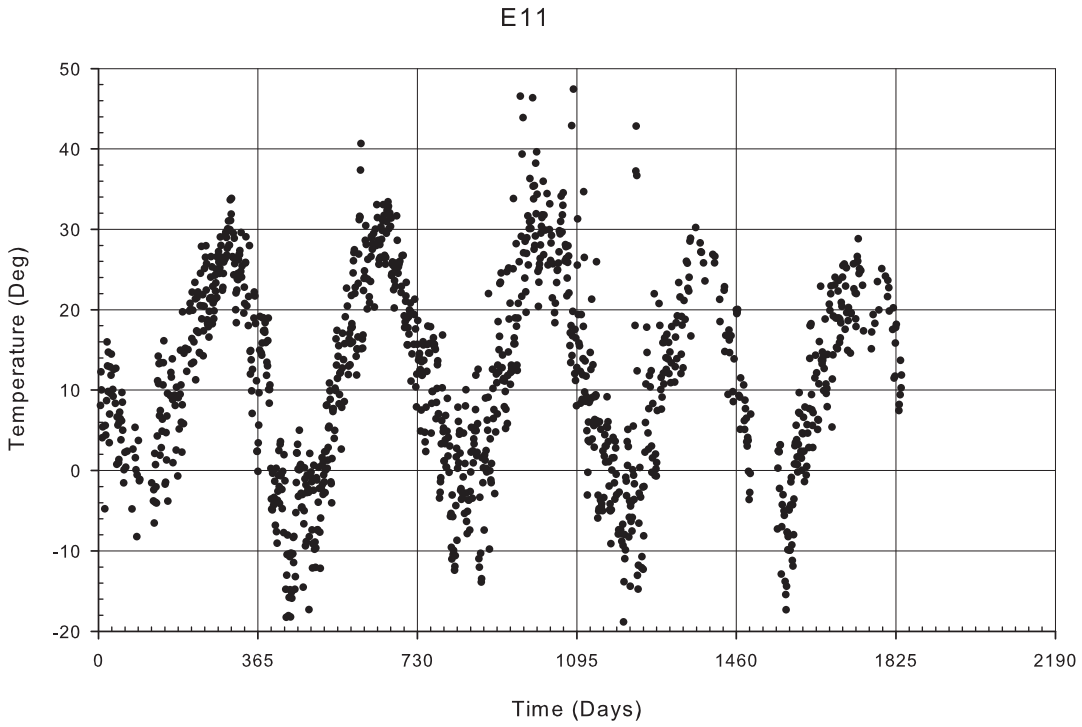

Figure A-117: Gage E11 filtered temperature data

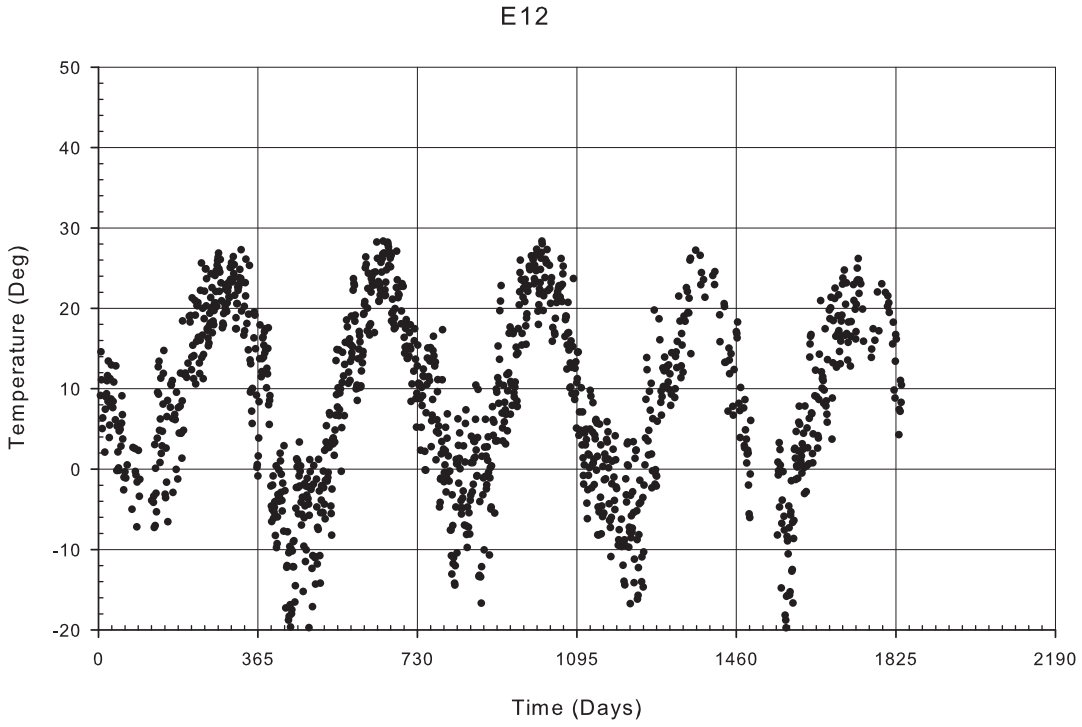

Figure A-118: Gage E12 filtered temperature data

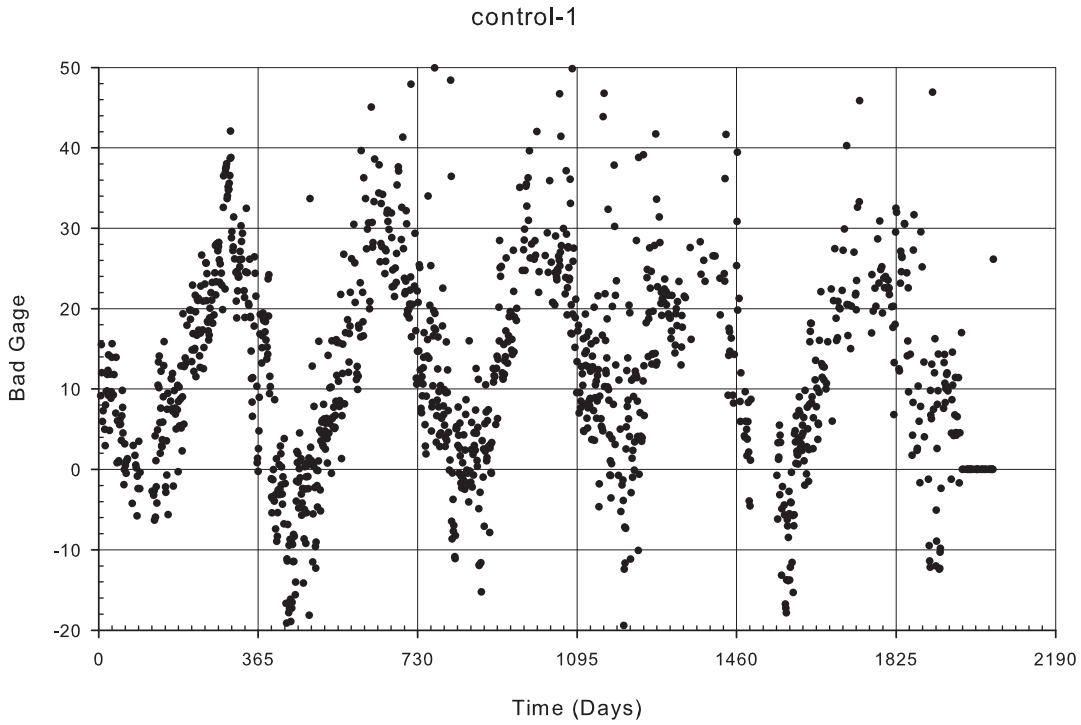

Figure A-119: Gage control-1 filtered temperature data

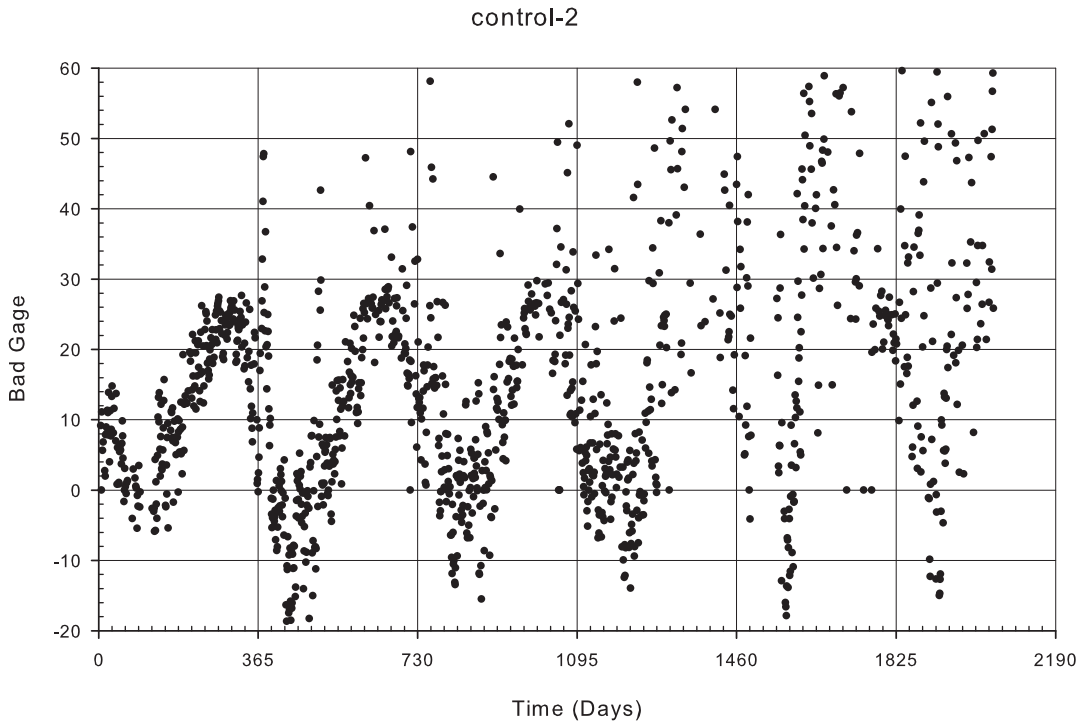

Figure A-120: Gage control-2 filtered temperature data

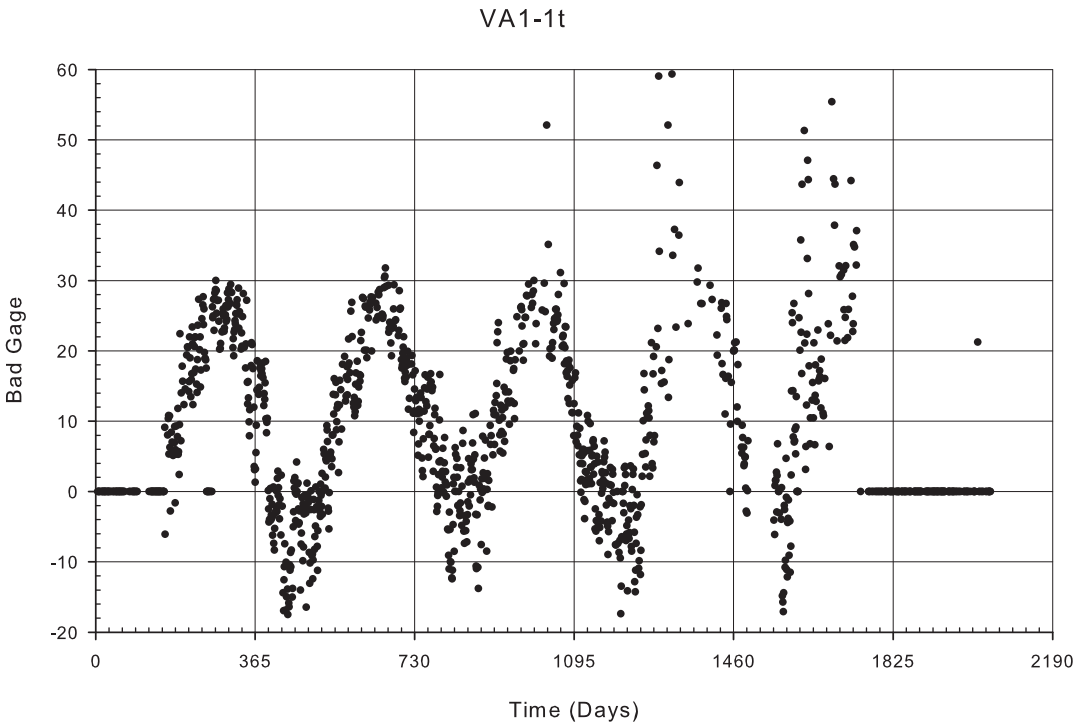

Figure A-121: Gage VA1-1t filtered temperature data

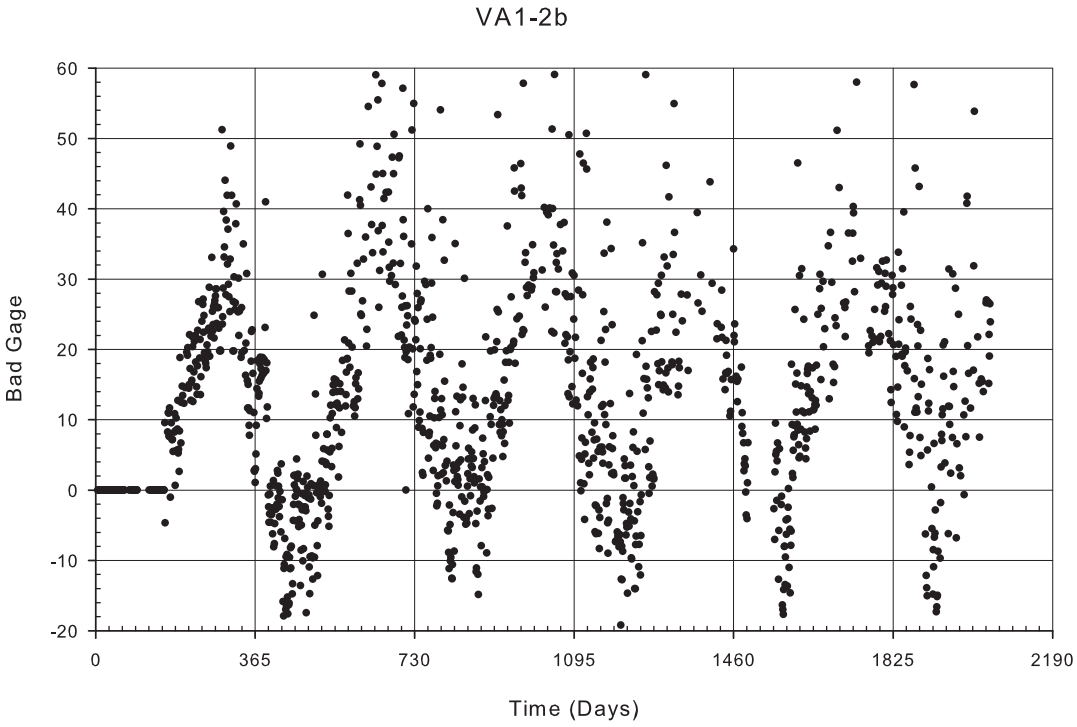

Figure A-122: Gage VA1-2b filtered temperature data

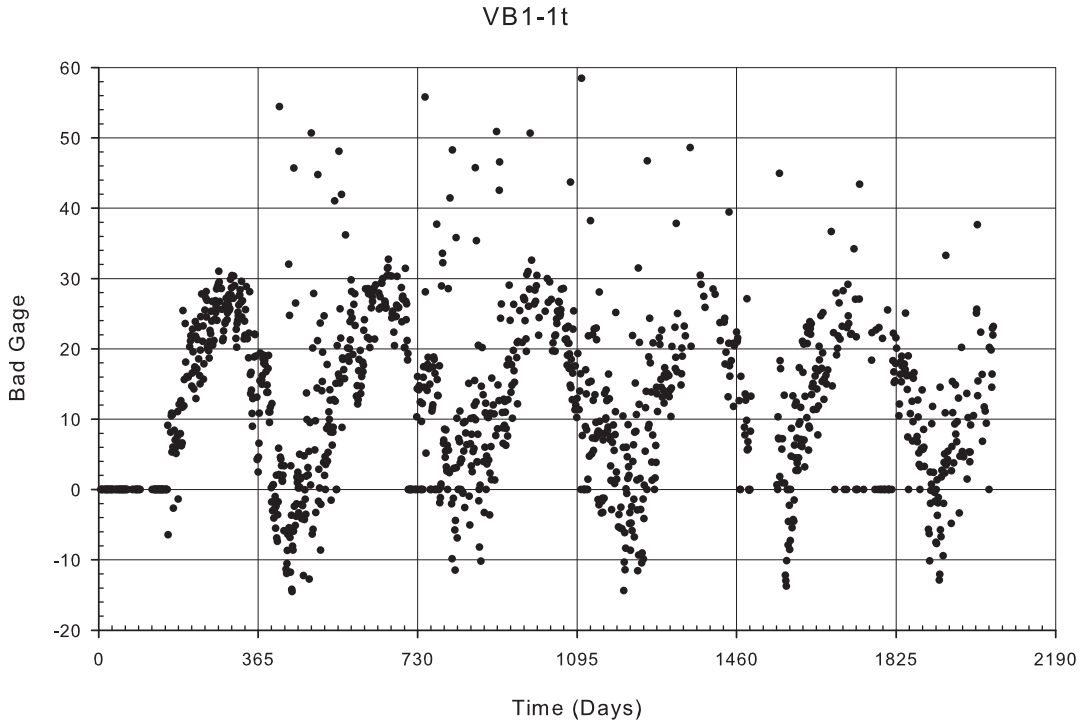

Figure A-123: Gage VB1-1t filtered temperature data

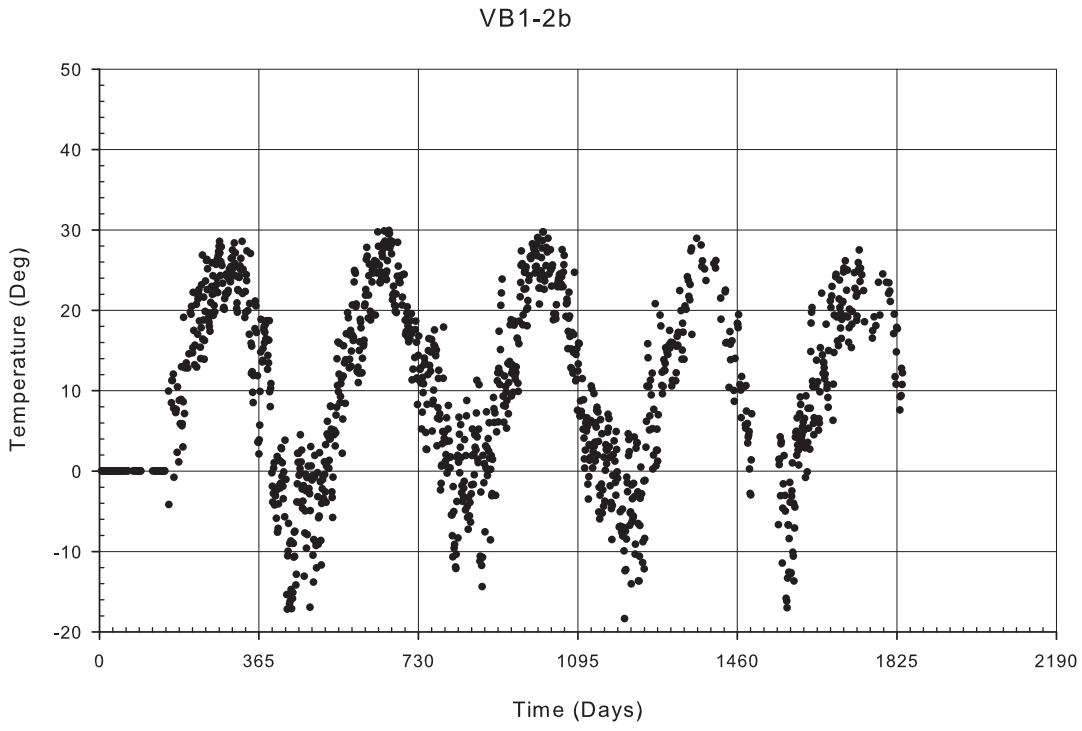

Figure A-124: Gage VB1-2b filtered temperature data

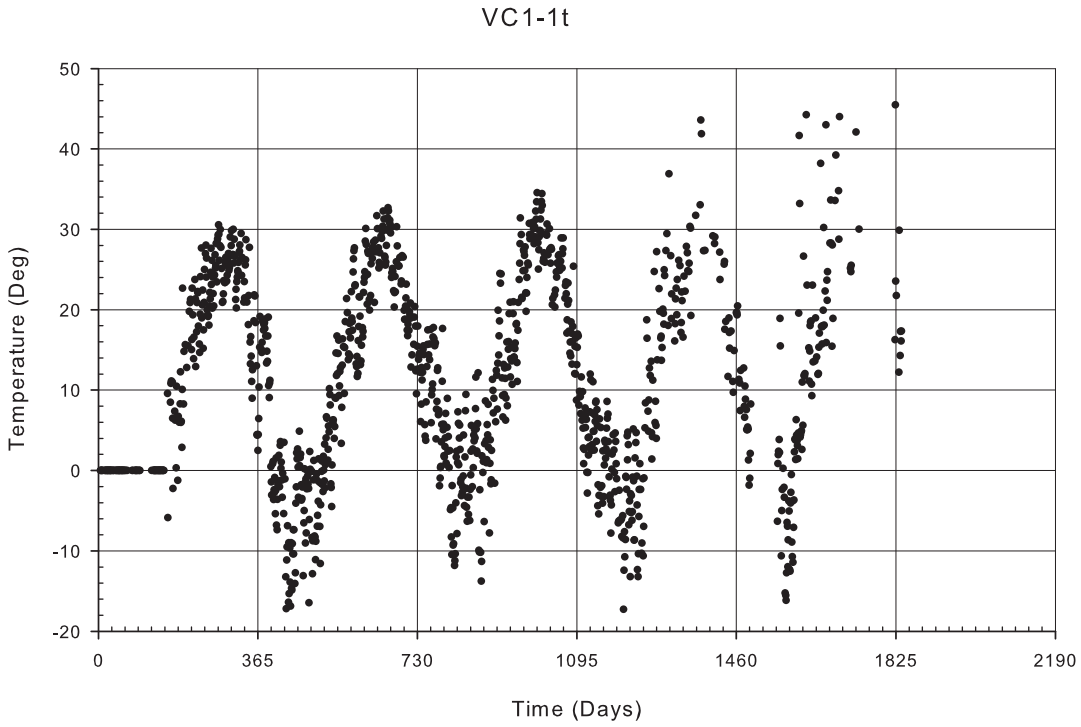

Figure A-125: Gage VC1-1t filtered temperature data

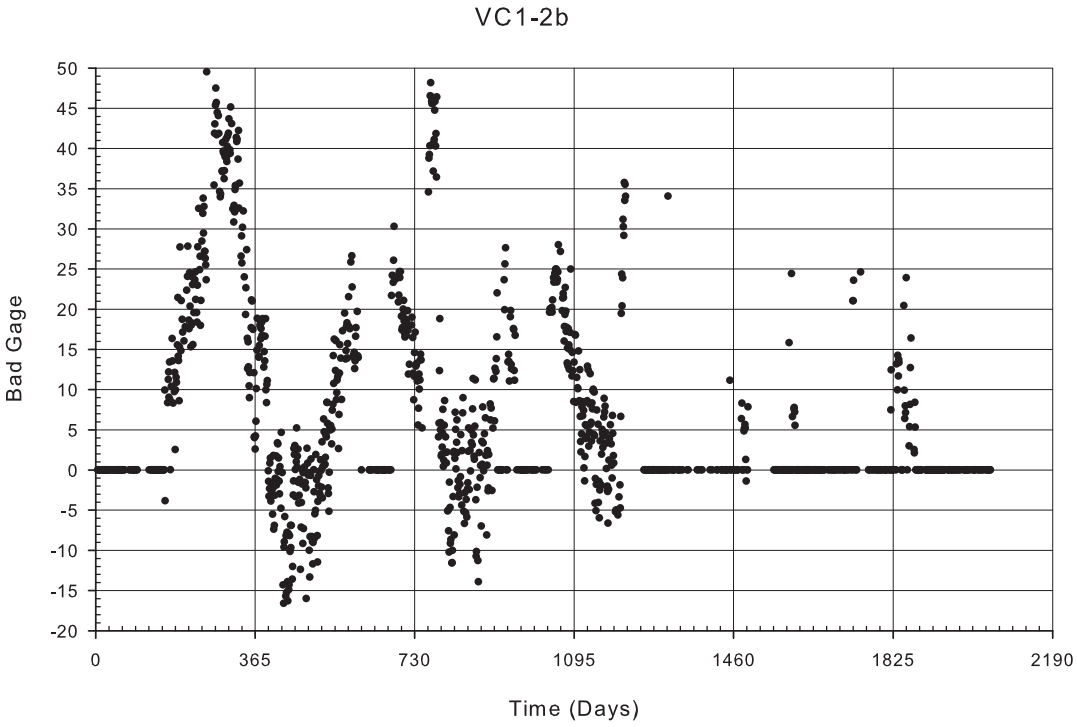

Figure A-126: Gage VC1-2b filtered temperature data

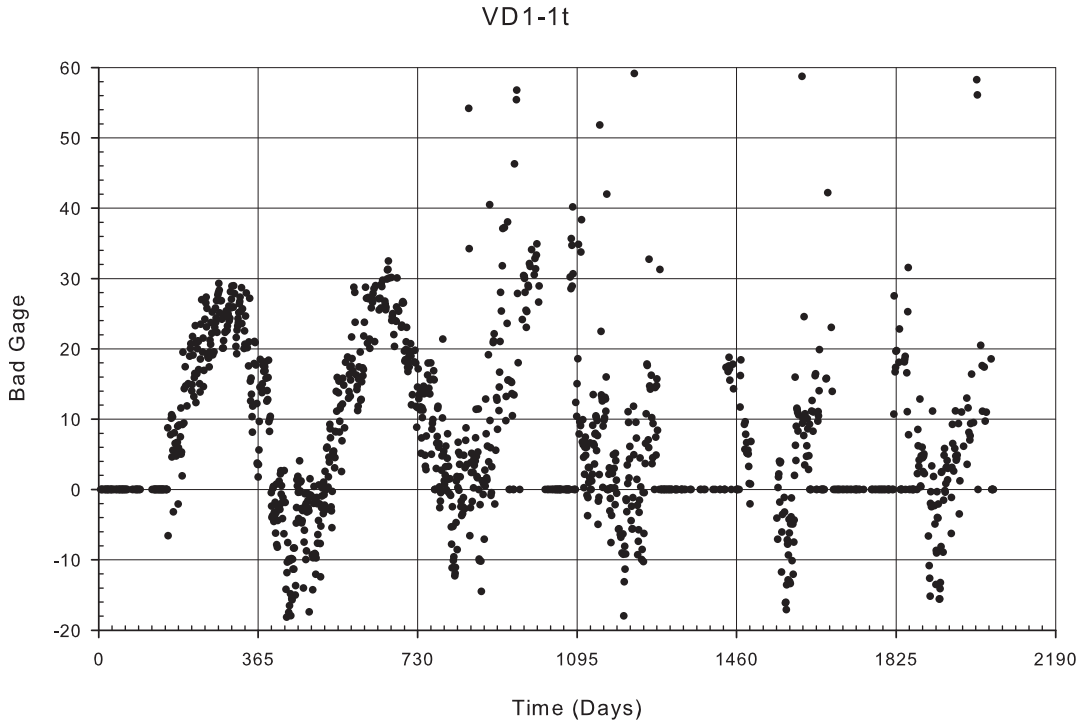

Figure A-127: Gage VD1-1t filtered temperature data

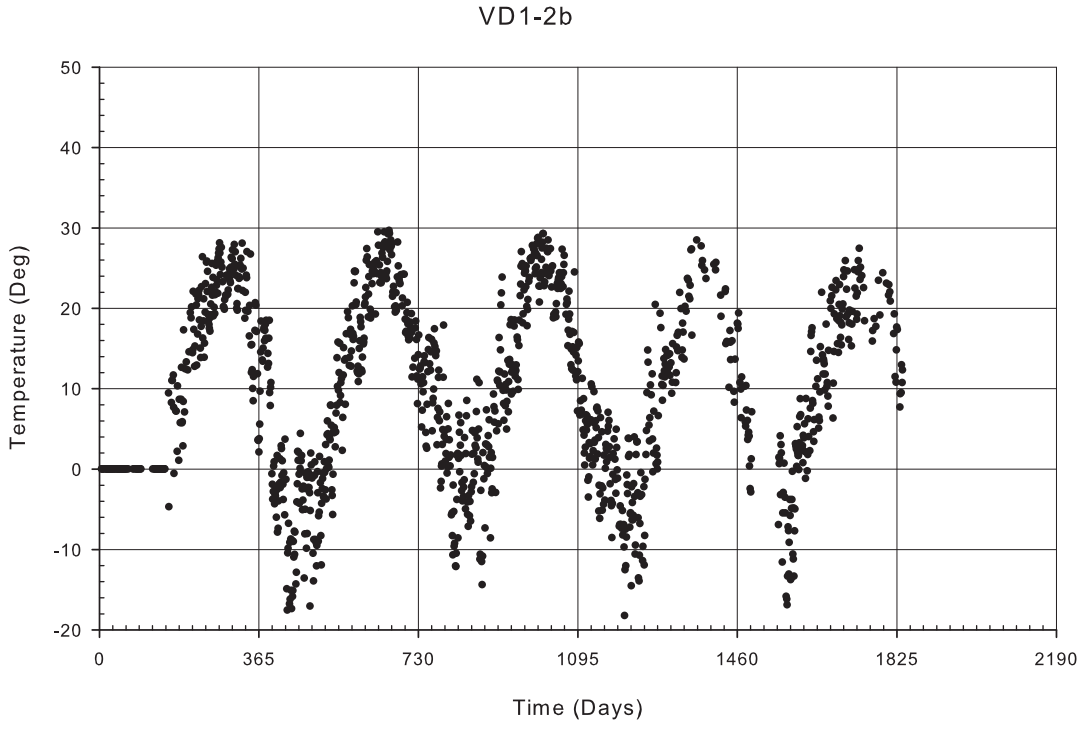

Figure A-128: Gage VD1-2b filtered temperature data

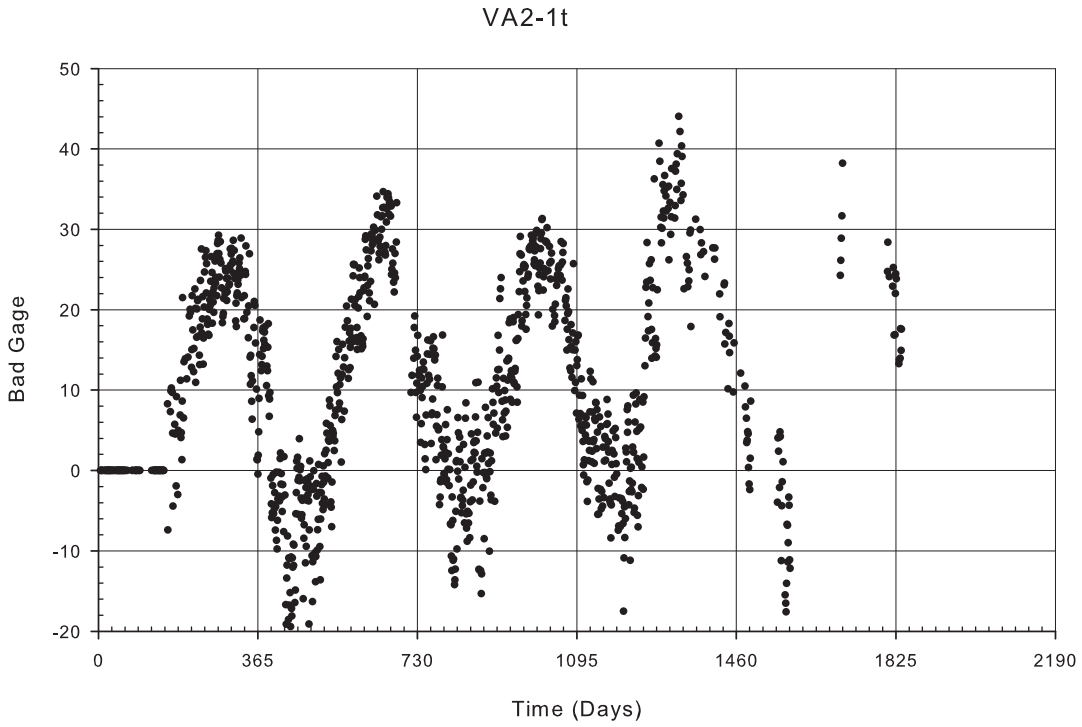

Figure A-129: Gage VA2-1t filtered temperature data

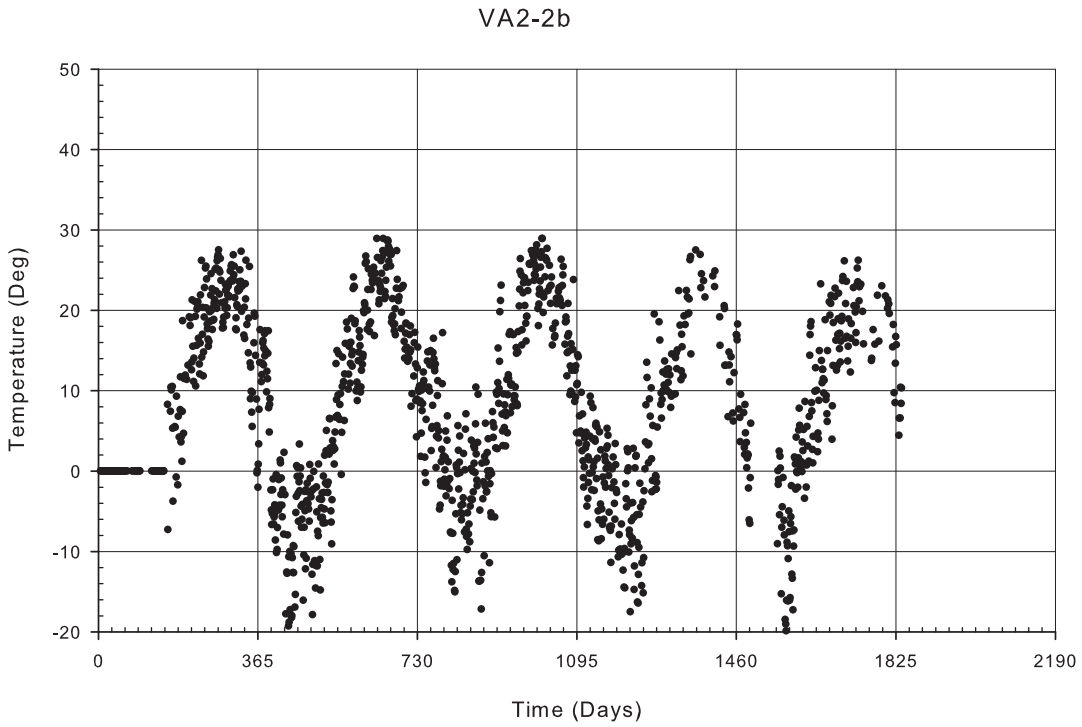

Figure A-130: Gage VA2-2b filtered temperature data

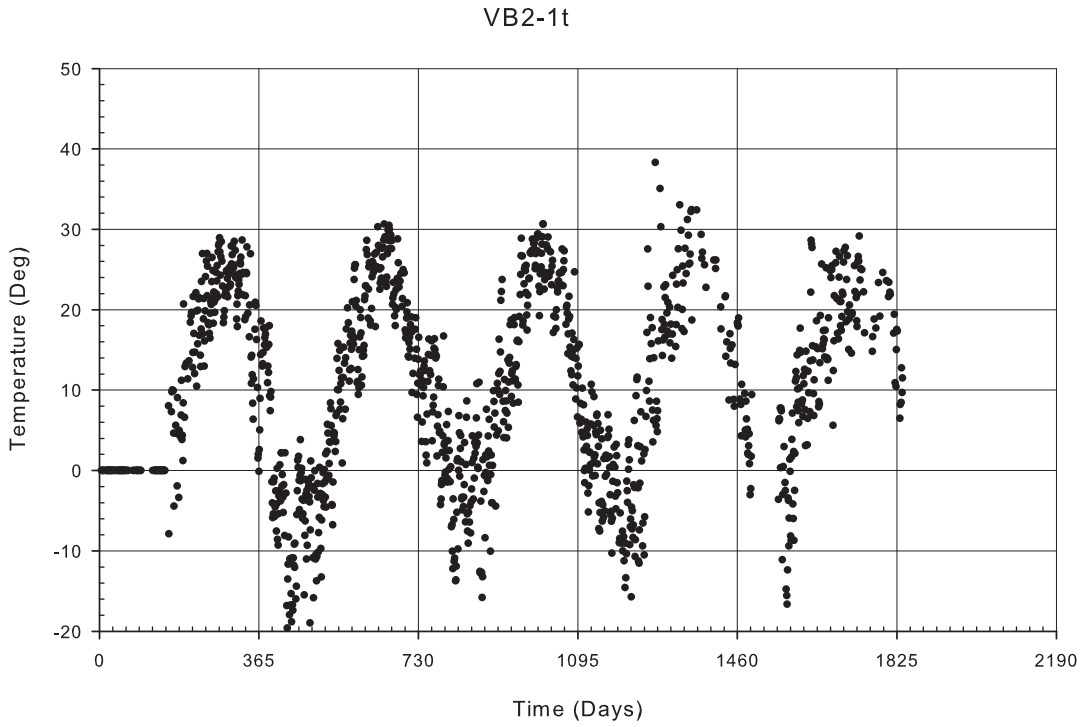

Figure A-131: Gage VB2-1t filtered temperature data

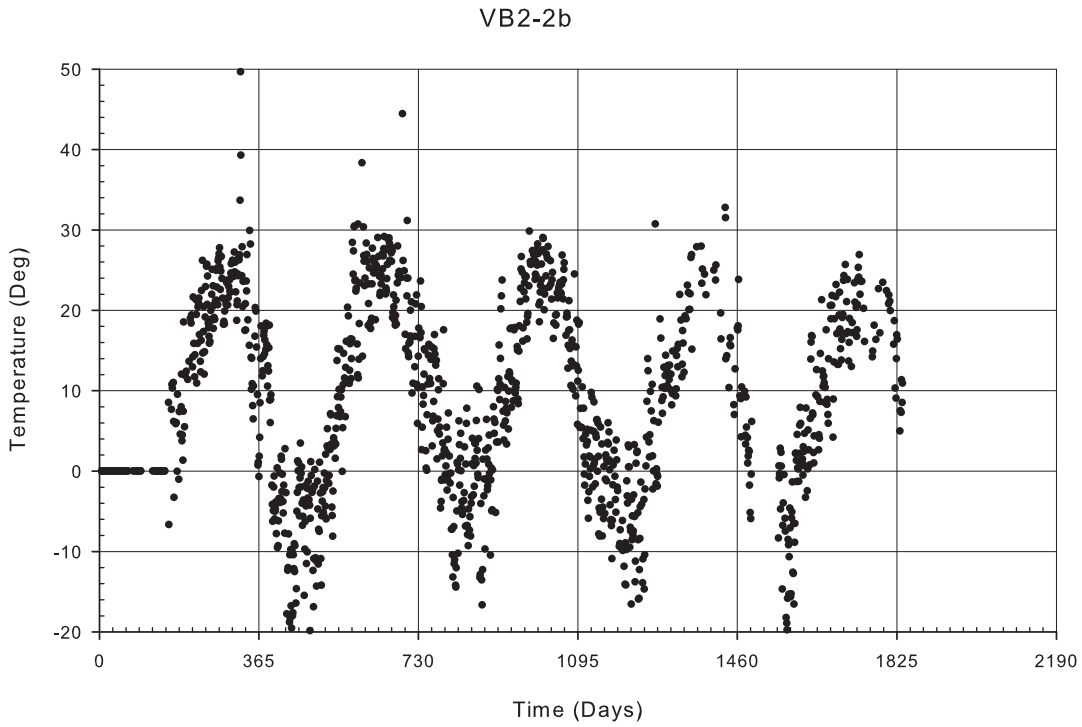

Figure A-132: Gage VB2-2b filtered temperature data

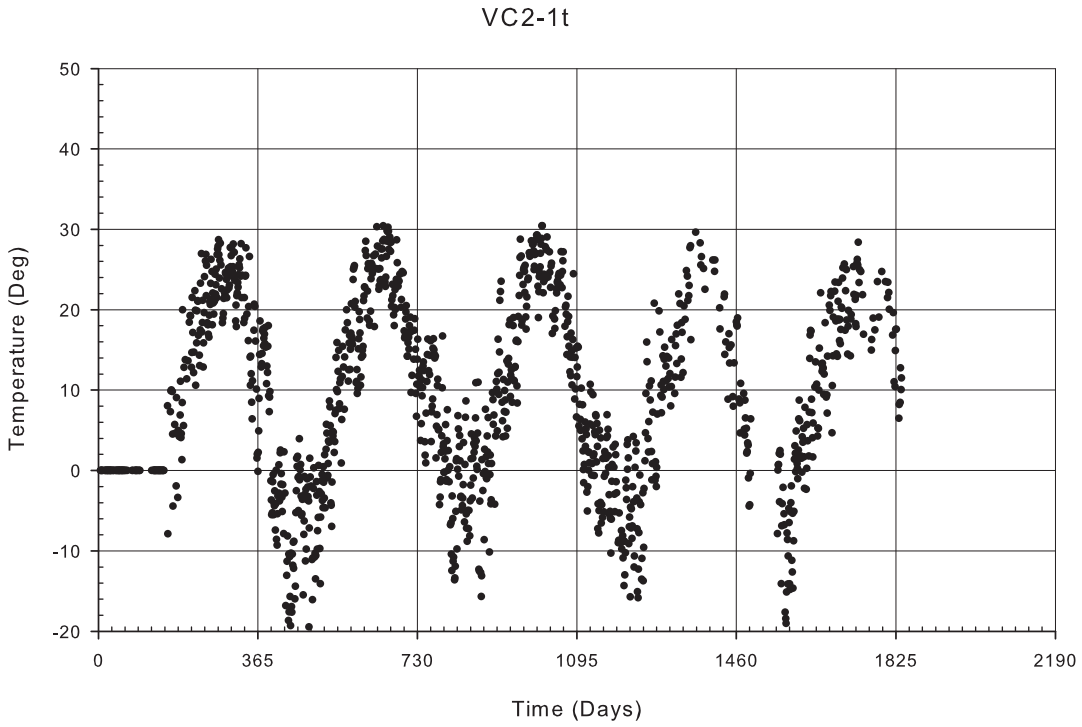

Figure A-133: Gage VC2-1t filtered temperature data

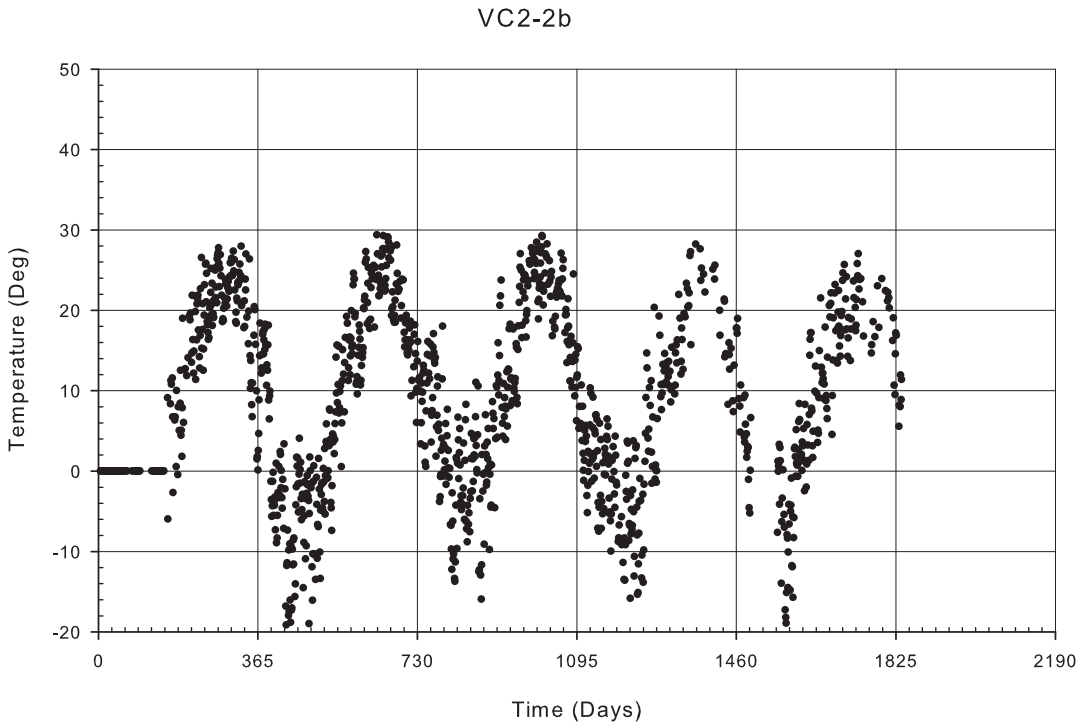

Figure A-134: Gage VC2-2b filtered temperature data

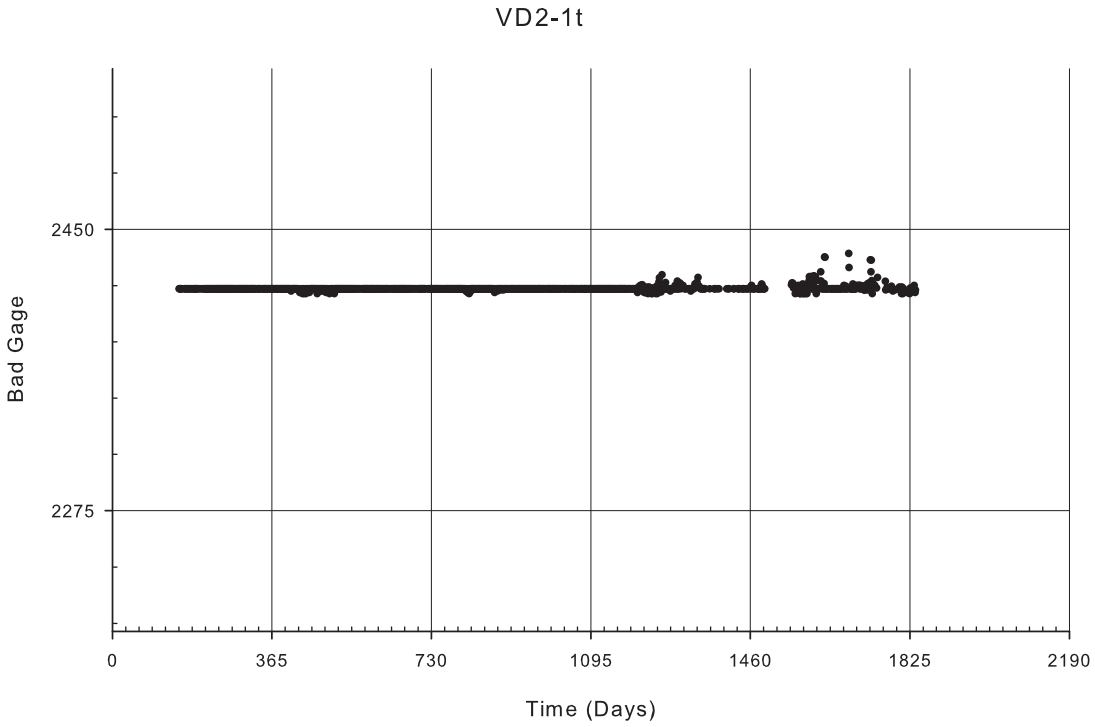

Figure A-135: Gage VD2-1t filtered temperature data

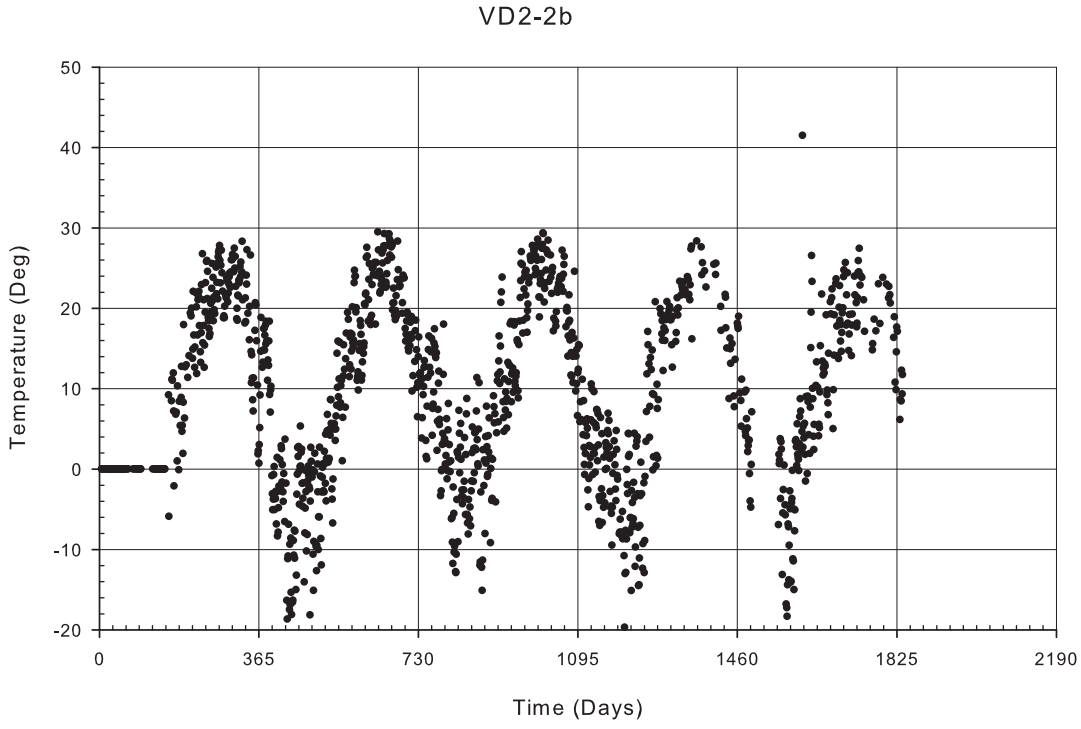

Figure A-136: Gage VD2-2b filtered temperature data

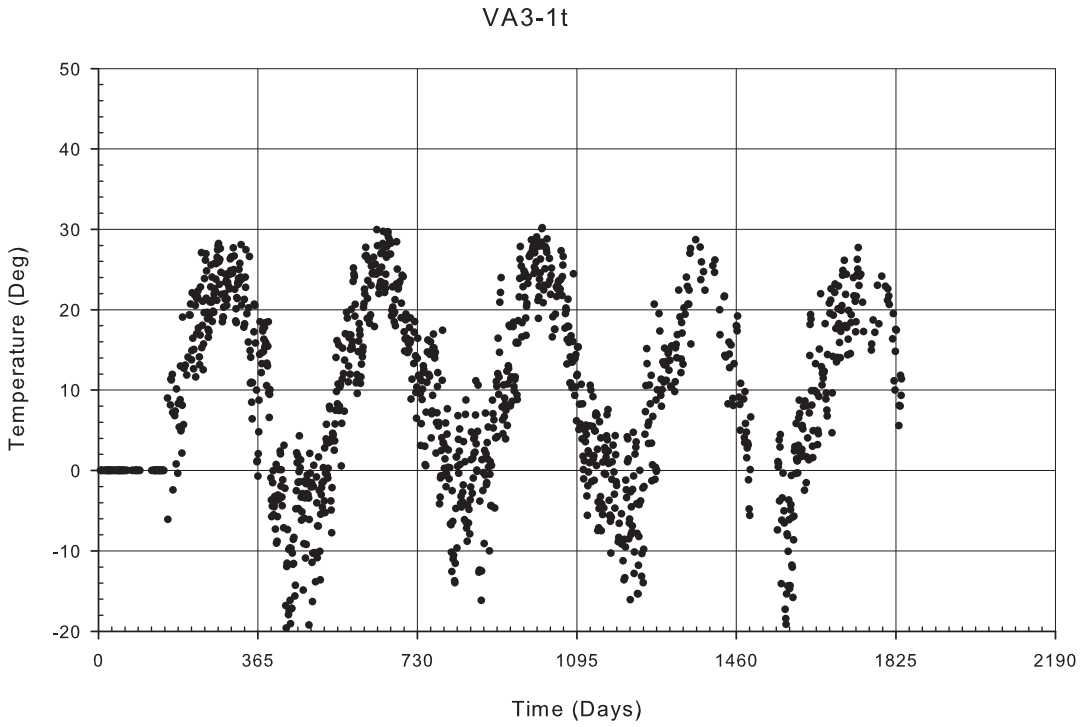

Figure A-137: Gage VA3-1t filtered temperature data

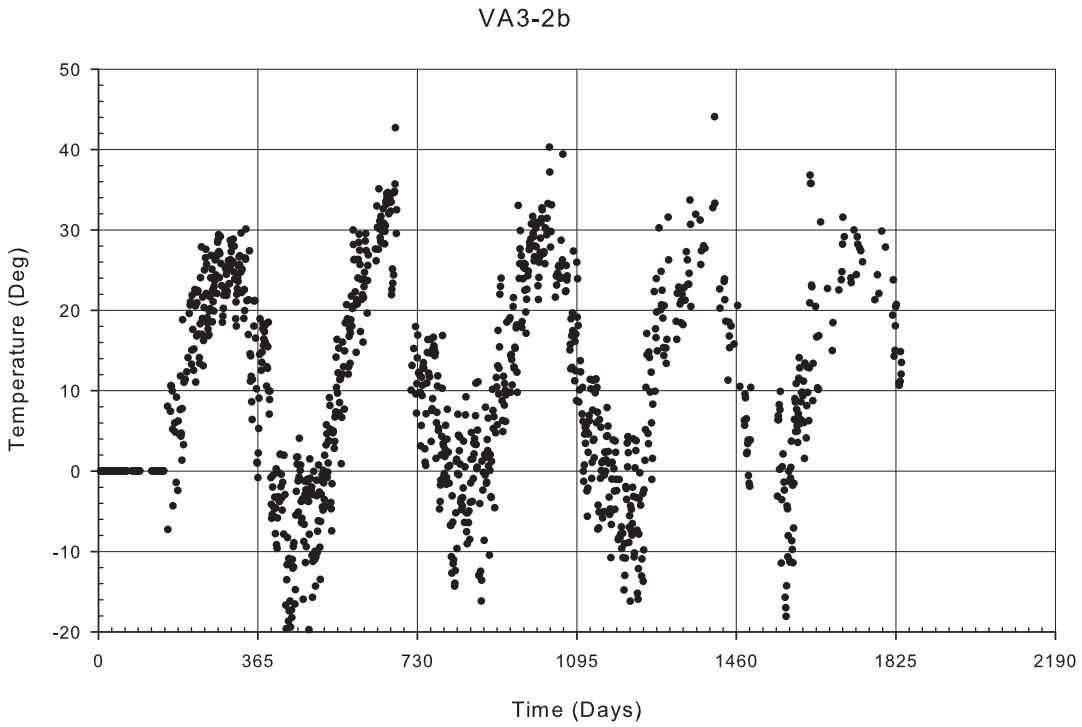

Figure A-138: Gage VA3-2b filtered temperature data

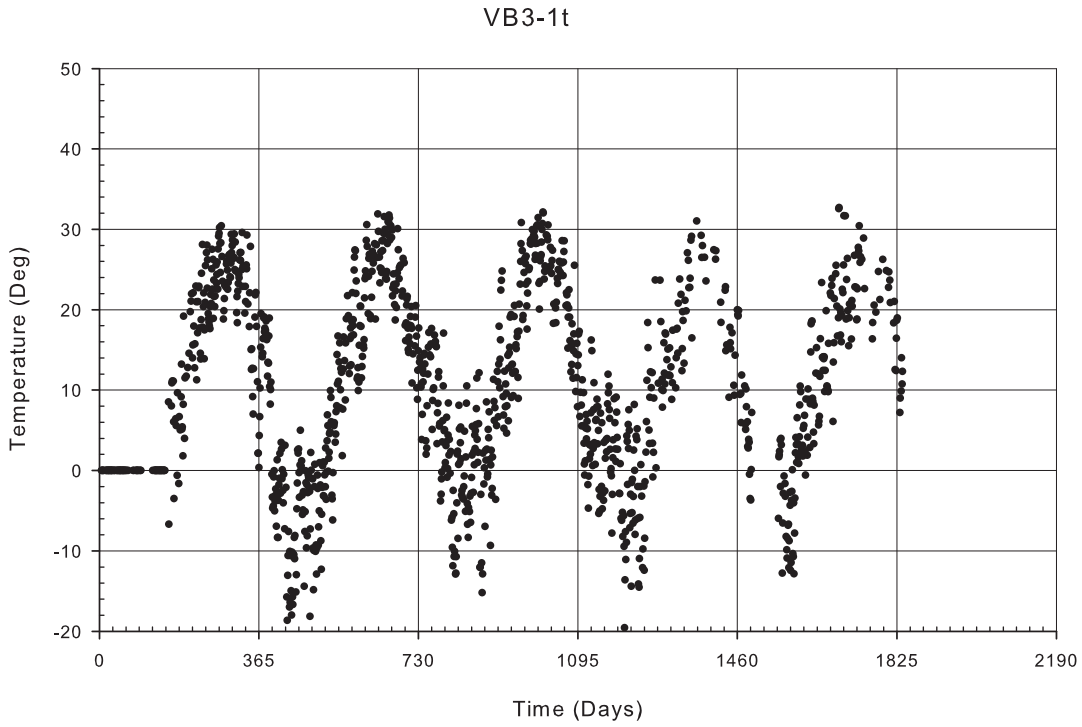

Figure A-139: Gage VB3-1t filtered temperature data

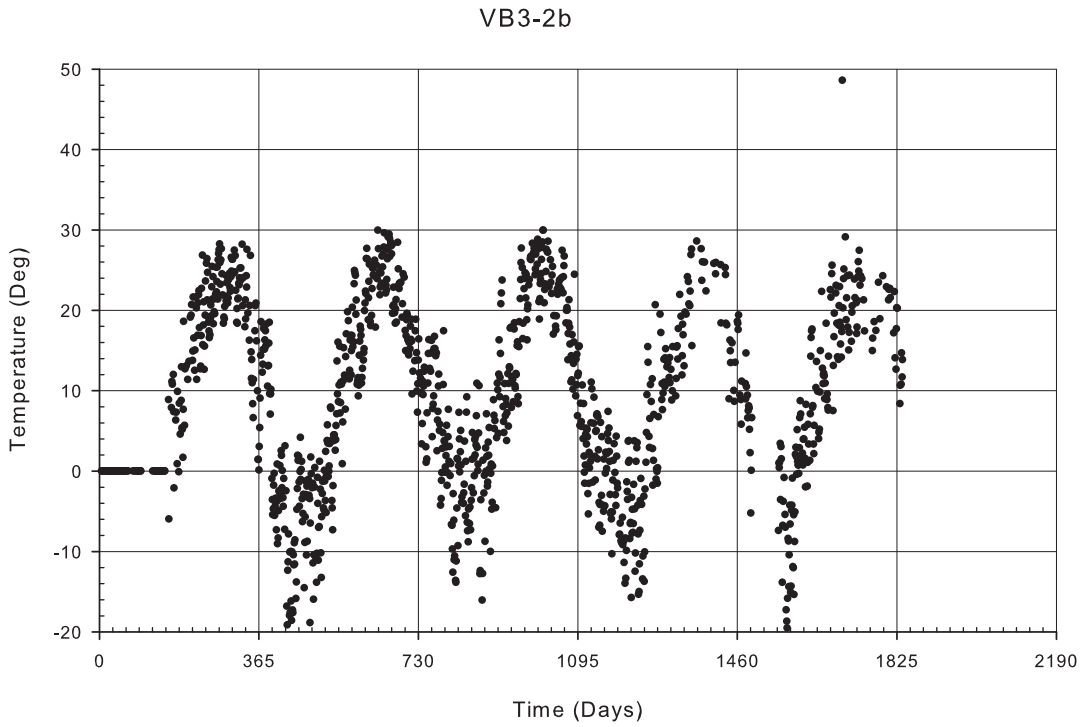

Figure A-140: Gage VB3-2b filtered temperature data

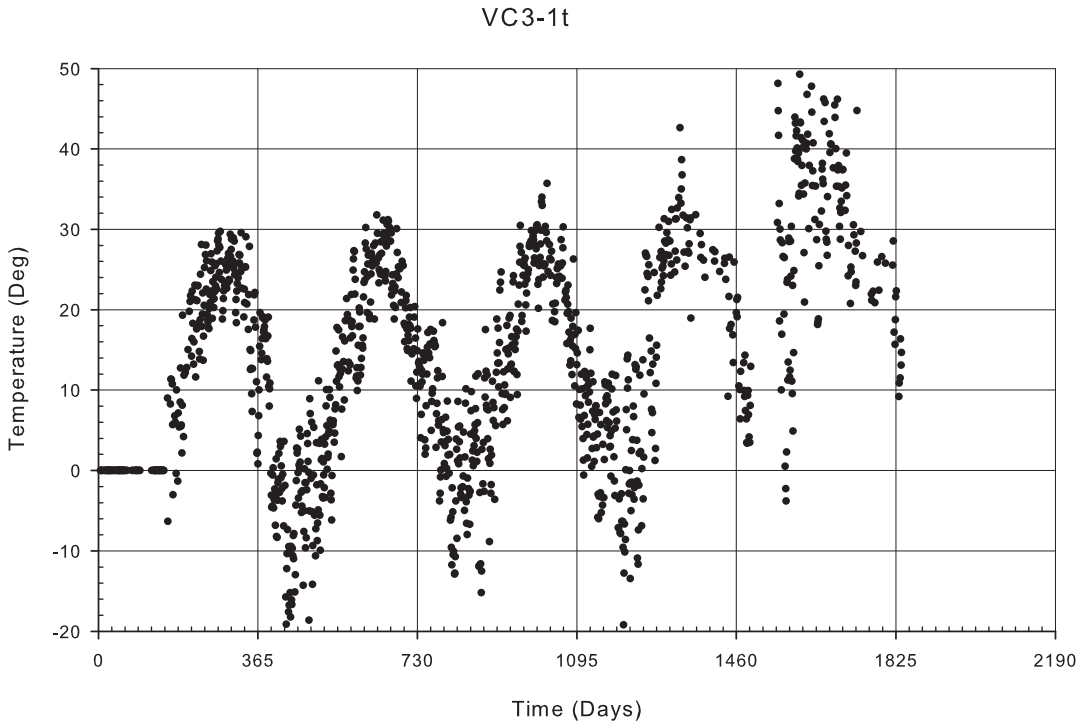

Figure A-141: Gage VC3-1t filtered temperature data

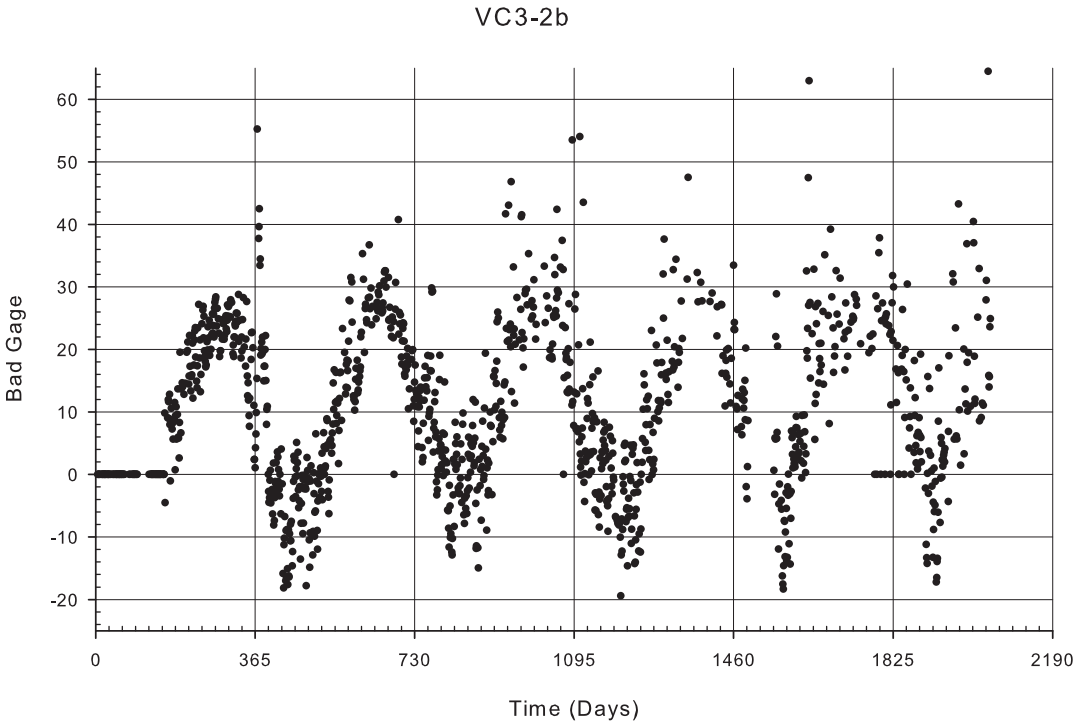

Figure A-142: Gage VC3-2b filtered temperature data

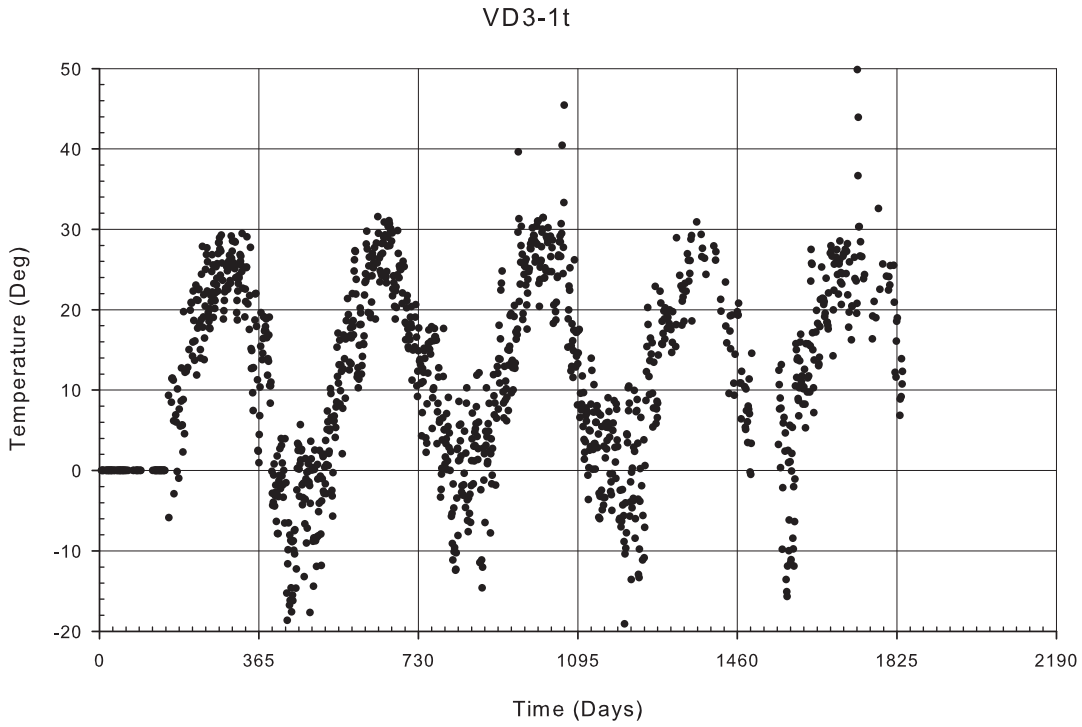

Figure A-143: Gage VD3-1t filtered temperature data

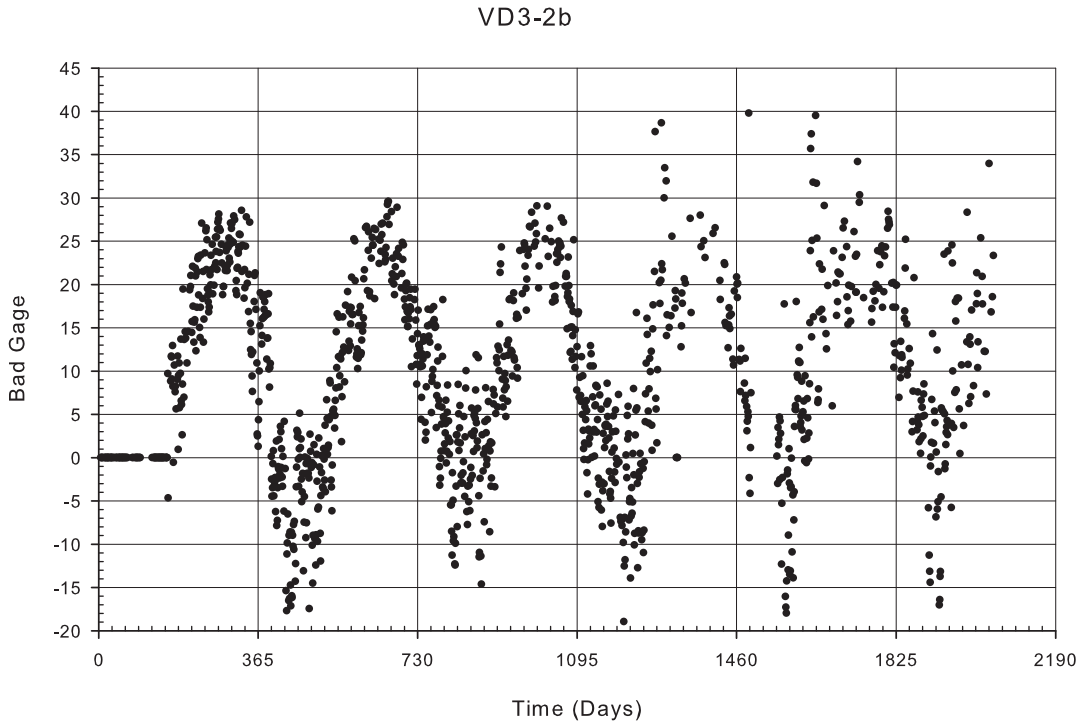

Figure A-144: Gage VD3-2b filtered temperature data

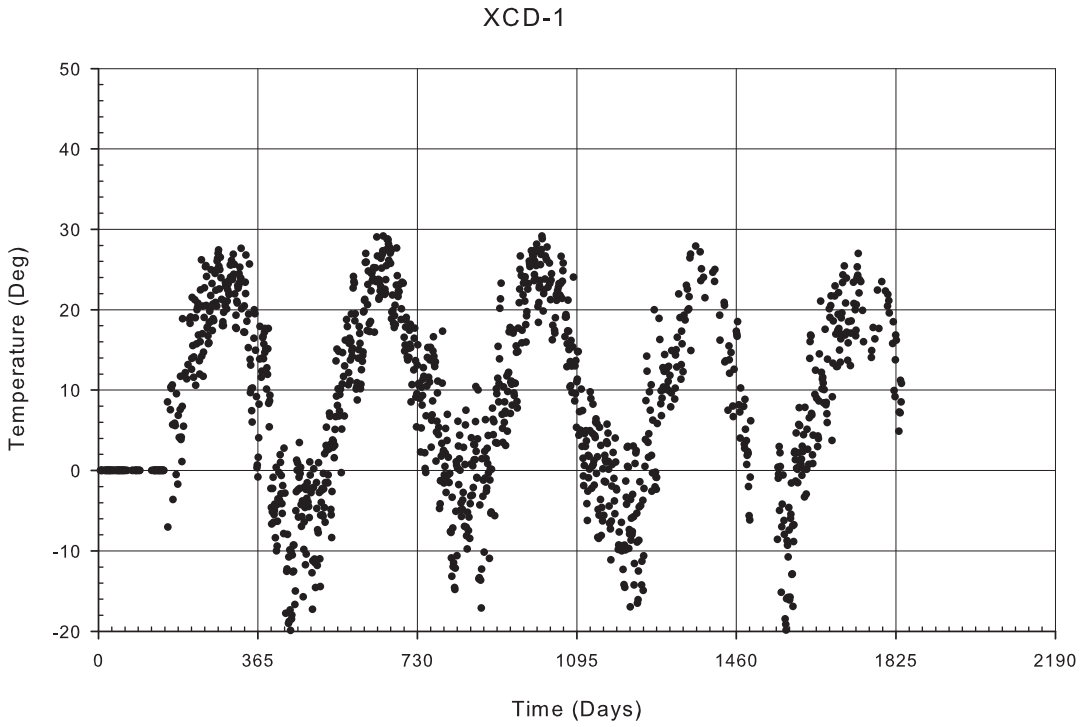

Figure A-145: Gage XCD-1 filtered temperature data

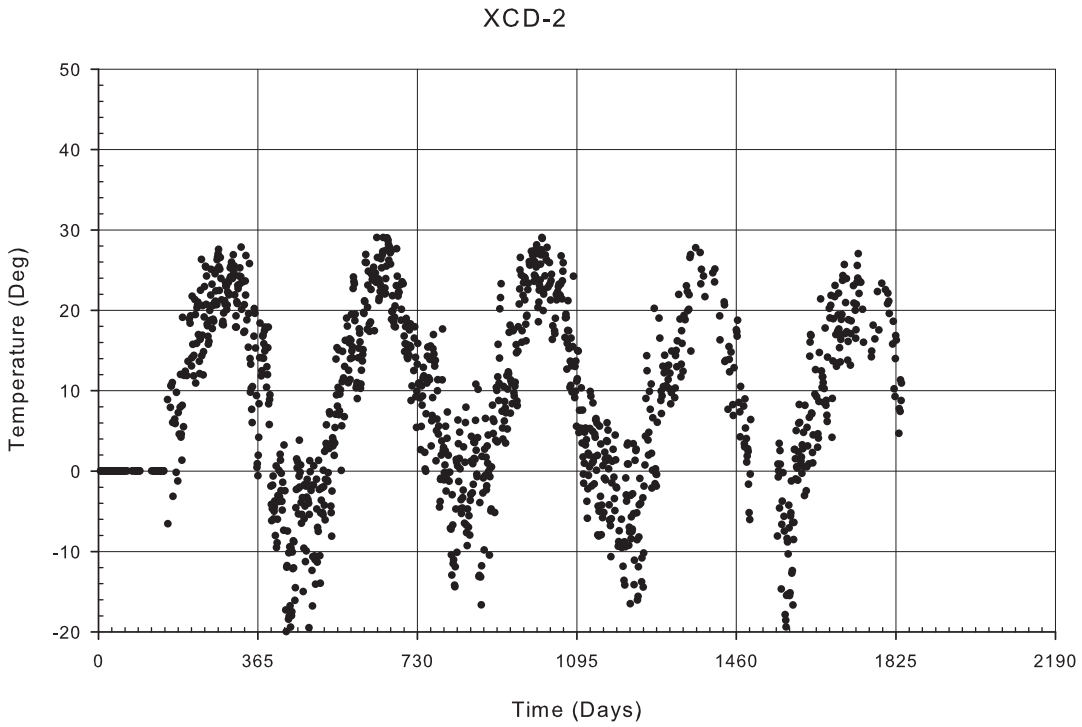

Figure A-146: Gage XCD-2 filtered temperature data

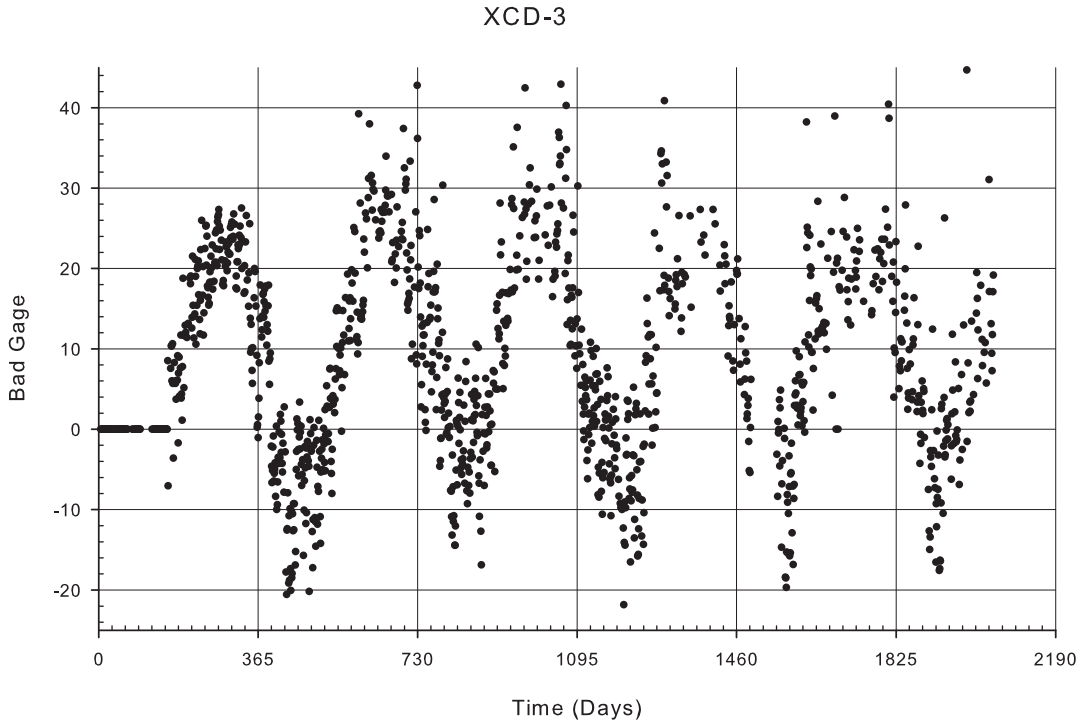

Figure A-147: Gage XCD-3 filtered temperature data

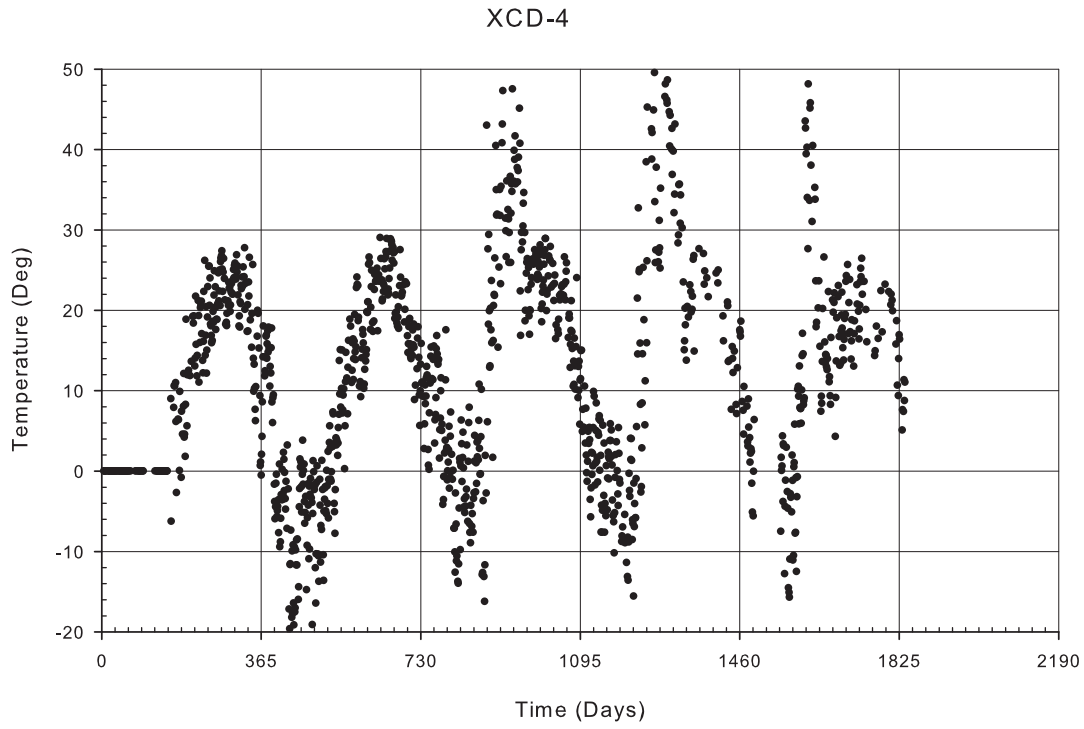

Figure A-148: Gage XCD-4 filtered temperature data

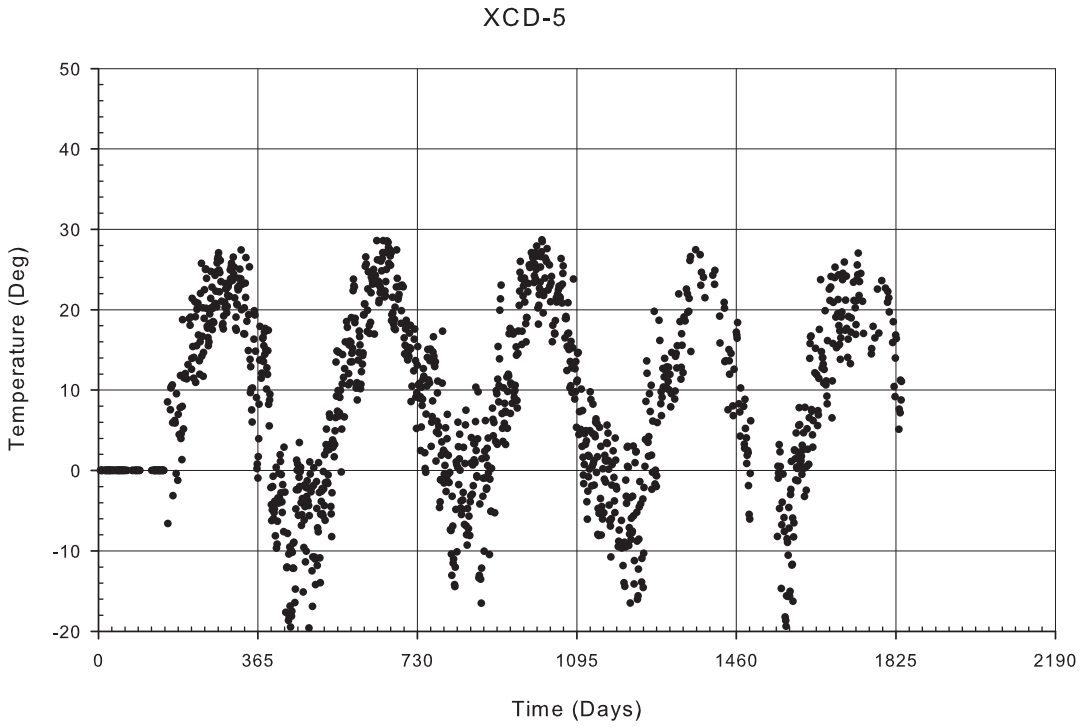

Figure A-149: Gage XCD-5 filtered temperature data

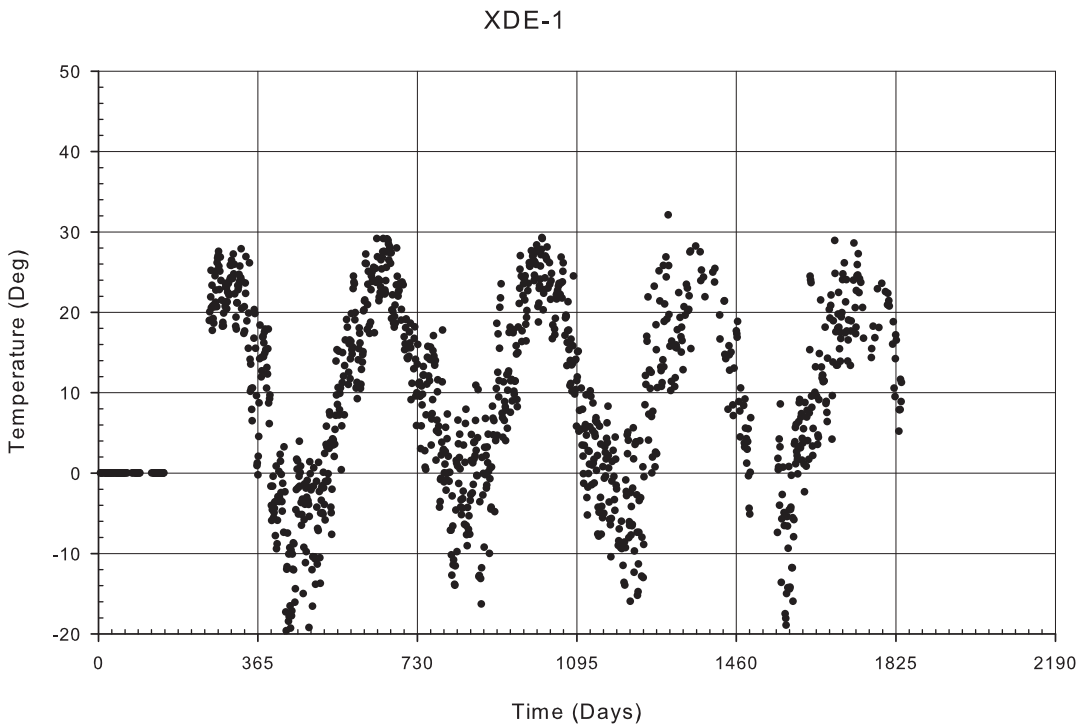

Figure A-150: Gage XDE-1 filtered temperature data

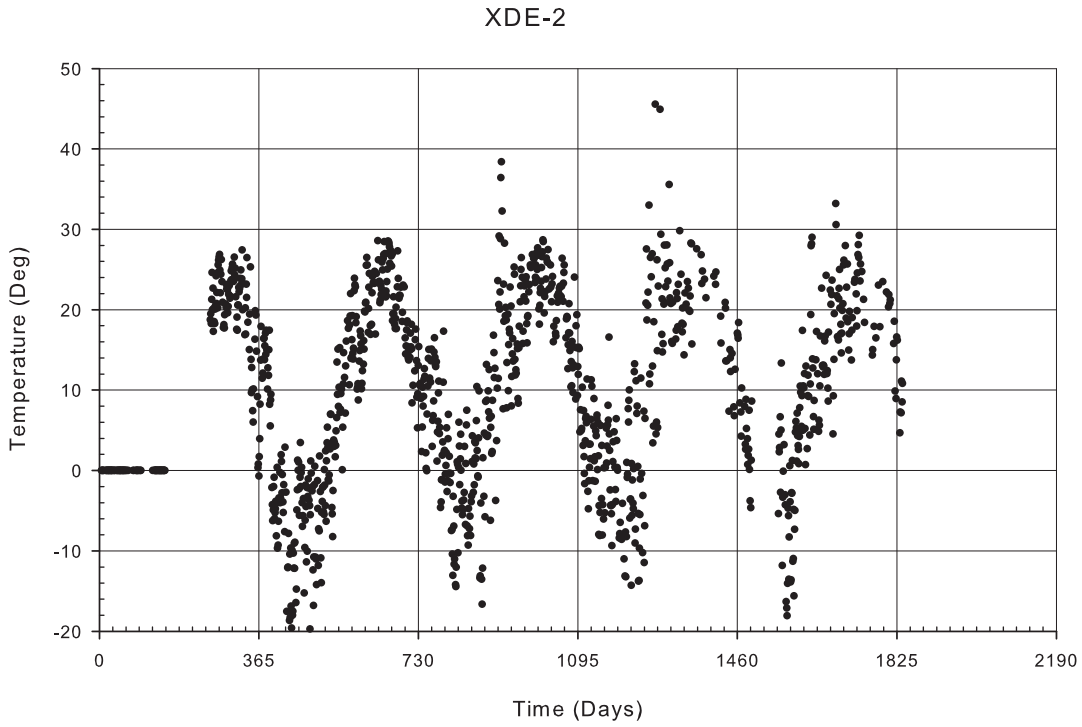

Figure A-151: Gage XDE-2 filtered temperature data

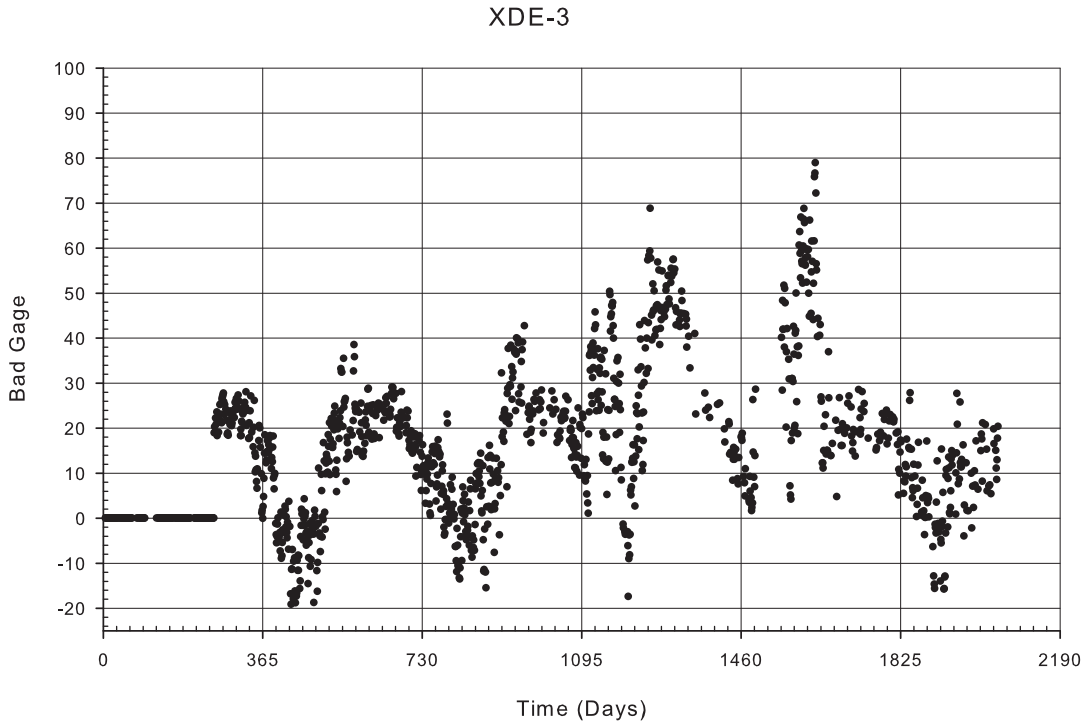

Figure A-152: Gage XDE-3 filtered temperature data

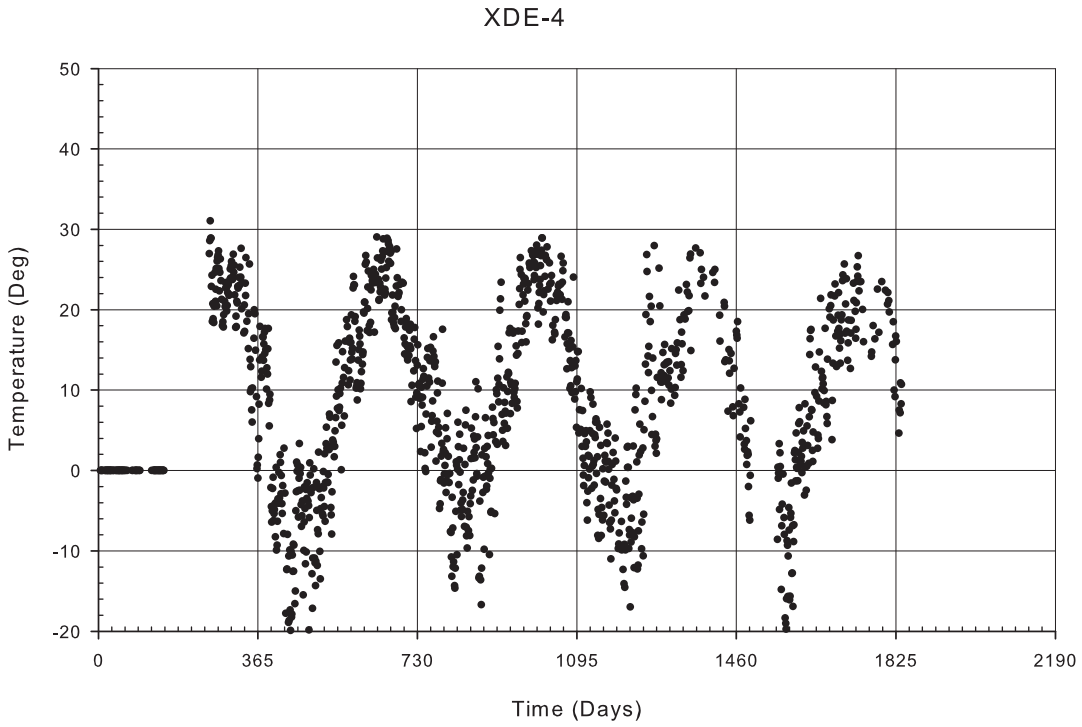

Figure A-153: Gage XDE-4 filtered temperature data

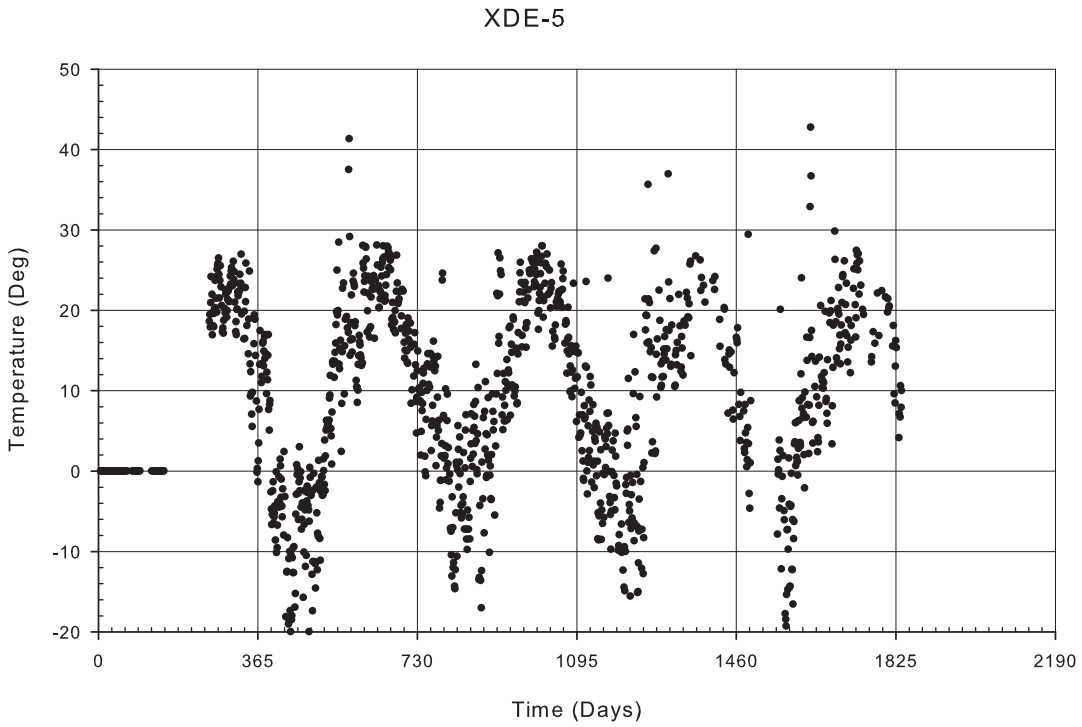

Figure A-154: Gage XDE-5 filtered temperature data

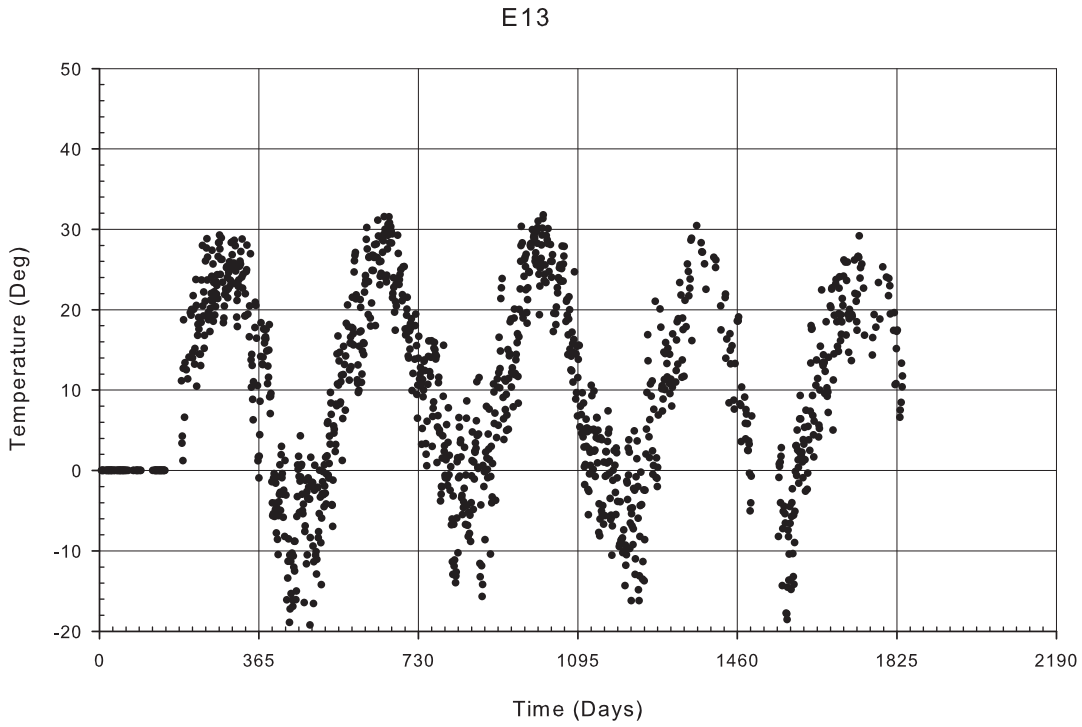

Figure A-155: Gage E13 filtered temperature data

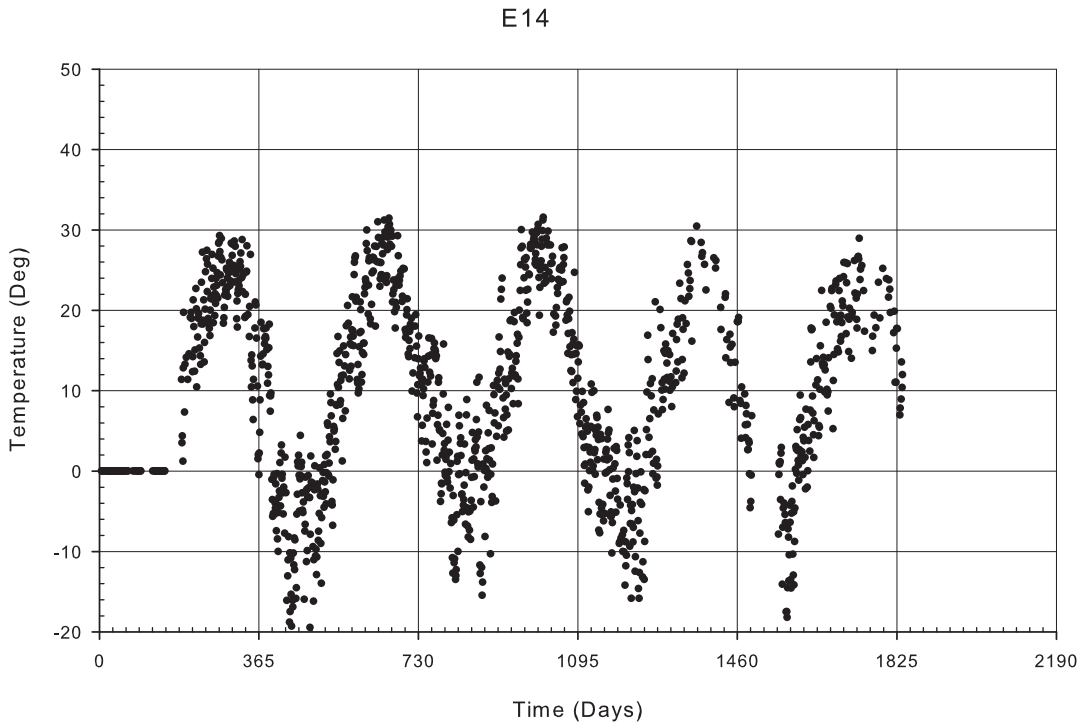

Figure A-156: Gage E14 filtered temperature data

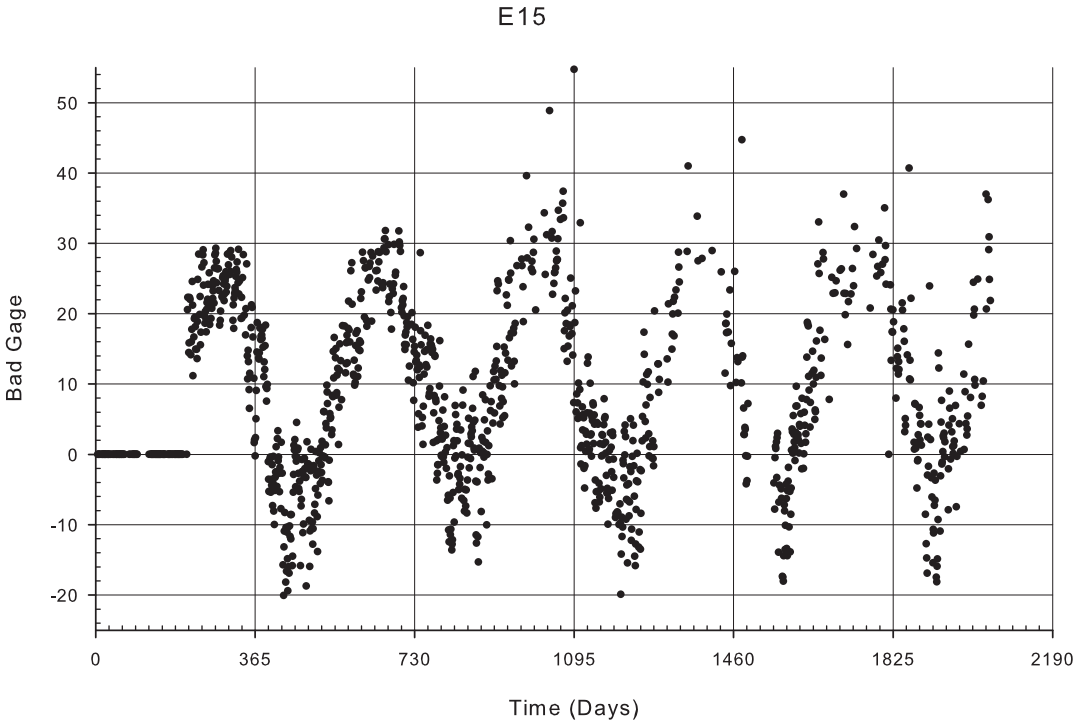

Figure A-157: Gage E15 filtered temperature data

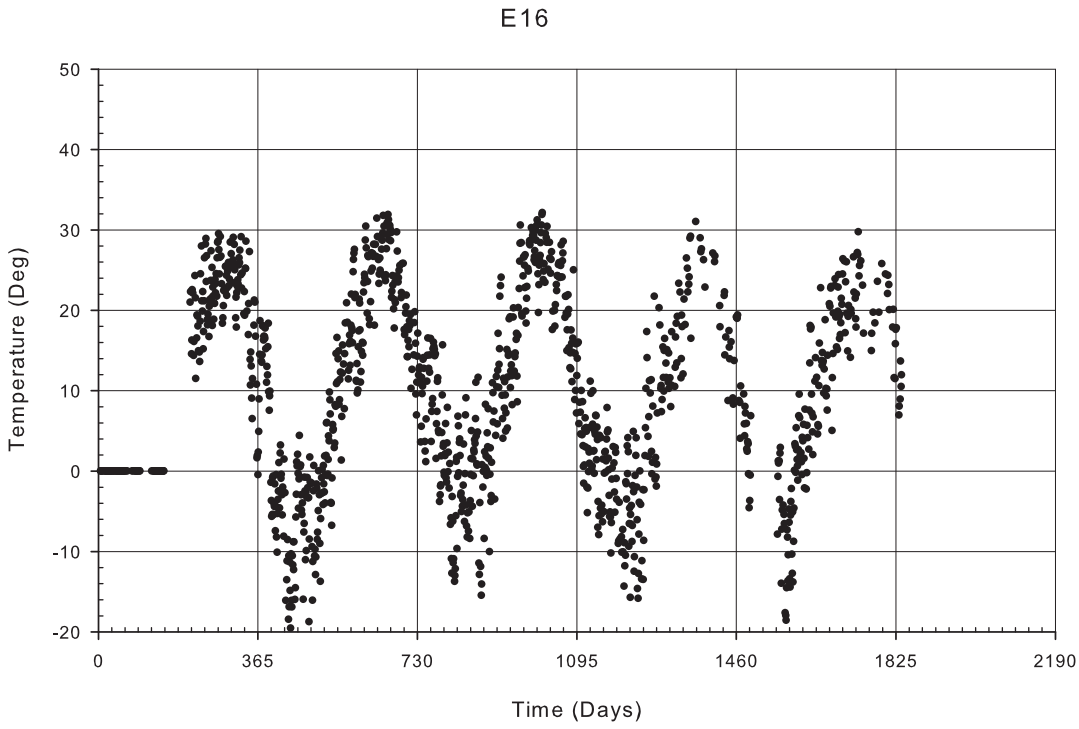

Figure A-158: Gage E16 filtered temperature data

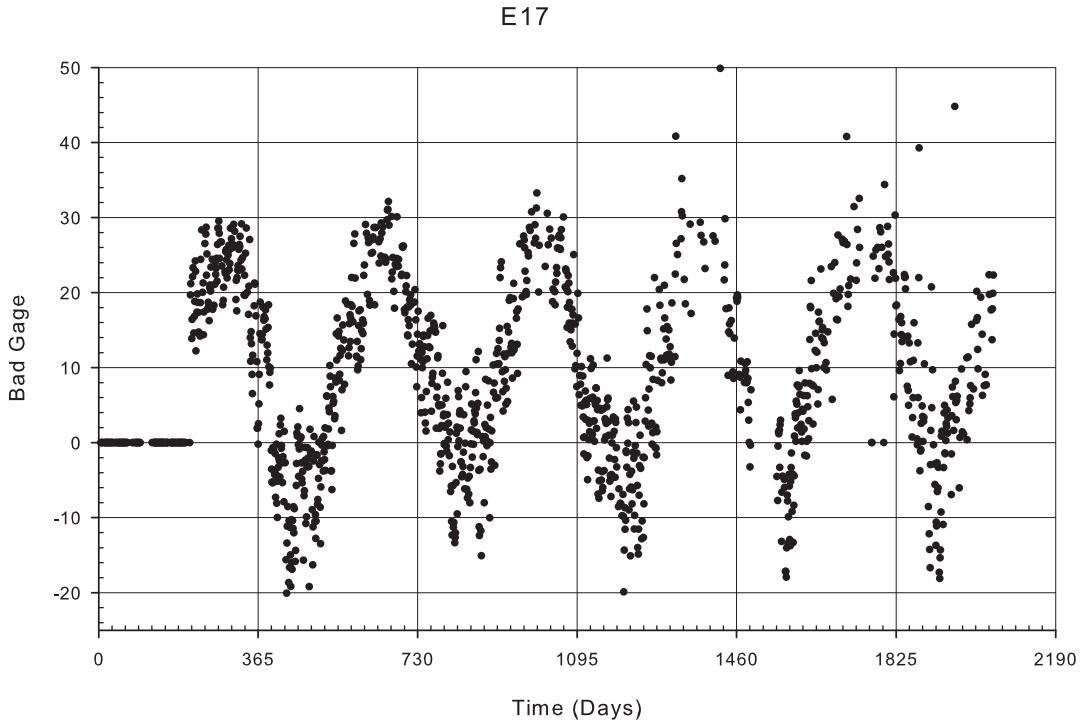

Figure A-159: Gage E17 filtered temperature data

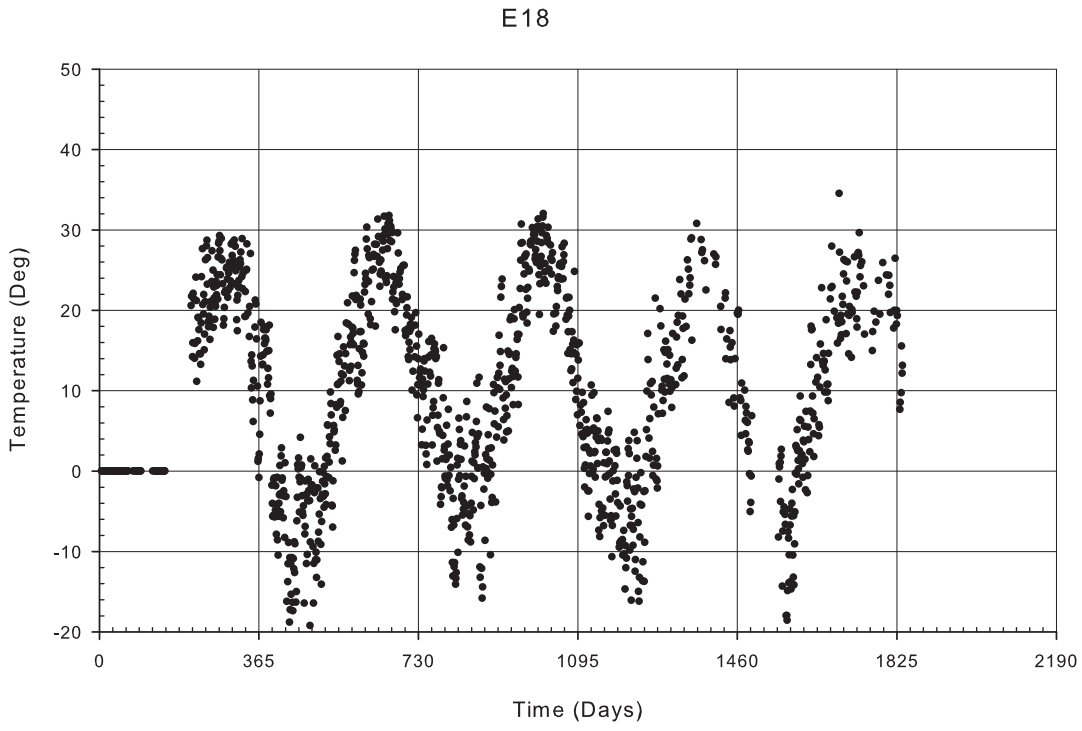

Figure A-160: Gage E18 filtered temperature data

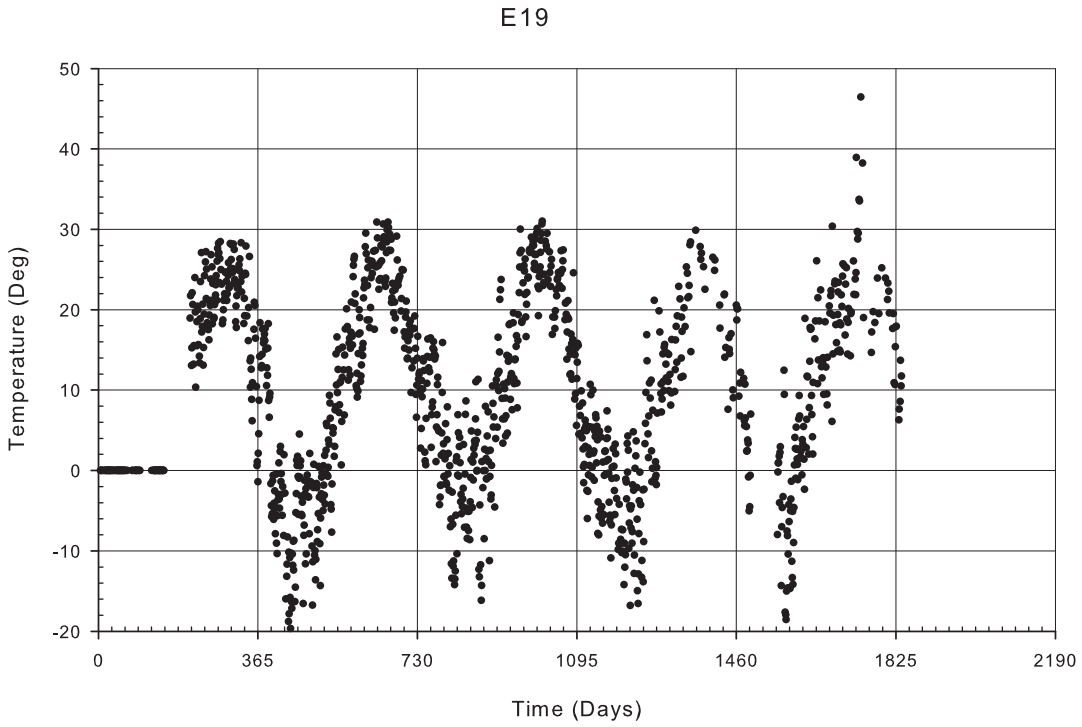

Figure A-161: Gage E19 filtered temperature data

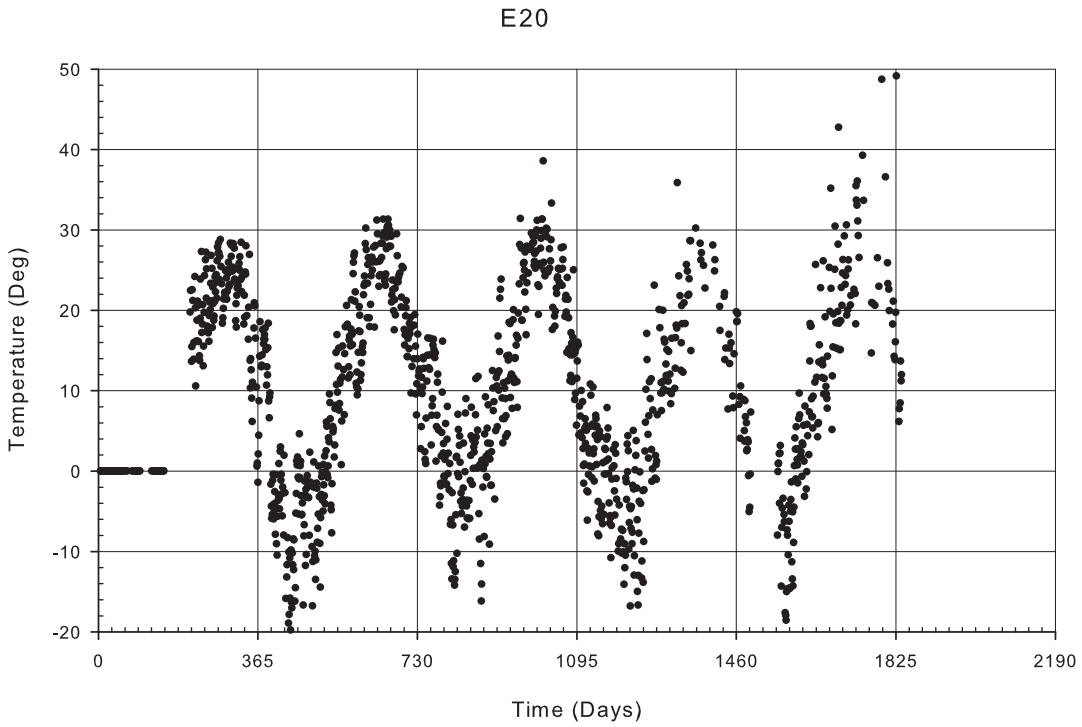

Figure A-162: Gage E20 filtered temperature data

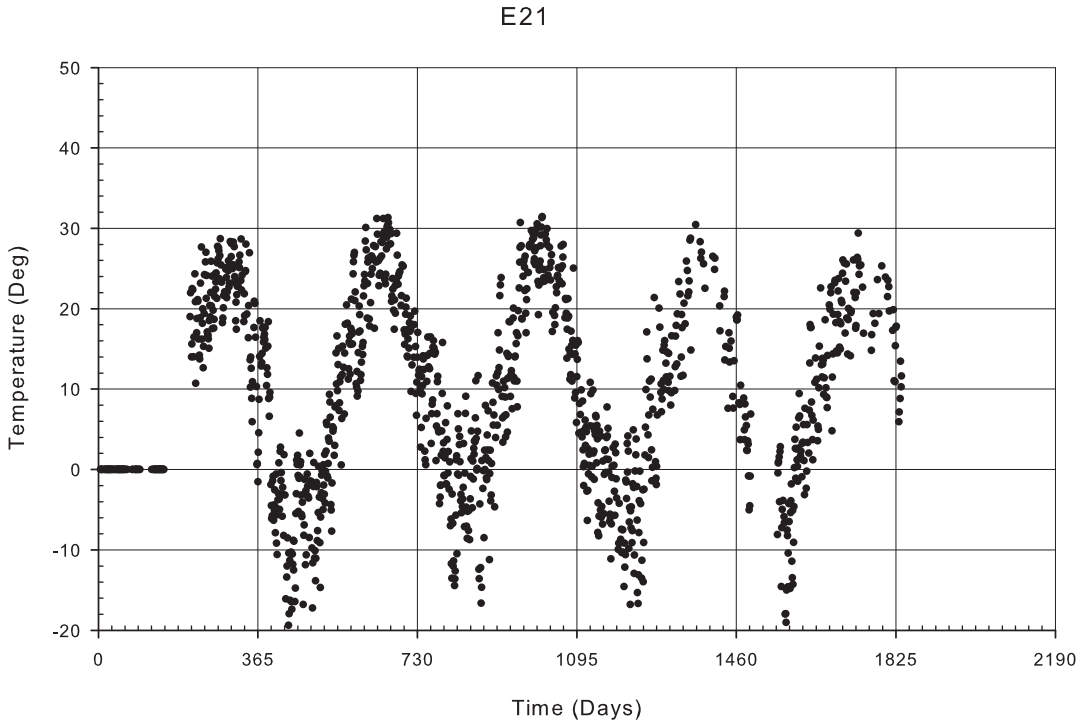

Figure A-163: Gage E21 filtered temperature data

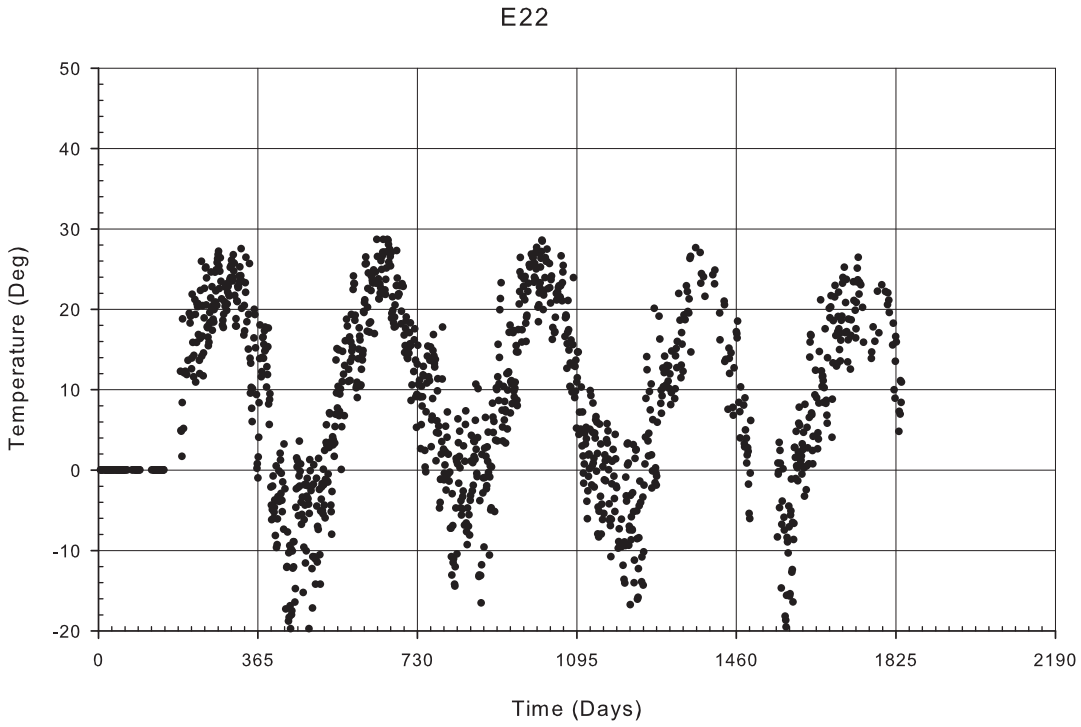

Figure A-164: Gage E22 filtered temperature data

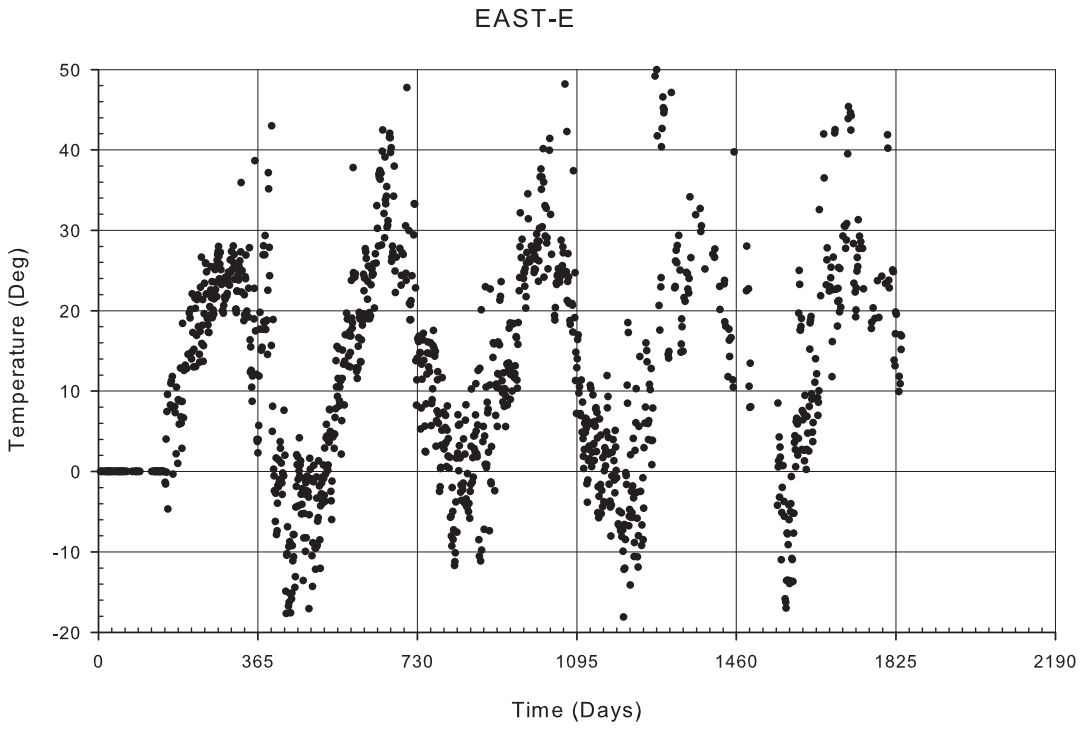

Figure A-165: Gage East-E filtered temperature data

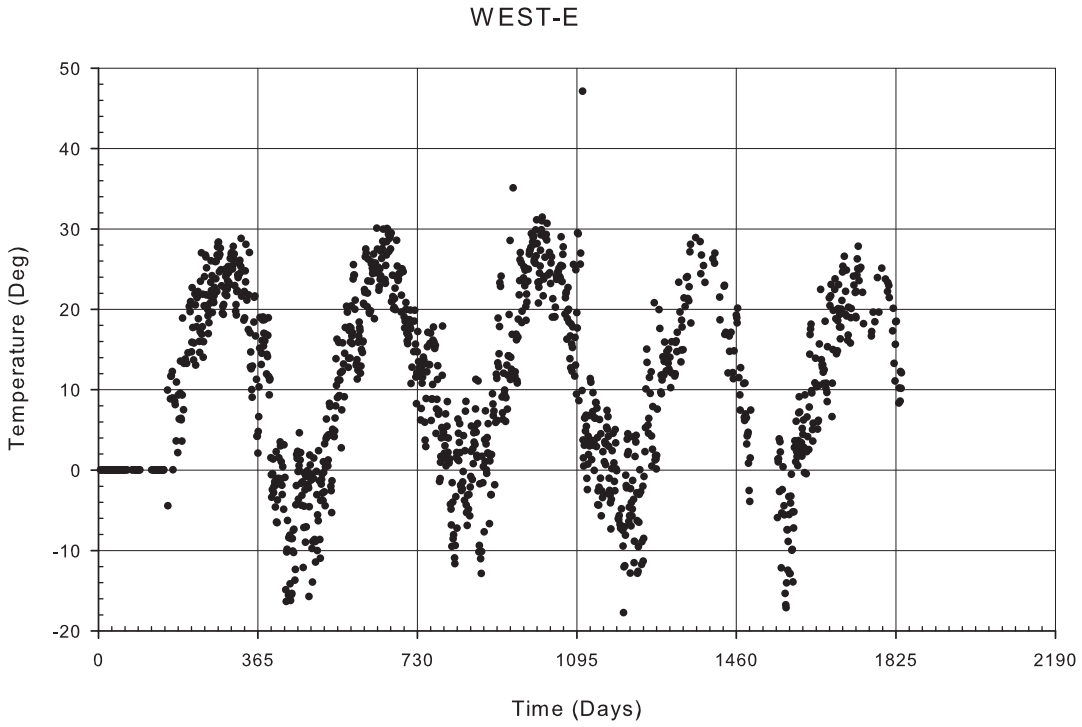

Figure A-166: Gage West-E filtered temperature data

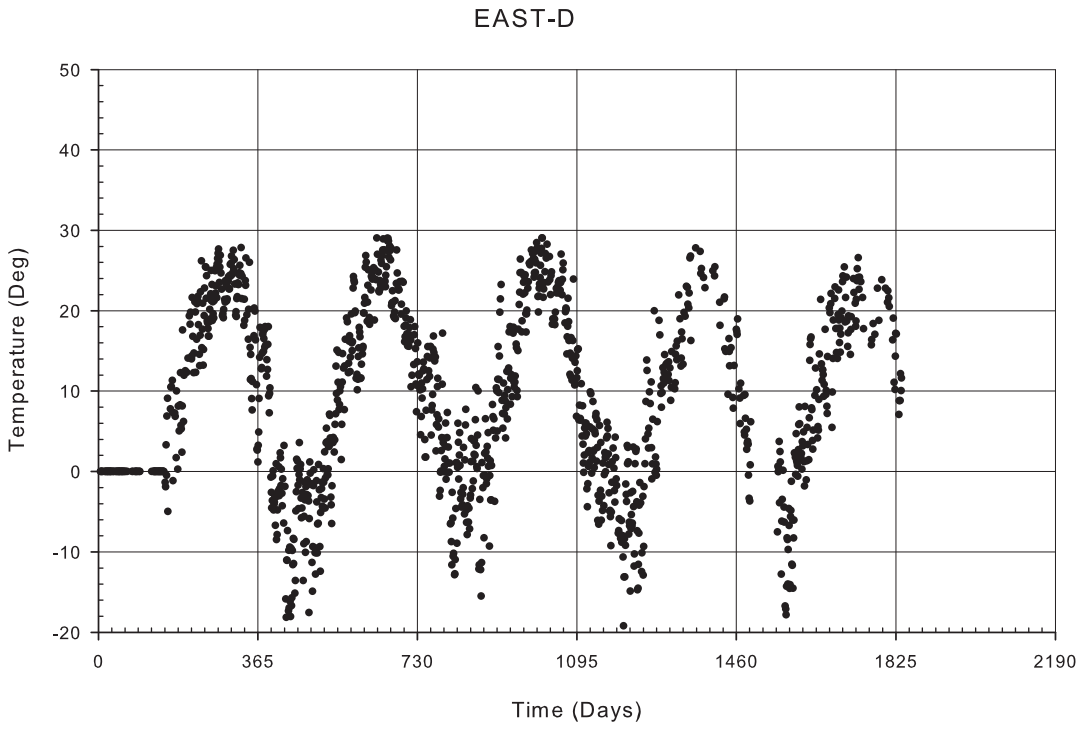

Figure A-167: Gage East-D filtered temperature data

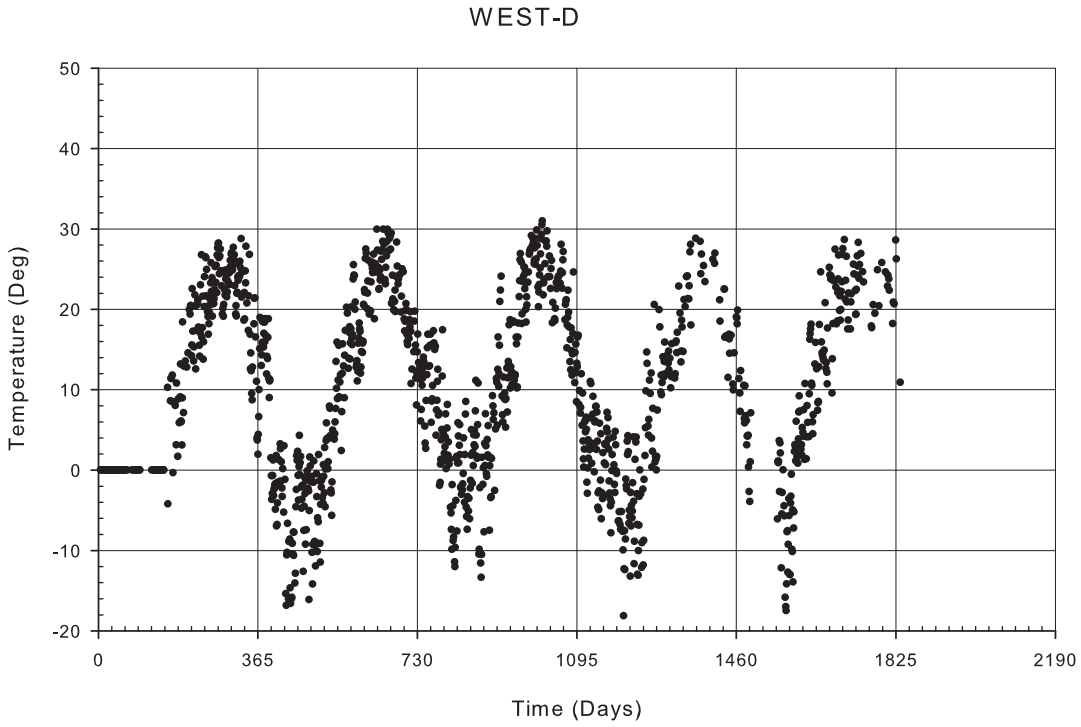

Figure A-168: Gage West-D filtered temperature data

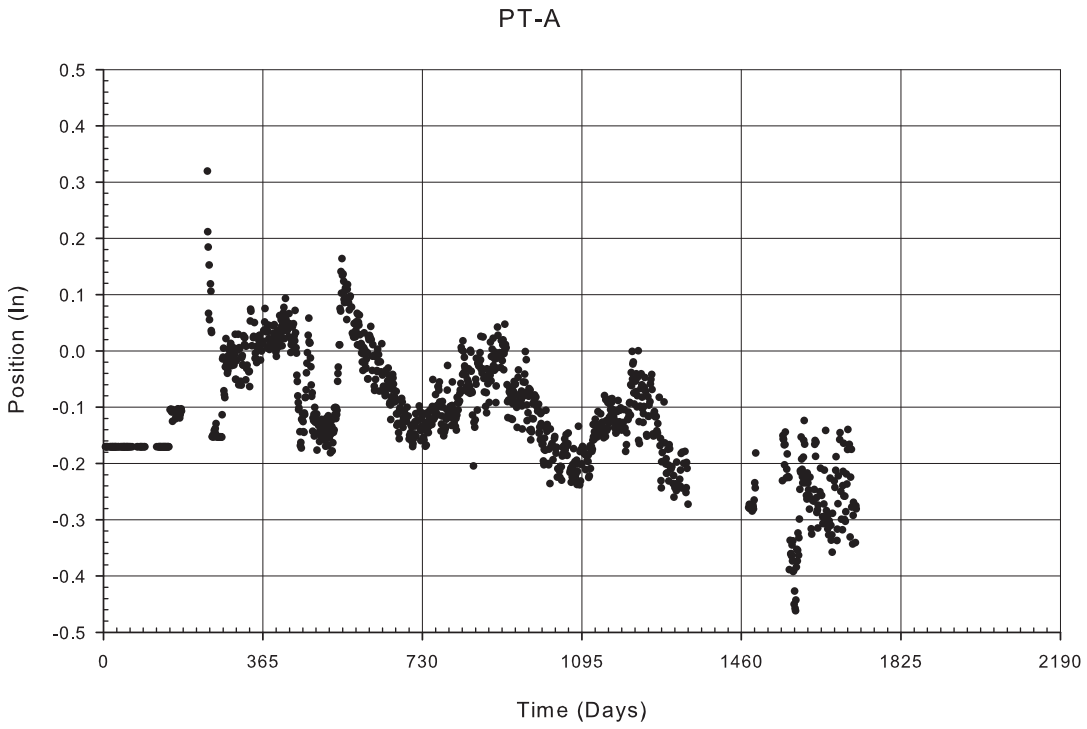

Figure A-169: Gage PT-A filtered position data

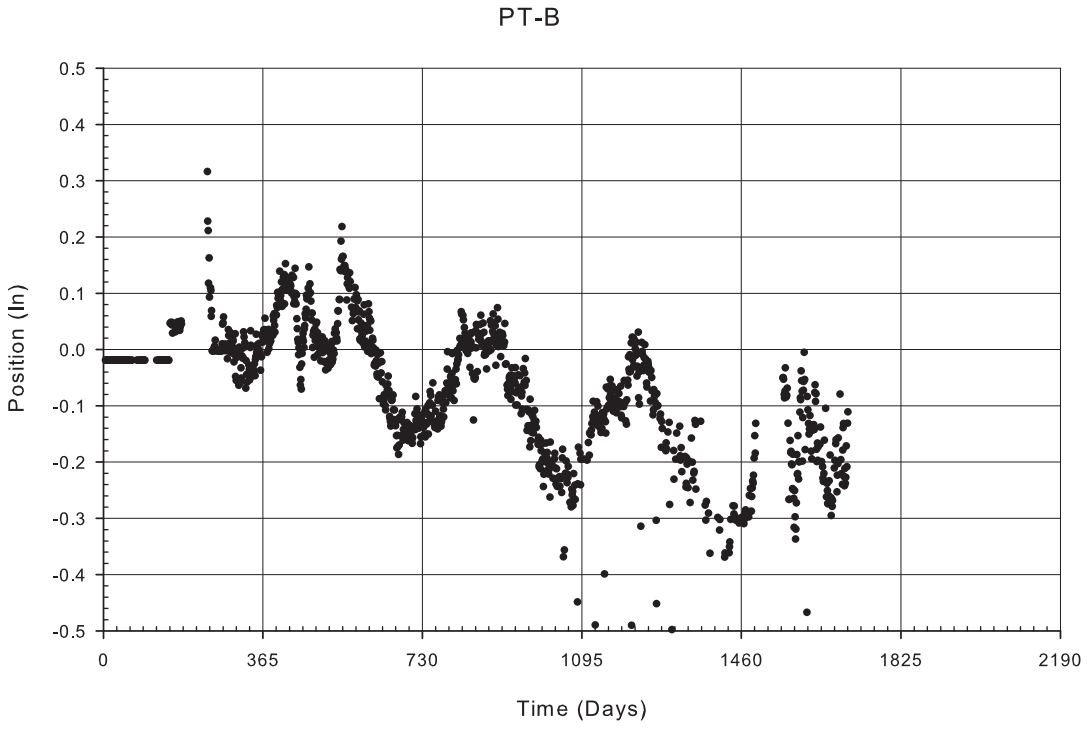

Figure A-170: Gage PT-B filtered position data

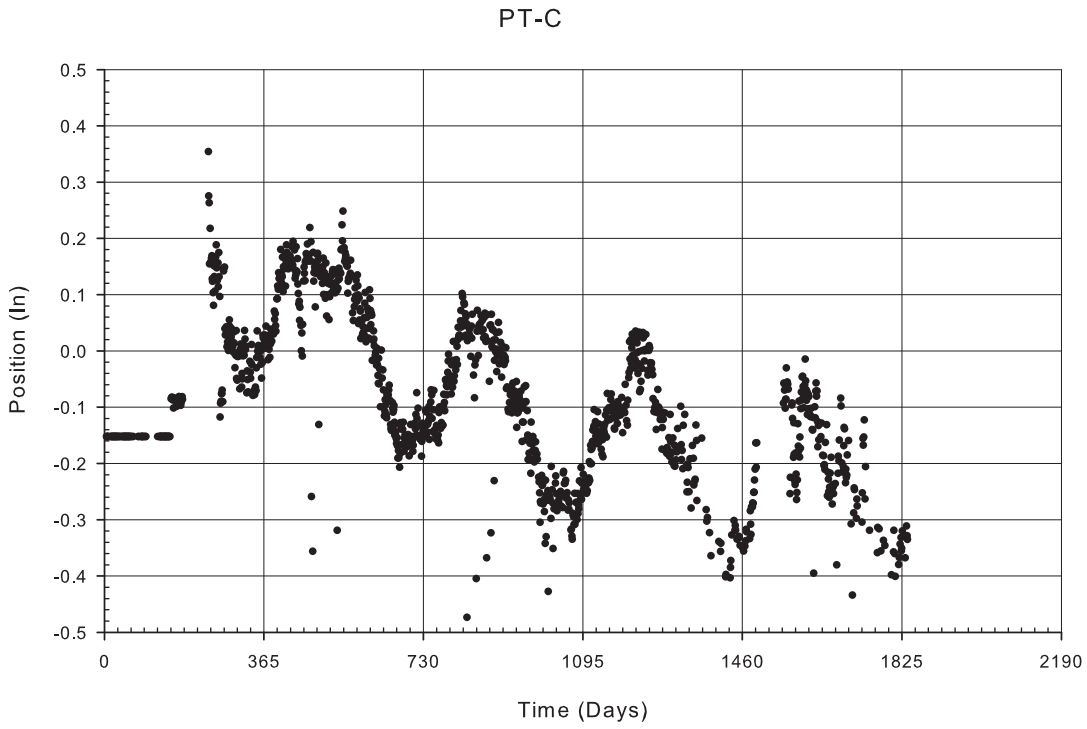

Figure A-171: Gage PT-C filtered position data

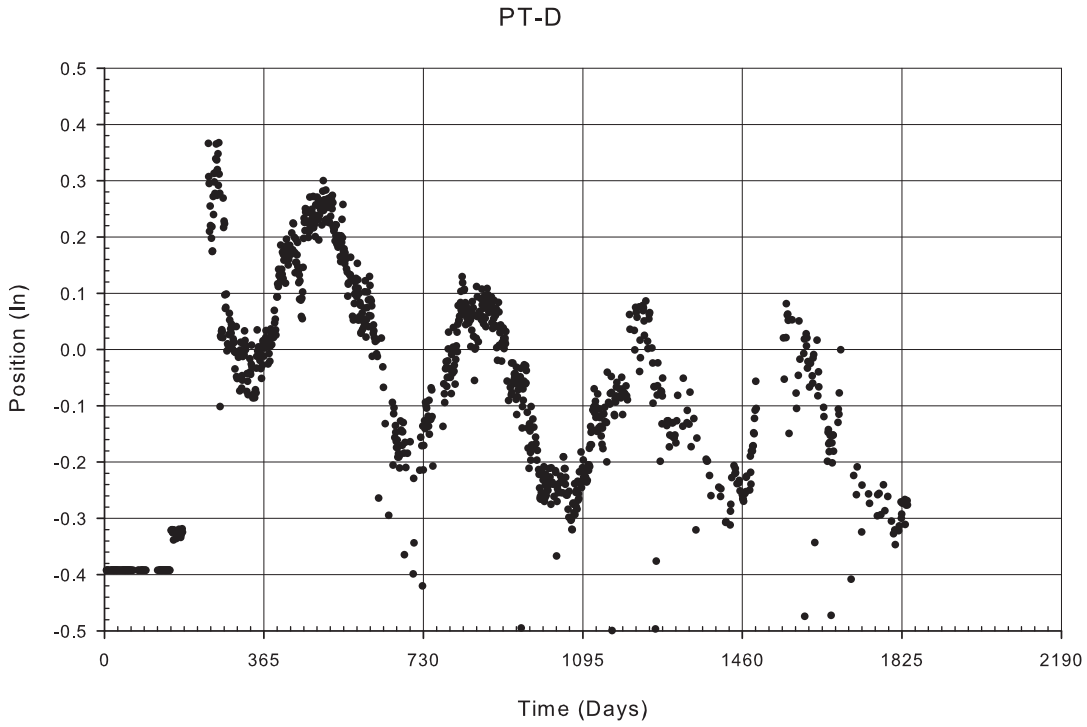

Figure A-172: Gage PT-D filtered position data

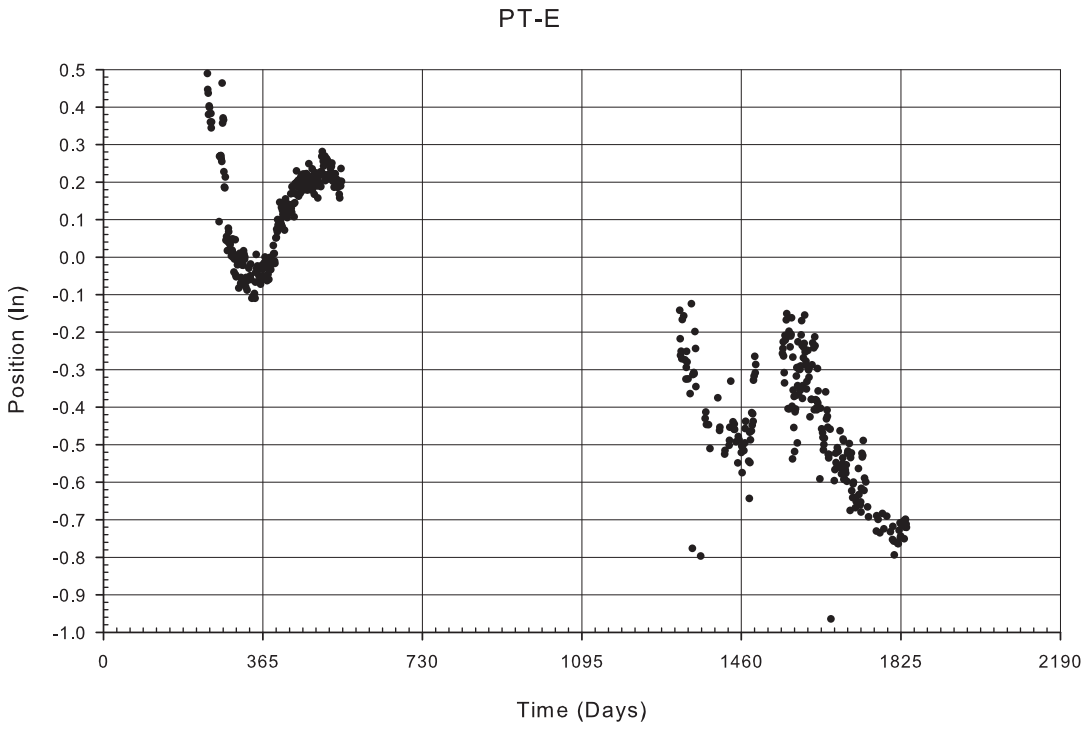

Figure A-173: Gage PT-E filtered position data

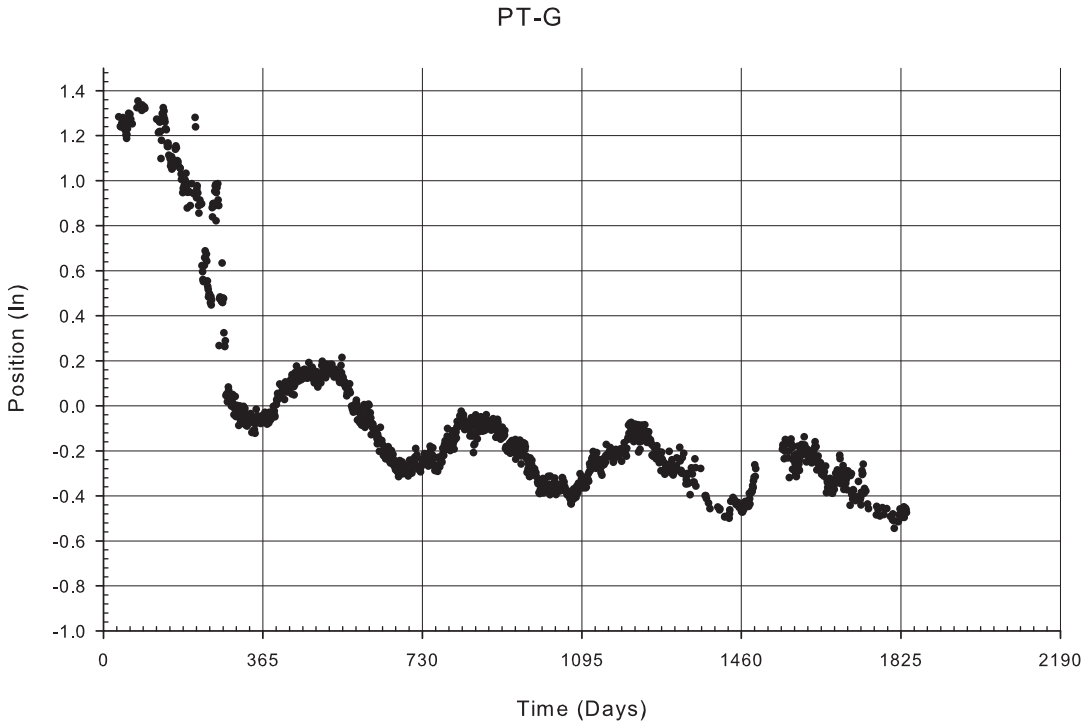

Figure A-174: Gage PT-G filtered position data

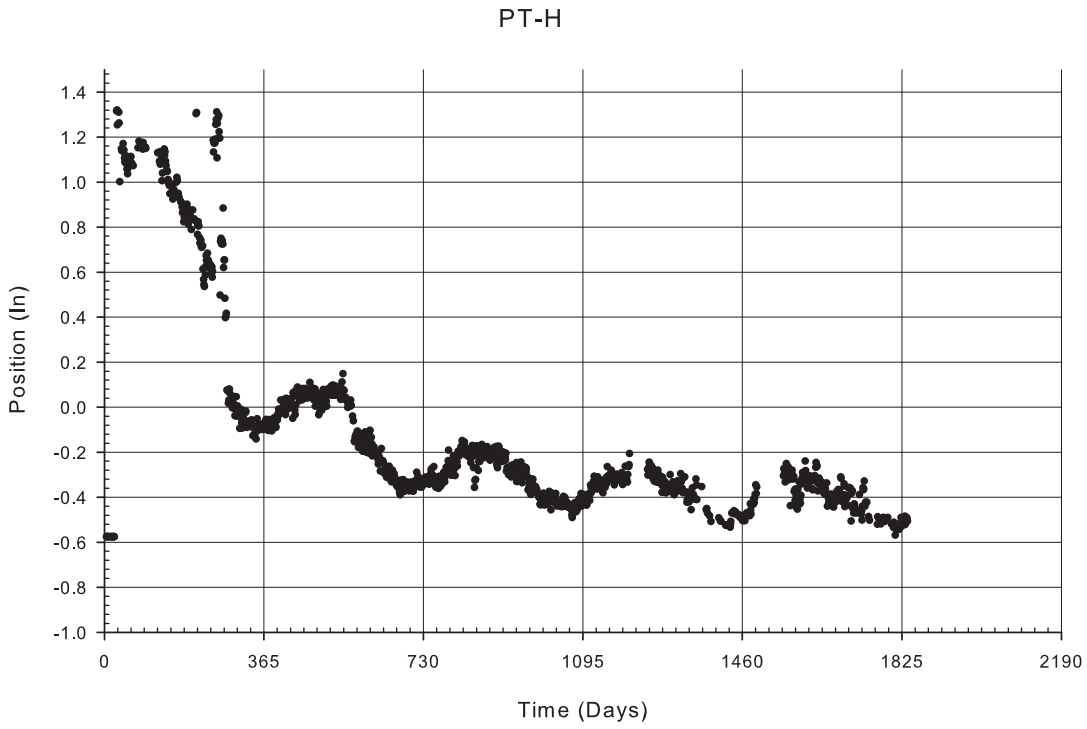

Figure A-175: Gage PT-H filtered position data

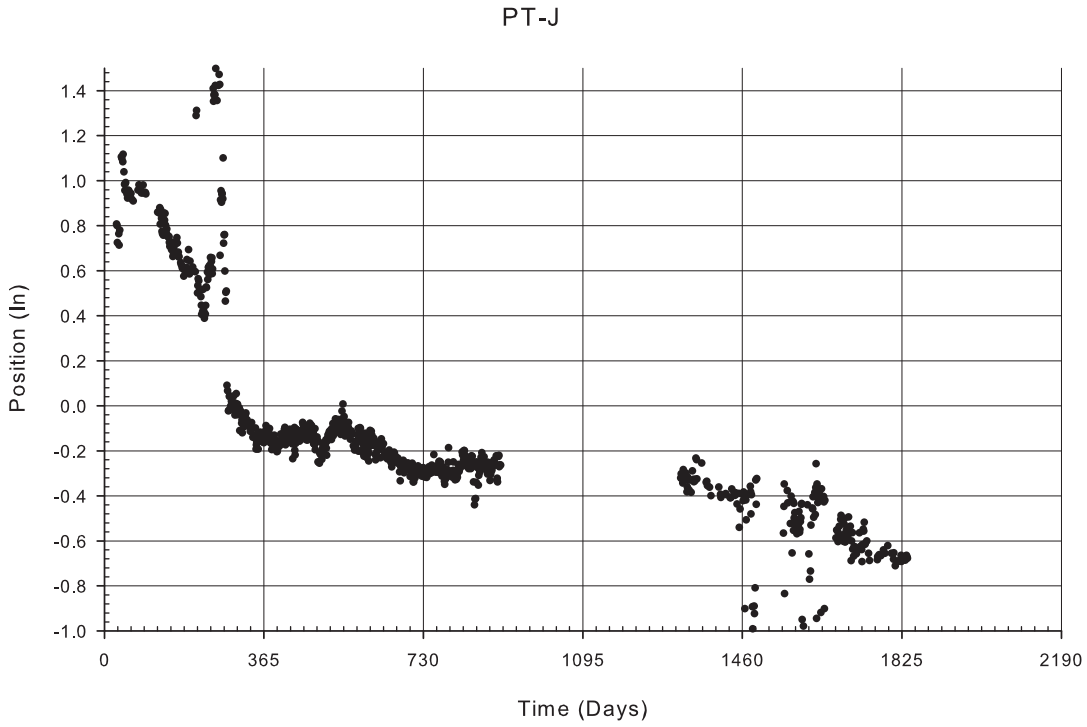

Figure A-176: Gage PT-J filtered position data

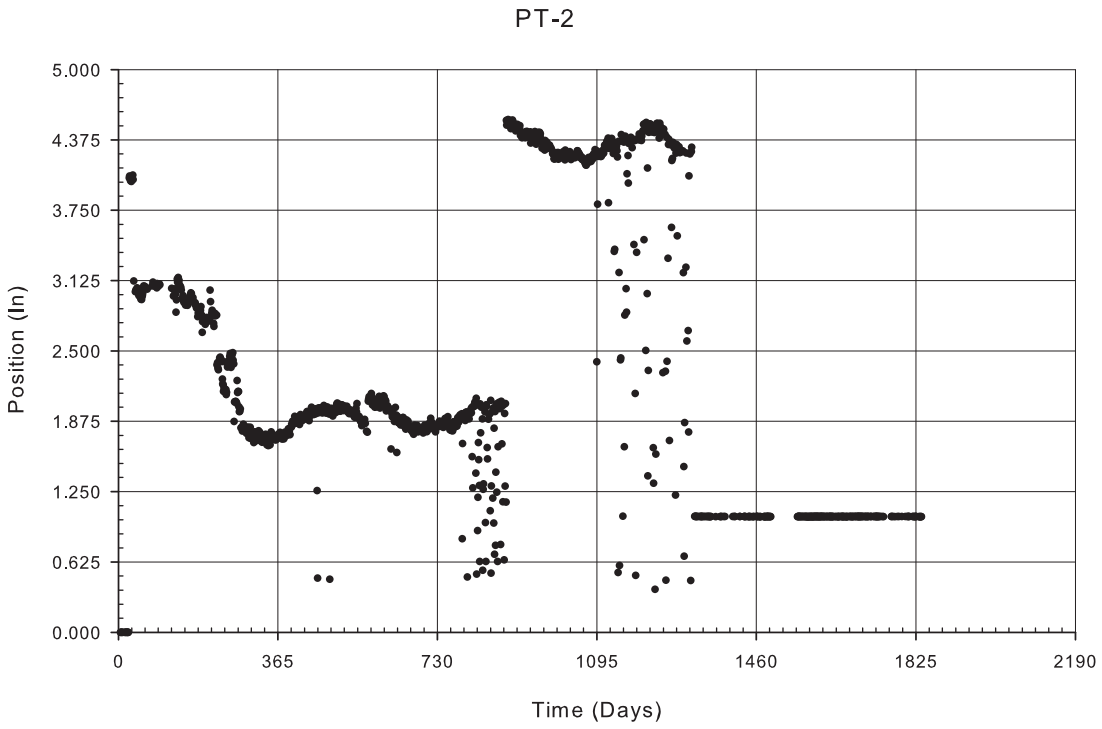

Figure A-177: Gage PT-2 filtered position data

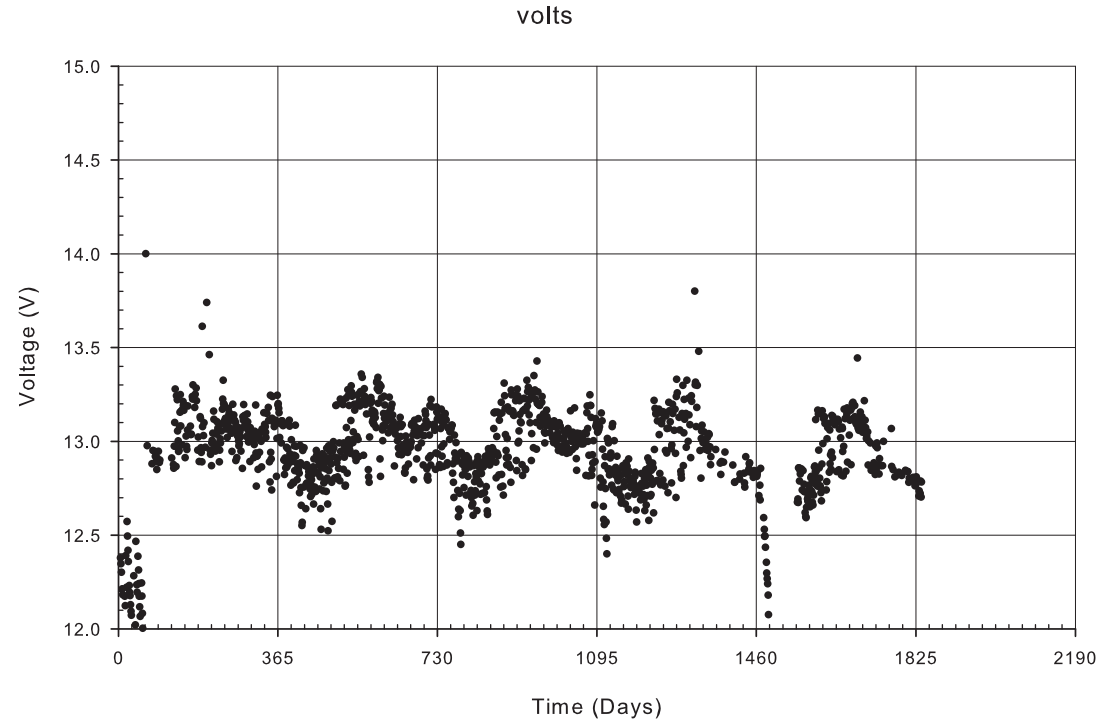

Figure A-178: System Voltage Data

Appendix

B Gaging Locations

MONITORING PLAN DETAILS FOR DODGE STREET OVER I-480

B.1 GAGE LOCATIONS

Redundant instrumentation to obtain the desired data adds to the project cost and produces massive data files. Therefore, a cost effective instrumentation strategy was devised by judiciously selecting the location of gages.

Using the 1997 AASHTO LRFD Bridge Design Manual, the bridge as designed by the Nebraska Department of Roads (NDoR) was analyzed. From the dead and live load analyses the gaging locations were chosen as described below. It was desirable to place gages on the East span because the distance to the ground is only 20' versus nearly 50' on the West span.

B.1.1 Spot-Weldable Gage Locations

The location of maximum positive bending moment from the Strength I combination was chosen as a gaging location. These strain readings will relate to the bending moment experienced by the girders. To obtain the amount of negative moment carried by girders, strain gages were also placed 2' East of the pier centerline. The gages could not be placed directly at the pier because of the bearing stiffeners there. Finally, spot-weldable gages were placed near the abutments so the amount of end restraint could later be determined and compared to the simple support assumed for

design. Figures B-1 and B-2 show the bridge sections where spot-weldable gages were placed on girders for Phase I and Phase II respectively.

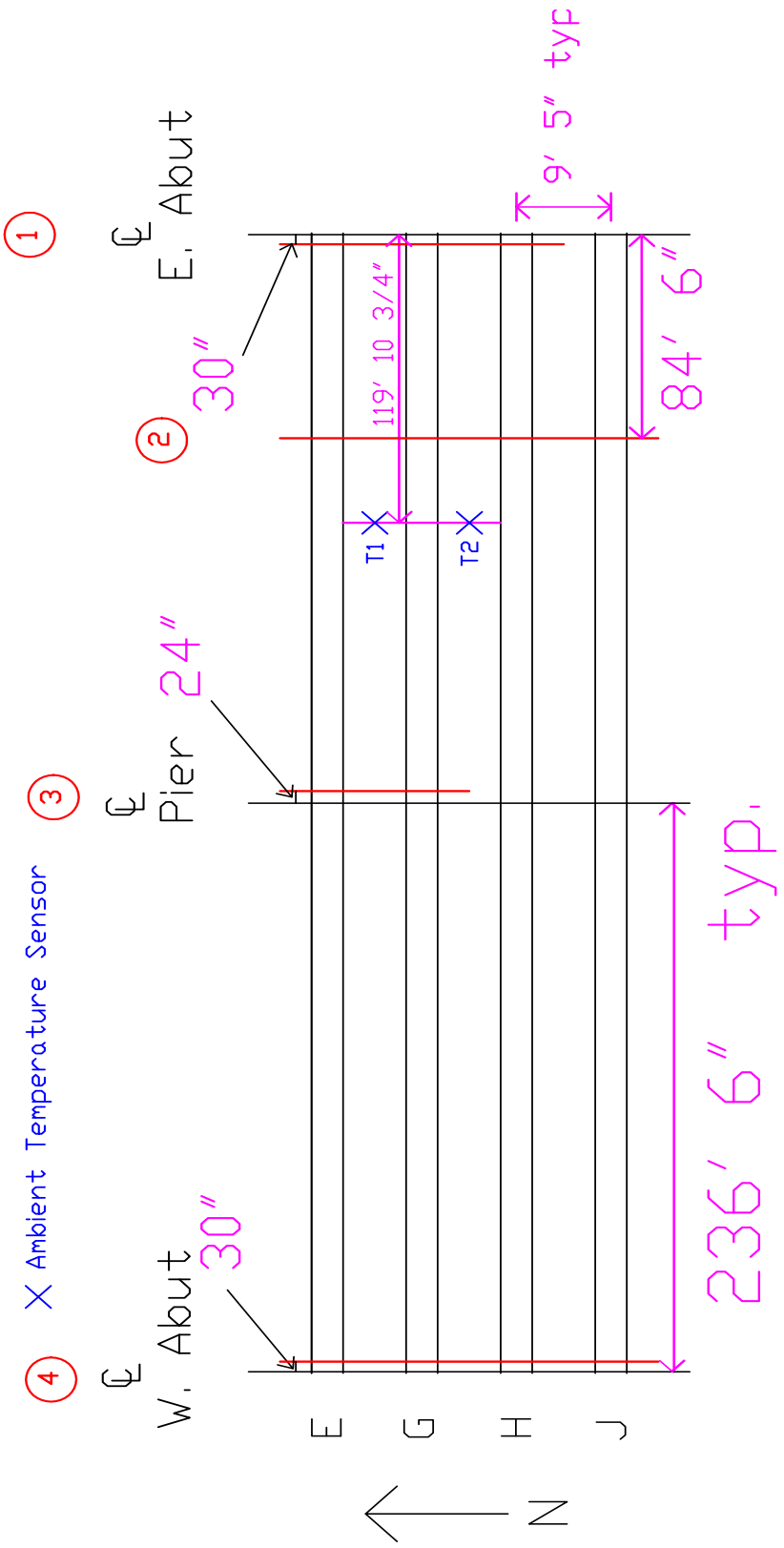

Figure B-1: Sections for spot-weldable steel strain gages for Phase I. Sections 1 and 4 are at the abutments, section 2 is at the maximum positive moment, and section 3 is at the pier

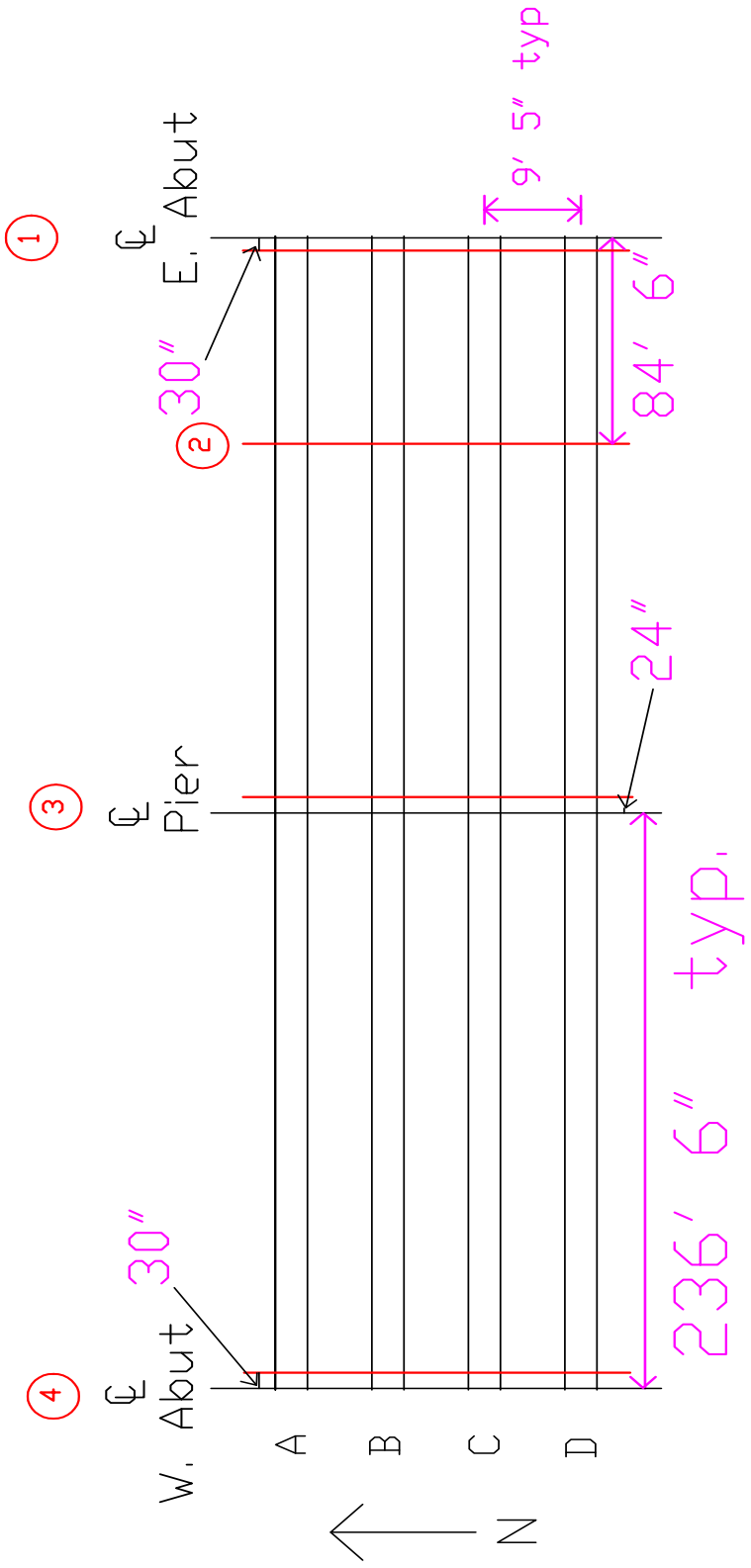

Figure B-2: Sections for spot-weldable steel strain gages for Phase II. Sections 1 and 4 are at the abutments, section 2 is at the maximum positive moment, and section 3 is at the pier

Looking at Figures B-1 and B-2 a few differences are evident in the gaging plans of Phase I and Phase II. For Phase I only the two girders closest to the closure pour were gaged at Section 3 versus all four girders for Phase II. Also, at Section 1 for Phase I, Girder J was not gaged. All gages were placed prior to girder erection.

Figures B-3 through B-6 show the gage placement on the girder at each section. The gages were centered on the flange at their respective position. To name the gages, the following convention was used: Vxy,1t or Vxy,2b. The V indicates it is a spot-weldable vibrating wire gage while x is the girder the gage is located on and the y is the section the gage is on. The 1t or 2b designates if the gage is located on the top or bottom flange, respectively. For example VG2,1t is the vibrating wire gage on Girder G of Section 2 on the top flange.

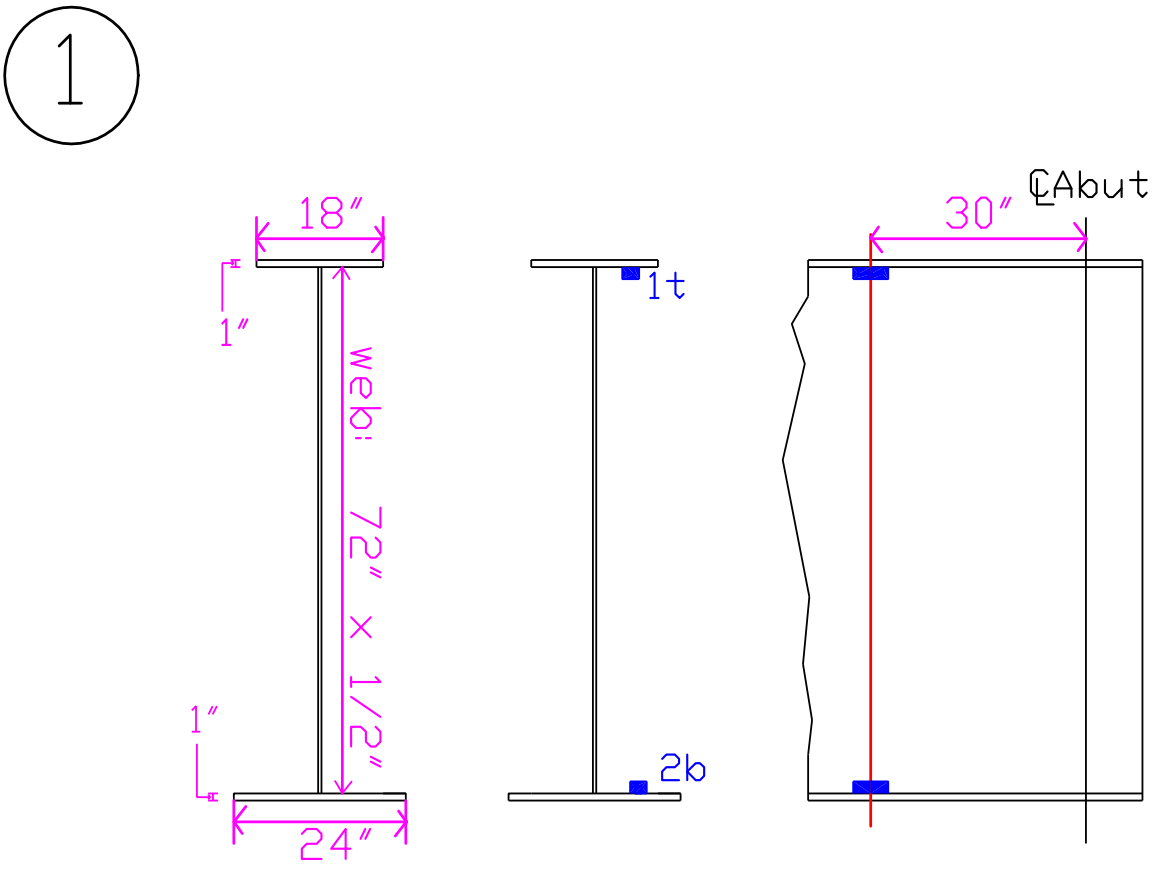

Figure B-3: Gaging Section 1 - East abutment

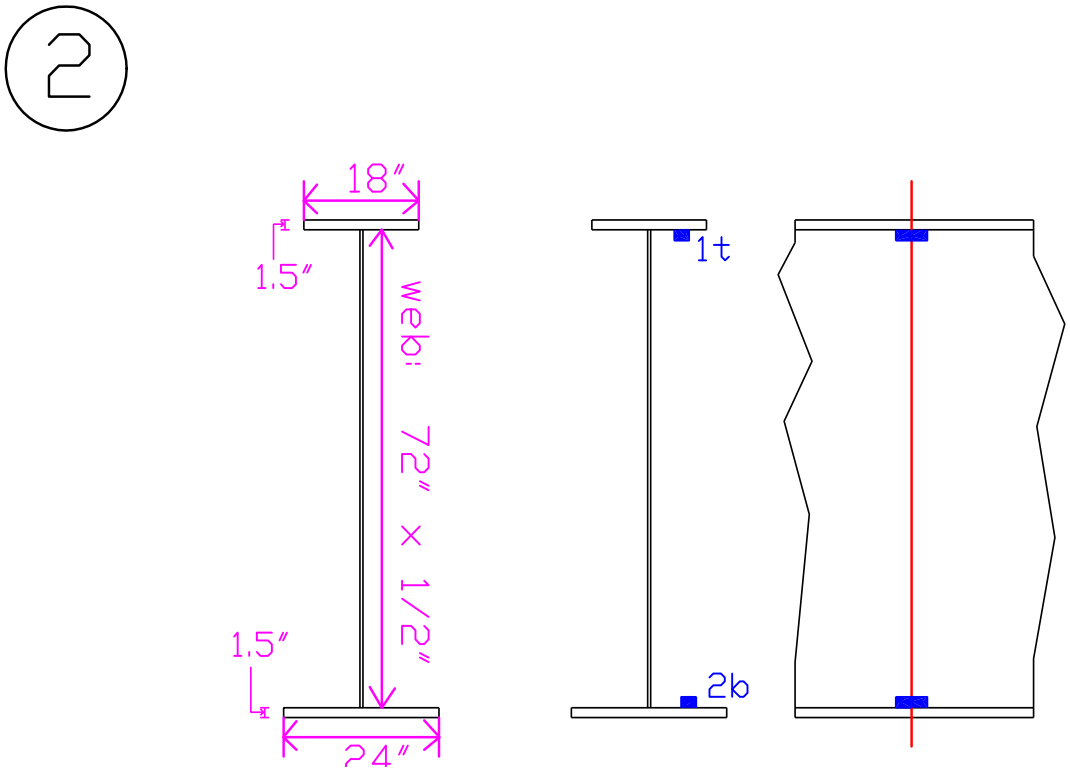

Figure B-4: Gaging Section 2 - maximum positive bending moment

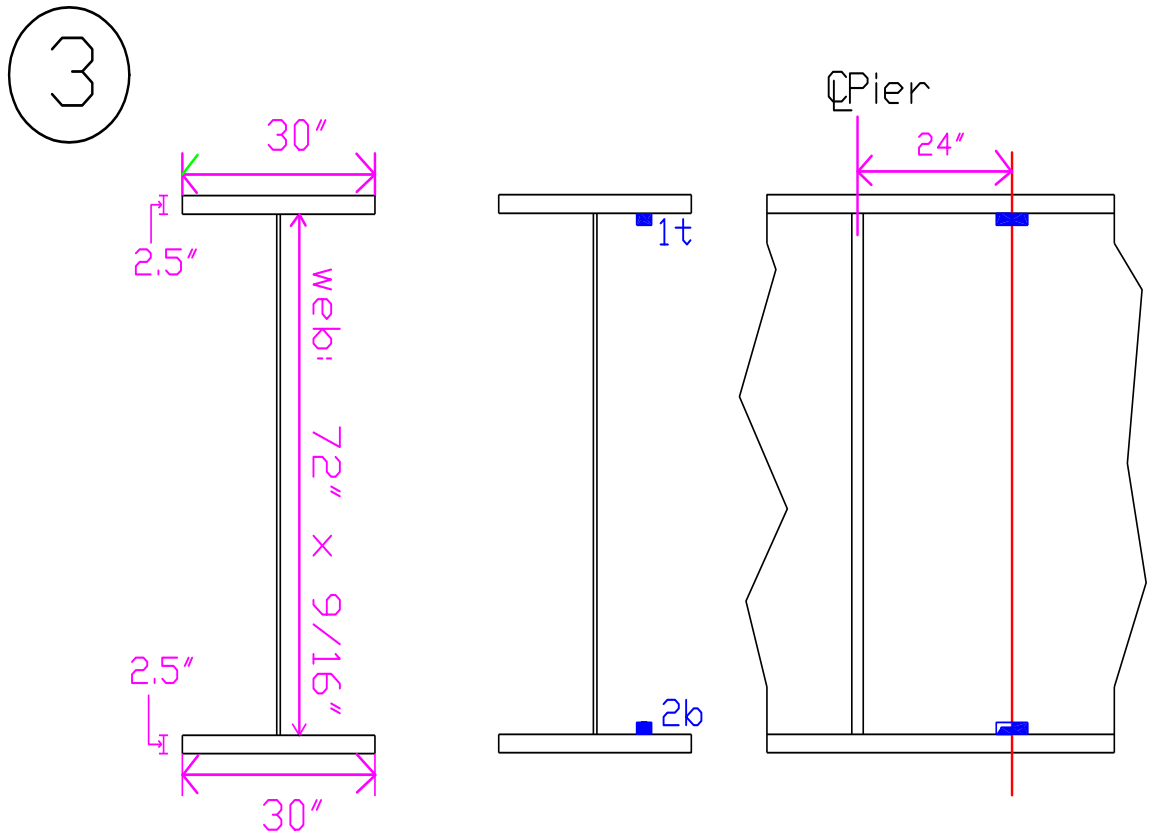

Figure B-5: Gaging Section 3 - maximum negative bending moment

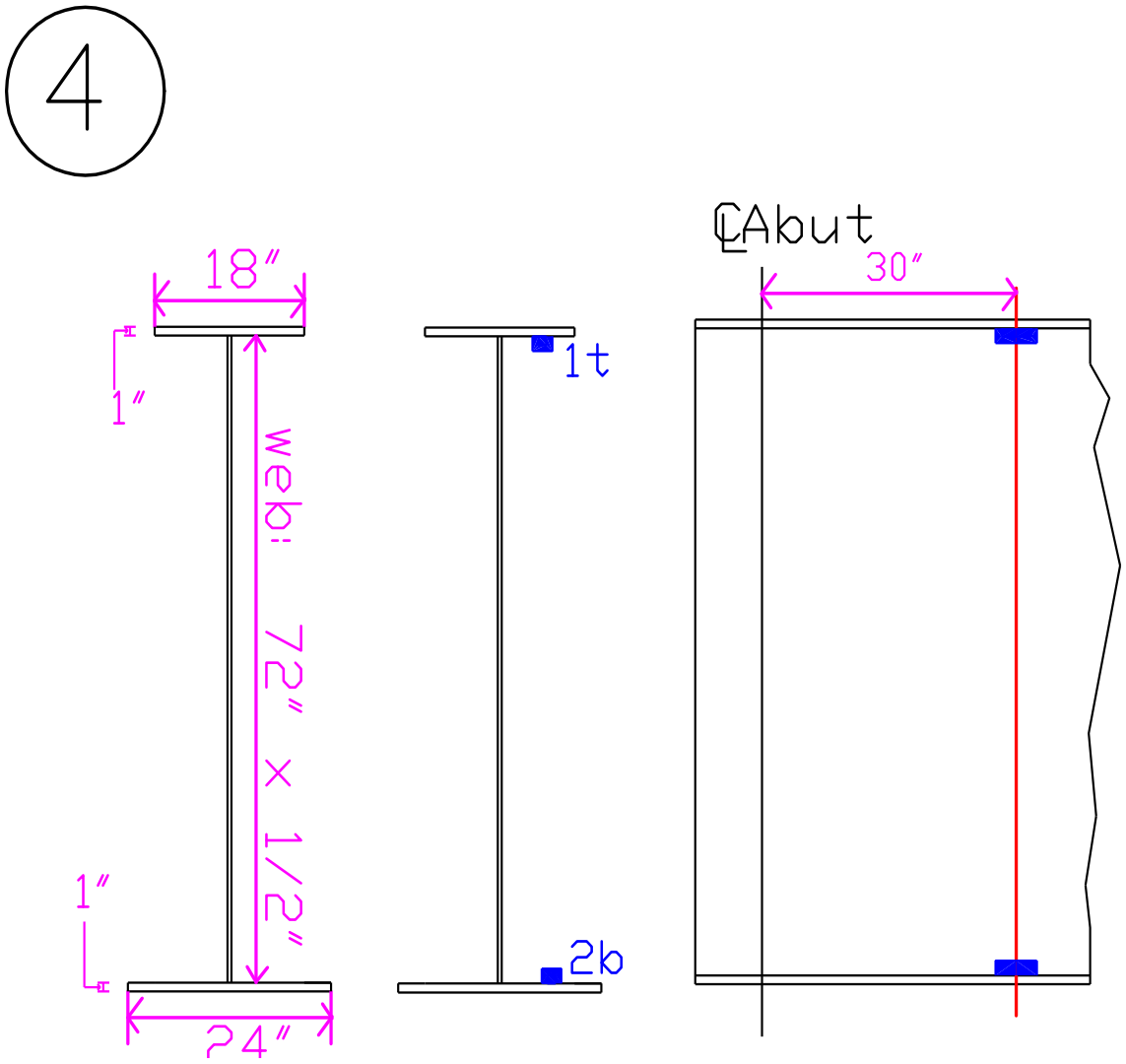

Figure B-6: Gaging Section 4 - West abutment

Two cross frames for Phase II and were also gaged. These strain readings will indicate how effective cross frames are in transmitting load in the transverse direction as the phases deflect relative to each other. The cross frames chosen to be gaged were the ones closest to the maximum positive moment section (Section 2). How these cross frames were gaged and their locations can be seen in Figures B-7 and B-8. The naming convention is as follows: XCD-1 to XCD-5 and XDE-1 to XDE-5. X indicates it is a cross frame gage, the two letters following that indicate what girders the cross frames

connect, and the number is a location. As can be seen there was one cross frame gaged in Phase II and one cross frame that connects the two phases.

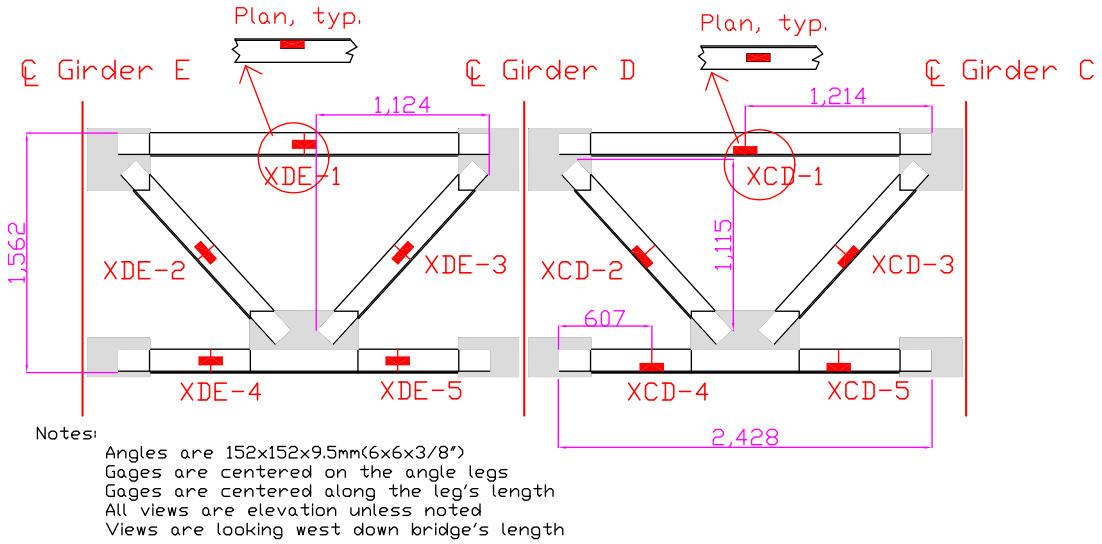

Figure B-7: Cross frame gage placement

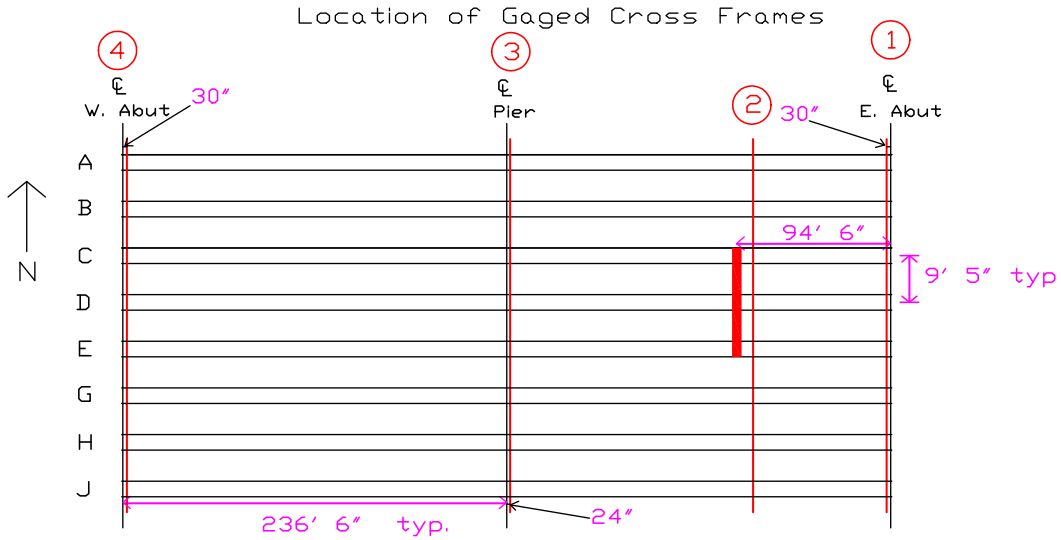

Figure B-8: Location of gaged cross frames

B.1.2 Embedment Gage Locations

To obtain concrete strain data, gages were placed at several locations and orientations in the deck. On Phase I, gages were placed directly above Girders E, G, H, and J at Sections 2 and 3 and orientated parallel to the girders. Several other gages were placed orientated perpendicular to girders at Sec-

tion 2. Another gage was placed at Section 2, 3" from the pour edge nearest the closure, orientated parallel to the girders. Finally, one gage was placed in a control specimen 7" deep x 6" wide x 18" long that was placed near the DAS to obtain the concrete's free shrinkage behavior. Figure B-9 shows the locations of Phase I embedment gages. Table B-1 indicates the distance from the bottom of the deck to the center of the gage for Phase I embedment gages.

Gage	Distance above deck	Section	Orientation
E1	4.25”	2	3” from N face of pour edge
E2	5.625”	2	Above CL Girder E parallel to girder
E3	3.875”	2	Between E&G perpendicular to girders
E4	5.25”	2	Above CL Girder G parallel to girder
E5	4.00”	2	Between G&H perpendicular to girders
E6	4.75”	2	Above CL Girder H parallel to girder
E7	4.25”	2	Above CL Girder J parallel to girder
E8	4.625”	3	Above CL Girder E parallel to girder
E9	5.25”	3	Above CL Girder G parallel to girder
E10	4.375”	3	Above CL Girder H parallel to girder
E11	4.125”	3	Above CL Girder J parallel to girder
E12	4.00”		In a 7” x 6” x 18” control specimen

Table B-1: Information on embedment gage location for Phase I

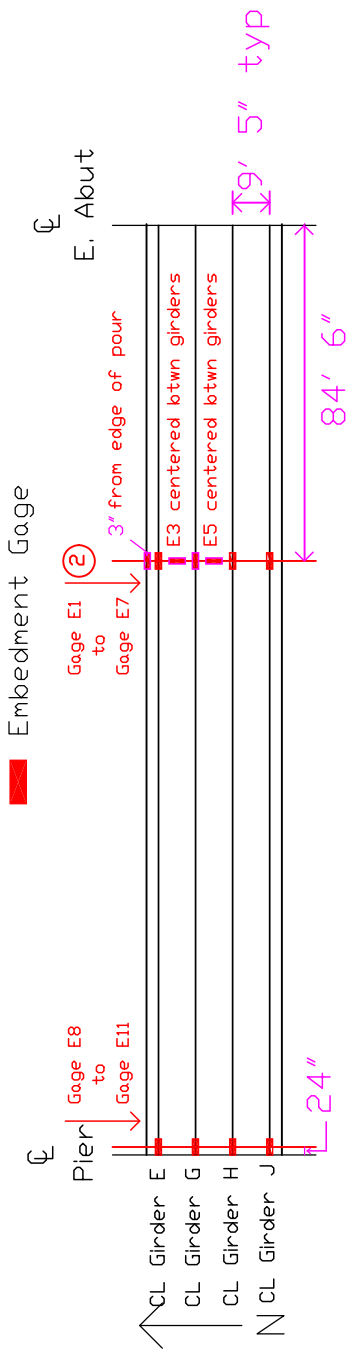

Figure B-9: Location of embedment gages for Phase I

Phase II has different embedment gage locations than Phase I as can be seen in Figure B-10. For this phase only two gages were placed in the bridge deck to preserve system resources so embedment gages could be placed in the closure pour region as seen in Figure B-11. Gages were placed in the closure pour because it joins the two phases and can carry high strains and

crack if differential settlement between the phases occurs. The gages will also provide long-term data on the closure region concrete behavior as it creep and shrinks. The gages in Phase II and the closure pour were all placed 4 inches above bottom of the deck. These gages are named with the prefix E and a number indicating their location.

Embedment gages were also placed in the Pier, East abutment, and West abutment for Phase I. The locations of these gages are in Figures B-12, B-13, and B-14 for the Pier, East abutment, and West abutment, respectively. On the East abutment the gages were placed over the second set of piles, which is behind the girder seat centerline. On the West abutment, gages

were centered along the width of the pile cap. This locates the gages directly below girder seats.

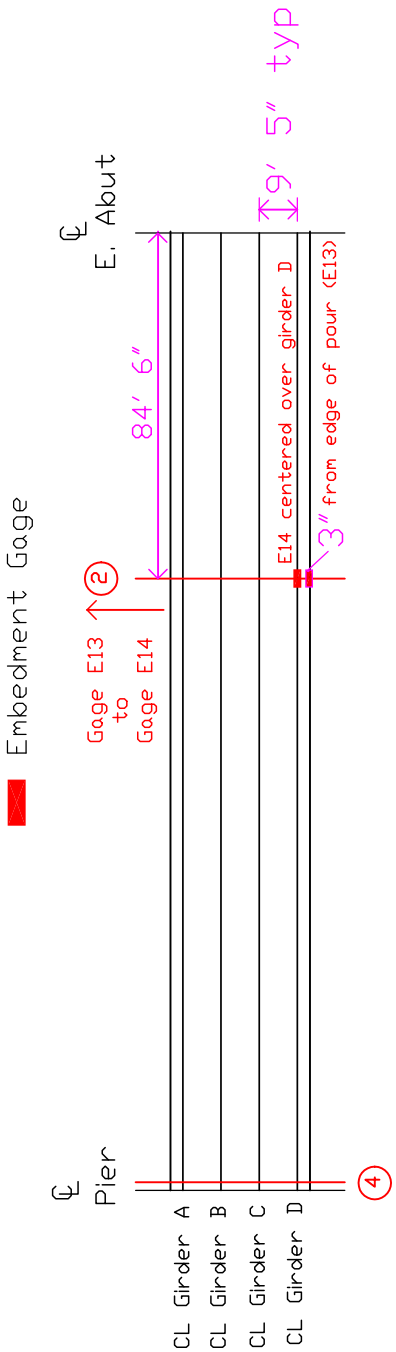

Figure B-10: Location of Embedment gages for Phase II

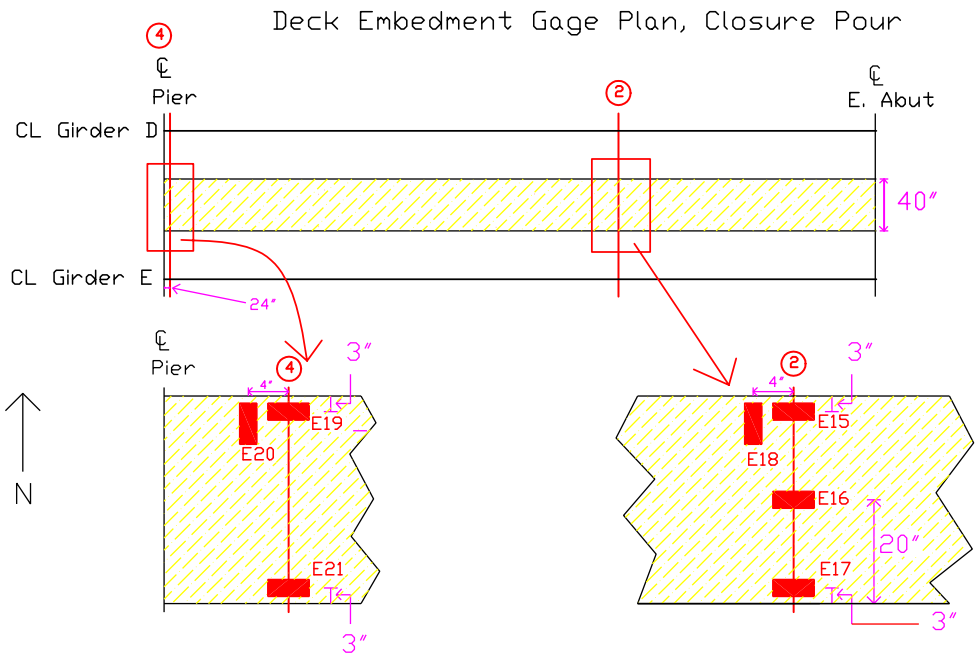

Figure B-11: Location of Embedment gages in the closure region

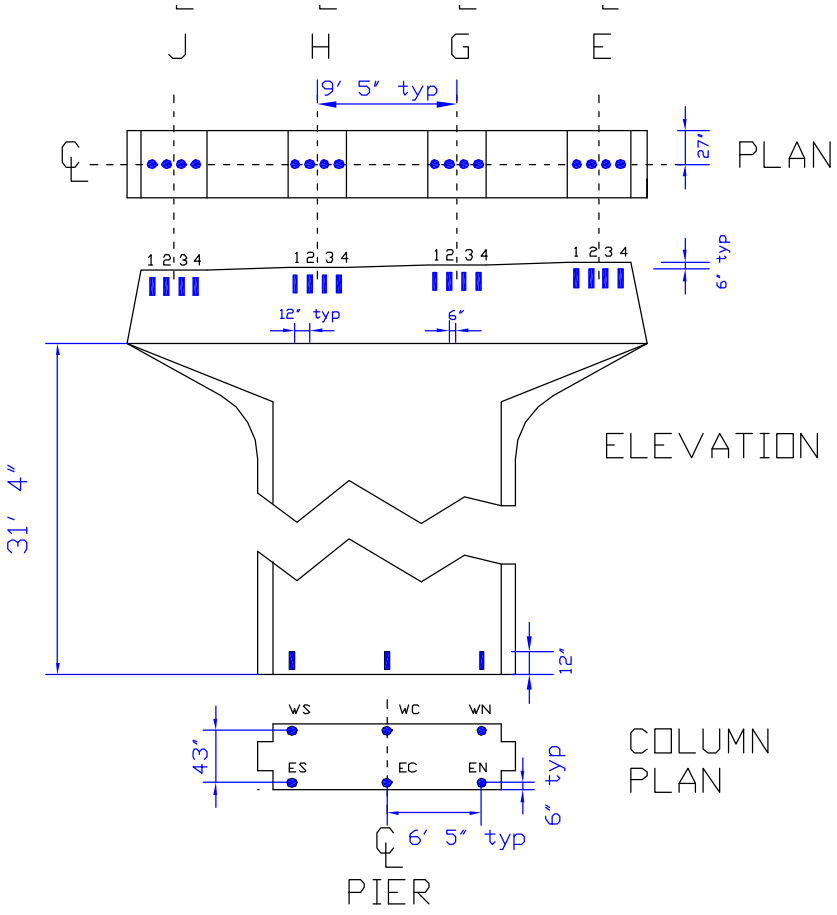

Figure B-12: Embedment gage locations in the Pier

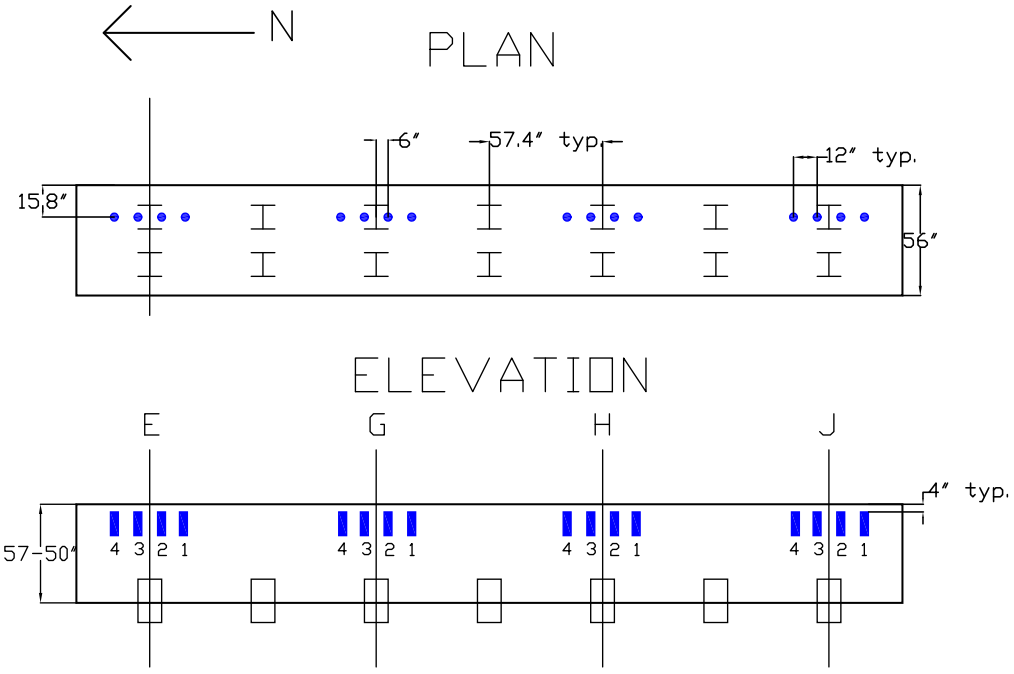

Figure B-13: Embedment gage locations in the East abutment

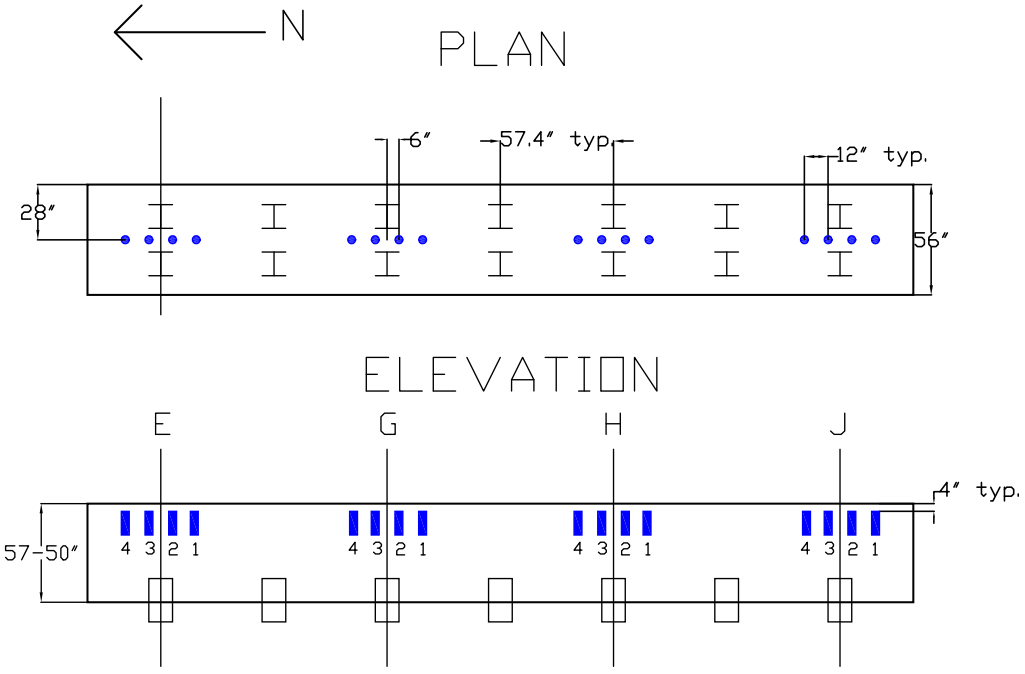

Figure B-14: Embedment gages in the West abutment

B.1.3 Displacement Measurement Locations

To obtain meaningful vertical displacement data it is desirable to measure deflection at the predicted location of maximum deflection, 0.4L. Potentiometers (pots) could not be placed exactly at this location because there is a roadway underneath the bridge. Therefore they were placed as close to the roadway as possible while still in a location that would not interfere with construction. The pots are tightly clamped to the underside of the girders while the other end is connected to a rigid test frame, which has its base cemented in the ground below the frost line. It is assumed the test frame does not move. This test frame can be seen in Figure B-15. At this location one pot is mounted on each girder of Phase I and II as seen in Figures B-16 and B-17. The pots monitor deflection during significant construction events and also long-term behavior. This data will indicate the amount of differential deflection occurring between the phases. The pots are named with the convention pot x, where x is the girder letter the pot is monitoring.

Girders D and E were instrumented at each abutment as seen in Figures B-16 and B-17 to measure the longitudinal displacement of each phase. These girders were chosen because they are adjacent to the closure pour and

should have the most effect on the closure region behavior. This data allows comparisons between the behaviors of the two phases.

Figure B-15: Test frame used to measure deflection. Note pots mounted on the underside of girders

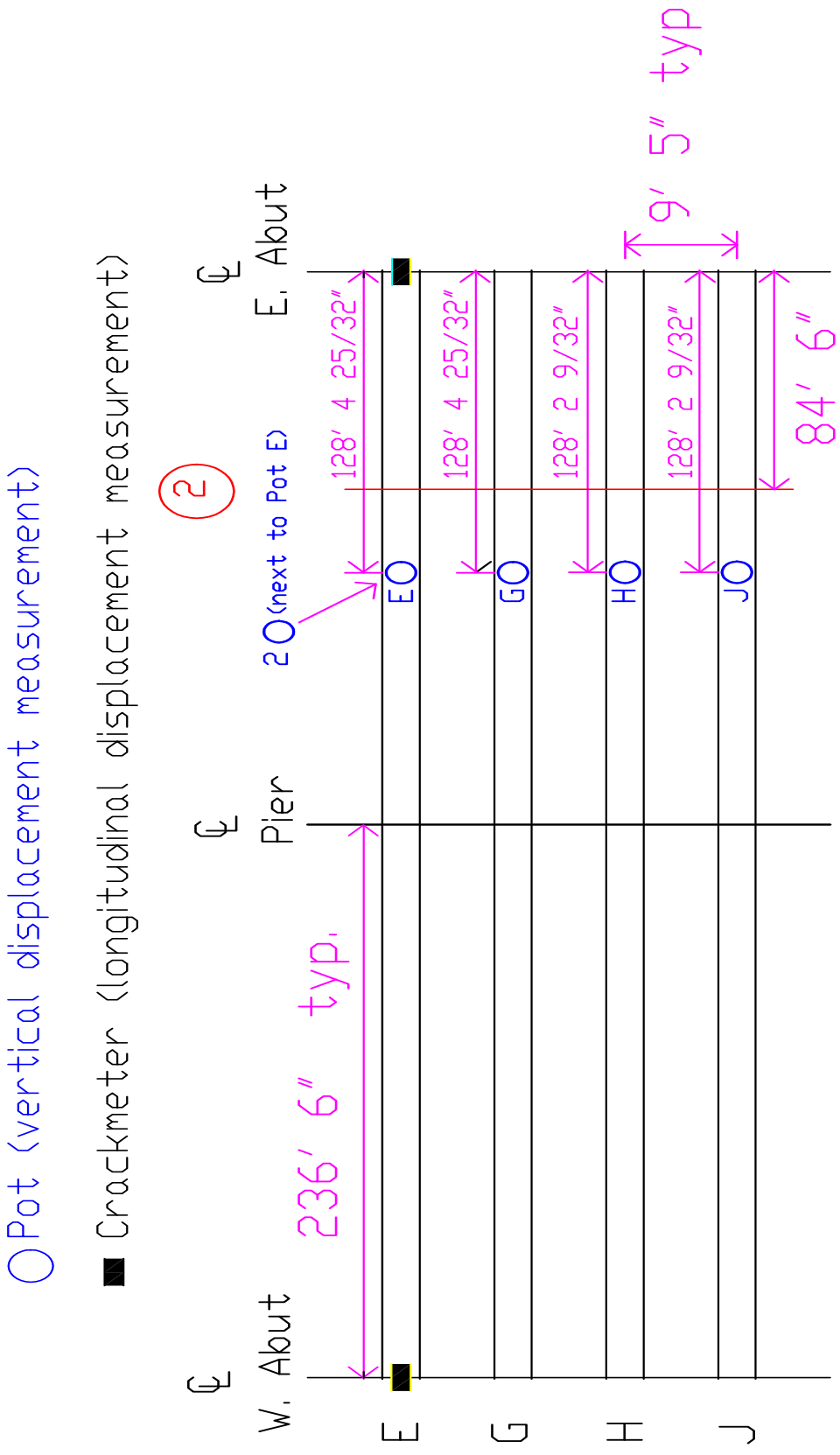

Figure B-16: Location of Displacement measurement for Phase I

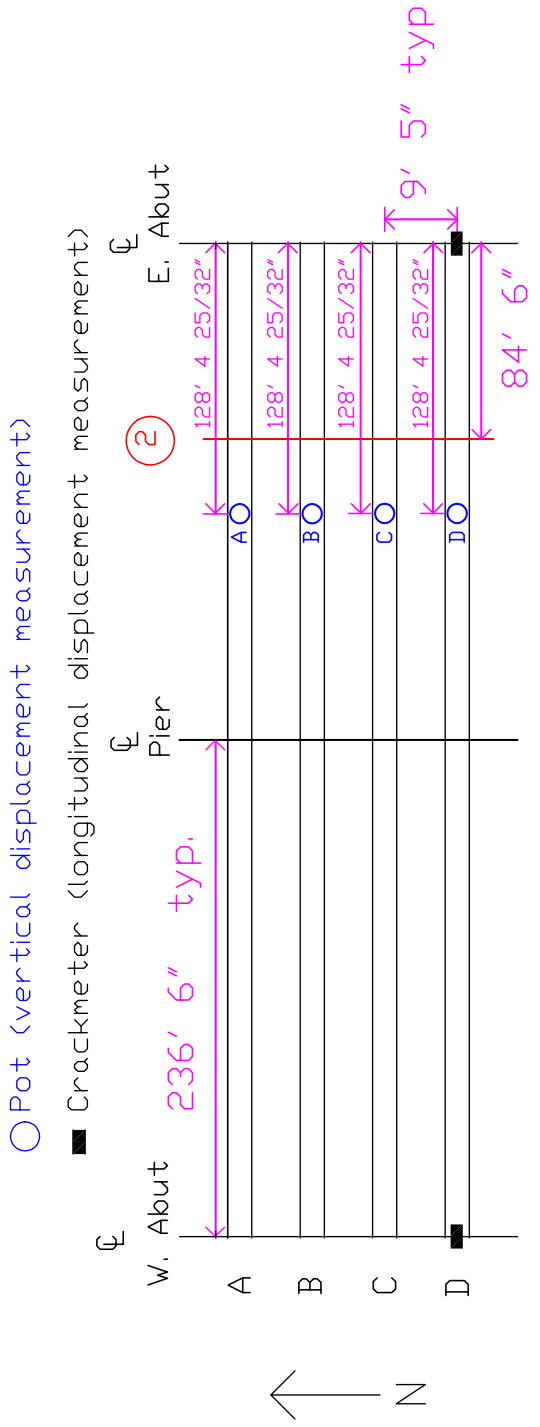

Figure B-17: Location of Displacement measurement for Phase II